IMAGING P-GLYCOPROTEIN FUNCTION: PREDICTION OF TREATMENT RESPONSE IN MESIAL TEMPORAL LOBE EPILEPSY

Maria Feldmann, MD

DEPARTMENT OF CLINICAL AND EXPERIMENTAL EPILEPSY

INSTITUTE OF NEUROLOGY

UNIVERSITY COLLEGE LONDON (UCL)

UNITED KINGDOM

THESIS SUBMITTED TO UNIVERSITY COLLEGE LONDON FOR THE DEGREE OF DOCTOR OF PHILOSOPHY, 2015

DECLARATION OF OWN WORK

I, Maria Feldmann, confirm that the work presented here is my own. Where information has been derived from other sources, I confirm that this has been indicated in the thesis. The scientific studies presented in this thesis reflect the contributions of a team of researchers including other colleagues from the Department of Clinical and Experimental Epilepsy, Institute of Neurology, University College London, Kings College, London, University of Liverpool and the Wolfson Molecular Imaging Centre, University of Manchester. Professor Joan Abbott and colleagues at Kings College performed the S100 protein analysis. Drs Joan Liu and Maria Thom from the Institute of Neurology, University College London, did the genetic and protein analysis. Dr Dickens and Professor Pirmohamed from the University of Liverpool helped with the PBMC analysis. The results of this collaboration are presented in Chapter IX and X. This thesis presents only studies where I conducted most steps of data collection, data analysis and the complete interpretation of the results following discussions at supervision meetings. I have outlined my own individual contribution to each of the studies published here and the contributions of my main co-workers and collaborators. All the figures and illustrations are my own. Information derived from other sources has been indicated and referenced in this thesis.

Signature

ABSTRACT

Background

Overexpression of multidrug efflux transporters at the blood–brain barrier, such as P-glycoprotein (Pgp), might contribute to pharmacoresistance by reducing target-site concentrations of antiepileptic drugs (AEDs). We assessed Pgp activity in vivo in patients with mesial temporal lobe epilepsy (mTLE).

Methods

Fourteen pharmacoresistant mTLE patients with unilateral hippocampal sclerosis (HS), three patients with pharmacoresistant epilepsy due to focal cortical dysplasia (FCD), eight seizure-free mTLE patients and 13 healthy controls underwent baseline PET scans with the Pgp substrate (R)-[^{11}C]verapami (VPM). Pharmacoresistant mTLE patients and healthy controls underwent a second VPM PET scan following infusion of the Pgp-inhibitor tariquidar (TQD). The transfer rate constant from plasma to brain, K_1, was estimated using a single-tissue compartment model with a VPM-in-plasma arterial input function. Analysis was performed on the first 10min of dynamic data containing limited radiolabeled metabolites. Regions were defined automatically using a brain atlas (ROI analysis), and ratios of VPM-K_1 values were calculated between a reference region (parietal cortex) and target regions. Parametric maps of VPM-K_1 were also generated using generalised linear least squares and was used for SPM voxel-based analysis. For the voxel-based analysis at baseline we created VPM PET images corrected for differences in whole brain radiotracer uptake. Furthermore, we compared VPM PET scans with epileptic tissues removed during epilepsy surgery and measured peripheral

markers of Pgp function: PBMC ABCB1 mRNA, ABCB1 polymorphism and S100B.

Findings

The ROI analysis revealed differences in VPM metabolism between mTLE patients and healthy controls which is caused by AED-mediated hepatic cytochrome P450 enzyme induction in mTLE patients requiring images to be normalised for global brain differences. When using ROI analysis and normalised VPM ratios there was no difference in VPM-K_1 ratios in pharmacoresistant compared to seizure-free mTLE patients or healthy controls. The ROI analysis after partial Pgp-inhibition with TQD showed attenuated global increases of VPM brain uptake in pharmacoresistant mTLE patients compared to healthy controls but there where no regional differences.

The voxel-based analysis at baseline revealed that pharmacoresistant mTLE patients had reduced VPM uptake compared to seizure-free mTLE patients and healthy controls in ipsi- and contralateral temporal lobes. Higher Pgp activity was associated with higher seizure frequency. After Pgp-inhibition with TQD pharmacoresistant mTLE patients had reduced increases of VPM brain uptake in the whole brain and ipsilateral hippocampus, implicating Pgp overactivity in the epileptogenic hippocampus. The difference in percentage change in VPM brain uptake after Pgp-inhibition with TQD inversely correlated with the difference in percentage area of Pgp immunopositive labeling in pharmacoresistant mTLE patients who underwent epilepsy surgery. Pharmacoresistant epilepsy patients with FCD had reduced VPM brain uptake in close proximity to the area of FCD but also extending to other ipsilateral

regions. There were no differences in peripheral markers of Pgp function between the three groups. Our results support the hypothesis of Pgp overactivity in pharmacoresistant epilepsy.

TABLE OF CONTENTS

LIST OF FIGURES

LIST OF TABLES

LIST OF ABBREVIATIONS

AED	Antiepileptic drug
AI	Asymmetry index
ANOVA	Analysis of Variance
ABC	ATP binding cassette
ABCB1	ATP-binding cassette subfamily B member 1
ABCC1	ATP-binding cassette subfamily C member 1
ATP	Adenosine triphosphate
BBB	Blood-Brain Barrier
BCRP	Breast cancer resistance protein
BCEC	Brain capillary endothelial cells
CA	Cornu Ammonis
CBF	Cerebral blood flow
CNS	Central nervous system
CP	Choroid Plexus
CSF	Cerebrospinal fluid
CsA	Cyclosporine A
DCE-MRI	Dynamic contrast-enhanced magnetic resonance imaging
DARTEL	Fast diffeomorphic registration algorithm
EEG	Electroencephalography

FCD	Focal cortical dysplasia
^{18}FDG	Fluorine-18 fluorodeoxy-glucose
FS	Febrile seizures
GABA	Gamma-aminobutyric acid
GBq	Gigabecquerel
GM	Gray matter
HC	Healthy control
HPLC	High-performance liquid chromatography
HRRT	High Resolution Research Tomograph
HS	Hippocampal sclerosis
ILAE	International League Against Epilepsy
keV	Kiloelectron volt
LOR	Line of response
MBq	Megabecquerel
MDR	Multidrug resistance
MNI	Montreal Neurological Institute
MRI	Magnetic resonance imaging
mRNA	Messenger ribonucleic acid
MRP	Multidrug resistance protein
MTLE	Mesial temporal lobe epilepsy

MTS	Mesial temporal sclerosis
NMDA	N-methyl-D-aspartate
PBMC	Peripheral blood mononuclear cells
PCR	Polymerase chain reaction
PET	Positron emission tomography
Pgp	P-glycoprotein
PR	Pharmacoresistant epilepsy patients
ROI	Region of interest
ROS	Reactive oxygen species
SD	Standard deviation
SE	Status epilepticus
SF	Seizure-free epilepsy patients
SPEC T	Single photon emission computed tomography
SPM	Statistical parametric mapping
TQD	Tariquidar
TLE	Temporal lobe epilepsy
VPM	[^{11}C]verapamil
WM	White matter

ACKNOWLEDGEMENTS

I am grateful to the many people who helped me make this PhD a most rewarding experience. I would like to thank Professor Matthias Koepp, for introducing me to the EURIPIDES project. His enthusiasm, guidance and passion for work inspired me throughout the project. I am grateful to Dr Marie-Claude Asselin for her support and teaching me how to perform PET studies and data analysis. I am also thankful to Professor Sanjay Sisodiya for his encouragement and help with data analysis and results interpretation.

This thesis would not have been completed without the support from the staff at the Wolfson Molecular Imaging Centre. I would like to thank Dr Shaonan Wang for his help with data analysis. I am grateful to the production and quality control team as well as the radiochemistry and blood analysis laboratory. I am also grateful to the radiographers Lindsay Cunningham, Mike Godfrey, Eleanor Duncan-Rouse and Gerben van der Vegte. Jose Anton Rodriquez helped with reconstruction of our PET scans, and Drs Rainer Hinz and Julian Matthews helped with data analysis and interpretation. I am also grateful to Lynne Macrae and Jenny Jamnadas-Khoda for their support with the research administration. I am thankful to The NIHR/Wellcome Trust Manchester Clinical Research Facility who looked after the patients and I so well and nothing was too much trouble.

Professor Joan Abbott did the S100 protein analysis. Drs Joan Liu and Maria Thom helped with the genetic and protein analysis and Dr Dickens and Professor Pirmohamed with the PBMC analysis.

I would also like to thank my colleagues and friends at the Department of Clinical and Experimental Epilepsy Drs Maria Centeno Soladana, Meneka Sidhu, Umair Chaudhary and Jason Stretton as well as Professor John Duncan for their support and scientific discussions.

I am grateful to the radiographers at the National Society for Epilepsy, Philippa Bartlett, Jane Burdett, and Elaine Williams for their help with the MRI scans.

The patients were generously referred by Professors Ley Sander, Sanjay Sisodiya, John Duncan, Matthew Walker, Dr Dominic Heaney and Dr Paul Cooper.

The patients and participants volunteered enthusiastically to give up their time in order to participate in these studies and often travelled from far distances. Their contribution to this work is greatest of all.

Funding for this project was provided by the European Community's Seventh Framework Programme (FP7/2007-2013) under grant agreement no 201380 (EURIPIDES) and the Wolfson Trust and the Epilepsy Society supports the Epilepsy Society MRI scanner.

My family supported me at all times, in particular my mother who despite her illness has always encouraged me to continue even in difficult times. My strongest thanks to my beloved husband Stephen and our daughter Anna Maria- you are my motivation and inspiration. I could not have done this without your unconditional love and support!

OUTLINE OF THESIS AND STATEMENT OF PERSONAL CONTRIBUTION

This thesis is structured as follows:

SECTION 1: BACKGROUND

Chapters I-III summarise the background that is important to understand the following work and outlines the objective of this thesis.

Chapter I: presents the current understanding of the mechanism of seizure generation, classification scheme of seizures and epilepsy, investigation tools applied to diagnose seizures and possible treatment options.

Chapter II: summarises the background of pharmacoresistance in epilepsy and discusses the different hypotheses of pharmacoresistant epilepsy. It focuses on the transporter hypothesis and presents the mechanisms of P-glycoprotein (Pgp) overexpression. It outlines preclinical and clinical studies investigating Pgp in mesial temporal lobe epilepsy (mTLE) and describes imaging studies examining Pgp function.

Chapter III: outlines the objectives and hypothesis of this thesis.

SECTION II: EXPERIMENTAL STUDIES

Chapter IV: describes the common methods used in the most experimental studies used in the thesis.

Chapters V-XI describe the experimental studies.

Chapters V and VI show the results of the region of interest analysis (ROI) of (R)-[11C]verapamil (VPM) PET at baseline and after partial Pgp inhibition

Chapter V: I present my work investigating Pgp function using VPM-PET in patients with mTLE. Using ROI analysis I show that there are differences in VPM metabolism between mTLE patients and healthy controls which is caused by AED-mediated hepatic cytochrome P450 enzyme induction in mTLE patients requiring images to be normalised for global brain differences. Additionally I show an association between Pgp activity and seizure frequency in mTLE patients. When using ROI analysis and normalised VPM images there was no difference in VPM-K_1 ratios in pharmacoresistant compared to seizure-free mTLE patients or healthy controls.

Chapter VI: by using ROI analysis I show attenuated global increases of VPM brain uptake after partial Pgp-inhibition by TQD in pharmacoresistant mTLE patients compared to healthy controls but there where no regional differences.

Chapters VII and VIII show the results of the voxel-based analysis of the same data. We hypothesise that the voxel-based analysis of the same data would complement the ROI findings.

Chapter VII: by using voxel-based SPM analysis normalised for global brain differences I show that at baseline there is lower focal VPM uptake indicating higher Pgp activity in pharmacoresistant compared to seizure-free mTLE patients and healthy controls. Furthermore, Pgp overactivity in the ipsilateral

hippocampus of pharmacoresistant mTLE patients correlates with seizure frequency.

Chapter VIII: I present the voxel-based SPM analysis after partial Pgp-inhibition by TQD showing attenuated increases of VPM uptake with a maximum effect in epileptogenic hippocampus.

Chapter IX: I show a correlation of Pgp overexpression revealed in postsurgical tissue with the Pgp overactivity demonstrated with voxel-based analysis after partial Pgp-inhibition by TQD in pharmacoresistant mTLE patients. Here I would like to thank Drs Joan Liu and Maria Thom from the Institute of Neurology, University College London, who did the immunohistochemisty study on the postsurgical tissue.

Chapter X: I present that there is no differences in peripheral markers of Pgp function measured with PBMC ABCB1 mRNA, ABCB1 polymorphism and S100B between the three groups. Professor Joan Abbott and colleagues at Kings College kindly performed the S100 protein analysis. Drs Joan Liu and Maria Thom from the Institute of Neurology, University College London, did the genetic analysis and Dr Dickens and Professor Pirmohamed from the University of Liverpool helped with the PBMC analysis.

Chapter XI: I extended our study including patients with focal cortical dysplasia (FCD) complementing the previous results of mTLE patients showing pharmacoresistant epilepsy patients with FCD had reduced VPM brain uptake in close proximity to the area of FCD but also extending to other ipsilateral regions.

SECTION III DISCUSSION AND CONCLUSION

Chapter XII in this section, I discuss the limitations, neurobiological and clinical applications as well as future research directions in the context of the principal experimental findings.

PUBLICATIONS ASSOCIATED WITH THIS THESIS

Feldmann M, Asselin MC, Liu J, Wang S, McMahon A, Anton-Rodriguez J, Walker M, Symms M, Brown G, Hinz R, Matthews J, Bauer M, Langer O, Thom M, Jones T, Vollmar C, Duncan JS, Sisodiya SM, Koepp MJ. P-glycoprotein expression and function in patients with temporal lobe epilepsy: a case-control study. Lancet Neurol. 2013;12(8):777-85.

Feldmann M, Koepp M. P-glycoprotein imaging in temporal lobe epilepsy: in vivo PET experiments with the Pgp substrate [^{11}C]-verapamil. Epilepsia. 2012; 53 Suppl 6:60-3

Feldmann M, Koepp M. Positronen-Emmissions-Tomographie. Zeitschrift fuer Epileptologie. 2012; 25: 208-21.

Walker M, **Feldmann M,** Matthews J, Anton-Rodriquez J, Wang S, Koepp M, Asselin M. Optimization of methods for quantification of rCBF using high resolution [^{15}O]H2O PET images. Phys. Med. Biol. 2012; 57:2251-227.

Walker, M., Asselin M, Julyan P, **Feldmann M**, Talbot P, Jones T, Matthews J. Bias in iterative reconstruction of low-statistics pet data: benefits of a resolution model. Physics in Medicine and Biology. 2011; 56(4): 931–949.

CONFERENCE ABSTRACTS RELATED TO THIS THESIS

Feldmann M, Asselin M-C, Wang S, McMahon A, Hinz R, Duncan J, Sisodiya S, Koepp M. P-glycoprotein overactivity in pharmacoresistant epilepsy patients with focal cortical dysplasia compared to healthy controls measured using (R)-[^{11}C]verapamil PET and the Pgp inhibitor tariquidar. In: Eur. J. Neurol. 21 (2014), Suppl. 1, p. 229. Presented at European Federation of Neurological Societies (EFNS) and European Neurological Society (ENS) Joint Congress of European Neurology; 2014. Istanbul, Turkey.

Wang S, **Feldmann M,** Hinz R, McMahon A, Koepp M, Jackson A, Asselin M-C. Robust kinetic model for quantification of P-glycoprotein (P-gp) function under altered metabolism and after P-gp inhibition using (R)-[^{11}C]verapamil and PET. Presented at IXth International Symposium on Functional Neuroreceptor Mapping of the Living Brain, 2012, Baltimore, USA.

Feldmann M, Asselin M-C, Wang S, Walker M, McMahon A, Hinz R, Brown G, Anton-Rodriguez J, Duncan J, Sisodiya S, Koepp M. P-glycoprotein overexpression in temporal lobe epilepsy: in-vivo PET experiment with the P-gp substrate and (R)-[^{11}C]verapamil and the P-gp inhibitor tariquidar. Presented at 65th American Epilepsy Society Annual Meeting, 2011. Baltimore, USA.

Wang S, Walker M, Matthews J, **Feldmann M,** Hinz R, Jackson A, Koepp, M, Asselin M-C. Optimisation of generating parametric maps for quantification of P-gp function in vivo using PET with (R)-[^{11}C]verapamil. Presented at XIIth PET Symposium. 2011. Turku, Finland.

Wang S, Hinz R, **Feldmann M,** McMahon A, Koepp M, Jackson A, Asselin M-C. Can partial volume correction of (R)-[^{11}C]verapamil PET data be performed using kinetic modelling? Presented at World Molecular Imaging Congress. 2011. San Diego, California, USA.

Feldmann M, Asselin M-C, Wang S, McMahon A, Walker M, Hinz, R, Duncan J, Sisodiya S, Koepp M. P-glycoprotein overexpression in patients with pharmaco-resistant temporal lobe epilepsy measured with PET and (R)-[^{11}C]verapamil. Presented at 10th International Conference on Quantification of Brain Function with PET, 2011, Barcelona, Spain.

Wang S, **Feldmann M,** Hinz R, Koepp M, Jackson A, Asselin M-C. Partial volume correction of (R)-[^{11}C]verapamil PET images using choroid plexus defined on contrast-enhanced MRI. Presented at 10th International Conference on Quantification of Brain Function with PET, 2011, Barcelona, Spain.

Feldmann, M, Asselin, M-C, Wang, S, Walker M, McMahon, A, Anton J, Hinz R, Sisodiya S, Duncan J, Koepp M. Pharmacoresistance in mesial temporal lobe epilepsy measured with (R)-[^{11}C]verapamil PET after inhibition of P-glycoprotein function by Tariquidar. Neurology, 16(9), A517-A517. Presented at 63nd American Academy of Neurology Annual Meeting. 2011. Honolulu, Hawaii, USA.

Feldmann M, Asselin M-C, Wang S, McMahon A, Walker M, Anton J, Hinz R, Sisodiya S, Duncan J, Koepp M. Tariquidar inhibition of P-glycoprotein activity in patients with temporal lobe epilepsy measured with PET and (R)-[^{11}C]verapamil. Neuroimage 52, suppl. 1 (2010), S148. Presented at VIIIth International Symposium on Functional Neuroreceptor Mapping, 2010, Glasgow Scotland, UK.

Wang S, **Feldmann M**, Hinz R, Asselin M-C, Jackson A. Imaging the choroid plexus for partial volume correction of (R)-[^{11}C]verapamil PET images. Presented at VIIIth International Symposium on Functional Neuroreceptor Mapping, 2010. Glasgow, Scotland, UK

Feldmann M, Asselin M-C, Sisodiya S, Wang S, Duncan J S, Koepp M J. Effect of P-gp inhibition in drug-resistant TLE using a single dose of Tariquidar. Epilepsia pp. 119 – 120. Presented at 63rd American Epilepsy Society Annual Meeting, 2009. Boston, USA.

CHAPTER I BACKGROUND

1.1 EPILEPSY

1.1.1 Introduction

Epilepsy is a common neurological disorder with an estimated prevalence in Europe of 4.3-7.8 per 1000 (Pugliatti M et al. 2007). Despite advances in antiepileptic drug (AED) therapy about one-third of patients with epilepsy are resistant to drug treatment (Regesta and Tanganelli 1999). Uncontrolled epilepsy can shorten lifespan, lead to bodily injury, neuropsychological and psychiatric impairment, and social disability (Kwan and Brodie, 2005). Patients who are pharmacoresistant often present with certain features of the epileptic condition, such as history of febrile seizures (FS), high frequency of seizures prior to treatment, early onset of seizures, structural brain lesions or psychiatric comorbidities (Regesta and Tanganelli, 1999). Most patients with refractory epilepsy are resistant to several, if not all, AEDs, even though these drugs act by diverse mechanisms (Kwan and Brodie, 2005).

Functional imaging, in particular positron emission tomography (PET) offers new hope for the development of better treatments by increasing our understanding of mechanisms underlying drug- resistance.

1.1.2 Definition

Clinically, epilepsy is characterised by recurrent spontaneous seizures. An epileptic seizure is an acute and transient event, which is manifested as a brief change in behaviour caused by the disorder, synchronous and rhythmic firing of

populations of neurons in the central nervous system (McNamara 1999). A wide diversity of epilepsy syndromes have been described based upon several characteristics, such as symptoms, seizure types and electroencephalographic patterns.

1.1.3 Classification of seizures

Classifications are required for the purpose of dividing heterogeneous disease patterns into homogeneous classes to understand the biology of the disease. They can highlight the causes, pathophysiology and management of the disease and it allows communication between physicians, teaching and scientific research, epidemiology and pharmacology of the disease (Engel 1998). The international league against epilepsy (ILAE) creates and updates the classification of epilepsies. The ILAE classification of seizures was first published in 1969 (Gastaut 1969; Gastaut 1970) and updated in 1981 for seizures (ILAE 1981) and 1989 for epilepsies (ILAE 1989). Classically two seizure types have been recognised: those arising from focal cortical disturbances and those characterised by synchronous discharge of both hemispheres. These correspond to partial and generalised seizures and can be differentiated both clinically and by their electroencephalographic (EEG) findings. This division formed the basis of the revised International classification of Epileptic Seizures introduced by the ILAE in 1981. In this classification system partial seizures are also divided further into “simple” and “complex”, depending on whether consciousness is retained or lost. However, the previous ILAE classifications were based on concepts that predate modern neuroimaging,

genomic technologies and concepts of molecular biology. On this background the ILAE released in 2010 (Berg et al. 2010) recommendations for the classification of seizures and epilepsies in an attempt to change the old terminology, in accordance with the technology and scientific advances that have occurred in the last several years (Beghi 2011). Changes to the ILAE's 1981 classification of seizures include that neonatal seizures are no longer classified separately, absence seizures are simplified into typical, atypical or absence with special features which now included myoclonic absence and eyelid myoclonica as well as epileptic spasms (Table 1). Additionally the distinction between simple partial and complex partial focal seizures was eliminated but the concept of impairment of consciousness/awareness is still preserved.

Table 1: International classification of seizures (ILAE 2010)

Generalised seizures
Tonic-clonic
Absence
Typical
Atypical
Absence with special features
Mycoclonic absences
Eyelid myoclonia
Mycloclonic
Mycloclonic
Mycloclonic atonic
Mycloclonic tonic
Clonic
Tonic
Atonic
Focal seizures
Unknown
Epileptic spasms

1.1.4 Aetiology

In the revision of the 1989 ILAE classification, both focal and generalised epilepsy and syndromes were divided according to the aetiology into “idiopathic” (epilepsies not associated with a structural lesion, neurologic abnormalities or cognitive impairment), “symptomatic” (seizures as a consequence of a focal abnormality) and “cryptogenic” (symptomatic aetiology suspected but aetiology not known). Epilepsy may be caused by brain trauma, infections of the central nervous system (CNS), cerebrovascular disease or brain tumours. Other neuropathological lesions associated with chronic epilepsy include hippocampal sclerosis (HS) and malformations of the brain and will be discussed in the next chapter. The aetiology also varies according to age. Children and adolescents are more likely to have epilepsy of unknown or genetic origin. Onset of epilepsy during adult life is more commonly associated with an underlying neurological disorder.

The new 2010 ILAE classification takes recent understanding and knowledge in genomics, neuroimaging and neurophysiology into account. Therefore the new classification replaced the term “idiopathic” with the term “genetic”. The epilepsy must be a direct result of a known or presumed genetic defect and the seizures are a core symptom of the disorder. An example would be Dravet syndrome due to a mutation in the sodium channel, voltage gated, type 1, alpha subunit (SCN1A). The term “symptomatic” is replaced by the term “structural/metabolic”. To be classified in this category the epilepsy has to be associated with a structural lesion or metabolic disease that has been shown in previous studies to

substantially increase the risk of developing epilepsy. Examples of structural lesions include stroke, trauma, infection, tuberous sclerosis and malformations of cortical development. The term “cryptogenic” is replaced by the term “unknown cause” (Berg et al. 2010).

A well known issue in epilepsy is the occurrence of pharmacoresistance. The importance of this issue is illustrated by the fact that about 20-30% of all people with epilepsy have poorly controlled seizures, or their seizures are refractory to drug treatment (Regesta and Tanganelli, 1999). Not all forms of epilepsy have the same rate of pharmacoresistance. Because of the high risk of therapy resistance, together with its relatively high prevalence, most studies on pharmacoresistance in epilepsy have involved mesial temporal lobe epilepsy.

1.2 MESIAL TEMPORAL LOBE EPILEPSY

1.2.1 Introduction

Temporal lobe epilepsy (TLE) is the most common focal epilepsy. 60-70% of focal epilepsies are believed to originate from the temporal lobe. The seizures associated with temporal lobe epilepsy consist of focal seizures with and without loss of awareness. The most common cause of TLE in surgical series is hippocampal sclerosis (HS), which can be reliably detected in vivo by magnetic resonance imaging (MRI) (Lee et al. 1998). Structural damage in TLE associated with HS is a condition that characterises mesial temporal lobe epilepsy (mTLE). Such damage and dysfunction frequently extends beyond the hippocampus into the parahippocampal and entorhinal cortex (Bonilha et al.

2004). As reviewed by Engel , patients often have a history of complicated FS or other initial precipitating injuries, such as head trauma or intracerebral infections, within the first four or five years of their life (Engel 1996). There is also an increased prevalence of a family history of epilepsy. In the latter half of the first decade of life habitual seizures start to occur, which in most cases initially can be brought under control by pharmacotherapy. Subsequently, the seizures often remit for several years until adolescence or early childhood. After this latent period habitual complex partial seizures develop, which are mostly insensitive to medication. At this stage, about 60% of the patients become pharmacoresistant.

1.2.2 Hippocampal structures and connections

The hippocampal formation is located in the medial part of the temporal lobe, lying on the floor of the temporal horn of the lateral ventricle. The hippocampus is one of a group of structures forming the limbic system and is a part of the hippocampal formation. This also includes the dentate gyrus, subiculum, and entorhinal cortex. The limbic system has been shown to play a critical role in all aspects of emotions, fear, learning and memory (Geinisman 2000; Geinisman, Disterhoft et al. 2000; Cardinal, Parkinson et al. 2002). The hippocampus is a crescent-shaped structure and its resemblance to a seahorse prompted the use of its Greek-derived name. The hippocampus is divided into four Cornu Ammonis (CA) zones, labelled CA1 – CA4. Areas CA1 and CA3 are the largest and most easily identified (Figure 1). The principal neurons in the CA are pyramidal neurons (90%). The CA1 pyramidal neurons are the main output neurons of the hippocampus and their axons are glutamatergic (Sweatt 2009).

The axons of the CA1 neurons project predominantly to the ipsilateral and contralateral entorhinal cortices and to the contralateral hippocampus via the fornix. Secondary efferents of the CA1 pyramidal neurons via the subicular neurons also project to subcortical regions, including the ventral striatum and mamillary bodies. The major input to the hippocampus arises from the entorhinal cortex. This input is termed the perforant path. Axons of the perforant path arise principally in layers II and III of the entorhinal cortex, with minor contributions from the deeper layers IV and V (Sharma et al. 2007). Axons from layers II/IV project to the granule cells of the dentate gyrus and pyramidal cells of the CA3 region, while those from layers III/V project to the pyramidal cells of the CA1 and the subiculum.

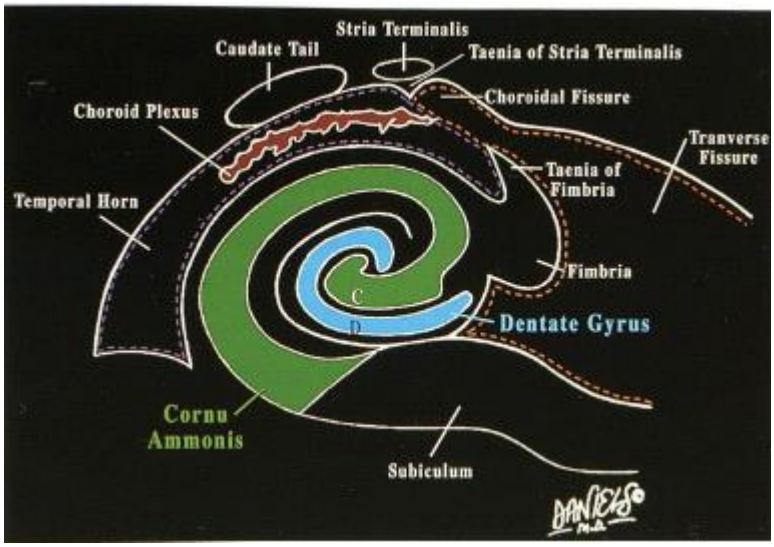

Figure 1: Structure of the hippocampus
The figure is from Mark et al. (Mark et al. 1993).

1.2.3 Hippocampal sclerosis

1.2.3.1 Neuropathology

Hippocampal sclerosis (HS) is the most common pathological finding in mesial temporal lobe epilepsy and found in approximately 70% of temporal lobe resections for pharmacoresistant partial seizures (Zentner et al. 1995). The presence of sclerosis is a good indicator for a positive outcome to surgery. Despite the strong association between HS and temporal lobe epilepsy, it remains unclear whether or not the relationship is causal-or if both conditions might reflect an underlying developmental abnormality of the hippocampus (Thom 2014). Macroscopically the hippocampus is firm and shrunken, sometimes with visible collapse of the CA1 subfield (Sommer's sector (Sommer 1880)). Microscopic findings include a characteristic pattern of neuronal loss and reactive gliosis. Under the general category of HS, several patterns have been recognised: 1) classical HS with neuronal loss in CA1 and the hilar region, 2) End-folium sclerosis or mesial temporal sclerosis type 3 (MTS type 3) with neuronal loss primarily in the hilar region, and 3) loss restricted to CA1 only (MTS type 2) (Thom et al 2011). Non-classical or atypical patterns of HS have been associated with poorer surgical outcomes than classical HS. Seizure free outcomes for MTS type 3 at one year are 25% to 28% compared to 66% to 77% for MTS type 2 and 72% to 84% for classical HS (Thom et al. 2010). In addition to neuronal loss and gliosis, there is also an associated mossy fibre sprouting, by which new axons arise from granular cells and extend upwards into the molecular layer of the dentate gyrus. It is thought that they may contribute to

epileptogenesis by forming potentially self-excitatory connection within the dentate gyrus. Additionally granular cell dispersion can be found with an increased width of the granular cell layer which is more than ten cells deep. However, these also occur on the opposite side and therefore may be a response to generalised seizure activity rather than signifying damage (Thom 2014).

1.2.3.2 Aetiology and pathogenesis

Animal models of limbic status epilepticus demonstrate hat HS can be acquired- and the pathological features in many cases are similar to those seen in humans (Coulter et al. 2002). MRI and post-mortem studies confirm that acute hippocampal damage may follow status epilepticus (Provenzale et al. 2008). A leading hypothesis suggests that an initial precipitating insult in childhood such as febrile convulsion may injure the hippocampus and that this “first hit” at a critical period of development may act as a template for progressive neuronal loss and gliosis (Thom 2009). The degree of vulnerability of hippocampal cells is most probably age dependant and is particularly prone to occur in the first years of life. Hippocampus sclerosis may then be seen as part of a scarring process which sooner or later leads to epileptic attacks. FS are the most common seizure disorders in childhood, occurring in 2-5% of children before the age of five years. The incidence of subsequent epilepsy is 2-8% (Baram et al. 2002). MRI studies in children with prolonged (>30 minutes) FS performed both in the acute stages (<48 hours after seizures) and chronic stages (4-8 months later) showed enlarged hippocampal volume and prolonged T2 relaxation time,

suggesting acute hippocampal oedema that resolves within several months of acute events (Scott et al. 2002). When seizures are prolonged maximum damage occurs at the seizure source. Although fever is the commonest provocation it is not the only potential stimulus and in both humans and animal models several epileptogenic stimuli cause the sequence of hippocampal followed by secondarily generalized seizures (Neville and Gindner 2010).

1.2.4 Clinical features of mTLE

Seizures take the form of focal seizures without (simple partial) and with loss of awareness (complex partial). Focal seizures (complex partial seizures) where patients loose awareness typically have gradual onset, slow evolution and last longer than most extra-temporal complex partial seizures (2-10 minutes) (Blair 2012). The typical complex partial seizure consists of three components discussed below.

1.2.4.1 Aura

Auras occur in approximately 80% of temporal lobe seizures (Ferrari-Marinho et al. 2012). They usually precede seizures with loss of awareness but can also occur in isolation. Speech usually ceases or is severely reduced, but repetitive vocalization may occur. If a patient has one seizure focus, the seizure semiology tends to be stereotyped. The most common aura is some type of visceral sensation such as nausea, butterflies, or a rising epigastric sensation (French et al. 1993). This may be accompanied by fear, and fear may exist alone as the second most common aura. Fear or anxiety is usually associated with seizures arising from the amygdala (Gloor et al. 1982). Other less common auras include

olfactory and gustatory hallucinations, alteration of visual perceptions (micropsia, macropsia), and distortions of memory (déjá vu, jamais vu). Olfactory sensations can signal the start of seizures in the Sylvian region or entorhinal cortex and visual illusions may be seen with seizures arising from the fusiform or the inferior temporal gyrus. Auditory hallucinations can consist of a buzzing sound, voices, or muffling of ambient sounds and occur if discharges arise from the superior temporal gyrus. Autonomic symptoms include alterations in heart rate, blood pressure, skin colour, pupil size, piloerection, and sweating (Panayiotopoulos 2005).

1.2.4.2 Motor arrest

Following the aura, a temporal lobe complex partial seizure begins with motor rest or absence (also called motionless stare). The patient stops ongoing activities and looks blank and stares. This is more common in mesial temporal lobe than extra-temporal lobe epilepsy (Shorvon 2010)

1.2.4.3 Automatisms

Automatisms are semi-purposeful involuntary motor activity occurring either in the course of, or after an epileptic seizure. Oroalimentary automatisms (eg, lip smacking, chewing, or swallowing), during which the patient is usually, but not always, unresponsive may be noted. Gestural automatisms, as well as reactive automatisms that can be ictal or postictal (or both), are commonly seen. A number of lateralizing features can occur (Kotagal et al. 1989; Williamson et al. 1998). When dystonic posturing occurs, it is contralateral to the side of seizure onset, whereas unilateral automatisms are ipsilateral (often in combination with

contralateral dystonic posturing). Head deviation early in the seizure is usually ipsilateral to the seizure focus, but head deviation late in the seizure is contralateral and often a prelude to generalization. Patients usually experience a postictal period of confusion and headache. Postictal aphasia suggests onset in the language-dominant temporal lobe. Post-ictal nose-rubbing is commonly seen in temporal lobe epilepsy and in 90% of cases is ipsilateral to the seizure focus. Amnesia is the rule for the blank spells and automatism but auras are often remembered. By definition, amnesia occurs during a complex partial seizure because of bilateral hemispheric involvement. The postictal phase may last for a longer period (several minutes). A complex partial seizure may evolve to a secondarily generalized tonic-clonic seizure but this is much less common (Panayiotopoulos 2005).

1.2.5 Electrophysiological features of mTLE

The human electroencephalogram (EEG) was discovered by the German psychiatrist, Hans Berger, in 1929. Its potential applications in epilepsy rapidly became clear, when Gibbs and colleagues in Boston demonstrated 3 per second spike wave discharged in what was then termed petit mal epilepsy. Electrical activity recorded by electrodes placed on the scalp or surface of the brain mostly reflects summation of excitatory and inhibitory post synaptic potentials in apical dendrites of pyramidal neurons in the more superficial layers of the cortex. Quite large areas of cortex, in the order of a few square centimetres, have to be activated synchronously to generate enough potential for changes to be registered at electrodes placed on the scalp. Mesial temporal

lobe epilepsy with unilateral hippocampus sclerosis shows anterior/mid temporal interictal spikes which are ipsilateral or predominate over the pathological temporal lobe (Smith 2005). In a third of patients the interictal discharges are present bilaterally during sleep. Strongly lateralised interictal discharges are predictive of side of seizure onset (Chung et al. 1991; Holmes et al. 1996). No definite EEG changes are usually seen with auras. Lateralized rhythmic 5-7 Hz ictal discharge accompanies a seizure in 80% of patients with mesial temporal lobe epilepsy. It typically occurs 10-40 seconds after clinical seizure onset. If present this activity correctly lateralises seizure onset in 95% of patients. Focal postictal slow activity is present in about 70% of seizures and if present is consistent with the side of seizure onset correctly in about 90% of patients (Verma and Radtke 2006).

1.2.6 Neuroimaging features of mTLE

1.2.6.1 MRI in mTLE

Modern neuroimaging and in particular MRI has revolutionised epilepsy surgery. The principal role of MRI imaging is to reveal cerebral lesions that might cause epilepsy as a clear-cut removal of a focal abnormality improves the chances of seizure freedom (Duncan 2010). Indeed, 70% of patients which have such lesions removed enter remission (Spencer and Huh 2008). High-resolution MRI at 1.5 T with tailored protocols might increase the yield of subtle lesions in surgical candidates by 30% relative to routine MRI (Wieshmann 2003).The ability of higher field magnets (3T) further increases the rate of detection of pathology in 20% of patients with refractory epilepsy and previously

unremarkable or inconclusive MRI (Duncan 2010). MRI in mTLE reliably detects HS with features such as unilateral hippocampal atrophy, decreased signal intensity seen on T1 and increased signal intensity on T2 (Jackson et al. 1990; Jackson et al. 1993). Hippocampal atrophy ipsilateral to EEG abnormalities is the most reliable predictor of seizure control following surgery with a specificity of 93% and a sensitivity of 83% (Lee et al. 1998). The presence of bilateral hippocampal disease is associated with poorer surgical outcome (Jack et al. 1992). Manual hippocampal volumetry can identify unilateral and bilateral hippocampal damage (Duncan 2010). These capabilities are important in the presurgical work up to identify subtle hippocampal damage and to ensure the other hippocampus is intact. Furthermore, automated hippocampal volume estimations have been developed (Hammers et al. 2007b; Bonilha et al. 2009; Chupin et al. 2009; Winston et al. 2013). Anatomic surface modelling of hippocampal atrophy also can identify abnormal hippocampal morphology that is not evident on conventional analysis (Hogan et al. 2008). The diffusity of water increases in the sclerotic hippocampus. Diffusion abnormalities have been found in hippocampi ipsilateral to the seizure onset that are normal on conventional MRI, suggesting that diffusion MRI might be more sensitive than standard structural MRI (Wehner et al. 2007).

Other quantitative techniques have shown unilateral high T2 relaxometry to be a useful identifier of hippocampal histopathology and to correlate with the severity of atrophy (Jackson et al. 1993). Abnormal T2 signal is seen in the contralateral hippocampus in 30%-40%. T2 relaxometry is also a sensitive measure of

amygdala pathology. Single voxel proton magnetic resonance spectroscopy as well as magnetic resonance spectroscopic imaging have demonstrated a reduction in temporal lobe N-acetylaspartate to choline plus creatine ratios in up to 75% of mTLE patients, correctly lateralizing in 55%. Bilateral abnormalities, however, have been reported using magnetic resonance spectroscopic imaging techniques in 45% of mTLE patients (Cendes et al. 1997; Li et al. 2000; Thom et al. 2010). It is unclear whether spectroscopy aids in the prediction of seizure freedom following surgery (Kuzniecky et al. 1999; Li et al. 2000). Functional MRI is used for language lateralisation and localisation (Binder et al. 1997; Koepp 2014).

1.2.6.2 Functional neuroimaging with PET and SPECT in mTLE

Positron emission tomography (PET) and single photon emission computed tomography (SPECT) are imaging techniques that can study CNS function in vivo. Thereby a radionuclide is synthetically introduced into a molecule of biological relevance and administered to a patient or animal. PET and SPECT cameras monitor the distribution of these radiotracers over time. In PET the radioisotope undergoes positron decay and emits a positron, which interacts with an electron in situ, producing a pair of annihilation photons moving in approximately opposite directions which can be detected outside the body by a PET camera (Sawle, 1995). In contrast with PET, the radiotracers used in SPECT emit a single photon (gamma ray) that is detected directly using collimators. By detecting photons "coincident" in time, PET provides more radiation event localization information and, thus, higher resolution images than

SPECT. Therefore the great advantage of PET over SPECT is a higher sensitivity, better temporal and spatial resolution and ability to provide a quantitative measure of radioactivity in tissues.

1.2.6.2.1 PET in mTLE

PET scanning was first applied to clinical epilepsy in the mid-1970s, the first published report was in 1978 (Kuhl et al. 1978). In 1984 Engel reviewed the clinical work accrued to that date. PET has the potential in differentiating clinical syndromes and elucidating epileptogenic mechanisms (Engel 1984). Initially 13N-labeled ammonia and fluorine-18 fluorodeoxy-glucose (^{18}FDG) were used, and still today ^{18}FDG remains the most common tracer employed in epilepsy (Shorvon 2009).

1.2.6.2.1.1 Glucose metabolism with ^{18}FDG in mTLE

.^{18}FDG measures glucose metabolism as an indirect marker of neuronal activity. Interictal hypometabolism at the ictal focus has been shown to be useful for the localisation of the epileptic zone. ^{18}FDG has a sensivity of 70-85% in patients with mTLE (Ryvlin et al. 1998; Won et al. 1999). However, in patients with extra-TLE the diagnostic sensivity is significantly lower: between 30-60% depending on the seizure focus (La Fougère et al. 2009). In particular ^{18}FDG is of value in selecting patients for temporal lobeectomy and for identifying epileptogenic areas in MRI-negative temporal lobe epilepsy, where PET correctly localises the lesion in 80% of cases (Won et al. 1999). In mTLE, focal hypometabolism ipsilateral to the lobe to be resected is a predictor of a good surgical outcome (Willmann et al. 2007). Among patients with mTLE, those who were seizure free

after temporal lobe resection were shown to have a greater proportion of the hypometabolic area resected than did individuals who continued with seizures (Vinton et al. 2007). This finding raises the possibility of tailoring the extent of resection according to the area of hypometabolism (Duncan 2010). Additionally ^{18}FDG often has a wider distribution than that of the seizure focus. For example many patients with mTLE present with an additional pronounced hypometabolism of the frontal lobe, which may represent inhibitory phenomena induced by the epileptogenic focus (La Fougère et al. 2009). Similarly networks of hypometabolism had some correlation with patterns of EEG spread of ictal activity. Hypometabolism has been noted in the thalamus or in the insular cortex and putamen associated with dystonic limb posturing in the ictus (Lee et al. 2009).

1.2.6.2.2 SPECT in mTLE

SPECT scanning was tried in the early 1980s initially using 123I isopropyl amphetamine or 133XE (Shorvon 2009). Soon iodine isotopes were replaced by radioactive technetium 99mTC-HMPAO administered by intravenous injection. 99mTc-HMPAO SPECT is used to image directly the regional increase in cerebral blood flow that occurs during an epileptic seizure, and thus to directly image the epileptic focus. The injection can be given during the seizure and the scan recorded in the subsequent three hours. This is a major advantage, as it does not require the patient to have a seizure in the scanner and the ictal image can be acquired at some time after the seizure is resolved. SPECT is a complementary rather than competing technology to PET. Ictal SPECT is

superior to interictal SPECT for the identification of the location or the lateralisation of epileptic seizures in mTLE, indicating sensitivities between 73-97% for ictal and only 50% for interictal SPECT (Devous, Thisted et al. 1998; Spanaki, Spencer et al. 1999; Zaknun, Bal et al. 2008). Cortical and subcortical changes in regional cerebral blood flow during seizures may begin with hyperperfusion in the epileptic zone follow by rapid extension to other regions through seizure spread and generalisation. If ictal injection is made within the first 30s of temporal lobe seizures onset, it reportedly shows diffuse temporal lobe hyperperfusion in 100% of patients but the longer the delay the lower the sensitivity (Van Paesschen 2004). A great advance of SPECT to improve the ability to detect and define the extent of epileptogenic lesions is the subtraction of ictal and interictal SPECT which should preferably be co-registered to MRI (O'Brien et al. 1999).

1.2.7 Epilepsy surgery in mTLE

Epilepsy is resistant to treatment in one third of patients. The effects of chronic uncontrolled epilepsy and multidrug therapy include progressive cognitive and behavioural decline as well as increased accident and death rates (Cascino 1990; Silfvenius 1999). In carefully selected patients, epilepsy surgery can control seizures, improve quality of life, and reduce the costs of medical care (Kuzniecky and Devinsky 2007). Surgical intervention is an appropriate consideration for 3% of people who develop epilepsy (Duncan 2011). Every year, for every 50 million people in the developed world 1000 individuals with refractory epilepsy are estimated to require evaluation for epilepsy surgery, with

50% of such patients proceeding to surgery (Lhatoo et al. 2003). Furthermore for each 50 million people a backlog exists of 5000 patients who would benefit from surgery (Lhatoo et al. 2003; Cascino 2008). Localisation-related seizures of temporal lobe origin have been considered to most likely benefit from surgery. In a randomised, controlled intention-to-treat trial including 80 patients, the 40 patients who had temporal lobe epilepsy surgery had a 58% chance of freedom form disabling seizures compared with 8% of patients who continued medical therapy ($p<0.001$) (Wiebe et al. 2001). The goal of epilepsy surgery is complete removal of the epileptogenic area without causing a permanent neurological deficit. Several different diagnostic techniques can be used to determine the ictal generator and epileptogenic zone. Structural and functional imaging, neurophysiological techniques and psychological testing help to identify the seizure focus and will be discussed in the paragraphs below. Even though there might be a high chance of seizure freedom, the risks and benefit of epilepsy surgery vary for each individual patient. Epilepsy surgery may be divided into two major categories: resective and functional. In adults, the most common surgical procedure for mTLE involves the medial temporal lobe—either an amygdalohippocampectomy (resection of the amygdala, hippocampal head and body, and adjacent parahippocampal gyrus) or an anteromedial temporal resection that also includes resection of the anterior, inferior, and middle temporal gyri (3-4 cm from the temporal tip) (Al-Otaibi et al. 2012).

1.2.7.1 Presurgical evaluation

A key aim of pre-surgical evaluation is to determine the epileptogenic zone and the relationship of this zone to eloquent areas of the brain. No single pre-operative investigation can determine the epileptogenic zone with complete reliability and when various investigation modalities are combined there may be variable degree of congruence (Rosenow and Lüders 2001).

1.2.7.2 Clinical history and seizure pattern

Neurological history and examination are carried out to identify any underlying disorder and to localise dysfunctional areas. Examination can also provide localizing features. Patients' history can also give information that may inform the odds of success, including patient age, age of epilepsy onset, epilepsy duration, the occurrence of secondary generalised seizures and status epilepticus and antecedent history, including the presence of head injuries, meningitis or FS.

1.2.7.3 Electrophysiology

Interictal and ictal scalp EEG recordings are critical determinants of surgical candidacy. Recordings of multiple seizures are required in some patients, especially when functional (e.g. interictal EEG) or imaging (e.g. MRI) data suggest more than one seizure focus (Kuzniecky and Devinsky 2007). Focal interictal abnormalities and concordant ictal EEG and behavioural changes during seizures can provide sufficient localisation for surgical intervention. However, identification of a structural abnormality consistent with electrophysiological data is desirable before surgery. An intracranial EEG

recording with seizure monitoring may be useful when the exact localisation of the epileptogenic zone is not conclusive enough from non-invasive evaluation (Zumsteg and Wieser 2000). The type of intracranial recording depends on the suspected pathophysiological substrate of the epilepsy and its location.

1.2.7.4 Neuroimaging

Modern neuroimaging and in particular MRI has revolutionised epilepsy surgery. The principal role of imaging is to reveal cerebral lesions that might cause epilepsy as a clear-cut removal of a focal abnormality improves the chances of seizure freedom (Duncan 2010). Indeed, 70% of patients which have such lesions removed enter remission (Spencer and Huh 2008). High-resolution MRI at 1.5 T with tailored protocols might increase the yield of subtle lesions in surgical candidates by 30% relative to routine MRI (Wieshmann 2003). The ability of higher field magnets (3T) further increases the rate of detection of pathology in 20% of patients with refractory epilepsy and previously unremarkable or inconclusive MRI (Duncan 2010). Nuclear medicine studies with ^{18}FDG-PET is highly sensitive for mTLE but its yield is low in extra-temporal TLE. It is in particular valuable when MRI is normal. Interictal SPECT has lower sensivity for localisation than does ^{18}FDG-PET (Rathore et al. 2014). But ictal SPECT can provide unique localisation data in patients with normal MRI or multiple lesions. Functional MRI is used for language lateralisation and localisation (Wehner and Lüders 2008). Magnetoenephalography can localise interictal epileptiform discharge and has a high correlation with intracranial ictal localisation (Knowlton et al. 1997).

1.2.7.5 Neuropsychology testing

Neuropsychological tests traditionally assess function in five cognitive domains, all of which can dissociate in the pathological brain. These are intelligence, language, memory, perception and executive or frontal lobe functions. In conjunction with MRI and other presurgical investigations, neuropsychological scores are used to asses s the suitability of patients for epilepsy surgery and can be used to predict post-operative outcome, in terms of cognitive change and seizure control (Baxendale and Thompson 2010). Neuropsychological assessment has an important role in evaluating candidates for temporal lobe surgery since the temporal lobe has long been implicated in memory function. Bilateral hippocampal excision is associated with profound anterograde amnesia. Unilateral resections are traditionally associated with material-specific memory dysfunction. The traditional view is that the dominant temporal lobe (usually left) is important for verbal memory processing and the non-dominant temporal lobe (usually the right) for non-verbal or visual processing (McAndrews and Cohn 2012). Neuropsychological performance has been related to surgical outcome. Patients with more focal neuropsychological deficits and less overall cognitive impairment should be expected to have better outcomes with respect to seizure frequency, given the absence of evidence of dysfunction extending beyond the resection zone (Wendling et al. 2013; Jutila et al. 2014). Patients at high risk of significant memory decline can be counselled pre-operatively and can be trained in compensatory strategies prior to the surgery when appropriate (Baxendale and Thompson 2010).

1.2.7.6 Outcome of surgery

The outcome of surgery should be measured not only in terms of seizure freedom, but also in terms of neuropsychology, neurological deficits, psychosocial adjustments and quality of life. The fraction of epileptogenic tissue removed is a major determinate of seizure outcome. Temporal lobe surgery results in approximately 70% of patients becoming seizure –free in the first two to three years after surgery, and a further 20% are improved. The overall mortality of temporal lobectomy is less than 0.5% and the risk of permanent hemiparesis is less than 1%. A transient hemiparesis can occur in up to 5% (Téllez-Zenteno et al. 2005). Memory problems and visual field defects that prevent driving can occur in up to 5% of those undergoing mesial temporal lobe resection (Georgiadis et al. 2013). Psychosis and depression are not uncommon following temporal lobe resection and most patients should be warned of the possibility of these following the surgery (Cleary et al. 2013a; Cleary et al. 2013b). In comparison, best medical therapies over a similar period yield a 5% chance of becoming seizure free and a 0.5 to 1.0% chance of death per a year from epilepsy (Wiebe et al. 2001). Hence surgery is a highly effective treatment for patients with medically refractory mTLE (Thom et al. 2010).

On the other hand one third of patients continue with seizures after surgical therapy. At the moment it is not clear why some patients fail to become or remain seizure-free after surgery. Recurrence of seizures in the first year following surgery is a predictor of poor outcome and may suggest that the epileptogenic zone has not completely been removed. There is an association

between the volume of tissue removed and seizure freedom following surgery (Siegel et al. 1990). Reports of patients who failed the first mesial temporal resection have shown significant improvement in outcome with an extension of the amount of mesial temporal tissue removed (Germano et al. 1994). The extent of the hippocampal resection itself has been shown to influence seizure free outcome with the resection that extends more posteriorly having a significantly greater proportion of patients who become seizure free (Wyler et al. 1995). Observations suggest that, despite early seizure control after surgery, tissue beyond the hippocampus and parahippocampal complex may be capable of generating seizures and that the seizure onset zone may involve the entire mesial temporal lobe (Thom et al. 2010).

CHAPTER II PHARMACORESISTANCE IN EPILEPSY

2.1 PHARMACORESISTANT EPILEPSY

2.1.1 Definition of pharmacoresistant epilepsy

The concept of pharmacoresistant epilepsy seems to be self-explanatory, but for some years a universally agreed definition remained elusive. In 2010 the International League against Epilepsy suggested that pharmacoresistant epilepsy be defined as failure of adequate response to two tolerated and appropriately prescribed AED schedules (whether as monotherapies or in combination) to achieve sustained seizure freedom (Kwan et al., 2010).

2.1.2 Seizure-freedom

The International League Against Epilepsy defined seizure freedom as absence of seizures for at least three times the longest preintervention interseizure interval in the previous year (Kwan et al., 2010).

2.1.3 Remitting-relapsing epilepsy

There is an intermediate pattern of pharmacoresistance, although there is no universally agreed definition for this condition. Bilevicus et al. (Bilevicius et al. 2010) define the intermediate seizure pattern as present if a patient still experiences occasional seizures despite adequate AED regimen, which had led to at least two periods of at least one year of being seizure free. On the other hand Neligan et al. (Neligan et al. 2011) defined seizures as intermittent when there was at least one previous period of remission of two years or more since seizure onset had occurred.

2.1.4 Neurobiological hypotheses for pharmacoresistance in epilepsy

There are several hypotheses that explain the mechanisms associated with pharmacoresistance in epilepsy. Current theories on the causes of drug resistance in epilepsy include the transporter hypothesis, the target hypothesis, the network hypothesis, the gene variant/methylation hypothesis and the intrinsic severity hypothesis. However, none of these hypotheses is currently a stand-alone theory that is able to convincingly explain how drug resistance arises in human epilepsy (Löscher et al. 2013).

2.1.4.1 The transporter hypothesis

The drug transporter hypothesis proposes that pharmacoresistance is related to increased expression of multidrug efflux transporter proteins such as Pgp. These proteins are thought to prevent AED entry by actively extruding AEDs from their target site (Sisodiya et al., 2002). Multidrug efflux transporters are highly expressed in capillary endothelial cells and astrocytic foot processes that form the BBB. They limit intracellular concentration of substrates by pumping them out of the cell through an active energy-dependant mechanism. Pgp (encoded by the adenosine triphosphate (ATP)-binding cassette subfamily B member 1 gene (ABCB1) was discovered more than thirty years ago (Juliano and Ling, 1976) and it is the multidrug efflux transporter protein we know most about in terms of its structure and mechanism. Epilepsy was the first CNS disorder for which pharmacoresistance was associated with enhanced expression of Pgp in the brain (Tishler et al., 1995). Pathologically elevated expression of Pgp has been found in resected brain tissue of patients with

pharmacoresistant mTLE undergoing surgery (Sisodiya et al., 2002) as well as in limbic brain regions of mouse and rat models of mTLE (Löscher and Potschka, 2005). It is currently not clear whether the endothelial and parenchymal overexpression of Pgp is a consequence of epilepsy, of uncontrolled seizures, of chronic treatment with AEDs, or is constitutive, i.e. present before the onset of epilepsy (Löscher and Potschka, 2005).

2.1.4.2 The target hypothesis

According to the target hypothesis, epilepsy pharmacoresistance occurs when intrinsic (genetic) or acquired (disease related) changes in drug targets make them less sensitive to AEDs (Schmidt and Löscher 2009). Two studies have provided evidence of reduced sensivity to carbamazepine in brain tissue from patients who were pharmacoresistant to carbamazepine and underwent resective surgery (Remy et al. 2003; Jandová et al. 2006). Since the carbamazepine was applied directly to the brain slices in these experiments circumventing the BBB and any transporter effects, reduced sensivity is presumably due to altered target sensivity. Both studies are restricted to carbamazepine only and it is unknown whether pharmacodynamic insensitivity in these tissues extended to AEDs with different mechanisms of action. The acquired version of the target hypothesis proposes that the pharmacodynamic sensivity of the AED target is modified by the disease state. For example there is a loss in benzodiazepine sensivity in a rat model of mTLE resulting from alterations in the subunit composition of the neurotransmitter gamma-aminobutyric acid $(GABA)_A$ receptors, which are the molecular target of

benzodiazepines (Brooks-Kayal et al. 1998). The $GABA_A$ receptor subunit composition can change in response to prolonged seizure activity, and pronounced inter-individual differences have been reported in human epileptic tissue (Loup et al. 2009). In addition, the consequences of $GABA_A$ receptor activation depend largely on chloride homeostasis and its modulation by chloride transporters. Changes in the expression rate of chloride transporters described in the epileptic brain can result in outward chloride fluxes mediating depolarization and excitation instead of hyperpolarization and inhibition (Deisz 2002). AEDs promoting $GABA_A$ -receptor mediated neurotransmission might lose their efficacy under these circumstances (Potschka 2013).

2.1.4.3 The inherent severity model of epilepsy

The inherent severity model of epilepsy suggests that there is a continuum in severity of the disease, which determines its relative response to medication (Rogawski and Johnson, 2008). Prospective studies of outcome in populations of patients with newly treated epilepsy have consistently shown that the single most important factor associated with the chance of remission of seizures is the frequency of seizures in the early phase of epilepsy, with an association between increased number of seizures in this period and poorer outcome. In a hospital-based, prospective cohort, patients with eleven or more seizures before treatment were more than twice as likely to be pharmacoresistant to their AEDs than patients with two or fewer seizures pre-treatment, independent of the time from the first seizure to starting treatment (Mohanraj and Brodie, 2006). Interestingly the same observation has been made in a chronic rodent model

where epilepsy with spontaneous recurrent seizures was induced by status epilepticus. Frequency of spontaneous recurrent seizures was determined by video-electroencephalography in a total of 33 epileptic rats before onset of treatment with phenobarbital. Thirteen (39%) rats did not respond to treatment with phenobarbital. Before treatment, average seizure frequency in non-responders was significantly higher than seizure frequency in responders, which, however, was due to six non-responders that exhibited more than three seizures per day. Such high seizure frequency was not observed in responders, demonstrating that high seizure frequency predicts pharmacoresistance in this model, but does not occur in all non-responders (Löscher and Brandt 2010).

2.1.4.4 The network hypothesis

According to this hypothesis, structural brain alterations and/or network changes (for example, hippocampal sclerosis) are involved in resistance to AEDs. The network hypothesis suggests that recurring episodes of excessive neuronal activity (i.e. seizures) induce structural changes and alterations of brain plasticity including axonal sprouting, synaptic reorganization, neurogenesis, and gliosis which contribute to the formation of abnormal neural networks. This in turn leads to loss of the inhibitory effect of the endogenous antiepileptic system and prevents AEDs from entering their targets, eventually leading to pharmacoresistance (Banerjee et al. 2014). Intractability to currently available AEDs may reveal the fact that there are many mechanisms for seizure generation in a given patient, and if one is inhibited other mechanisms still exist. The alterations of brain plasticity including axonal sprouting, synaptic

reorganization, neurogenesis and gliosis would not be the etiological factors, but rather adaptive changes in response to seizures. However, poorly controlled seizures may induce progressive alterations of brain plasticity, eventually forming aberrant neural network and causing pharmacoresistance. Thus, the formation of aberrant neural network may be a potential contributing and etiological factor for pharmacoresistant epilepsy (Fang et al. 2011).

2.1.4.5 The gene variant hypothesis/methylation hypothesis

The fifth hypothesis is the gene variant or methylation hypothesis, which suggests that there is an inherent resistance that is governed by genetic variants of proteins that are involved in the pharmacokinetics and pharmacodynamics of AED activity. The methylation hypothesis indicates that seizures are associated to long-lasting epigenetic mechanisms such as acetylation, methylation, phosphorylation, ubiquitination of DNA and alterations in multidrug transporter molecules that contribute to the development of pharmacoresistance in epilepsy Recently Kobow et al. (Kobow et al. 2013) discussed the potential role of epigenetic alterations as an underlying pathogenic process of pharmacoresistance in epilepsy. Epigenetic regulation is a key mechanism to define the versatile activity states of a gene, whereby a set of chromatin-modifying actions leads to a change in genetic activity, without affecting DNA sequence itself. These biochemical cascades and signals have been shown to play a major role in various pathologic conditions, including cancer and cancer-related drug resistance. It has also been shown that seizures induce epigenetic changes in the hippocampus in experimental TLE models (Huang et al. 2002)

and in human TLE specimens compared to controls (Kobow et al. 2009) suggesting a pathophysiological impact of promoter methylation in human epilepsies. Additionally, it has been demonstrated that targeting a single molecular entity that modulates multiple molecular pathways by transcriptional repressors, such as neuron-restrictive silencer factor (NRSF; also known as REST), or via epigenetic mechanisms, offers new strategies for epilepsy therapies (McClelland et al. 2011; Kobow et al. 2013; Kullmann et al. 2014).

Still, none of the prevailing pharmacological hypotheses is able to fully explain the neurobiological basis for pharmacoresistance and most of the experimental data suggest that multifactorial rather than single alterations underlie pharmacoresistance (Schmidt and Löscher 2009).

2.2 BACKGROUND TRANSPORTER HYPOTHESIS

The discussion regarding a putative contribution of efflux transporters to drug resistance has been initiated by a study reporting overexpression of the BBB transporter Pgp in human epileptic tissue from patients with pharmacoresistant epilepsy (Tishler et al., 1995). The transporter hypothesis has gained interest in recent years, because if true, it would allow overcoming drug resistance by either inhibiting or bypassing Pgp or other involved efflux transporters (Hughes 2008; Löscher and Langer 2010).

2.2.1 Blood-brain barrier

The blood-brain barrier (BBB) is a physical and metabolic barrier between the brain and the systemic circulation (Pardridge 1999). The BBB is composed of a monolayer of brain capillary endothelial cells. Unlike capillaries in other parts of the body, the cerebral capillaries are joined by tight junctions, which restrict solute flux between the blood and the brain. The brain capillary endothelial cells are surrounded by extracellular matrix, pericytes, and astrocyte foot processes (Loescher and Potschka 2005). Circulating molecules gain access to the brain via one of two processes: 1) lipid-mediated transport of small nonpolar molecules through the BBB by free (passive) diffusion, or 2) catalyzed transport (Pardridge 1999; Loescher and Potschka 2005).

The endothelial cells of the BBB contain numerous membrane transporters involved in the influx and efflux of essential substrates (Lee et al. 2001). ABC efflux transporters, such as Pgp, at the BBB limit the brain uptake of a variety of therapeutic agents, including compounds that are relatively lipophilic and would

be predicted to permeate the endothelial lining of the brain microvasculature (Golden and Pollack 2003). Pgp is located at the luminal (apical = blood-facing side) membrane of endothelial cells (Beaulieu et al. 1997; Schinkel and Jonker 2003). Thus, Pgp substrates entering the endothelial cells from the blood are immediately pumped back into the blood. As a consequence, the net penetration of substrate compounds from the blood into the brain tissue can be dramatically decreased. In the absence of Pgp in the BBB, the brain penetration of Pgp substrate drugs can increase up to ten - to 100-fold, with sometimes dramatic consequences for the toxicity of compounds (Schinkel and Jonker 2003). Furthermore, blockade of BBB Pgp by cerebral application of Pgp inhibitors significantly increases the brain concentration of various drugs, again being in line with Pgp functioning as an efflux transporter in the BBB (Löscher and Potschka 2005a).

Clear expression of Pgp in astrocytes is especially seen in certain pathological states such as epilepsy (Sisodiya 2003).

In contrast to Pgp, data on the other ABC transporters in the BBB are much more limited (Schinkel and Jonker 2003). At least six multidrug resistant proteins (MRP) (MRP1-6) are expressed at the BBB of different species (Begley 2004). However, the exact subcelluar localization (apical vs basolateral) of most of these MRPs in brain capillary endothelial cells remains to be determined (Löscher and Potschka 2005).

2.2.2 Blood-cerebrospinal-fluid barrier

There is a shift in the appreciation of the contribution of the blood-cerebrospinal-fluid (CSF) barrier to the drug transport between blood and brain. Several drug efflux transporters are present in epithelial cells of the blood-CSF barrier. However, in contrast to the BBB, the exact functional role of efflux transporters in these other brain barrier is less well understood (Löscher and Potschka 2005a). The blood-CSF barrier is located at the choroid plexus (CP) and the outer arachnoid membrane. The blood- CSF barrier plays a vital role in the selectivity and permeability of the CP membrane to various nutrients and xenobiotics (Lee et al. 2001). The CP, which is the main source for CSF production, is a leaf-like highly vascular organ that projects into the ventricles of the brain and functions as a highly regulated solute- and drug-permeability barrier. The apical surface area has a same size range as the luminal surface area of the endothelial cells of the BBB, thereby providing a similarly large surface for solute exchange (Löscher and Potschka 2005a). The CP is comprised of fenestrated, highly permeable capillaries at the blood side that are surrounded by stroma and a monolayer of epithelial cells that face the CSF and are joined together by tight junctions (Lee et al. 2001). Once a solute or drug has crossed the capillary wall, it must penetrate the epithelial cells before entering the CSF (Löscher and Potschka 2005a).

The molecular identity and localization of the proteins responsible for the influx and efflux of drugs and metabolites at the CP are currently explored. Transport of drugs and metabolites involves mainly the solute carrier and ABC transporters

(Lee et al. 2001; Ghersi-Egea and Strazielle 2002; De Lange 2004). Rao et al. (Rao et al. 1999) first described the expression of Pgp and MRP1 in the epithelia of the CP and their contribution in a bipolar permeation barrier for selected drugs crossing the blood-CSF barrier (Löscher and Potschka 2005a). It was concluded that Pgp localizes sub-apically at the CP with transport into the direction of CSF, whereas MRP1 localizes basolaterally, conferring transport to the blood side of epithelial cells (Rao et al. 1999). Thus, in the choroidal epithelium, Pgp and MRP1 seem to have opposing drug-transport functions. The basolateral localization of MRP1 at the CP epithelium was subsequently confirmed by other groups (Wijnholds et al. 2000). However, in general, the role of these and other drug transporters in blood-CSF barrier function is only incompletely understood and more studies need to be done (Löscher and Potschka 2005a).

2.2.3 ABC transporters: function and role in pharmacoresistance

Active drug efflux transporters of the ATP binding cassette (ABC)-containing family of proteins have a major impact on the pharmacological behaviour of most of the drugs in use today. The penetration of drugs into a range of important pharmacological sanctuaries, such as brain, testis, and fetus, and the penetration into specific cell- and tissue compartments can be extensively limited by ABC transporters (Schinkel 1999; Schinkel and Jonker 2003). ABC transporters are expressed in many tissues including the intestine, liver, kidney, brain and they maintain chemical homeostasis by mediating the transport of molecules across a membrane irrespective of concentration gradient. These transporters are encoded by 49 genes in the human genome and have been

grouped into seven subfamilies (designated ABCA-ABCG) based on sequence homology (Dean et al. 2001; Gottesman et al. 2002; Szakacs et al. 2006). ABC transporters in their functional form comprise a minimum of four core domains that form the permeation pathway for transport of substrates, and two nucleotide binding domains that hydrolyze adenosine triphosphate (ATP) to power this process. Resistance to treatment by multiple drugs has been associated with the expression of ABC transporters in the target tissue. Three ABC proteins appear to account for most observed multidrug resistance (MDR) in humans and rodents (Sharom 2008); P-glycoprotein (Pgp/MDR1/ABCB1), MDR-associated protein (MRP)1 (ABCC1) and breast cancer resistance protein ABCG2 (variously known as BCRP, ABCP for its high expression in placenta or MXR for mitoxantrone resistance) (Litman et al. 2001). I will focus on these three most important multidrug transporters; however the family of mammalian ABC transporters is far more extensive and functionally highly diverse (Jones and George 2004).

2.2.3.1 P-glycoprotein

Pgp was discovered more than 30 years ago (Juliano and Ling 1976) and it is the ABC protein we know most about in terms of its structure and mechanism. Pgp is generally expressed at higher levels in epithelial cell surfaces throughout the body. It is found exclusively at the apical surface of cells in the kidney proximal tubule, canalicular membrane of hepatocytes, pancreas, the villous membrane of the small and large intestine and the adrenal gland (Thiebaut et al. 1987; Croop et al. 1989). Pgp is also located in blood-tissue barriers, including

the placenta and endometrium, blood-inner ear barrier, blood-mammary tissue barrier, blood-testis barrier, blood-nerve barrier, blood- brain barrier (where it is exclusively oriented to transport substrates toward blood) and epithelial cells of the blood-CSF barrier (Rao et al. 1999; Eckford and Sharom 2009). Pgp either restricts drug-entry to the body via the gastrointestinal tract and excretes metabolites into the urine or gastrointestinal tract or prevents their access from the blood to the fetus and sensitive organs such as the brain and testis (Eckford and Sharom 2009).

Pgp is a phosphorylated glycoprotein with an apparent molecular weight of 170kDA (Löscher and Potschka 2005a). There are two types of human Pgp: type I, encoded by the MDR 1 gene (ABCB1), which confers the drug resistance phenotype and promotes drug efflux at the blood-brain barrier, and type II, encoded by (ABCB2), present in the canalicular membrane of hepatocytes and functioning as phosphatidylcholine translocase (Demeule et al. 2002). The MDR1 gene in humans is located on chromosome seven and has 28 exons (Fromm 2004). Structurally the transporter consists of two interwoven transmembrane regions, each containing six transmembrane helices and an ATP-binding site located intracellularly. The transmembrane helices of Pgp allow it to bind and induce efflux of a broad range of substrates with varying affinities (Ambudkar et al. 1999). Although substrates for Pgp tend to be hydrophobic or weak base molecules with a planar ring system, Pgp is considered polyspecific because it can recognize a wide range of substrates including antiarrhythmics,

antihistamines, cholesterol-lowering statins and human immunodeficiency virus protease inhibitors ((Gottesman et al. 2002), Figure 2).

2.2.3.2 Multidrug resistance protein

The multidrug resistance protein (MRP) 1 was discovered in 1992 by Cole (Cole et al. 1992) and co-workers and the MRP family of proteins comprised nine characterized members (MRP1-9) also named ABCC1-6 and 10-12, respectively. Among MRP proteins, MRP1 is the most studied and like Pgp, MRP1 is an ATP-dependent transporter. It is expressed at low levels throughout many normal tissues and cell types in the body, but it is more highly expressed in the adrenal gland, bladder, CP, colon, erythrocytes, kidney, lung, placenta, spleen, stomach, testis, helper T-cells and muscle (both skeletal and cardiac) (Eckford and Sharom 2009). In contrast to Pgp and MRP2, it is localized on the basolateral membranes in polarized cells (Evers et al. 1996). The basolateral localization of MRP1 serves to protect sensitive tissues. For example, basolateral expression of MRP1 in the CP allows the protein to transport drugs from the cerebrospinal fluid to the blood to protect sensitive nervous tissues (Rao et al. 1999). MRP1 is a 190-kDa protein containing 1531 amino acids and its cognate gene is located on chromosome 16p13.11 (Conseil et al. 2005). MRP1 functions mainly as a co-transporter of amphipathic organic anions. It can transport hydrophobic drugs or other compounds that are conjugated or complexed to the anionic tripeptide glutathione, glucuronic acid, or to sulfate (Schinkel and Jonker 2003), Figure 2).

2.2.3.3 Breast cancer resistance protein

In the early 1990s several groups began reporting non-Pgp, non-MRP1-mediated pharmacoresistance in a variety of drug selected cell lines (Nakagawa et al. 1992 ; Kellner et al. 1997). The gene responsible for the novel phenotype was first cloned by Doyle and colleagues from a breast cancer cell line and was therefore called BCRP for breast cancer resistance protein (Doyle et al. 1998). Like Pgp, the breast cancer resistance protein (BCRP) is also localized to the apical face of polarized membranes. It is found in epithelial cells of the intestine, human placenta syncytiotrophoblasts, liver bile canaliculi, prostate, brain, lobules and lactiferous ducts of the mammary gland, and renal tubules, as well as the endothelium of veins and capillaries, including those at the blood-brain barrier and the placenta (Doyle et al. 1998; Eckford and Sharom 2009). Based on messenger ribonucleic acid (mRNA) analysis ABCG2 was more strongly expressed at the BBB than Pgp or MRP1 (Eisenblätter et al. 2003).

The tissue distribution of BCRP shows extensive overlap with that of Pgp, suggesting that it might have a similar role as Pgp in the pharmacological handling of substrate drugs. It appears to transport both positively and negatively charged drugs, including sulfate conjugates and the list of its substrates is rapidly expanding, highlighting the importance of this protein (Sharom 2008), Figure 2).

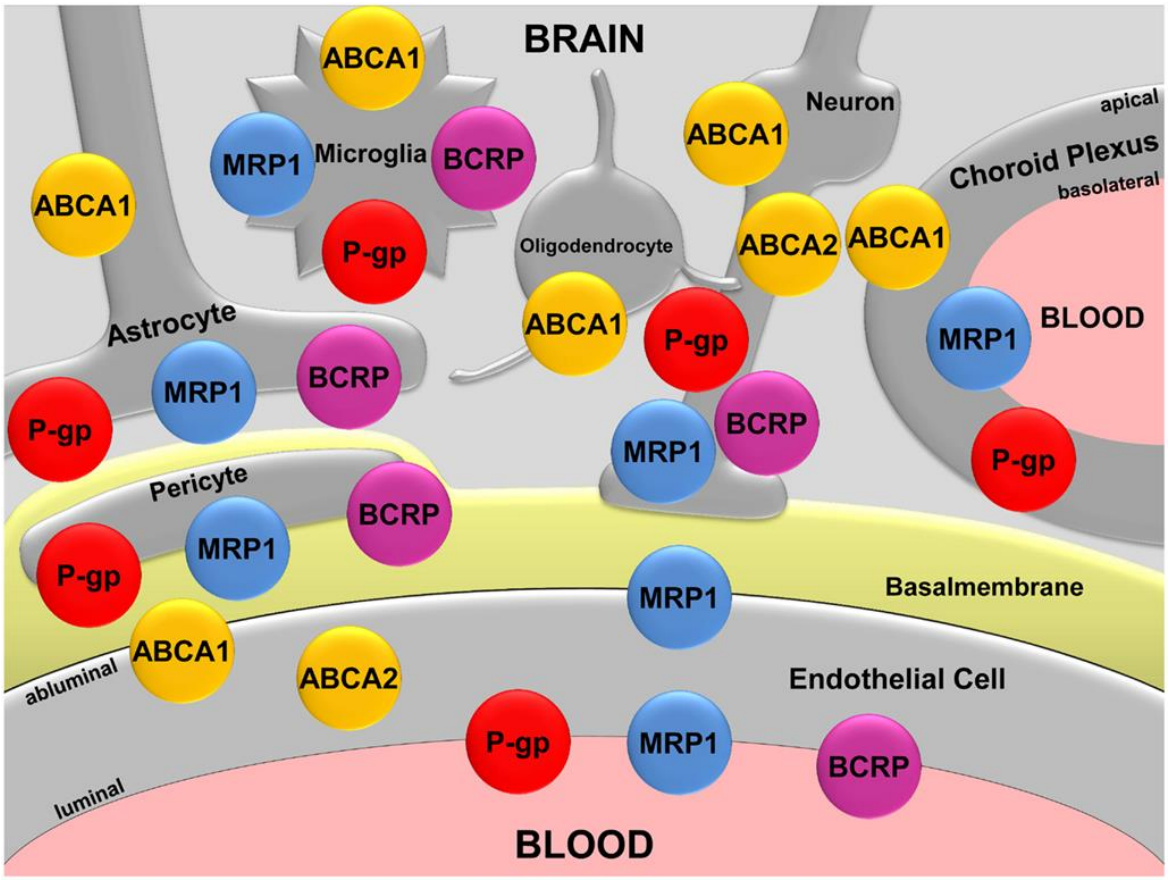

Figure 2: Multidrug transporter localisation in brain
Pgp, P-glycoprotein; BCRP, breast cancer resistance protein, MRP, multidrug resistance protein. ABCA, ATP-Binding Cassette, Sub-Family A (ABC). Figure is from Wolf et al. (Wolf et al. 2012).

2.3 MECHANISMS OF PGP OVEREXPRESSION IN PHARMACORESISTANT MTLE

An important question is whether the overexpression of efflux transporters in epileptic brain tissue is constitutive or acquired/induced, or both mechanisms may be at play. A constitutive overexpression could occur as a result of a genetic predisposition, or it could be intrinsic to the development of the specific pathology. It is also conceivable that overexpression is acquired such as induction by recurrent seizures or even the AEDs intended to prevent them

(Kwan and Brodie 2005). I will discuss the evidence for the possible various mechanisms in the following paragraphs.

2.3.1 Seizures induce Pgp overexpression

In rats and mice, experimentally induced seizures have been shown to increase the expression of Pgp in brain capillary endothelial cells (BCECs), astrocytes and neurons (Löscher and Potschka 2005a). Zhang et al. (Zhang et al. 1999) reported increased Pgp expression in the hippocampus following intracerebroventricular injection of kainate in rats, causing neuronal injury. This increase in Pgp expression was observed in reactive astrocytes as early as one day after injection, peaked at two weeks but was still visible at ten weeks. Seeger et al. (Seegers et al. 2002) studied Pgp expression at 24 hours and ten days after status epilepticus (SE) (to differentiate between seizure related changes and changes developing during epileptogenis). Pgp increased significantly 24 hours after kainate-induced SE in BCECs at the dentate gyrus, amygdala, piriform and parietal gyrus. Additionally in the brain parenchyma of rats 24 hours after SE, a significant increase in Pgp expression was observed in the piriform and parietal cortex, dentate gyrus and hippocampus. However, the alterations in Pgp expression were only transient and disappeared ten days after the SE, except for the dentate hilus and the CA1 sector of the hippocampus, in which a significant increase in parenchymal Pgp was observed ten days after the status. Following systemic injection of kainate in mice, expression of mdr-1, the gene encoding Pgp, was found to be increased in the hippocampus for three-24 hours after the seizures but returned to control level by 72 hours (Rizzi

et al. 2002). Recently Pekcec et al. (Pekcec 2009) studied Pgp expression in brain tissue sampled from epileptic dogs following spontaneous status epilepticus or seizure clusters to avoid a putative bias of status epilepticus induction. They demonstrated a significant upregulation of Pgp in the hippocampal hilus (82% above control), the dentate gyrus granule cell layer (132% above control) and parietal cortex of canines (123% above control) one-seven days following a seizure. In further support of the temporal increase of Pgp after seizures is the study by Bankstahl and co-workers in two rat SE models. Immunohistochemical staining of Pgp did not indicate any increase of Pgp expression in brain capillary endothelial cells during SE, whereas significant overexpression was determined in both models 48 hours after SE. Seven days after SE, Pgp expression had returned to control levels (Bankstahl and Löscher 2008). Löscher and Potschka (Löscher and Potschka 2005b) suggested that the excitatory neurotransmitter glutamate, which is excessively released by seizures, is involved in the seizure-induced over-expression of Pgp in the brain. This suggestion was based on a report by Zhu and Liu (Zhu and Liu 2004), showing that glutamate up regulates the expression and functional activity of Pgp in rat BCECs in vitro. They suggested that glutamate upregulates Pgp expression in BCECs by an N-methyl-D-aspartate (NMDA) receptor-mediated mechanism, which could play a role during ischemic and anoxic injury. Bankstahl et al. (Bankstahl et al. 2008a) recently examined this hypothesis and evaluated whether glutamate is involved in seizure-induced upregulation of Pgp in brain capillaries after systemic-administration of pilocarpine, a model of mTLE. Their data shows that the administration of the glutamate receptor

antagonist MK-801 after convulsive SE prevents the upregulation of Pgp in brain microvessels in the hippocampus, indicating that SE-induced glutamate release is involved in the regulation of Pgp expression after seizures. Additionally MK-801 reduces the neuronal damage after prolonged seizures which may offer a therapeutic option. The activation of the NMDA receptor by glutamate is known to generate reactive oxygen species (ROS) and Zhu and Liu (Zhu and Liu 2004) suggested that ROS may mediate the effect of glutamate on Pgp expression. Generation of free radicals such as ROS has been suggested to play a key role in neuronal damage developing after SE. It is generally believed that excitotoxic cell death is due to excessive activation of NMDA receptors by glutamate, leading to excessive activation of calcium ion influx through the receptor's associated ion channels and subsequent free radical production, including ROS. Based on this hypothesis, ROS is likely to be the link between seizures induced glutamate release and over-expression of Pgp. The data from these animal studies indicate that Pgp overexpression is a result of sustained seizure activity but not of the processes underlying development of epilepsy.

2.3.2 Brain inflammation and epilepsy

It is widely accepted that neurons are the cause of seizures and targeting of neuronal ion channels, GABA, and glutamate receptors has been, for decades, the mainstream pharmacological approach to eradicate seizures. Although the ultimate effectors of seizures are neurons, recent advances in experimental neurology have revealed that inflammation can precipitate seizures or sustain seizure activity (Marchi et al. 2014). Two distinct inflammatory processes have

been linked to seizures. Neuroinflammation is present in epileptic brain where it exacerbates seizures or increases their frequency (Vezzani et al. 2011). By contrast, systemic inflammation can cause epileptiform neuronal discharge via loss of ionic (e.g., potassium (Traynelis and Dingledine 1988) and neurotransmitter (e.g., glutamate (Heinemann et al. 2012; Marchi et al. 2014) homeostasis. Although neuroinflammation directly affects neurovascular and glial function, the effects of systemic inflammation are mediated or facilitated by loss of BBB function (Rivest 2010). BBB disruption can be triggered by a direct insult to the endothelium (Marchi et al. 2007) or by systemic factors, including activation of circulating leukocytes and release of molecular mediators that increase vascular permeability (Librizzi et al. 2012; Marchi et al. 2014). Pro-inflammatory and anti-inflammatory cytokines, chemokines, and prostaglandins are responsible for the production of an early immune response. Numerous studies have confirmed enhanced inflammatory signalling in chronic rodent models and in tissue from patients with TLE (Aronica and Crino 2011; Vezzani et al. 2013). Genetic and pharmacological modulation of the synthesis and secretion of inflammatory mediators and of their receptors can influence seizure thresholds, severity and duration in mouse and rat TLE models (Vezzani et al. 2013). Anti-inflammatory drugs, such as steroids and intravenous immunoglobulins, are useful in selected pharmacoresistant epileptic syndromes, whereas fever, immunization, and trivial infection can precipitate seizures, providing a solid link between inflammation and seizures (Vezzani and Granata 2005). In addition, inflammatory mediators seem to contribute to disease-associated alterations, which can exert an effect on antiepileptic drug

responses. For instance, cytokines can modulate the expression, sub-unit composition and functional state of antiepileptic drug targets (Balosso et al. 2009; Vezzani et al. 2013).

2.3.2.1 Pgp overexpression and brain inflammation

Experimental data indicate that seizure activity is one of the main factors up-regulating Pgp in the epileptic brain (Rizzi et al. 2002; Seegers et al. 2002; Volk and Loescher 2005) and glutamate can affect Pgp expression (Zhu and Liu 2004). Further downstream events in the signalling cascade have been identified and Bauer et al (Bauer 2008) have shown that cyclooxygenase-2 (COX-2) is a central factor of a cascade that drives the transcriptional activation of the Pgp-encoding gene in the epileptic brain. COX is an enzyme that is responsible for the formation of prostanoids, including prostaglandins, prostacyclin and thromboxane. These lipid mediators play important roles in inflammation and pain and in normal physiological functions. Pharmacological inhibition of COX can provide relief from the symptoms of inflammation and pain. It has been proven that COX-2 mediates Pgp regulation in response to excess glutamate concentrations such as those occurring during epileptic seizures (Bauer et al. 2008). It is known that glutaminergic signaling increases COX-2 expression and that at least in rat mesangial cells COX-2 activation leads to increased Pgp (Sorokin 2004). Furthermore, both the nonselective COX inhibitor indomethacin as well as the selective COX-2 inhibitor celecoxib counteracted Pgp increase by glutamate exposure of isolated rat brain capillaries. Van Vliet et al. tested the efficacy of COX-2 inhibitors in a chronic rodent model,

overexpressing Pgp (Van Vliet et al. 2004; van Vliet et al. 2007). A sub-chronic 2-week treatment with the highly selective cyclooxygenase-2 inhibitor SC-58236 in the chronic epileptic state kept Pgp expression at control levels (Van Vliet et al. 2010). These data substantiate that COX-2 inhibition can block repeated induction of Pgp by ongoing seizure activity, thereby allowing Pgp to return to control levels. Furthermore, enhanced Pgp expression in chronic epileptic rats was associated with a significant reduction in the brain penetration of the antiepileptic drug phenytoin. Importantly, the brain delivery of phenytoin was significantly enhanced by subchronic COX-2 inhibition in rats with recurrent seizure activity (Van Vliet et al. 2010). These data provided evidence that COX-2 inhibition may help to increase concentrations of AEDs at the target sites and that COX-2 inhibition could be a novel therapeutic concept to overcome pharmacoresistance in epilepsies (Potschka 2010).

2.3.3 Genetic polymorphism and Pgp expression

Several studies have tested for an association between Pgp expression in patients with epilepsy and polymorphism in drug transporter genes (Löscher and Langer 2010). One of these, a single nucleotide polymorphism in exon 26 (C3435T) of the MDR1 gene is associated with altered expression, functionality and substrate specificity of the MDR1 product Pgp. Based on an initial report by Siddiqui (Siddiqui et al. 2003), a series of studies supported the hypothesis that the C3435T polymorphism is associated with resistance to multiple AEDs (Löscher et al. 2009). Several recent genetic association studies have also indicated an association of the 3435CC genotype with increased Pgp expression

and drug resistant epilepsy (Löscher et al. 2009). In contrast however are other studies which did not find a link between ABCB1 and response to AEDs (Löscher et al. 2009). Two metaanalyses including 11 studies up to September 2007 involving 3371 patients and including 22 studies up to February 2010 involving 6755 patients respectively provided no support for an association between pharmacoresistance and ABCB1 (Bournissen et al. 2009; Haerian et al. 2010). The inconsistency between the studies might be caused by different inclusion criteria (definition of pharmacoresistance, co-morbidities, co-medication and population structure). A recent study pointed out the importance of stratification by patient age and aetiology of epilepsy (Sanchez et al. 2010). Another issue are the selection of AEDs included in the studies as the inclusion of drugs which have not been confirmed as Pgp substrates will bias the data (Potschka 2010). Another factor complicating genetic association studies is related to data indicating that the C3435T polymorphism might have contrasting consequences on Pgp expression in different ethnic subgroups. This is in line with the observation that an association in the opposite directions has been described in studies in Asian patients as compared to studies reporting an association in a Caucasian patient population (Kasperaviciute and Sisodiya 2009).

2.3.4 The effect of Pgp and gender

Pgp expression is known to differ between men and women; for example, hepatic Pgp expression is 2.4-fold lower in females, although there are large interindividual differences in Pgp levels (Schuetz et al. 1995). However, little is

known about gender differences in Pgp function at the BBB and in patients with epilepsy which again may be under gender specific hormonal influences (Bebawy and Chetty 2009). Assema et al. (van Assema et al. 2012) examined the effect of gender and age at the BBB in 35 healthy men and women in three different age groups using VPM PET scans. They found increased volume of distribution (VT) of VPM with aging in several large brain regions in men. Young and elderly women showed comparable VT values. Young women had higher VT compared with young men (van Assema et al. 2012). It is known that (both endogenous and synthetic) progesterone/progestins and estrogens can have an effect on Pgp function (Bebawy and Chetty 2009). To date no studies have investigated the relationship between VPM PET measurements and actual hormone levels. Interestingly, a preclinical study has found differences in brain uptake of verapamil comparing female mice to male mice, which suggested a modest increase in Pgp expression and/or function in female animals (Dagenais et al. 2001). But this is in contrast to the findings of the clinical study in humans, in which a higher VT was found in young women than in young men, suggesting reduced Pgp function in young women (van Assema et al. 2012). Further studies are needed to assess whether this discrepancy is due to differences in hormonal status or species differences in transporter expression and/or activity at the BBB.

2.3.5 Are antiepileptic drugs Pgp substrates?

A central question of the transporter hypothesis is whether AEDs are substrates for Pgp. Only then, could overexpression of Pgp crucially contribute to

pharmacoresistance in epilepsy. So far evidence has been reported that phenytoin, phenobarbital, lamotrigine, levetiracetam, topiramate, and carbamazepine and oxcarbazepine metabolite are substrates of human Pgp (Luna-Tortes et al. 2008; Luna-Tortós et al. 2009). On the other hand data argue against a transport of valproic acid and carbamazepine (Baltes et al. 2007a; Luna-Tortos et al. 2008). In addition, transport of AEDs has been evaluated in a human colon carcinoma cell line. In these in vitro assays no evidence was obtained that carbamazepine, vigabatrine, gabapentin, phenobarbital, or lamotrigine are substrate of Pgp (Owen et al. 2001; Crowe and Teoh 2006). Moreover, Rivers et al. reported that carbamazepine, valproic acid, phenytoin, lamotrigin, and primidone are not likely to be substrates of Pgp based on their investigations in breast and cancer cell lines (Rivers et al. 2008). Although in vitro and in vivo transport assays have indicated that several antiepileptic drugs are substrates of Pgp, and that some AEDs are transported by ABC transporters, the data however is controversial. Although apparently a simple question, obvious difficulties exist in research evaluating the transporter substrate characteristics of AEDs. AEDs can pass the BBB efficaciously when efflux transporters such as Pgp are expressed at basal level. However, their brain penetration is limited once a relevant over expression occurs. Highly lipophilic compounds can rapidly diffuse through membranes of endothelial cells and might be less sensitive to an impact of active transports. Furthermore differences in the affinity to the transporter molecule might exist. Respective differences need to be taken into consideration when choosing an in vitro assay to explore the substrate specificities of AEDs. It has also been recently

demonstrated that the transport of AEDs depends on concentration and it is therefore of particular relevance to test potential Pgp substrates at clinically relevant concentrations (Zhang et al. 2010). Additionally, recent data also suggests that the substrate recognition or transport efficacy by Pgp differs between human and mouse for certain AEDs (Baltes et al. 2007b; Sills 2008). Such differences might explain in part the controversial data which have been reported for AED transport by Pgp from different species (Kwan and Brodie 2005).

2.3.6 Antiepileptic drugs induce Pgp overexpression

Some studies have indicated that antiepileptic drugs might contribute to the induction of Pgp overexpression (Potschka 2010). Lombardo et al. (Lombardo et al. 2008) reported that carbamazepine, phenobarbital, and phenytoin induce Pgp and other transporters in rat brain endothelial cell lines via and interaction with the pregnane x receptor and the constitutive androstane receptor. In contrast Ambroziak el al. (Ambroziak et al. 2010) did not observe effects of these AEDs on expression and functionality of Pgp. Therefore definite conclusions regarding the impact of AEDs require further future efforts (Potschka 2010).

2.4 NEUROIMAGING OF PGP WITH PET

Although increased transporter expression has been demonstrated in animal models of pharmacoresistant epilepsy and in human tissue that had been resected in surgery it may not be functionally relevant (Rogawski and Johnson, 2008). Non invasive brain imaging of multidrug efflux transporter function in pharmacoresistant and seizure-free epilepsy patients is a strategy to evaluate whether the overexpression of multidrug efflux transporters at the BBB as postulated in the transporter hypothesis has any functional consequences that underlie pharmacoresistance in epilepsy. Additionally, PET tracers for multidrug efflux transporters could be useful to identify epilepsy patients with increased multidrug efflux transporter activity who will benefit from treatment with multidrug efflux transporter modulation drugs and therefore hold great promises for individualized medicine (Sisodiya and Bates 2006).

Almost all efforts to develop multidrug efflux transporters ligands have focused on Pgp expressed at the BBB or in tumours. To date three different categories of imaging probes have been described to measure multidrug efflux transporters in vivo (Mairinger et al., 2011). 1) Radiolabeled transporter substrates usually developed from drugs known to be substrates for Pgp. More recently 2) radiolabeled transporter inhibitors as well as 3) radiolabeled prodrugs.

2.4.1 Radiolabeled transporter substrates

2.4.1.1 [^{11}C]verapamil

[^{11}C]verapamil (VPM) is the best validated PET tracer to image Pgp function to date. Verapamil, a calcium channel blocker, has been found to be a substrate for Pgp at low concentrations (which are used in PET) but also inhibits the Pgp transporter ATP hydrolysis (which initiates substrate extrusion) at high concentrations (Ambudkar et al., 1999). As it is well characterised both pharmacologically and with regards to its metabolic pathways it was thought to be a suitable candidate for a PET tracer to quantify Pgp function in vivo non-invasively. In 1996 Elsinga et al. were the first to use PET to study multidrug resistance and to measure Pgp function. They developed a method using racemic (±) verapamil as a PET radiotracer and studied its tissue distribution in vivo in rats and in vitro with seizure-free and pharmacoresistant human ovarian carcinoma cell lines (Elsinga et al. 1996). The racemic (±) verapamil consists of two enantiomers, the (S) - and (R)- verapamil. In vivo pharmacokinetics and pharmacodynamics of both enantiomers in animals and humans are different and the (S)-verapamil is more actively metabolised than the R-form, resulting in a 2.5 higher concentration of the (R)-enantiomer in plasma (Vogelgesang et al. 1984). Furthermore (R)-verapamil exerts only 5-10% of the calcium channel blocking activity of the (S)-enantiomer and (S)-verapamil is ten times more potent in prolonging PR-intervals in humans (Echizen et al. 1985). As the enantiomers of verapamil have different pharmacokinetics, the quantification of racemic (^{11}C)verapamil may be difficult. For this reason Luurtsema et al.

developed a synthesis of (R)-[^{11}C]verapamil and they found that the metabolism was slower than that of the racemic verapamil. (Luurtsema et al. 2002; Luurtsema et al. 2005). (R)-[^{11}C]verapamil is a high-affinity substrate of Pgp and is therefore very effectively transported by Pgp at the BBB. This results in low brain uptake of this radiotracer thus making it difficult to elicit regional differences in cerebral Pgp function. A possible strategy to overcome the limitation of the low brain uptake of Pgp substrate radiotracer is to perform PET scans after partial blockade by Pgp modulating drugs such as cyclosporine A (CsA) or tariquidar (TQD) (Löscher and Langer, 2010). The third-generation Pgp inhibitor TQD is safer than the non-selective CsA for use in human subjects and was shown to lack interaction with metabolism and plasma protein binding of (R)-[^{11}C]verapamil (Bankstahl et al., 2008;Wagner et al., 2009). Blocking Pgp with an inhibitor allows the radiotracer to enter the BBB and hence increase its uptake and signal in the brain.

2.4.1.2 [^{11}C]-N-desmethyl-loperamide

The radiotracer [^{11}C]-N-desmethyl-loperamide has the advantage that it is metabolised to a lesser extent than (R)-[^{11}C]verapamil. It has been used in rats (Farwell et al. 2013) as well as monkeys (Liow et al. 2009) and the first human studies using PET with [^{11}C]-N-desmethyl-loperamide at baseline (Seneca et al. 2009) and after Pgp inhibition with TQD (Kreisl et al. 2010) have been recently carried out. At baseline there is virtually no uptake of this radiotracer in the brain. After 2 mg/kg of TQD the brain uptake of radioactivity increased only slightly (approximately 30%). In contrast, 4 and 6 mg/kg of TQD increased brain uptake

two- and four-fold, respectively. Until now, [^{11}C]-N-desmethyl-loperamide has not been used clinically to study disease in patients. On the other hand, [^{11}C]-N-desmethyl-loperamide is a high affinity Pgp substrate that virtually shows no brain uptake which makes it unsuitable to map regional differences in Pgp function at baseline.

2.4.2 Radiolabeled Antiepileptic drugs

It is also possible to label AEDs with a positron emitter. [^{11}C]phenobarbital and [^{11}C]phenytoin have been shown to be weak substrates for Pgp and are expected to have higher brain uptake than the high-affinity Pgp substrate [^{11}C]verapamil (Stavchansky et al. 1978; Luna-Tortos et al. 2008). They could therefore be better suited to assess regional differences in Pgp function (Mairinger et al., 2011), in particular Pgp overexpression. A study in eight patients with pharmacoresistant partial epilepsy and two patients without epilepsy showed that [^{11}C]phenytoin concentration ratios were lower in the visual cortex in epilepsy patients who had an average value of 1.32 (range 1.05-1.66) compared to 1.61 (1.34-1.87) in nonepileptic patients (Baron et al. 1983). But whether phenytoin concentrations are lower within the epileptic focus was not addressed in this study (Baron et al. 1983).

2.4.3 Other radiolabeled Pgp substrates

Several more radiolabeled drugs and radioligands have been investigated as PET tracers for Pgp. The radioligand [^{18}F]MPPF has been developed as an alternative to short lived (^{11}C)-labelled tracers for PET studies of serotonin 5-HT_{1A} receptors. In microPET studies, treatment with CsA globally increases the

uptake of [^{18}F]MPPF in rat brain indicating that [^{18}F]MPPF must be a Pgp substrate (Laćan et al. 2008). So far [^{18}F]MPPF has been used in animal studies together with the third generation Pgp inhibitor TQD to study Pgp activity (Bartmann et al. 2010; La Fougère et al. 2010). By using [^{18}F]MPPF with TQD Bartmann et al. (Bartmann et al. 2010) revealed differences in Pgp function between pharmacoresistant and seizure-free epileptic rats. Tariquidar pre-treatment increased the magnitude of [^{18}F] MPPF K_1 in the hippocampus by a mean of 142% in the non-responders, which significantly exceeded the 92% increase observed in the responder group. The same treatment decreased the mean magnitude of [^{18}F] MPPF in the hippocampus by 27% in non-responders, without comparable effects in the responder group (Bartmann et al. 2010). Additionally, Bartmann et al. (Bartmann et al. 2010) demonstrated that the impact of TQD on the brain kinetics of [^{18}F]MPPF correlates with the pharmacosensitivity toward phenobarbital in a rodent model of chronic pharmacoresistant epilepsy, in which pharmacoresistance proved to be associated with Pg overexpression (Potschka 2010). Moreover, preliminary results obtained in a clinical study with ten mTLE patients showed that the Pgp inhibitor CsA significantly increased the [^{18}F]MPPF binding potential by 14% in most brain regions, regardless of their involvement in seizure generation or propagation (Hammers et al. 2010). On the other hand, a recent study using [^{18}F]MPPF PET in mice and non-human primates together with CsA (Tournier et al. 2012) revealed discrepancies in the Pgp-mediated transport of [^{18}F]MPPF between mice and non-human primates. Their in vitro data indicates that [^{18}F]MPPF is not a substrate of human P-gp and that the effect of the Pgp

inhibitor CsA on the brain transport of [^{18}F]MPPF in non-human primate is related to an increase in the free fraction of tracer in the plasma, concluding that it is unlikely that the kinetics of [^{18}F]MPPF brain transport and distribution are affected by Pgp activity in humans. In contrast in situ brain perfusion showed that Pgp restricted the permeability of the mouse BBB to ^{3}H-MPPF (Tournier et al. 2012).

The PET radioligand [^{11}C]flumazenil which is clinically used for the assessment of $GABA_A$ receptor mediated inhibition in epilepsy and to localize epileptic foci prior to epilepsy surgery has also been suggested to be a Pgp substrate (Ishiwata et al. 2007; Froklage et al. 2012). [^{11}C]flumazenil was recently used to detect regional differences in Pgp functionality in five different brain regions of control and kainate-treated rats, a model for TLE, before and after TQD administration. The study showed that the $GABA_A$ receptor density (Bmax) was reduced in kainate-treated rats, compared with controls and that there were region-specific Pgp differences, with the hippocampus showing the highest Bmax (Syvänen et al. 2012).

Furthermore, [^{11}C]colchicine (Mehta et al., 1994), [^{11}C]daunorubicin (Elsinga et al., 1996), [^{11}C]carvedilol (Bart et al., 2005), [^{11}C]-GR218231 (de Vries et al., 2005), [^{18}F]paclitaxel (Kurdziel et al., 2003), various 64Cu-labeled copper complexes (Packard et al., 2002), 67Ga/68Ga radiopharmaceuticals (Sharma et al., 2005), [^{11}C]TMSX, [^{11}C]MPDX, ^{11}C]donepezil (Ishiwata et al. 2007), [^{11}C]carazolol and [^{18}F]fluorocarazolol (Doze et al., 2000) have been used to study Pgp. However, only limited in vivo data have been reported so far and it is

not yet clear if these radiotracers are useful for PET studies to image Pgp function in human.

2.4.4 Radiolabeled transporter inhibitors

Another complementary approach to assess the Pgp system with PET is the use of radiotracers which bind to Pgp without being transported. Such radiotracers would asses the transporter distribution and give a signal increase rather than a decrease (as will Pgp substrates) in brain regions that overexpress Pgp (Löscher and Langer, 2010). Several PET radiotracers based on the Pgp inhibitors have been reported to date: [^{11}C]laniquidar, [^{11}C]MC-18, [^{11}C]quinidine [^{11}C]elacridar and [^{11}C]tariquidar (Bauer et al. 2010; Mairinger et al. 2012; Bauer et al. 2013; Syvänen et al. 2013). These new radiotracers have so far only been tested in animal models of naïve, transporter knock-out and epileptic rodents with rather surprising results. The cerebral uptake was lower than expected at baseline and increased several-fold rather than decreased after administration of unlabelled inhibitors (Bauer et al. 2010; Bauer et al. 2013; Syvänen et al. 2013). These radioligands were administered at very low (tracer) concentrations and could behave differently than at high concentrations. It is hypothesized that the low brain uptake, i.e. the rather substrate-like behaviour of these radiotracers, could be caused by other multidrug efflux transporters (such as BCRP) at the BBB transporting the radiotracers out of the brain (Mairinger et al. 2011).

2.5 NEUROIMAGING OF PGP WITH SPECT

[^{99m}Tc]sestamibi was originally developed as a K+ analog for imaging myocardial ischemia. It has been shown to be a substrate for Pgp (Luker et al., 1997). In humans, [^{99m}TC]sestamibi was reported to image Pgp efflux transport in multidrug resistant cancers (Luker et al., 1997). However, it was found not to be an ideal substrate radioligand as it is not a selective substrate for Pgp but also for other multidrug efflux transporters (such as MRP1) (Hendrikse et al., 1998). Furthermore in contrast to PET, SPECT does not enable quantitative measurements of uptake and efflux kinetics of Pgp substrates and thus has only limited use in studying Pgp function in the BBB (Löscher and Langer, 2010).

2.6 PRECLINICAL STUDIES OF PGP IN MTLE

2.6.1 Preclinical epilepsy models

2.6.1.1 Knockout mice and natural mutants

Investigations in genetically deficient animals, which lack a functional form of one or more drug efflux transporter, have contributed to a significant extend to the current knowledge about the physiological and pharmacological function of these transporters. Genetically deficient mice have been generated by knockout technologies with the purpose of studying the role of specific transporters. Furthermore, subpopulations of animals with spontaneous mutations in multidrug transporter genes have been identified for different species. The in vivo impact of Pgp in the BBB has been intensely studied in knockout mice lacking the Pgp isoform mdr1a (mdr1a (-/-)mice) or mdr1a and mdr1b Pgp (md1a/1b (-/-) mice). Mdr1a knockout mice lack the mdr1a isoform of Pgp all

over the body and in the brain capillary endothelial cells. The animals are viable and fertile but are more susceptible to developing a severe, spontaneous intestinal inflammation (Löscher and Potschka 2005).

2.6.1.2 Animal models of epilepsy

Animal models of epilepsy are a valuable tool to study models of seizure onset, neurologic changes during seizures, and new pharmacologic tools for seizure propagation or pharmacoresistance. For epilepsy research various animal models are available, each with their specific characteristics. Globally, these models are categorized into models of seizures and those of epilepsy (Sarkisian 2001). Examples of seizure, or acute, models are the cortical stimulation model and the maximal electroshock model. The amygdala kindling model is also an acute model, as most animals do not develop spontaneous epilepsy. The models of epilepsy, chronic models, can be subdivided into models of genetic epilepsy and models of acquired (symptomatic) epilepsy (Löscher 2011). The first category includes both animals with spontaneous mutations and animals with induced mutations, resulting in epileptic symptoms and behavior. In animals of the acquired or symptomatic epilepsy models, status epilepticus (SE) is induced by electrical stimulation (amygdala, perforant path, and hippocampus) or through the administration of chemical convulsants (pilocarpine or kainic acid) in previously non-epileptic rats, which results in the development of spontaneous seizures after a latent period of days to weeks.

2.6.1.2.1 Kindling model

Since its introduction by Goddard in 1967 (Goddard 1967), the kindling model has been used extensively as an animal model of epilepsy. Kindling can be induced by the repeated administration of a mild electric stimulus to the rat brain via an implanted electrode into a limbic structure such as the amygdala, hippocampus, entorhinal cortex or other brain areas. Over a period of several stimulations session the rat reliably displays stage five seizures, according to the Racine scales (Racine 1972). The pathophysiology of kindling is very similar to that of human mTLE. For example, kindling leads to structural and functional changes characterized by neuronal cell loss, gliosis, neurogenesis and mossy fiber spouting (Arida et al. 2009).

2.6.1.2.2 Pilocarpine model

The pilocarpine and the kainic acid model are probably the most commonly studied chemical-inductive models for mTLE. Pilocarpine, a potent muscarinic cholinergic agonist, is administered as a single high dose (300-380mg/kg) to rats or mice. It acutely induces sequential behavioral and electrographic changes, indicative of sustained epileptic activity, resulting in widespread damage to the forebrain in (Arida et al. 2009). After 15-25 minutes this results in motorlimbic seizures and leads to SE within 50-60 minutes after pilocarpine administration that last for up to 12 hours. After a silent period of a few days animals start exhibiting spontaneous recurrent seizures. Morphological analysis of the brain after pilocarpine-indcued SE demonstrates cell loss in the hippocampal subfields CA1 and CA3 and in the hilus of the dentate gyurs, in the septum, olfactory

tubercle, amygdala, piriform cortex, neocortex and thalamic nuclei (Arida et al. 2009).

2.6.1.2.3 Kainic acid model

The excitotoxic glutamate analogue kainite can be systemically or intracerebrally injected into an animal and rapidly produce acute seizures. In rodents, large doses of the drug induce severe acute seizures with subsequent SE, which is followed by a quiescent period of usually several weeks (Arida et al. 2009). This latent period is followed by the development of spontaneous recurrent seizures. Injections of kainic acid were shown to lead to cell death in the hippocampus, amygdala, entorhinal cortex and medial thalamic nuclei (Ben-Ari et al. 1980).

2.6.2 Preclinical studies of Pgp in epileptic rats

In animals, models of temporal lobe epilepsy, such as the kindling and kainate models, have been used to study the molecular mechanisms of pharmacoresistance. In these models a large group of kindled or epileptic rats is treated with AEDs. Subsequently subgroups of animals that either respond (pharmacosensitive/seizure-free) or do not respond (pharmacoresistant) to AEDs are selected. Pgp is overexpressed in endothelial cells and ectopically in astrocytes, after induction of sustained limbic seizures in rodents (Volk and Loescher 2005). Upregulation of the mRNA of the MDR1 gene was detected in rat brain during both acute and spontaneous seizures caused by status epilepticus. Because limbic seizures were induced in these studies in otherwise normal rodent brain, these experimental findings indicate epileptic activity per se can increase the expression of Pgp. More recently Volk and Löscher (Volk and Löscher 2005) used a rat model of temporal lobe epilepsy to examine whether Pgp expression differs in AED responders from non-responders rats. In this model, spontaneous recurrent seizures develop after status epilepticus induced by amygdala kindling. They showed that phenobarbital-resistant epileptic rats exhibit significantly higher endothelial expression of Pgp in limbic brain regions compared to drug-responsive rates providing further support for the hypothesis of Pgp overexpression in pharmacoresistant epilepsy. Furthermore in another study with amygdala epileptic kindled rats significant upregulation of Pgp was reported in brain capillary endothelial cells of limbic brain regions. In these rats, brain-to-plasma concentration ratios of phenytoin in the hippocampus were about 30% lower than those measured in control rats (Potschka and Löscher

2002). When kindled rats were divided into phenytoin responders and non responders, non responders exhibited a significantly higher expression of Pgp in capillary endothelial cells in the epileptogenic focus (Potschka et al. 2004). Moreover, no differences in Pgp expression were observed in the adjacent piriform cortex indicating that the Pgp expression between non-responders and responders are restricted to the kindled focus (Potschka et al. 2004). Rizzi et al. (Rizzi, et al. 2002) reported that mdr1 mRNA is overexpressed in mouse hippocampus after the induction of limbic seizures. Then phenytoin was systemically administered to the mice, its brain-to-plasma ratio was 30% less than in mice not subjected to seizures thus indicating reduced drug-concentrations on brain.

Moreover, targeting Pgp by modulators can enhance the efficacy of AEDs. The co-administration of the unselective inhibitor verapamil proved to potentiate the anticonvulsant efficacy of the AED oxcarbazepine (Clinckers et al. 2005). The third generation selective modulator tariquidar (TQD) increased the efficacy of phenytoin in a chronic rat model where spontaneous recurrent seizures where induced by amygdala kindling (Brandt, et al. 2006). However, putative species differences in the substrate spectrum of the transporters need to be taken into account when extrapolating from rodent data to the clinical situation.

2.6.3 Preclinical imaging of Pgp function

PET analysis with [^{11}C]-verapamil to assess Pgp function at the BBB within the intact CNS was first validated using *mdr1a* knockout mice and showed lower [^{11}C]-verapamil uptake in the wildtype mice compared to those in the *mdr1a*

knockout mice (Hendrikse, et al. 1998). In addition it was possible to prove that the reversal of Pgp function can be monitored by PET. The unselective Pgp inhibitor CsA increased the [^{11}C]-verapamil accumulation to levels comparable to this in mdr1a knockout mice (Hendrikse et al. 1998). This concept was subsequently replicated in two further studies using the racemic [^{11}C]-verapamil and the unselective inhibitor CsA at different doses resulting in dose dependent increases of [^{11}C]verapamil by Pgp modulation after CsA (Bart et al. 2003; Syvaenen et al. 2006). Furthermore Bankstahl et al. (Bankstahl et al. 2008b) performed paired (R)-[^{11}C]verapamil PET scans in a group of 7 healthy Wistar rats before and after administration of the new third-generation Pgp inhibitor TQD (15 mg/kg). After TQD administration, the distribution volume of (R)-[^{11}C]verapamil was 12-fold higher than baseline and the influx rate constant K_1 of (R)-[^{11}C]verapamil into the brain, was about eight-fold higher after tariquidar hereby, demonstrating that (R)-[^{11}C]verapamil PET combined with TQD administration is a promising approach to measure Pgp function at the BBB. Recently Kuntner et al. used (R)-[^{11}C]verapamil PET in rats before and after the administration of different doses of the selective Pgp inhibitors TQD and elacridar (Kuntner et al.). They demonstrated that the median effective dose (the dose required to achieve 50% of the desired response in 50% of the population=ED 50) for TQD is 3.0 +/- 0.2 mg/kg. Furthermore, PET scans after 3 mg/kg TQD resulted in regionally different enhancement of brain activity distribution, with lowest distribution volume in cerebellum and highest distribution volume in thalamus pointing to regional differences in cerebral Pgp function and expression in rat brain.

2.6.4 Preclinical imaging of Pgp function in pharmacoresistant epilepsy

Following the promising results of (R)-[^{11}C]verapamil in healthy Wistar rats a proof of concept study was performed in rats 48 hours after pilocarpine-induced SE. Both control and post-SE rats underwent (R)-[^{11}C]verapamil PET scans after administration of tariquidar at 3mg/kg (Bankstahl et al., 2011). Regional PET data was analyzed and Pgp expression was independently quantified in the same brain regions using immunohistochemical staining (Bankstahl et al., 2011). In brain regions with increased Pgp expression (cerebellum, thalamus, hippocampus) in SE rats the influx rate constants from blood to brain, K_1, of (R)-[^{11}C]verapamil were significantly decreased relative to control animals, thereby supporting the hypothesis of regionally increased cerebral Pgp function in epilepsy. A further PET study with another Pgp substrate radiotracer [^{18}F]MPPF confirmed the hypothesis of Pgp overexpression in pharmacoresistant epilepsy. Bartmann et al. (Bartmann et al., 2010) evaluated BBB Pgp function in rats with seizure-free and pharmacoresistant mTLE. The authors showed that TQD (5 mg/kg) pre-treatment increased the magnitude of [^{18}F]MPPF K_1 in the hippocampus by a mean of 142% in AED non-responders, which significantly exceeded the 92% observed in the AED responder group. Therefore PET imaging approach with combined use of a Pgp substrate radiotracer and a Pgp modulator seems to be appropriate to non-invasively determine Pgp efflux function at the BBB.

2.7 CLINICAL STUDIES OF PGP IN MTLE

Evidence for increased expression of Pgp has mainly been derived from epileptic tissues removed during epilepsy surgery from patients with pharmacoresistant epilepsy (Kwan and Brodie 2005). Tishler et al. (Tishler et al., 1995) were the first to measure MDR1 expression in 19 patients undergoing resective epilepsy surgery, 15 of whom had mTLE receiving temporal lobeectomy for a mixture of pathologies (mostly hippocampus sclerosis). MDR1 mRNA level was found to be >ten times higher in 11 of the 19 resected samples compared with controls. In addition Pgp was detected by immunohistochemical staining in astrocytes where it is not normally present, suggesting novel expression. Following Tishler and colleagues' report multiple follow-up studies have confirmed this initial finding in patients with different types of epilepsy and different pathologies. Dombrowski et al. (Dombrowski, Desai et al. 2001) applied cDNA array and found overexpression of MDR1, MRP2 and MRP5 in endothelial cells isolated from temporal lobe blood vessels of brain specimens from five pharmacoresistant patients undergoing temporal lobeectomy. Sisodiya et al. demonstrated both Pgp and MRP1 in astrocytic cells, but not in capillary endothelial cells, in the hippocampus in cases of hippocampal sclerosis (Sisodiya, Lin et al. 2002). More recently Aronica et al. (Aronica, Özbas-Gerçeker et al. 2004) performed detailed immunostaining studies in brain sections from 16 patients with hippocampal sclerosis and found upregulation for Pgp and MRP2 in capillary endothelium consistent with an enhanced barrier function. MRP1 was detected in glial foot processes around blood vessels, possibly functioning as a "second line" defence mechanism. In addition, novel

expression of Pgp, MRP1 and MRP2 was found in reactive astrocytes within the hippocampus in the CA1 and hilar regions. A recent post-mortem study showed Pgp overexpression in the sclerotic hippocampus of individuals with pharmacoresistant epilepsy, but not in post mortem seizure-free individuals or non-epileptogenic tissue with electrode-related injuries (Liu et al. 2012). Additionally, Pgp over expression has been studied in malformations of cortical development. Focal cortical dysplasia tissue removed from patients with pharmacoresistant epilepsy showed intralesional induction of MRP1 in dysplastic neurons, balloon cells and glial processes around blood vessels, whereas Pgp overexpression was observed primarily in the glial component and endothelial cells (Sisodiya, Lin et al. 2001).

2.7.1 Clinical Imaging of Pgp function

Pgp function at the BBB of healthy humans has been imaged and quantified using [^{11}C]-verapamil and [^{11}C]-N-desmethyl-loperamide (Kannan et al. 2009) . Recent studies have shown, however, that imaging of Pgp function at the BBB in humans may need to take into consideration a subject's age and the genetic polymorphisms of Pgp. Bartels et al. (Bartels et al. 2009) studied the Pgp function using [^{11}C]-verapamil PET in seventeen healthy volunteers with age 18-86. Analysis with statistical parametric mapping showed significantly decreased Pgp function in older subjects than in younger subjects in the internal capsule and corona radiata white matter and in orbitofrontal regions; thereby suggesting that Pgp function declines with increasing age. Furthermore, haplotypes of nucleotide polymorphisms at positions 1236, 2677 snf 3435 of the MDR1 gene

have been shown to alter Pgp activity in vivo and to alter substrate specificity in vitro. However, imaging studies with [^{11}C]-verapamil show that pharmacokinetics were unaffected in healthy volunteers who expressed either the TTT or the CGC (wild-type) haplotype (Brunner et al. 2005; Takano et al. 2006).

The promising concept of performing (R)-[^{11}C]verapamil PET scans after blockade of Pgp was recently translated into healthy human subjects (Wagner et al., 2009). Five healthy volunteers underwent paired (R)-[^{11}C]verapamil PET scans before and after intravenous administration of tariquidar (2 mg/kg of body weight). TQD administration resulted in significant increases in K_1, +49% +/- 36% of (R)-[^{11}C]verapamil across the BBB. The data from this first human study were re-analyzed region wise using an automated atlas approach to define 43 different brain regions as well as parametric maps. No regional differences in TQD-induced Pgp inhibition were detected, suggesting that there were no regional differences in Pgp function in healthy human brain (Bauer et al., 2010b). Shortly after, Eyal and co-workers confirmed the results in a study with [^{11}C]-verapamil before and during infusion of CsA (2.5 mg x kg(-1) x h(-1)) (Eyal et al., 2010). Thereby K_1 estimates were similar across gray-matter regions of the brain and the magnitude of Pgp inhibition was comparable across BBB-protected brain structures.

2.7.2 Clinical imaging of Pgp function in pharmacoresistant epilepsy

The use of PET to determine Pgp function in epilepsy patients has only started recently. A pilot study by Langer et al. (Langer et al., 2007) used PET and the radiotracer (R)-[^{11}C]verapamil to test for differences in Pgp activity between

epileptogenic and non-epileptogenic brain regions of patients with pharmacoresistant unilateral mTLE. Although statistical significance could not be reached it supported the hypothesis of Pgp overexpression. They observed increased influx rate constants from blood to brain, $K_{1,}$ and efflux rate constants from brain to blood, $k_{2,}$ in several temporal lobe regions that are known to be involved in seizure generation and propagation ipsilateral compared to contralateral. Additionally, parameter asymmetries were most prominent in parahippocampal and ambient gyrus, amygdala, medial anterior temporal lobe and lateral anterior temporal lobe. In contrast to temporal lobe volumes of interest asymmetries were minimal in regions not involved in epileptogenesis located outside the temporal lobe. A caveat of (R)-[^{11}C]verapamil is that the peripheral metabolism of the radiotracer is significantly faster in epilepsy patients compared to healthy controls. This is most likely caused by hepatic cytochrome P450 enzyme induction of AEDs (Abrahim et al., 2008). The difficulty is that these radiometabolites which are generated from the (R)-[^{11}C]verapamil are also taken up into the brain tissue independent of Pgp function and compromise the quantitative measurement of Pgp function especially when comparing different study groups such as patient and healthy controls. A study in nine patients suffering from pharmacoresistant mTLE showed a reduction of [^{18}F]MPPF for 5-HT_{1A} receptors in the epileptogenic temporal lobe compared with control values, possibly indicating Pgp overexpression (Merlet et al., 2004;Didelot et al., 2008). At steady state, brain:blood, [^{11}C]phenytoin activity was lower in the visual cortex, resulting in an average value of 1.32 (range 1.05.-1.66) in epilepsy patients compared to 1.61

(range 1.34-1.87) in non-epileptic patients (Baron et al., 1983). Whether [^{11}C]phenytoin concentration were lower in the epileptogenic focus was not addressed in this study.

Genetic polymorphism of Pgp might play a role pharmacoresistant mTLE. Only two imaging studies have been performed so far to investigate the role of Pgp and of its polymorphisms in pharmacoresistant mTLE. In a pilot study with seven patients with mTLE no apparent relationship between the ABCB1 genotype and the R-[^{11}C]verapamil efflux rate constant k_2 could be described but the sample size was small (Langer et al. 2007). On the other hand a SPECT study in patients with epilepsy the 3435CC genotype was associated with reduced brain uptake of (99mTc)sestamibi, which was correlated with drug resistance (Jensen et al. 2006). Furthermore, cerebrospinal fluid concentrations of phenobarbital were significantly lower in epilepsy patients with the 3435CC genotype (Basic et al. 2008).

CHAPTER III OBJECTIVES OF THE PROJECT

Our main objective is to validate radiotracers for Pgp activity as biomarkers for drug resistance using pharmacoresistant and seizure-free epilepsy as a biological model, the required proof-of-concept of a non-invasive molecular imaging-based tool. Epilepsy is the ideal condition for testing suitability of these imaging biomarkers, as either surgical specimens or whole brains are available for direct in-vivo / ex-vivo comparative analysis.

1. To determine test-retest variability in pharmacoresistant and seizure-free mTLE patients using PET and (R)-[^{11}C]verapamil
2. To determine the effects of chronic epilepsy and therapeutic AEDs on brain Pgp function
3. To determine the effects of the Pgp inhibitor TQD on the cerebral uptake of (R)-[^{11}C]verapamil

3.1 HYPOTHESIS

We hypothesise that:

1. In pharmacoresistant mTLE patients, the uptake of the Pgp substrate VPM is reduced in the epileptogenic relative to contralateral regions and compared to seizure-free mTLE patients and healthy controls.
2. Seizure activity worsens variability in pharmacoresistant mTLE patients compared to seizure-free mTLE patients and healthy controls.
3. The third-generation Pgp inhibitor tariquidar increases (R)-[^{11}C]verapamil uptake, but this increase is attenuated in epileptogenic

regions compared to contralateral regions of mTLE patients and to healthy controls

4. This difference is expected to be correlated with the level of Pgp expression as measured independently using immunohistochemistry.

CHAPTER IV COMMON METHODOLOGY

4.1 POSITRON EMISSION TOMOGRAPHY IMAGING

PET is a non-invasive quantitative imaging technique which can provide information about physiological and pharmacokinetic processes in vivo. These processes can be measured by intravenous injection of a radiotracer labelled with a positron emitter such as ^{15}O, ^{13}N, ^{11}C and ^{18}F. A positron is an electron with a positive electric charge. The positron travels at most a few millimetres (2-5mm) in tissue before combining with an electron. These two particle then annihilate, resulting in the simultaneous emission of two 511 keV gamma photons in opposite directions. A PET scanner is equipped with a large number of scintillation detectors arranged in a ring surrounding the object of interest. When two opposing detectors register a photon simultaneously (coincidence detection), the line along which the annihilation took place (line of response, LOR) can be determined. A PET scan consists of the collection of large numbers of these coincidence events, which take place over time. Using mathematical reconstruction methods, the location of these coincidences, and thus the location or distribution of the compound can be calculated as a function over time (Cherry 2001). PET is a powerful diagnostic tool, particular in oncology, neurological disorders and cardiovascular disease. It is possible to acquire kinetic data with a time resolution of a few seconds. This offers the possibility to image relatively rapid physiological and pharmacological processes. Furthermore, PET is very sensitive, having the ability to detect picomolar or fetomolar concentrations of ligand in the tissue of interest.

Additionally, it is quantitative, providing the potential to measure physiological or pharmacological parameters in absolute units.

4.1.1 PET data acquisition

PET scans were performed at the Wolfson Molecular Imaging centre in Manchester on the High Resolution Research Tomograph (HRRT; CTI/Siemens Molecular Imaging, TN, USA) (Figure 3). This is a dedicated brain PET scanner comprising eight flat panel detectors, with transaxial and axial field of views of 31.2. and 25.2cm, respectively. Depth-of interaction information is provided by a dual-layer scintillator (10mm LSO, 10 mm LYSO). Point source resolution varies across the field of view from approximately 2.3 to 3.2 mm (full-width-at-half maximum) in the transaxial direction and from 2.5 to 3.4 mm in the axial direction.

Figure 3: The HRRT PET scanner
On the left hand side is the custom-built BGO detector. The HRRT PET scanner is located at the Wolfson Imaging Centre, University of Manchester.

4.1.2 Head positing and transmission scans

During scanning subjects' heads were rested in the HRRT head holder. An external position tracker (Polaris Vicra, Northern Digital Inc., Waterlook, Canada) monitored the head movement during emission and transmission scans by tracking the position with the reflective tool attached to the vertex of a customized neoprene swim cap. Head movement was reduced by the snug fit of the cap within the head holder and the use of Velcro forehead and chin straps. Attenuation and scatter correction was enabled by a six minute transmission scan at the end of the dynamic emission scan using a 1.1 gigabecquerel (GBq)

$^{137}C_S$ single photon emission source (662 kiloelectron volt (keV)), the energy window for the transmission scan is 550-800 keV. The delayed and prompt coincidence events were recorded using an energy window of 400-650keV.

4.1.3 Arterial plasma input function

Radiolabeled metabolites appear in plasma after a short delay following intravenous injection of the parent tracer. Arterial blood sampling is essential in order to determine the availability of the radiotracer in the brain. Therefore prior to scanning, a 22 gauge cannula was inserted into the radial artery after subcutaneous infiltration with 1-2% lidocaine and arterial blood was sampled for the duration of the PET scan. Radioactivity in arterial blood was assayed continuously for the first 15 minutes at a rate of 5ml minutes^{-1} using a custom-built bismuth germanium oxide detector (Ranicar et al. 1991). These were combined with discrete blood samples at 5, 10, 15, 20, 30, 40, 50 and 60 minutes to calibrate the on-line blood sampling system and to determine the partition of radioactivity between plasma and erythrocytes. The plasma samples except those at 15 and 50 minutes were also analysed to measure fractions of parent tracer and radiolabeled metabolites. The arterial plasma input function was generated by combining the continuous plasma (15 minutes) with the interpolated discrete plasma samples and corrected by the fractions of VPM to total radioactivity.

Some radiolabelled metabolites of VPM are taken up into brain independently of Pgp-function and so compromise the quantitative estimation of VPM-K_1. Increased VPM metabolism in epilepsy patients has previously been reported

and is most likely caused by AED-mediated hepatic cytochrome P450 enzyme induction (Abrahim et al. 2008). To limit the effect of radiolabeled metabolites, we performed kinetic analysis using a single-tissue compartment model on the first 10 minutes of dynamic PET data (Muzi et al. 2009). For the voxel-based analysis, weighted generalized linear least squares were employed to generate parametric maps of K_1.

4.1.4 Radiochemistry

(R)-[^{11}C]verapamil was produced based on the procedure reported by Luurtsema et al (Luurtsema et al. 2002). The total radiosynthesis time was 40-45 minutes giving 2.4-5.9 GBq of formulated product at the end of the radiosynthesis.

The average product characteristics at the end of synthesis were: radiochemical purity 98.37%, co-injected stable VPM 1.08ug/mL and the specific activity was 156.71GBq/umol.

4.1.5 Metabolite-corrected (R)-[^{11}C]verapamil arterial input function

Following administration of VPM a number of radio-metabolites are formed on the timescale of a 60 minute scan. Luurtsema et al. (Luurtsema et al. 2002) referred to these as high-performance liquid chromatography metabolites (HPLC) and polar metabolites, reflecting their partition by a solid phase extraction cartridge. The HPLC metabolites retained on the cartridge were eluted and analysed by HPLC (Shimadzu Prominence HPLC, instrument control and data acquisition Shimadzu Lab Solutions version 1.11 SP1). The polar

metabolites are not retained on the cartridge because of their polarity and they are therefore lost and not accounted for. We have developed an in-house method based on in-line solid phase extraction and HPLC that avoids sample acidification and exposure to atmosphere or vacuum where there is potential for loss of polar metabolites (assumed to be [^{11}C]-formaldehyde [^{11}C]-formate and [^{11}C]-bicarbonate, all three possible polar metabolites are volatile at acidic pH). This in-house method ensures capture of these polar metabolites and allows for them to be accounted for.

4.1.6 Scanning protocol

The protocol aimed to scan subjects with VPM on the same day whenever possible with a two and a half hour break out of the camera between scans. In all subjects, a six minute [^{15}O]H2O scan to measure regional cerebral blood flow (rCBF) was performed (reported in (Walker et al. 2012)), followed ten minutes later by a 60 minute VPM scan to assess Pgp function. For each scan [^{15}O]H2O was administered as an intravenous bolus over 15 seconds and VPM was administered as an intravenous bolus over 20 seconds. The pharmacoresistant patients and healthy controls underwent a second set of [^{15}O]H2O and VPM scans on the same day 60 minutes after a 30 minute intravenous infusion of 2 or 3mg/kg TQD (Figure 4). The seizure-free mTLE patients also underwent a second set of [^{15}O]H2O and VPM scans on the same day to assess test-retest reproducibility but did not receive TQD. The injection doses for the baseline scans in pharmacoresistant, seizure-free patients and healthy controls were 535 ± 37 MBq, 543 ± 41 MBq and 559 ± 23 MBq, respectively as well as 552 ± 48

MBq and 535 ± 63 MBq for pharmacoresistant patients and healthy controls for all the blocking scans.

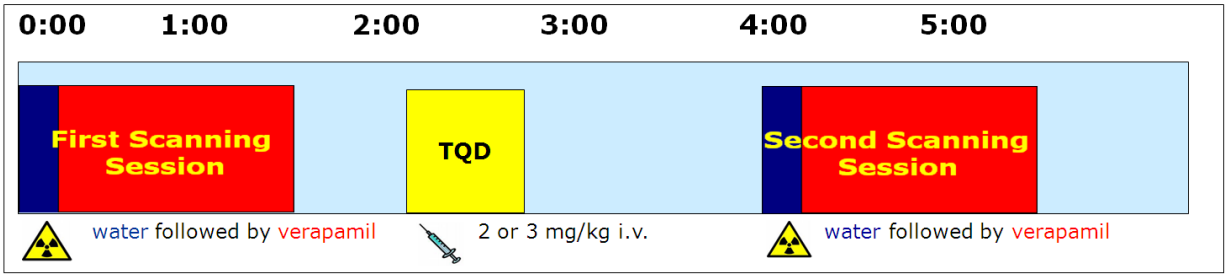

Figure 4: Scanning protocol of [^{15}O]H2O and VPM PET scans

Initially a dose of 2 mg/kg TQD was administered to pharmacoresistant patients based on previously published data (Wagner et al. 2009). To prove our basic assumption about partial Pgp inhibition increasing the difference between areas of Pgp overactivity and normality, we scanned a further seven pharmacoresistant patients and six healthy controls with 3 mg/kg TQD (Kuntner et al. 2010). Baseline- and inhibitor-scans were acquired in fixed order because of the long half- life of TQD (18-36 hours).

The dynamic 3D acquisition in list mode lasted 60 minutes for the VPM-PET scan and was reconstructed into 28 frames, a variable background frame followed by 6 x 5 seconds, 5 x 10 seconds, 3 x 30 seconds, 3 x 60 seconds, 3 x 120 seconds, 6 x 300 seconds and 2 x 600 seconds.

4.1.7 Image reconstruction

4.1.7.1 Image reconstruction for regional analysis

The images were reconstructed using ordinary Poisson (OP)-OSEM with 16 subsets and ten iterations. The transmission scan, acquired after the emission scan, was segmented and co-registered to the first ten minutes of emission data in order to correct for head motion prior to use in attenuation and scatter corrections (Anton-Rodriguez et al. 2010).

4.1.7.2 Image reconstruction with motion correction for parametric images

The VPM-PET images for the voxel-based analysis were reconstructed using OP-OSEM with resolution modeling (RM-OP-OSEM) (Sureau et al. 2008) with 16 subsets and 20 iterations. To correct for head motion a frame-by-frame motion correction approach was used (Anton-Rodriguez et al. 2010): 1) the transmission scan was co-registered to non-attenuation corrected VPM-PET image from the first 6 minutes of the dynamic scan using the software Vinci (version 2.55). 2) The whole dynamic scan was then reconstructed without attenuation correction into 28 frames. 3) Each frame was co-registered to the reference frame using the software Vinci and the individual transformation matrices were saved. 4) The transformation matrices were applied to co-registered transmission scan (in reference frame space) to move the transmission scan in individual frame space. 5) The whole dynamic scan was reconstructed using the transmission scan in individual frame space with attenuation and scatter corrections. 6) The transformation matrices were then

applied to individual reconstructed dynamic frames to co-register individual frames into reference frame space.

4.1.8 PET data correction

4.1.8.1 Attenuation

Attenuation is the loss of true coincidences detection events, due to photons being absorbed within the body or being scattered out of the detector field of view. Those photons may interact with the body; then the photons are scattered or/and absorbed by the body causing the true emission to be attenuated. Then any signal measured will be lower than expected. The loss of true coincidence event detection due to attenuation in PET imaging can range between 50 to 95%, especially in a large person. The reconstructed image is affected increasing noise, artefacts and distortion. The most accurate attenuation correction methods are based on measured transmission scans acquired before, during or after the emission scan (Kuhl et al. 1966). Alternatively, methods using segmented areas can compensate for photon attenuation in reconstructed images (Bailey 1998). In PET the correction for attenuation is exact, as attenuation is independent of the origin of the annihilation along a LOR. In other words, the probability of transmission for a pair of annihilation gamma rays travelling on a particular LOR, can be determines as the ratio of the number of gamma rays counted in the LOR from the transmission source with and with attenuation object in place. The main advantage of attenuation correction is an improved anatomic delineation and the ability to quantify tracer uptake.

4.1.8.2 Scatter

The scatter event is originated from a single annihilation, but one (or both) photons change its trajectory while they are crossing the body or within the detector space. If the photon is registered by the detection system, the event collected does not have the information of the annihilation point. The problem is that the scatter events in some systems cannot be distinguished electronically from true events. The events together with the true events are used to reconstruct the PET image, resulting in a low contrast image with an overestimation of activity concentration. The sensivity to scattered coincidences is greater in 3D mode than in 2D mode and therefore accurate scatter corrections are required. The commonly used scatter correction method for modern PET estimates scatter events based on simulation, such as Watson (Watson 1997; Watson 2000). The algorithm uses the attenuation map obtained from a transmission scan together with the emission data and a model of the scanner geometry and detector systems to calculate the percentage of photons falling on each detector using the Klein-Nishina formula (Klein and Nishina 1929). The Klein-Nishina formula gives the differential scattering cross-section as a function of scattering angle. Generally this methods are highly accurate but if the activity is outside the field of view these methods starts to fail and more complete treatments of scatter which are more time consuming can be used (Markiewicz et al. 2007).

4.1.8.3 Random correction

Depending on the length of the timing window, there is a probability that two single photons originated from two different annihilation points can be measured in coincidence in a particular LOR. This event is referred as “random”. The created event does not include useful information about the radio tracer distribution within the body. The distribution of random coincidences is fairly uniform across the field of view, causing an incorrect isotope concentration if not corrected. Random events can be measured by introducing the delayed coincidence window (e.g. many times longer than the coincidence time window). The random coincidence events can be estimated using the coincidence events recorded during the delayed time window. After estimating the random events using the delayed time window, the random events can either be subtracted from the prompt events or more optimally be taken into account during image reconstruction (Yamamoto et al. 1986; Brasse et al. 2005).

4.1.8.4 Normalisation correction

Detectors in the PET scanner vary in their manufacture and performance. These variations lead to differences in the relative sensitivity between detectors and subsequently leading to different sensitivity for each LOR. This difference in sensitivity is accounted for by scanner normalisation. Normalisation coefficient can be measured by two methods: direct normalisation and component-based normalisation. The direct normalisation measures the normalisation coefficient by calculating the sensivity along each LOR. This is preformed by exposing the detectors to a rotating source. The difference between the expected count rate and detected count rate can represent the detector sensitivity. Component

based normalisation splits the normalisation coefficient into a few components. Each of the components is calculated as the final normalisation coefficient (Defrise et al. 1991; Oakes et al. 1997).

4.2 MAGNETIC RESONANCE IMAGING

PET allows the imaging of functional properties in the living tissue, whereas other modalities (CT/MRI) provide structural information at significantly higher resolution and better image quality (Turkheimer et al. 2008). Magnetic resonance imaging (MRI) is commonly used synergistically in PET studies to allow both anatomic and functional correlation. Fusion between functional and structural images is made practical by co-registering the two image modalities. MRI uses the magnetic properties of hydrogen and its interaction with both a large external magnetic field and radiowaves to produce highly detailed images of the human body. The human body primarily consists of fat and water which have many hydrogen atoms (approximately 63% of hydrogen atoms). The hydrogen atom has only one proton and consequently possesses a magnetic moment allowing its use for magnetic resonance imaging. The basis of MRI is the directional magnetic field, or moment, associated with charged particles in motion. Nuclei containing an odd number of protons and/or neutrons have a characteristic motion or precession. Because nuclei are charged particles, this precession produces a small magnetic moment. When a human body is placed in a large magnetic field, many of the free hydrogen nuclei align themselves with the direction of the magnetic field. To obtain an MR image of an object, the

object is placed in a uniform magnetic field of 0.5-3 Tesla. As results, the objects hydrogen nuclei align with the magnetic field and create a net magnetic Moment

4.2.1 MRI acquisition

For all subjects, a T1-weighted MRI brain scan was acquired on a 3 Tesla GE Excite II scanner (General Electric, Waukesha, Milwaukee, WI, USA). Standard imaging gradients with a maximum strength of $40mTm^{-1}$ and slew rate 150 $Tm^{-1}s^{-1}$ were used. All data were acquired using an eight-channel array head coil for reception and the body coil for transmission.

4.3 IMAGE ANALYSIS

The dynamic image set, describing the uptake and subsequent wash-out of the tracer following intravenous injection, and the arterial plasma input function, describing the kinetic processes in the tissue, can be used to derive regional parameters such as the transport rate constant from blood to tissue, K_1, the efflux rate constant k_2 and the ratio of radioactivity concentration in tissue to that of plasma at equilibrium (Innis et al. 2007). These parameters are derived via modelling techniques. A tracer kinetic model provides the basis for operational equations for estimates of these physiological parameters form the acquired data (Gunn et al. 2001). The essential underlying assumption is that the observed time course of tissue radioactivity is the convolution of the arterial input and tissue response function which describes the physiological process under study at each voxel.

4.3.1 Compartment model

Compartment models are the commonest form of a tracer kinetic model used in PET (Gunn et al. 2001). A compartment is a volume within which the tracer rapidly becomes uniformly distributed. In order to interpret the observed PET data over time, we assume there are physiologically separate pools of tracer substances as “compartments”. A model which is too complex results in parameter estimates with large variances. In practice, simplified models and operational equations are developed in which the number of compartments are reduced by grouping them unto functional compartments that contain substructures for which no or only partial information is provided. The number, definition and interrelationship of compartments in a compartmental model are developed from knowledge of the biological properties of the radiotracer in question.

4.3.1.1 Single tissue compartment model

It has been shown that the single tissue compartment model adequately describes the kinetics of VPM (Lubberink et al. 2006). Hereby, the function of Pgp is measured as decrease in K_1 as its entry into the brain is blocked (Kannan et al. 2009). Pgp is situated in the lipid bilayer (Figure 5) and captures substrates before they enter the intracellular compartment. Therefore, if Pgp captures all of the substrate while in transit through the membrane its effect is entirely on K_1. However, if some of the substrate escapes and has time to interact with the intracellular milieu, and if there is an efflux from the cell later, Pgp will both decrease K_1 and increase k_2 (Kannan et al. 2009).

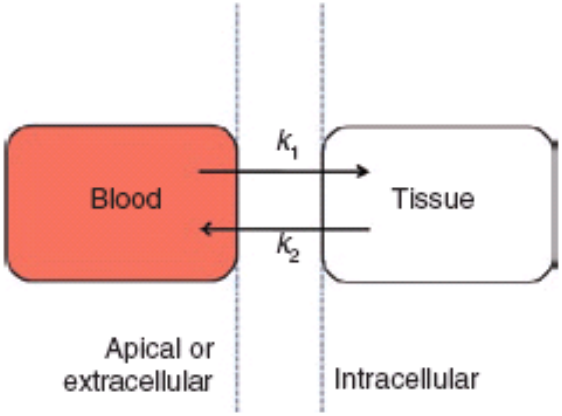

Figure 5: The single input, single tissue compartment model.
K_1 is the transport rate from blood to brain and k_2 is the transport rate from brain to blood. The figure is from Kannan et al. (Kannan et al. 2009).

The single tissue compartment model is the simplest compartment model and only has one tissue compartment. The first compartment is the arterial blood. From arterial blood, the radiotracer passes into the second compartment, known as the free compartment. Data obtained by PET camera are a summation of these compartments. The parameters can be estimated by fitting the model to measure PET data with arterial radioactivity concentrate as input function. The arterial radioactivity concentration must be measure separately from PET data acquisition (Watabe et al. 2006).

4.3.2 Region of interest analysis

Cerebral region of interests (ROIs) can be produced either manually or automatically. The manual delineation requires an experienced operator to draw the ROI on the raw T1 MR image. The procedure is time consuming, and gives rise to observer bias and partial volume effect. Alternatively, fully automatic ROI definition is reproducible and comparable with manual intervention. There are

currently a few fully automated methods for cerebral ROI definition. Babalola et al (Babalola et al. 2009) compared four different automated methods of segmenting subcortical brain structures and concluded that brain atlas based labelling and active appearance modelling are the most successful methods against the gold standard manual delineation. Predefined brain atlases are required for atlas based ROI labelling serving as prior anatomical knowledge of the brain. Typically a brain atlas is created in a template space (e.g. Montreal Neurological Institute (MNI) space). To register the brain atlas from template space to individual space MRI normalisation is necessary. A template MR image can be normalised into individual MR space and the non-linear transformation can be applied to the brain atlas to move the atlas into individual space. Three steps are usually required to create individual anatomical ROIs for the PET analysis:

a. Segmentation of MR images to separate components of gray matter (GM), white matter (WM) and cerebrospinal fluid (CSF).
b. Because the brain atlas is commonly generated in MNI space the brain atlas has to be registered into an individual MRI space to be used. The procedure involves non-rigid registration and is commonly referred to a normalisation.
c. MRI-PET registration. After the ROI definition those ROIs should be moved into PET space for PET data analysis. This is performed through MRI-PET image co-registration. Since this is within subject registration, it is also an affine rigid body registration.

4.3.2.1 MR Image segmentation

Normal MRI brain image without the skull can be generally classified into three main tissue components: GM, WM and CSF. The MR Image segmentation can be generally divided into two main categories: Structural segmentation and statistical segmentation. There are many structural based segmentation methods proposed in the literature, such as region growing and edge detection but they are generally not thought to be very robust. Statistical approaches classify tissue classes based on the intensity distribution of the image (i.e. histogram). The simplest method is to threshold the image to segment different tissue types. However, if a hard threshold is chosen, it is likely to be inaccurate. Several conditions can make the separation of statistical brain segmentation worse because the spatial information is not taken into account, which requires the brain image to be well defined with low noise level and higher spatial resolution. To achieve this efforts have been spent to correct for head motion artefact and non-uniformity of the image.

4.3.2.2 MRI image normalisation

MR image registration can be divided into within-subject registration and between–subject registration. Within-subject registration is simply applied to register MR images from the same subject but acquired under different conditions (e.g. different positions, scanner, MR sequences or image modalities). Usually rigid-body registration (three translations, three rotations) is performed to align two brain MR images because they are from the same brain. However, between-subject image registration will require non-rigid image registration which is often referred to as spatial normalisation. The aim of the

MR image normalisation is to map once space to another space. An affine transformation including 12 parameters is used (three rotations, three translations, three shears and three zooms). Rigid-body transformation (three rotation and three translations) can be seen as a simplified form of affine transformation. For the analysis we used statistical parametric mapping (SPM, http://www.fil.ion.ucl.ac.uk/spm/software/spm8, Wellcome Trust Centre for Neuroimaging, London, UK). This normalisation algorithm starts with a 12 degree of freedom affine registration to initialise the normalisation process, followed by an iterative non-linear registration which estimates the non-linear warping field (or deformation field) from template MR image to target MR image. The affine transformation and non-linear deformation field define the mapping information from one MR space (i.e. brain atlas template MR) to another MR space (i.e. individual MR).

4.3.2.3 Multi-modality Image Registration using MR images

After generating the brain ROIs in individual MR space, the next step is to register those ROIs into PET space. Because this process is a within subject registration rigid body registration is appropriate. As PET and MR are images provide functional and anatomical information they are hugely different from each other. An accurate MRI-to-PET co-registration can be achieved by maximizing the normalized mutual information. The MRI-to-PET co-registration used in this study is discussed in the next chapter 4.3.2.4 for the ROI analysis and in chapter 4.3.3.2 for the voxel-based analysis.

4.3.2.4 Cerebral region of interest generation

We used a maximum probability brain atlas (Hammers et al. 2003), to define ROIs on the 3T T1-weighted MR images. First the brain was extracted from the MR image using the FMRIB Software Library (FSL)'s BET toolbox (Smith 2002). Secondly, the extracted brain was segmented in to GM, WM and CSF with correction for spatial intensity variations across the image (bias correction). Thirdly, the GM maps were thresholded at 50% to generate a GM mask. Fourthly, an MR template was normalised (using non-linear registration) to the bias corrected MR image using SPM 8 (Ashburner and Friston 1997). Finally, the normalised brain atlas was multiplied by the GM masks to generate GM ROIs.

The co-registration from MRI space to VPM-PET space was performed via the [^{15}O]H2O scan using SPM 8. First, the bias corrected MR image was co-registered to a summation image of the whole dynamic [^{15}O]H2O scan smoothed with a 4-mm Gaussian filter and the transformation was saved (TX1). Second, a summation image of the first ten minutes of the dynamic VPM-PET scan, assuming to have negligible head motion, was also smoothed with a 4-mm Gaussian filter. Third, the smoothed VPM-PET image was co-registered to the smoothed [^{15}O]H2O scan and the transformation saved (TX2). Fourth, the transformation from the MRI space to VPM-PET space was calculated by combining the two transformations ($TX=TX1 \times TX2^{-1}$). Finally, the GM ROIs were transferred into VPM-PET space by applying the combined transformation (TX) and nearest neighbour interpolation.

Tissue time-activity curves of each ROI were generated by overlaying these ROIs to the dynamic PET using Tacstats (in-house software).

All GM ROIs excluding the ventricles were combined to generate the whole brain GM ROI. Eight additional ROIs were selected. Six different temporal lobe ROIs (lateral anterior temporal lobe, inferior temporal gyrus, occipitotemporal gyrus., parahippocampal and ambient gyrus, posterior temporal lobe, anterior superior temporal gyrus) and the extratemporal control ROI (superior parietal gyrus) as well as cerebellum and whole brain. The abbreviations for the ROIs are as follows: Ant TL lat, lateral anterior temporal lobe; Inf-Mid TL, inferior temporal gyrus; Occ TL, occipitotemporal gyrus.; ParaH, parahippocampal and ambient gyrus; Post TL, posterior temporal lobe; Sup TL ant, anterior superior temporal gyrus; Sup PL, superior parietal gyrus.

4.3.3 Voxel based Analysis

4.3.3.1 Statistical Parametric Mapping

SPM is generally used to identify functionally specialised brain responses and is the most prevalent approach to characterising functional anatomy and disease-related changes. It does this characterisation by treating each voxel separately and by performing voxel-wise statistical analysis in parallel creating an image of statistics. SPM refers to the construction of spatially extended statistical processes to test hypotheses about regionally specific effects. SPMs are image processes with voxel values that are, under the null hypothesis, distributed according to a known probability density function (usually Gaussian). These statistical parametric maps, are 3D projections of statistical functions that are

used to characterise significant regional brain differences in imaging parameters. Corrections for the implicit multiple comparisons, when making inferences based upon the statistical parametric map are confounded by spatial correlations. The theory of Gaussians fields is used to provide values that are corrected for the brain volume analysed (Friston 1997).

4.3.3.2 Pre-processing for SPM Analysis

All the image pre-processing steps were performed using the SPM 8 software (http://www.fil.ion.ucl.ac.uk/spm/software/spm8, Wellcome Trust Centre for Neuroimaging London, UK). First, the MR images from all subjects were segmented into GM, WM and CSF using the New Segmentation option (Ashburner and Friston 2005). During this segmentation fast diffeomorphic registration algorithm (DARTEL) parameters were also saved (Ashburner 2007). Second, a DARTEL template was created using the pharmacoresistant and seizure-free mTLE patients as well as the healthy controls. This DARTEL template was made symmetrical and centered following the method by Didelot et al. (Didelot et al. 2010) and normalized to MNI space. Third, summation VPM-PET images were smoothed with a 4mm Gaussian filter and co-registered with the corresponding native space MR images which was skull stripped and smoothed with a 6-mm Gaussian filter. Fourth, the co-registered VPM-PET images and the individual gray matter probability maps (from the previous segmentation step) were right-left reversed, providing the flipped counterpart. Fifth, the unflipped and flipped gray matter probability maps were normalised to the symmetric and centered DARTEL template. The normalisation parameters

were saved and applied to the co-registered unflipped and flipped VPM-PET images, resulting in all VPM-K_1 maps being in MNI space. Because of spill in from the CP into the neighbouring hippocampus (Figure 6), the CP, the region with the highest VPM uptake, was individually masked out of the VPM-K_1 maps using individual threshold values (see for further details in following paragraph "Manual delineation of CP and generation of CP mask").

To normalize the effect of the different metabolism between the three groups, ratio images were created by first dividing the mean gray matter whole brain of the VPM-K_1 of all patients and controls by the individual mean gray matter whole brain VPM-K_1 and then multiplying the individual masked VPM-K_1 parametric maps with this value. The masked VPM-K_1 maps and ratio images were finally smoothed using an isotropic 8-mm Gaussian filter. These images were then used for the voxel-based SPM analysis which was restricted to voxels belonging to the gray matter by applying the gray matter probabilistic map thresholded at $x > 0.3$ to the symmetric and centered DARTEL template (see generation of Gray matter mask in next paragraph).

4.3.3.3 Generation of Gray matter mask

The voxel-based SPM analysis was restricted to voxels belonging to gray matter by applying a mask obtained by thresholding at $x > 0.5$ the probabilistic map of GM within the SPM distribution (/spm8/apriori/gray.nii). This mask was then multiplied with the invert of the CP mask (creation of CP mask described in chapter below "Generation of CP") to mask out voxel belonging to the CP contaminating into surrounding ROIs such as the hippocampus. This gray matter

mask was then applied to the SPM analysis, to sample the gray matter of the parametric images and remove the CP spill over into regions around it.

4.3.3.4 Generation of choroid plexus mask

The hippocampus cannot be correctly analyzed quantitatively in VPM-PET images due to a serious spill-over of activity (partial volume effects) from the adjacent CP, the region with by far the highest signal intensity (Figure 6).

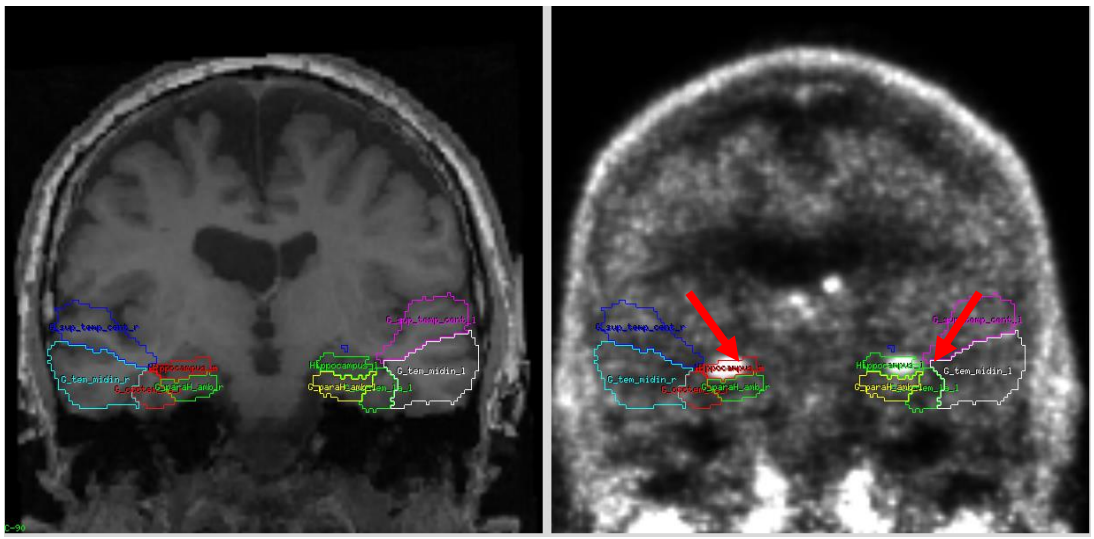

Figure 6: T1-weighted MR image and VPM-PET summation image
The MR image is on the left and the PET summation image is on the right. The images show ROIs in the temporal lobe. The arrow indicates the spill in from the CP in the adjacent hippocampus.

Therefore the ROI CP was masked out manually using the FMRIB Software Library (FSL, Release 5.0, 2012, The University of Oxford). We first created a binary mask of the CP applying individual thresholds to smoothed VPM-K_1 maps using an isotropic 4 mm Gaussian filter (figure 7 b) and in a second step this binary mask was inverted and in a third step the inverted CP mask was multiplied to the original VPM-K_1 maps (figure 7 c) so that the CP is masked out on the original VPM-K_1 maps.

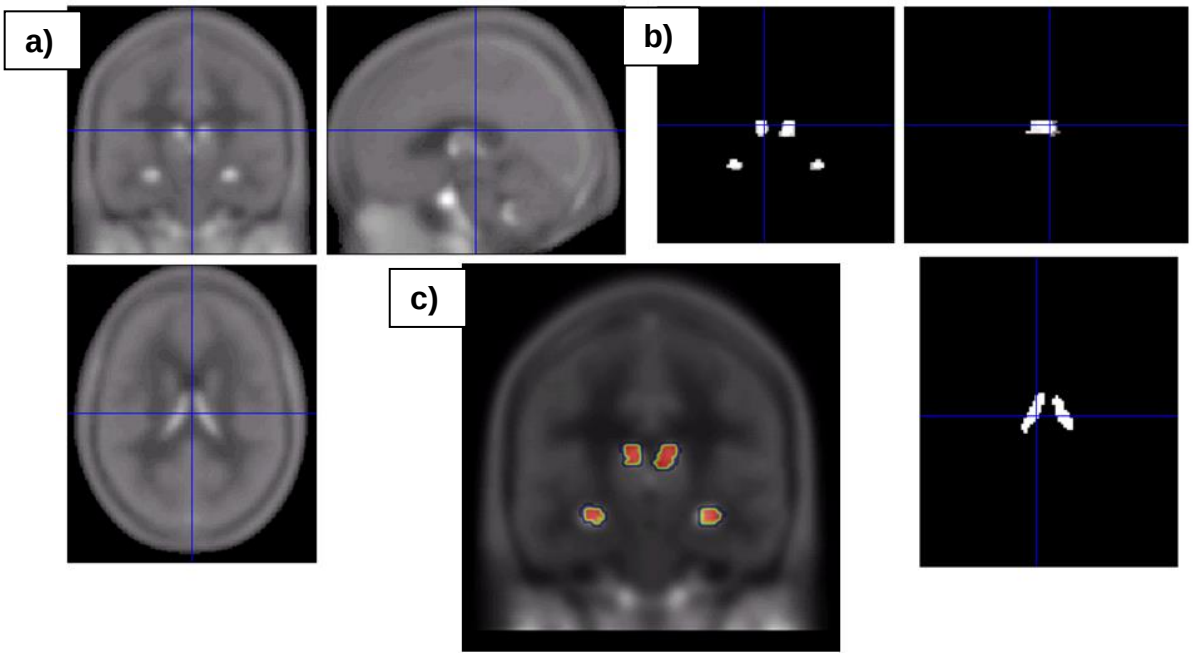

Figure 7: Generation of CP mask on VPM-PET Images
Picture (a) shows the high VPM upatake in the CP on a VPM PET summation image. Picture (b) shows a binary CP mask. Picture (c) illustrates the CP mask on VPM PET summation image.

4.4 STATISTICAL ANALYSIS

4.4.1 Statistical Analysis for region of interest analysis

The analyses were performed using SPSS 19.0 (SPSS Inc., Chicago). We used independent t-tests to compare the means between two groups. To compare multiple groups, we used analysis of variance (ANOVA), calculated Pearson correlation coefficients for normally distributed data, or Spearman's rank-order correlations otherwise. For pharmacoresistant mTLE patients only, we performed correlation analyses of VPM brain uptake at baseline with seizure frequency, for both whole brain and temporal lobe, the focus region for all mTLE patients. Differences were considered to reach statistical significance when $p < 0.05$.

4.4.2 Statistical Analysis for voxel-based analysis

We used independent t-tests to compare the means between two groups. To compare multiple groups, we used ANOVA, calculated Pearson correlation coefficients for normally distributed data, or Spearman's rank-order correlations otherwise. For pharmacoresistant patients only, we performed correlation analyses of VPM brain uptake at baseline with seizure frequency, for both whole brain and ipsilateral hippocampus, the focus region for all mTLE patients. The analyses were performed using SPSS 19.0. All comparisons were 2-tailed unless otherwise specified. Differences were considered to reach statistical significance when $p < 0.05$. We compared voxel-by-voxel parametric VPM-PET images of pharmacoresistant to seizure-free mTLE patients and healthy controls using factorial design analysis within SPM 8, considering age and gender as confounders and we used group and laterality as between-subjects factors assuming unequal variances between groups. The analysis was restricted to voxels belonging to grey matter by applying an additional probabilistic map with a threshold of 30% grey matter probability. Significance for activations in whole brain for areas without a-priori hypothesis was set at $p<0.001$. Based on a-priori hypothesis that P-glycoprotein is altered in the temporal lobes, activations within temporal lobe regions are considered significant for $p<0.01$ (uncorrected). In view of the smaller size of the hippocampus, we report changes for this region at $p<0.05$.

4.5 RECRUITMENT

4.5.1 MTLE Patients

We recruited 16 pharmacoresistant (PR, six male, median age 39.5 years, range 18-56) and eight seizure-free (SF) mTLE patients (three male, median age 45 years, range 23-53) with unilateral hippocampus sclerosis as well as three pharmacoresistant epilepsy patients with focal cortical dysplasia (two male, median age 37, range 24-62) between October 2008 and November 2011, from consultant-led outpatient clinics at the National Hospital for Neurology and Neurosurgery, a tertiary, nation-wide referral centre with an additional local catchment area of three million people in North London. Pharmacoresistance was defined as on-going seizures despite two tolerated and appropriately prescribed AEDs (Kwan et al. 2010). Seizure-free mTLE patients had active epilepsy for at least three years, but were free of all seizures on AEDs for at least one year prior to PET scanning. Seizure semiology and onset was concordant with side of HS, as verified with prolonged and repeated EEG recordings when epilepsy was active. Pharmacoresistant mTLE patients were matched to seizure-free mTLE patients according to gender, age and antiepileptic drugs. The numbers of patients needed for the study were based on power calculations using standard formulae (Dupont and Plummer Jr 1990). Six patients are usually required to allow a detailed analysis of the validity and reproducibility of radiotracers (Hammers et al. 2007a). The published test-retest variability of (R)-[^{11}C]verapamil brain uptake is 5% (Lubberink et al. 2006). For comparisons of groups with assumed unequal variance, group sizes of 13

patients with pharmacoresistant mTLE and six seizure-free mTLE control patients are sufficient to detect a moderate effect size (dt=0.7, at a=0.05, two-tailed and b=0.08). Assuming a failure rate of 20%, we aimed to recruit at least 16 pharmacoresistant and eight seizure-free mTLE patients, and 16 healthy controls for inclusion in our study (Figure 8).

4.5.1.1 MTLE Patients' inclusion/exclusion criteria

The inclusion criteria included, males and females aged 18−60, diagnosis of temporal lobe epilepsy (from history, clinical examination, EEG and imaging data and other data if available, e.g. video−EEG with ictal recordings, neuropsychology), currently treated with AEDs known to be a substrate for Pgp or multidrug resistance protein-1 (MRP1), willing and able to give informed consent. Exclusion criteria included relevant medical, particularly neurological, condition other than temporal lobe epilepsy (e.g. subjects with a history of stroke will have abnormal brain anatomy which would interfere with analyses), notably history of alcohol or benzodiazepine abuse, high-quality volumetric MRI identified structural abnormalities other than hippocampal sclerosis or prolonged EEG recordings (ictal video-EEG telemetry for pharmacoresistant mTLE) identified other than mesio-temporal seizure-onset, standard MRI exclusion criteria, participation in another trial involving medicinal products in the last three months or in another procedure involving ionising radiation in the past year, inability to give informed consent or pregnancy.

4.5.2 Healthy controls

Seventeen healthy controls (eight male, median age 45 years, range 35-55) were recruited locally by newspaper advertisement and posters displayed in the community. Males and females were included aged 35−55 (age limits were chosen in order not to expose younger persons to the radiation dose, Figure 8).

4.5.2.1 Healthy controls inclusion/exclusion criteria

Subjects were required to be in good health on the basis of medical history, vital signs, physical examination and laboratory investigations. Exclusion criteria included relevant medical, particularly neurological, condition, notably history of alcohol or benzodiazepine abuse, regular or recent intake of medication known to be a substrate (e.g.: amiodaron, digoxin, steroids, loperamide, colchicine, amytriptyline, b-blockers, erythromycin, rifampicin) or inhibitor (e.g.: CsA, quinidine, ketoconalzole) for Pgp or MPR1, standard MRI exclusion criteria, participation in another trial involving medicinal products in the last three months or in another procedure involving ionising radiation in the past year, inability to give informed consent, or pregnancy. Controls were matched for age and gender with the patients. Prior to PET scanning, subjects were asked to refrain from using alcohol with the preceding 24 hours.

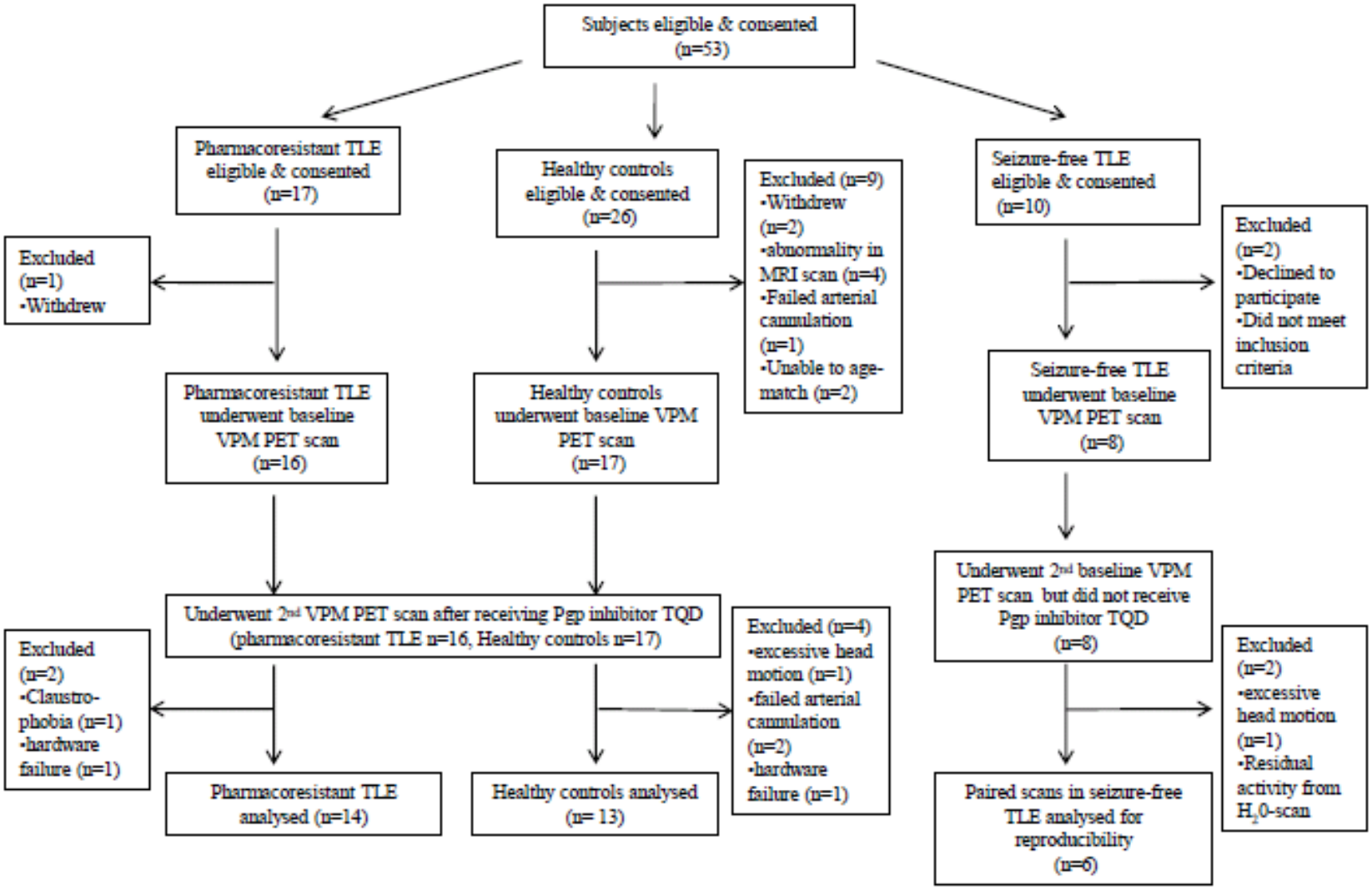

Figure 8: Flowchart of subjects' recruitment and selection process

The study was approved by the London – City Road and Hampstead Ethic Committee previously known as Moorfields and Whittington Research Ethics Committee then East Central London REC 1 and by the United Kingdom Administration of Radioactive Substances Advisory Committee (ARSAC). All subjects provided written informed consent after receiving written and verbal explanation of the study.

CHAPTER V (R)-[^{11}C]VERAPAMIL PET AT BASELINE IN PHARMACORESISTANT AND SEIZURE-FREE MTLE PATIENTS VERSUS HEALTHY CONTROLS – REGION OF INTEREST ANALYSIS

5.1 BACKGROUND

Pgp has been shown to contribute to pharmacoresistance in rodent epilepsy models: (i) pharmacoresistant rats exhibit higher endothelial Pgp-expression in limbic regions ipsilateral to the seizure focus compared to seizure-free rat (Volk and Loescher 2005), (ii) seizures transiently increase Pgp-expression at the BBB (Bankstahl and Löscher 2008), (iii) increased Pgp-expression is associated with decreased brain concentration of Pgp-substrate AEDs (van Vliet et al. 2007) and (iv) Pgp-inhibition enhances AED efficacy (Brandt et al. 2006). Human studies showed increased Pgp-expression at the BBB, ex-vivo in epileptogenic tissues removed at surgery from patients with pharmacoresistant epilepsy (Tishler et al. 1995; Sisodiya et al. 2002; Aronica et al. 2004) or post-mortem (Liu et al. 2012). The functional relevance of this increased expression in humans cannot be assessed ex-vivo. Using in-vivo positron emission tomography (PET) experiments with the Pgp-substrate (R)-[^{11}C]verapamil (VPM), we studied pharmacoresistant and seizure-free patients with mesial temporal lobe epilepsy (mTLE) due to unilateral hippocampal sclerosis (HS) as well as healthy controls, testing the hypotheses that Pgp-activity is higher in pharmacoresistant than seizure-free mTLE patients and healthy controls, and that Pgp overactivity is most pronounced in the epileptic focus.

5.2 METHODS

The common methods are described in Chapter 4, and the specific methods for this study are described here.

5.2.1 Subjects

Seventeen healthy controls and 16 pharmacoresistant and eight seizure-free mTLE patients with unilateral HS were included in this study. Data from four healthy controls and two pharmacoresistant mTLE patients were excluded due to technical problems: failure to sample arterial blood for input function (n=2); hardware failure (n=2), excessive head motion (n=1), claustrophobia (n=1). Therefore, 14 pharmacoresistant mTLE patients, eight seizure-free mTLE patients and 13 healthy controls were included in the data analysis (Figure 7).

5.2.2 Radiochemistry

(R)-[^{11}C]verapamil was synthesised as previously described (refer to section 4.1.4).

5.2.3 PET Image acquisition

The PET scans were performed at the Wolfson Molecular Imaging Centre, Manchester, UK, on the High Resolution Research Tomograph (CTI/Siemens, TN, USA). A 60 minute VPM-PET scan was acquired following intravenous bolus injection over 20 sec of 555 MBq of VPM. Arterial blood was sampled continuously for the first 15 minutes and discrete blood samples taken thereafter to measure the plasma radioactivity concentrations due to unmetabolised VPM for use as the input function in the kinetic modeling of the dynamic PET data (Lubberink et al. 2006). Seizure-free mTLE patients also underwent a second

scan on the same day in order to assess test-retest reproducibility (calculated as the absolute difference between test and re-test scans, divided by the average of the two scans). A 6 minute transmission scan was acquired at the end of the dynamic VPM scan using a 1.1-GBq 137Cs single photon (662 keV) point source for attenuation and scatter corrections.

5.2.4 MRI data acquisition

For all subjects, a T1-weighted MRI brain scan was acquired on a 3-Tesla GE Excite II scanner (General Electric, Milwaukee, WI, USA) for co-registration with the PET images, as previously described in section 4.2.1.

5.2.5 PET data analysis

The dynamic VPM-PET data were reconstructed and corrected for head motion as described in section 4.1.7 and 4.1.8 (Anton-Rodriguez et al. 2010). For the ROI analysis, regions were defined automatically using a maximum probability brain atlas as previously described in section 4.3.2.

Ratios of VPM-K_1 values were calculated between a reference region (parietal cortex) and target regions.

The asymmetry index (AI) was calculated as:

$$AI(\%) = \frac{ipsi - contra}{contra} \text{x}100$$

All image processing steps were performed in SPM 8, Wellcome Trust Centre for Neuroimaging London, UK as previously described in section 4.3.2.

5.2.6 Statistical Analysis

The statistical analyses were performed using SPSS 19.0 as previously described in section 4.4.1 and the level of significance was set at $p<0.05$.

5.3 RESULTS

Fourteen pharmacoresistant mTLE patients (six men, median age 38 years, range 18-56), eight seizure-free mTLE patients (three male, median age 45 years, range 23-53) and 13 healthy controls (seven men, median age 45 years, range 35-55) were studied for comparison. The pharmacoresistant mTLE patients had seizures (median: nine focal seizures with impaired awareness/month; range: 1-30) despite current treatment with a median of two AEDs (range: 1-4) and trials of a median of five AEDs (range 2-12) in the past. The eight seizure-free mTLE patients had been seizure-free for at least 12 months (median: 3.5 years; range: 1-12) and were taking a median of two AEDs (range: 2-3) at the time of scanning, with a median of three AEDs (range: 1-6 AEDs) tried previously. Patients' characteristics are summarized in Table 2.

Table 2: Clinical data of pharmacoresistant and seizure-free mTLE patients

Pat No	Gender/ Age (yrs)	Age at onset of epilepsy (yrs)	Interval last CPS (PR:days SF:yrs)	Duration of epilepsy (yrs)	Seizure frequency /month	Current AEDs (dose: mg/day)	Hippo volume (Ratio) / laterality)
Pharmacoresistant patients 2mg/kg TQD							
1	M/43	5	21	38	2	PHT(325),CLB(20), VPA(1500),LEV(2000) CBZ(1000)	47 /L
2	F/38	18	12	20	12	ZON(150),CLB(10)	69 / R
3*	F/56	11	2	45	18	LTG(200),PGB(300), LEV(750),OXC(600)	76 / R
4	M/30	19	6	11	15	CLB(20) VPA(1600),CBZ(1200)	63 / L
5	M/56	1	3	55	2	TPM(150), CBZ (400)	65 / L
6*	F/50	12	4	38	8	PHT(350),LTG(100)	82 / R
7*	F/18	2	6	16	10	LEV(3000),TPM(200)	70 / L
Pharmacoresistant patients 3mg/kg TQD							
8	F/52	4	2	48	8	LTG(500),PHT(225)	74 / R
9	F/27	8	6	19	10	CLB(20)	63 / L
10*	M/51	35	60	16	2	LEV(3000),CBZ(1600)	83 / R
11*	F/20	15	4	5	10	LEV(2250),CBZ(400), LTG(275)	76 / L
12	M/38	2	28	36	1	VPA(1000),LTG(200)	63 / L
13	F/37	33	1	4	30	LEV(2000),LTG(250)	58 / L
14	M/24	11	3	13	4	LEV(2000),CBZ(1200)	78 / L
Seizure-free patients							
1	F/50	25	3	22	n.a.	LTG(400),LEV(2000)	73/R
2	M/39	23	2	14	n.a.	CBZ(800),LEV(2000)	90/L
3	F/42	18	7	17	n.a.	CBZ(1600),CLB(40)	72/L
4	F/40	17	12	11	n.a.	VGB(500),CBZ(1400)	70/L
5	F/48	5	1	42	n.a.	PHT(450),CNZ(2), VPA(2000)	60/L
6	M/53	19	4	30	n.a.	PHT(300),LEV(1000), LTG(300)	79/R
7	M/50	35	10	5	n.a.	CBZ (1400),VGB(1500)	58/L
8	F/23	1	2	20	n.a.	LTG(50),LEV(3000), CLB(10)	58/R

M, male; F, female; R, right; L, left; CPS, complex partial seizure; PR, pharmacoresistant patients; SF, seizure-free patients; AED, antiepileptic drug; hippo, hippocampus; LEV, levetiracetam; LTG, lamotrigine; OXC, oxcarbazepine; CBZ, carbamazepine; VPA, valproic acid; PHT, phenytoin; CLB, clobazam; PGB, pregabalin; TPM, topiramate; ZON, zonisamide; VGB, vigabatrin, CNZ, clonazepam;*patients who underwent epilepsy surgery.

There was no difference in age (p=0.290) and weight (p=0.319) between the two mTLE patient groups and the healthy controls. There was no difference in injected doses of VPM/kg body weight between the three groups at baseline (pharmacoresistant mTLE patients: 540 ± 37 MBq, seizure-free mTLE patients: 536 ± 43 MBq, healthy controls: 558 ± 21 MBq; p=0.292).

5.3.1 Test-retest variability

The test-retest reproducibility (calculated as mean absolute difference) of VPM-K_1 in temporal lobe of epilepsy patients was 5.6% (n=6) for the seizure-free mTLE patients who underwent paired PET scans with VPM at baseline on the same day. There was no order effect of the time of day when the scans are performed, as indicated by the mean difference between test-retest scans of -0.8% in the temporal lobe.

5.3.2 Differences in VPM metabolism between mTLE patients and healthy controls

The function of Pgp can be quantified in-vivo using standard compartmental models (Lubberink et al. 2006). As we administer the Pgp substrate PET tracer VPM intravenously, its entry into the brain is limited, and this is measured as a decrease in K_1, the influx rate of the radiolabelled Pgp substrate. Thus, reduced VPM-K_1 equates to higher Pgp brain-to-blood transport (Abrahim et al. 2008; Muzi et al. 2009).

Metabolites of VPM are taken up into brain tissue independent of Pgp function (Abrahim et al. 2008) and so compromise the quantitative measurement of VPM-K_1. To limit the effect of radiolabeled metabolites, kinetic analysis of PET

data was performed using a single-tissue compartment model on the first ten minutes of dynamic data after VPM radiotracer injection as described in section 4.1.3 (Muzi et al. 2009).

Ten minutes after tracer injection, the fraction of unmetabolised VPM was indeed higher for healthy controls (mean±s.d.: 0.69±0.08) than for both mTLE patient groups ($p<0.001$), but not different between pharmacoresistant (0.49±0.11) and seizure-free (0.47±0.13) mTLE patients ($p=0.680$, Figure 9). Increased VPM metabolism in epilepsy patients has previously been reported and this is most likely caused by AED-mediated hepatic cytochrome P450 enzyme induction (Abrahim et al. 2008).

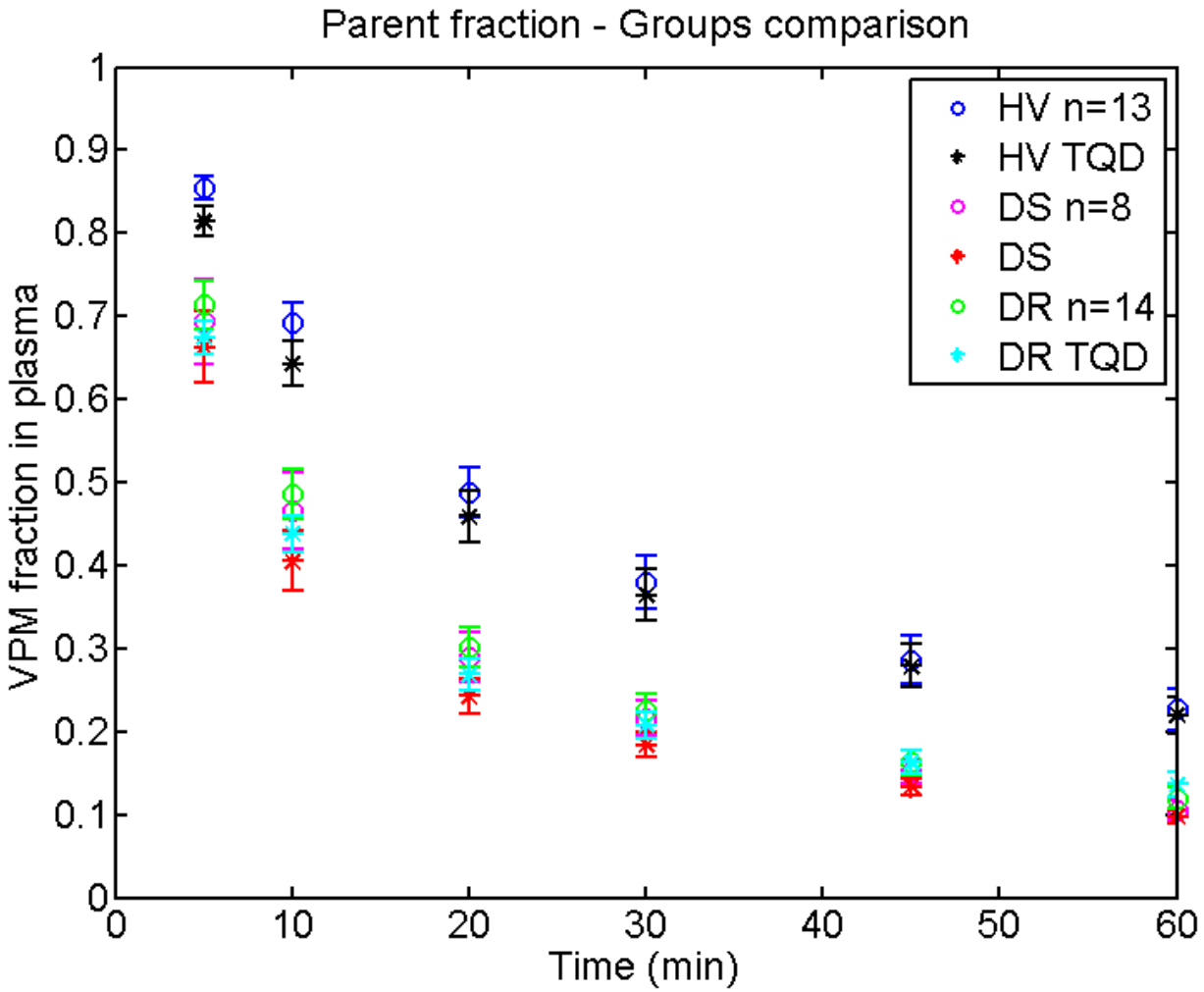

Figure 9: Differences of VPM metabolism between the three groups
VPM fraction in plasma is shown over 60 minutes for 13 healthy controls (HV), 8 seizure-free mTLE patients (DS) and 14 pharmacoresistant (DR) mTLE patients before and after tariquidar (TQD). Error bars represent SEM.

Despite minimising the effect of different VPM metabolism between controls and patients by only using the first ten minutes of data, we found a significant difference in VPM-K_1 globally across all analysed brain regions. VPM-K_1 values in whole brain were lower in healthy controls (mean ± SEM, 0.036±0.003 ml/min/cm3) compared to pharmacoresistant mTLE patients (0.049±0.004 ml/min/cm3; p=0.012) but not different compared to seizure-free mTLE patients (0.045±0.004 ml/min/cm3; p=0.138). There was no difference between seizure-free and pharmacoresistant mTLE patients (p=0.441, Figure 10).

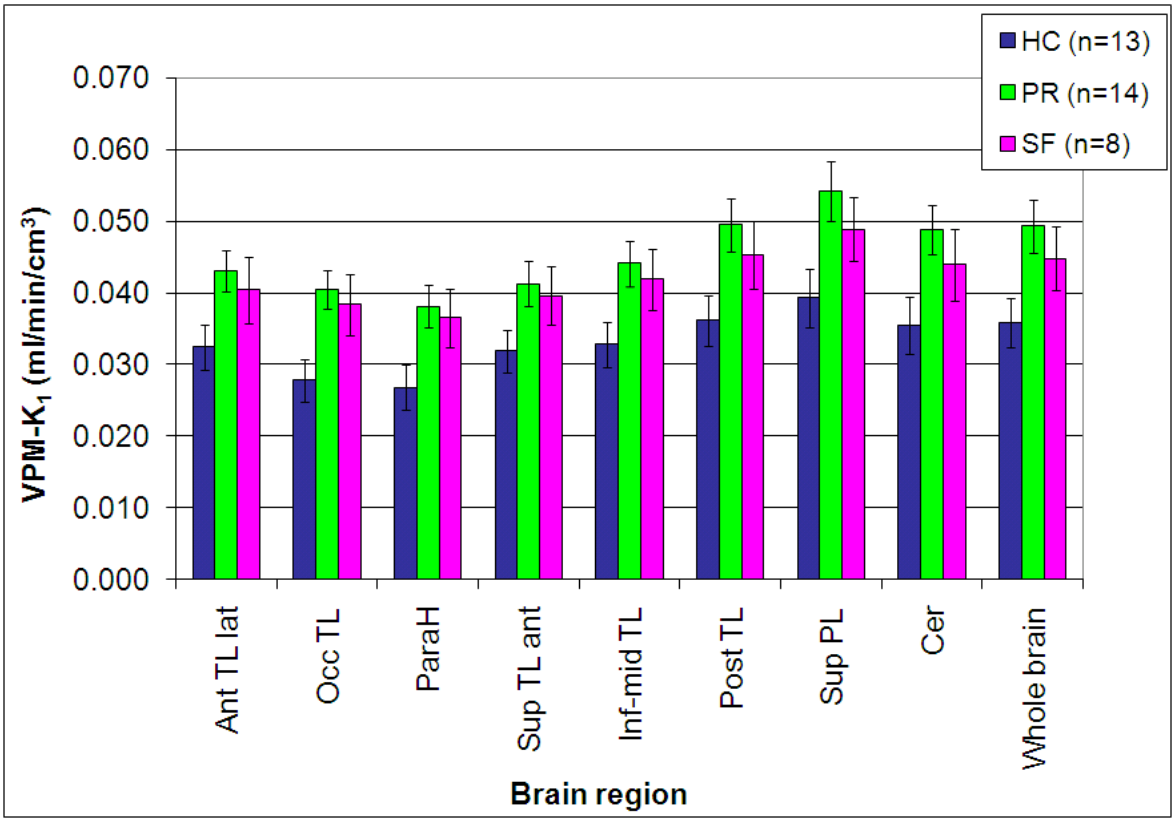

Figure 10: VPM-K_1 across eight brain regions and whole brain
VPM-K_1 is shown at baseline for 13 healthy controls (HC), 14 pharmacoresistant (PR) and eight seizure-free (SF) mTLE patients in six temporal lobe regions of interests (ROI) and the extratemporal ROI (superior parietal gyrus) as well as cerebellum and whole brain. Ant TL lat, lateral anterior temporal lobe; OccTL, occipitotemporal gyrus; ParaH, parahippocampal and ambient gyrus; Sup TL ant, anterior superior temporal gyrus; Inf-mid TL, inferior temporal gyrus; Post TL, posterior temporal lobe; Sup PL, superior parietal gyrus; Cer, cerebellum. Error bars represent SEM.

5.3.3 Differences in asymmetry index in pharmacoresistant mTLE

At baseline seizure-free mTLE patients had significantly different AI in anterior temporal lobe compared to healthy controls (p= 0.30) but AI was not significantly different compared to pharmacoresistant mTLE patients (p=0.69). There was no significant difference in the AI index for any of the other brain regions for pharmacoresistant, seizure-free mTLE patients or healthy controls (p>0.111, Figure 11).

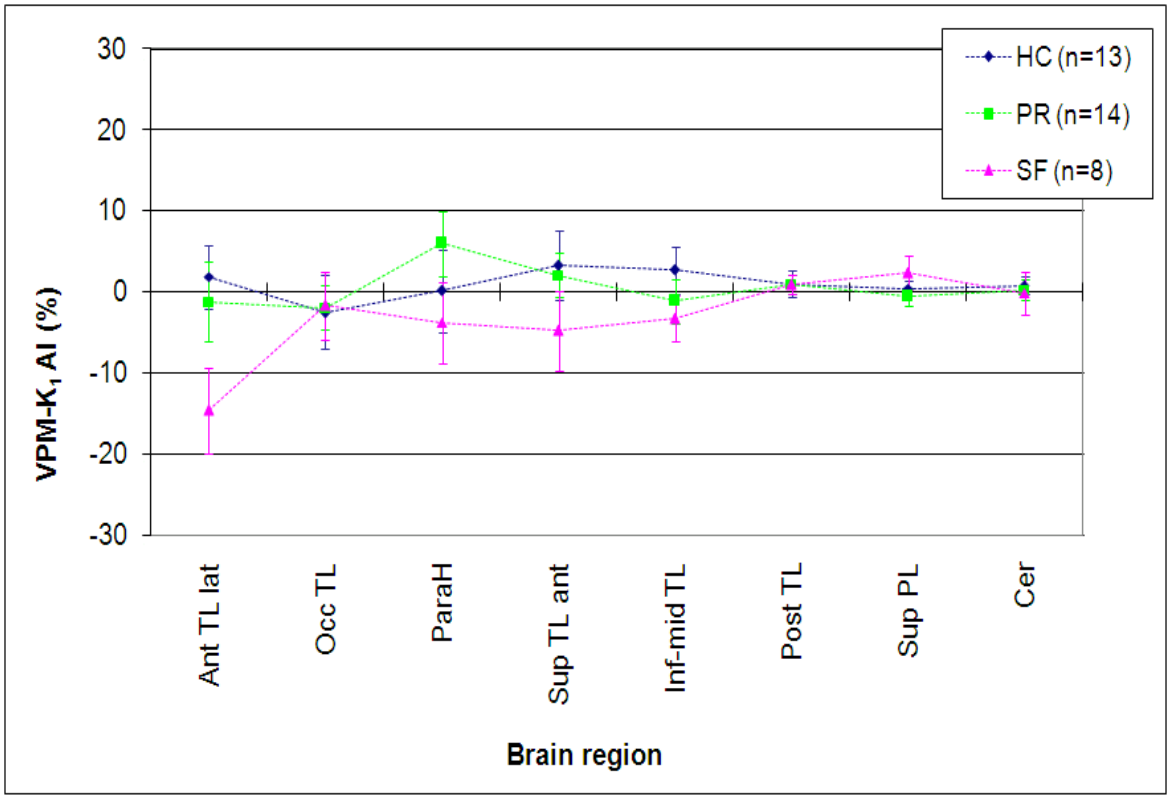

Figure 11: Differences in asymmetry index of VPM-K_1 at baseline
Asymmetry index is shown at baseline for 13 healthy controls (HC), 14 pharmacoresistant (PR) and eight seizure-free (SF) mTLE patients in six temporal lobe ROIs and the extratemporal ROI (superior parietal gyrus) as well as cerebellum and whole brain. Ant TL lat, lateral anterior temporal lobe; OccTL, occipitotemporal gyrus; ParaH, parahippocampal and ambient gyrus; Sup TL ant, anterior superior temporal gyrus; Inf-mid TL, inferior temporal gyrus; Post TL, posterior temporal lobe; Sup PL, superior parietal gyrus; Cer, cerebellum. Error bars represent SEM.

5.3.4 Frequent seizures increase Pgp activity

In pharmacoresistant mTLE patients, VPM-K_1 correlated inversely with average monthly seizure frequency, measured at the time of the baseline PET scan (correlation for whole brain: r =-0.535, p= 0.030; temporal lobe: r =-0.588, p= 0.017; Figure 12 and 13). There was no correlation of VPM-K_1 with the interval of seizures before the PET scan in the pharmacoresistant mTLE patients (correlation for whole brain: r =0.119., p= 0.349; temporal lobe: r =0.056, p= 0.428), duration of epilepsy (correlation for whole brain: r =-0.138, p= 0.327; temporal lobe: r =-0.103, p= 0.368) or age at first onset of epilepsy (correlation for whole brain: r =0.085., p= 0.391; temporal lobe: r =0.054, p= 0.431).

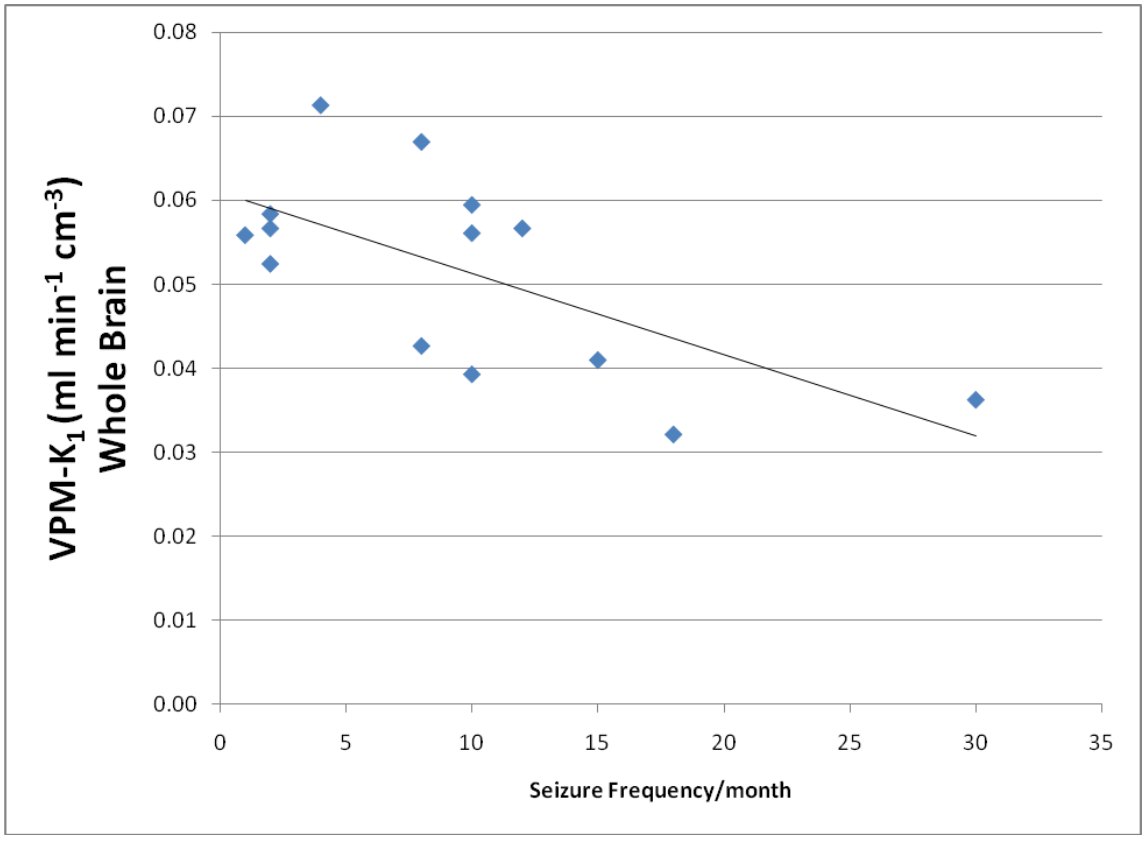

Figure 12: Correlation of seizure frequency and VPM-K_1 for whole brain
Monthly seizure frequency is shown for the 14 pharmacoresistant mTLE patients.

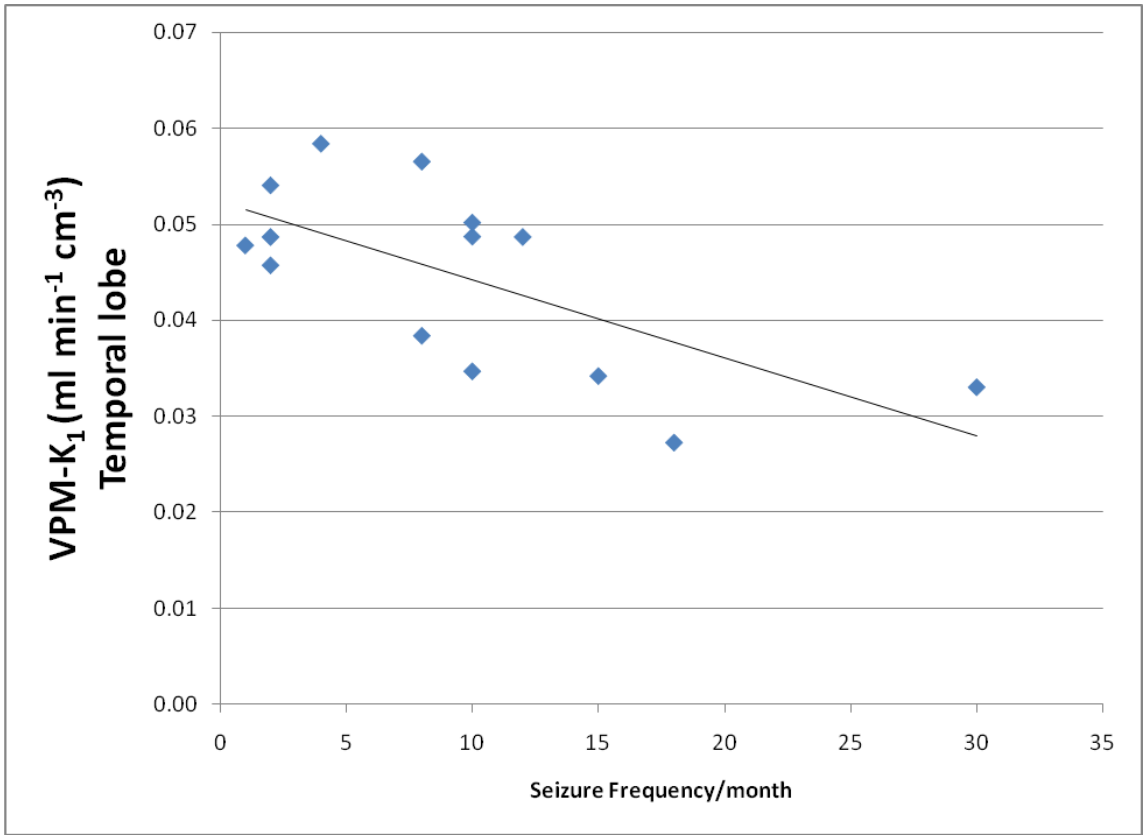

Figure 13: Correlation of seizure frequency and VPM-K_1 for temporal lobe
Monthly seizure frequency is shown for the 14 pharmacoresistant mTLE patients.

5.3.5 Shorter interval of seizures to PET scan increases Pgp activity

In seizure-free mTLE patients a shorter interval of last seizure to PET scan correlates with lower VPM-K_1 (correlation for whole brain: r =0.627, p= 0.048; temporal lobe: r =0.590, p= 0.062, figure 14). No correlations were found for seizure-free mTLE patients with duration of epilepsy (correlation for whole brain: r =-0.285, p= 0.247; temporal lobe: r =-0.367, p= 0.185), or age of onset of epilepsy (correlation for whole brain: r =0.285, p= 0.247; temporal lobe: r =-0.22, p= 0.480).

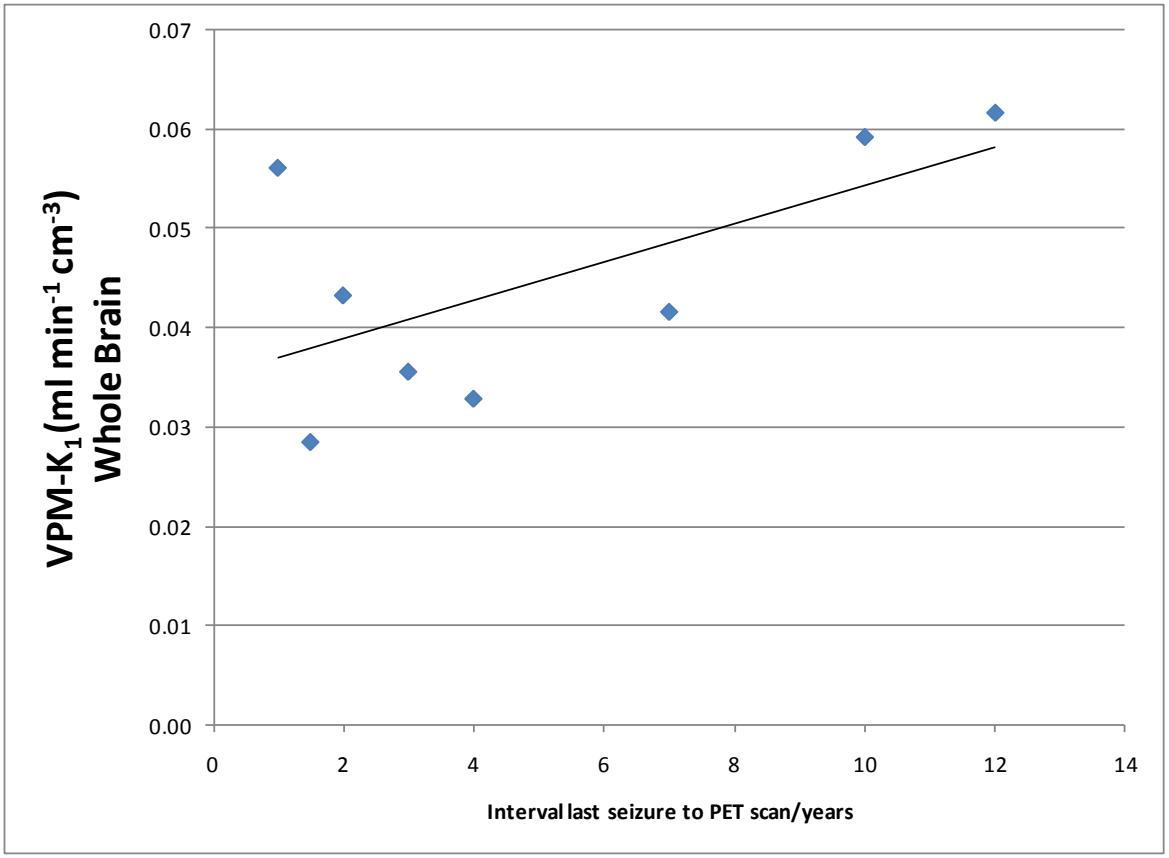

Figure 14: Correlation of interval of last seizure to PET scan and VPM-K_1 for whole brain

Interval of last seizure to PET scan is shown for the eight seizure-free mTLE patients.

5.3.6 Ratios of VPM-K_1 lessens dependency on VPM parent fractions

Because of the significant difference in VPM metabolism between mTLE patients and controls, we calculated ratios of VPM-K_1 values between a reference region (parietal cortex and for whole brain) and target regions. By taking the VPM-K_1 ratios the VPM-K_1 dependency on VPM fraction in plasma lessens (Figure 15, 16 and 17).

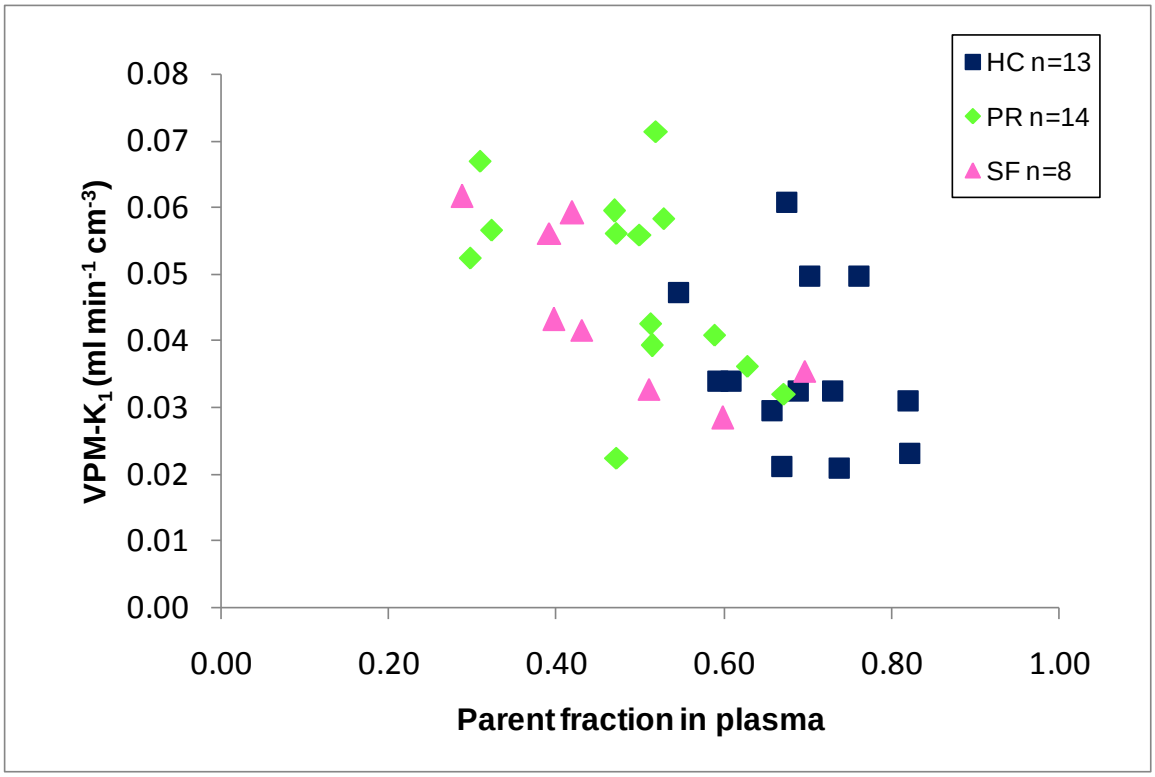

Figure 15: Correlation of VPM-K_1 with VPM fraction in plasma
Correlation of VPM-K_1 values with VPM fraction in plasma at ten minutes is shown for 13 healthy controls (HC), 14 pharmacoresistant (PR) mTLE patients and eight seizure-free (SF) mTLE patients.

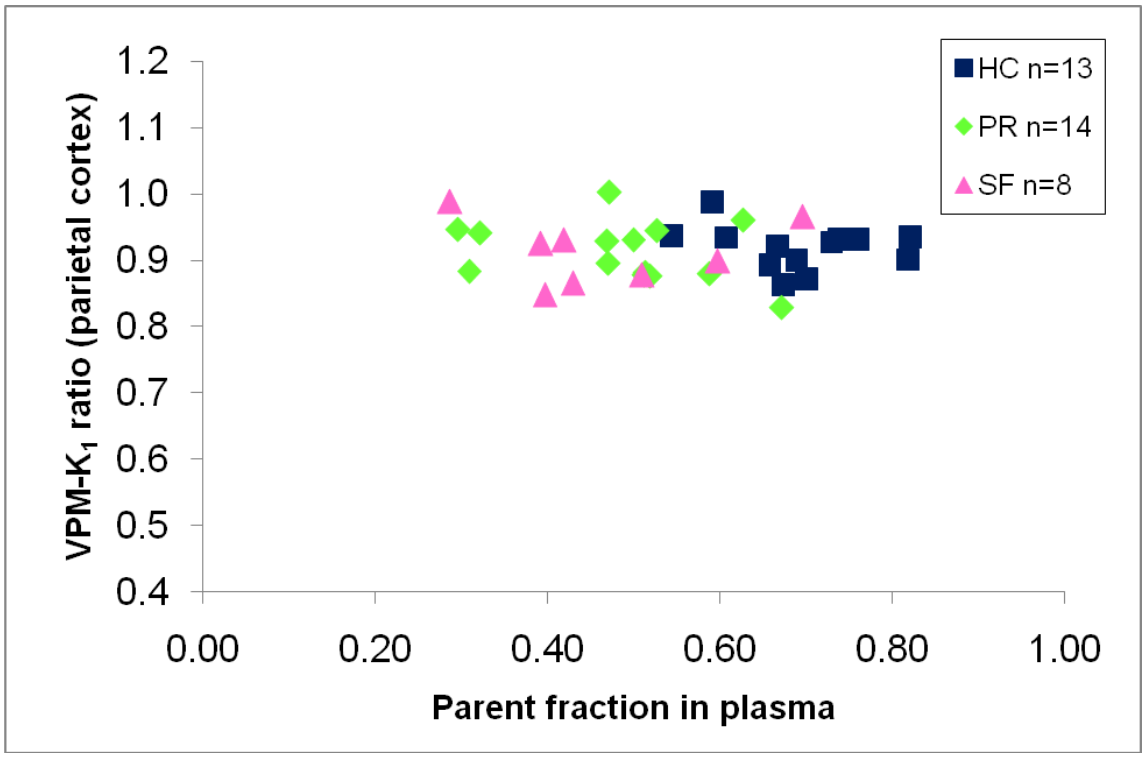

Figure 16: Correlation of ratios of VPM-K_1 (parietal cortex) with VPM fraction in plasma

Correlation of VPM-K_1 ratios (parietal cortex) with VPM fraction in plasma at ten minutes is shown for 13 healthy controls (HC), 14 pharmacoresistant (PR) mTLE patients and eight seizure-free (SF) mTLE patients.

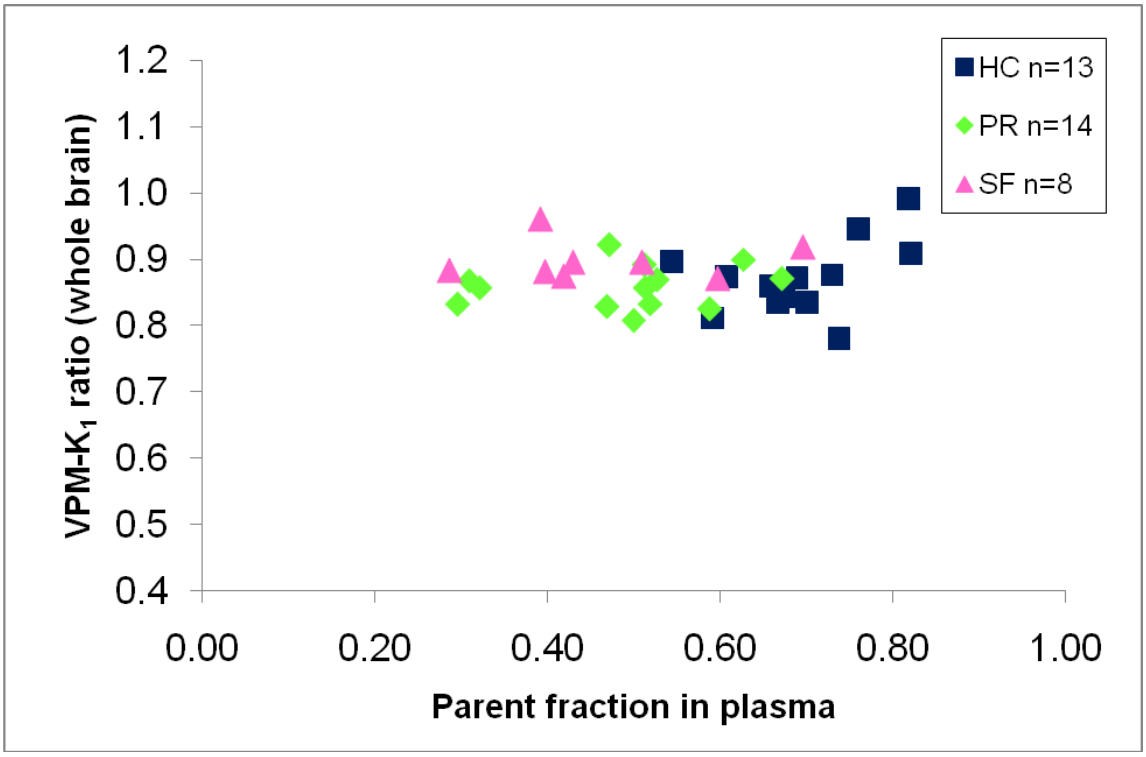

Figure 17: Correlation of ratios of VPM-K_1 (whole brain) with VPM fraction in plasma

Correlation of VPM-K_1 ratios (whole brain) with VPM fraction in plasma at ten minutes is shown for 13 healthy controls (HC), 14 pharmacoresistant (PR) mTLE patients and eight seizure-free (SF) mTLE patients.

5.3.7 Baseline ratios of VPM-K_1 are not different between groups

For multiple regions of interest, there was no difference between VPM-K_1 ratios at baseline for healthy controls and seizure-free mTLE patients (p=0.673) or between pharmacoresistant mTLE patients and healthy controls (p=0.308) or between pharmacoresistant and seizure-free mTLE patients (p=0.190, Figure 18).

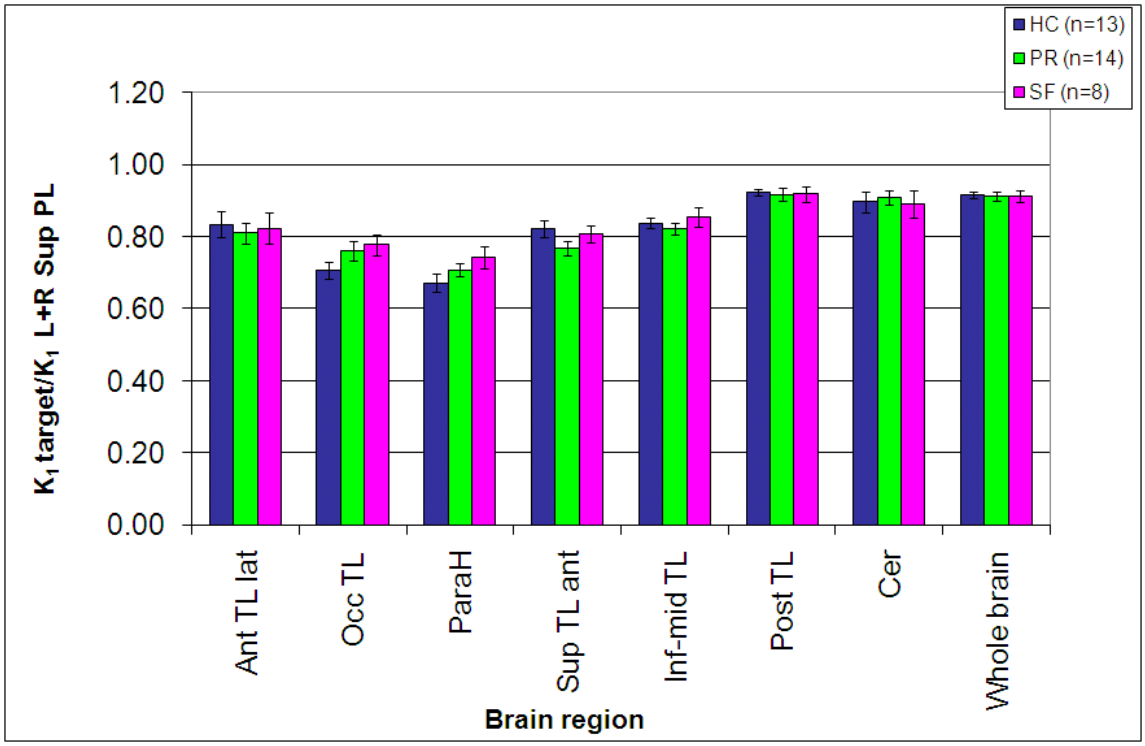

Figure 18: Ratios of VPM-K_1 between target regions and reference region (superior parietal gyrus)

Ratios between reference region (superior parietal gyrus) and target regions (6 different temporal lobe ROIs as well as cerebellum) are shown at baseline for 13 healthy controls (HC), 14 pharmacoresistant (PR) mTLE patients and eight seizure-free (SF) mTLE patients. Ant TL lat, lateral anterior temporal lobe; OccTL, occipitotemporal gyrus; ParaH, parahippocampal and ambient gyrus; Sup TL ant, anterior superior temporal gyrus; Inf-mid TL, inferior and middle temporal gyrus; Post TL, posterior temporal lobe; Cer, cerebellum. Error bars represent SEM.

Additionally, there was no difference between VPM-K_1 ratios at baseline normalised for global whole brain differences for healthy controls and seizure-free mTLE patients (p=0.068) or between pharmacoresistant mTLE patients and healthy controls (p=0.685) or between pharmacoresistant and seizure-free mTLE patients (p=0.134, Figure 19).

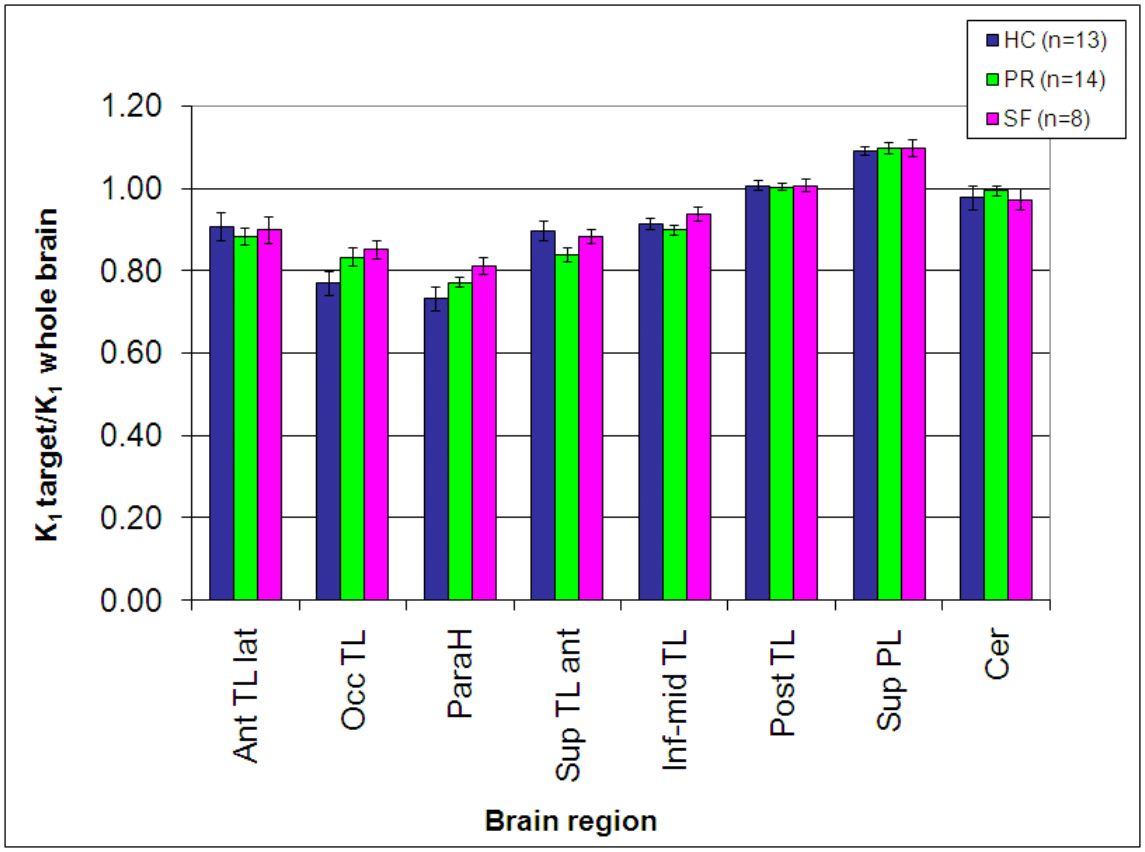

Figure 19: Ratios of VPM-K_1 between target regions and reference region (whole brain)

Ratios between reference region (whole brain) and target regions (6 different temporal lobe ROIs as well as superior parietal lobe and cerebellum) are shown at baseline for 13 healthy controls (HC), 14 pharmacoresistant (PR) mTLE patients and eight seizure-free (SF) mTLE patients. Ant TL lat, lateral anterior temporal lobe; OccTL, occipitotemporal gyrus; ParaH, parahippocampal and ambient gyrus; Sup TL ant, anterior superior temporal gyrus; Inf-mid TL, inferior and middle temporal gyrus; Post TL, posterior temporal lobe; Sup PL, superior parietal gyrus; Cer, cerebellum. Error bars represent SEM.

5.4 DISCUSSION

Despite minimising the effect of different VPM metabolism between healthy controls and patients by using only the first ten minutes of data, we found a significant difference in the fraction of unmetabolised VPM, which was higher for healthy controls than for both mTLE patient groups, but not different between pharmacoresistant and seizure-free mTLE patients. Whole brain VPM-K_1 was lower in controls than in pharmacoresistant mTLE patients and seizure-free

mTLE patients but there was no difference between seizure-free and pharmacoresistant mTLE patients. VPM undergoes extensive metabolism and the peripherally-generated VPM radiometabolites pass into the brain independently of Pgp activity compromise quantitative VPM-K_1 measurement; levels of such metabolites are higher in patients than controls. This is most likely caused by antiepileptic drug-mediated hepatic cytochrome P450 enzyme induction (Abrahim et al. 2008). We therefore we created individual VPM-K_1 ratios, which were normalized for global whole brain differences and to a reference region (parietal cortex). These normalised ratios were then used for further analysis to detect regional differences between healthy controls and the two patient groups. However, at baseline by using the ROI analysis we could not detect a difference of VPM-K_1 ratios between healthy controls or between pharmacoresistant and seizure-free mTLE patients. The difficulty is that VPM is a high-affinity substrate of Pgp and is therefore very effectively transported by Pgp at the BBB. This results in low brain uptake of this radiotracer thus making it difficult to elicit regional differences in cerebral Pgp function. To overcome this limitation, dynamic PET scans after partial blockade by Pgp modulating drugs such as cyclosporine A (CsA) or tariquidar (TQD) can be undertaken (Löscher and Langer 2010). Here, it is important that Pgp is only partially blocked as complete blockade results in radiotracer uptake which is only caused by passive diffusion and is independent of Pgp function. Furthermore, we may not have detected differences between the three groups because the ROI analysis is less sensitive than voxel-based analysis for this radiotracer with low brain uptake and small differences between groups. By employing voxel-based SPM analysis we

may improve sensitivity of statistical analysis, and elicit differences between pharmacoresistant, seizure-free mTLE patients and healthy controls.

At baseline we observed an association between Pgp activity and seizure frequency. Pharmacoresistant mTLE patients who had frequent seizures had higher Pgp activity. Similarly, seizure-free mTLE patients who had shorter intervals of their last seizure to their PET scan had higher Pgp activity. In rodent models of TLE, Pgp expression increases significantly as early as 24 hours after experimentally induced status epilepticus (Rizzi et al. 2002; Seegers et al. 2002; Bankstahl and Löscher 2008). The excitatory neurotransmitter glutamate, which is excessively released by seizures, upregulates Pgp expression in brain capillary endothelial cells, astrocytes and neurons in the dentate gyrus, amygdala, hippocampus, piriform and parietal gyrus (Zhang et al. 1999; Seegers et al. 2002; Zhu and Liu 2004; Bankstahl et al. 2008a; Bankstahl et al. 2011). A recent post-mortem study showed Pgp overexpression in the sclerotic hippocampus of individuals with pharmacoresistant epilepsy, but not in post mortem tissue of seizure-free individuals or non-epileptogenic tissue with electrode-related injuries (Liu et al. 2012) indicating that seizures are necessary, but not sufficient, for increased Pgp expression. These findings suggest that (i) there is measurable, localized Pgp overactivity in pharmacoresistant mTLE which is related to seizure activity; (ii) Pgp overexpression is not seen in seizure-freedom. Pgp overactivity might thus explain why pre-treatment seizure density is one factor predicting poor response to AEDs.

5.5 CONCLUSION

At baseline apparent VPM-K_1 values were lower in healthy controls compared to mTLE patients but pharmacoresistant and seizure-free mTLE patients were not different. There are differences in VPM metabolism between mTLE patients and healthy controls which are caused by AED-mediated hepatic cytochrome P450 enzyme induction in mTLE patients requiring images to be normalised for differences (either to the global whole brain or to a target region, for example the parietal lobe) when comparing mTLE patients with healthy controls. We observed an association between Pgp activity and seizure frequency in mTLE patients. At baseline using the ROI VPM analysis there was no difference in VPM-K_1 ratios in pharmacoresistant compared to seizure-free mTLE patients or healthy controls. However, the differences between groups could be accentuated by using a Pgp inhibitor such as TQD and employing voxel-based SPM analysis.

CHAPTER VI (R)-[^{11}C]VERAPAMIL PET AFTER PARTIAL PGP INHIBITION WITH TARIQUIDAR IN PHARMACORESISTANT MTLE PATIENTS COMPARED TO HEALTHY CONTROLS – REGION OF INTEREST ANALYSIS

6.1 BACKGROUND

Verapamil (VPM) is a high-affinity substrate of Pgp and is therefore very effectively transported by Pgp at the blood-brain barrier (BBB). This results in low brain uptake of this radiotracer thus making it difficult to elicit regional differences in cerebral Pgp function. A possible strategy to overcome this limitation of low brain uptake of Pgp substrate radiotracers is to perform dynamic PET scans after partial blockade by Pgp modulating drugs such as Cyclosporin A (CsA) or Tariquidar (TQD) (Löscher and Langer 2010). Blocking Pgp with an inhibitor allows the radiotracer VPM to enter the BBB and hence increases its uptake and signal in the brain. To test the functional relevance of the VPM baseline difference, we performed experiments with the third-generation Pgp inhibitor TQD. We determined whether there were regional variations in Pgp activity as assessed by differences in VPM-K_1 before and after partial TQD inhibition in pharmacoresistant mTLE patients and healthy controls. We hypothesize that the uptake of VPM is reduced after Pgp inhibition with TQD in pharmacoresistant mTLE patients in the epileptogenic relative to contralateral regions and compared to healthy controls.

6.2 METHODS

The common methods are described in Chapter 4, and the specific methods for this study are described here.

6.2.1 Subjects

Pharmacoresistant mTLE patients and healthy controls were recruited as previously described in section 4.5. Thirteen healthy controls (from the age range 35-55 years) and 14 pharmacoresistant mTLE patients (from the age range 18-60 years) with unilateral hippocampal sclerosis (HS) were included in this part of the study. Clinical details of the pharmacoresistant mTLE patients are in table 2.

6.2.2 Radiochemistry

(R)-[^{11}C]verapamil was synthesized as previously described in section 4.1.4.

6.2.3 PET Image acquisition

The PET scans were performed at the Wolfson Molecular Imaging Centre, Manchester, UK, on the High Resolution Research Tomograph (CTI/Siemens, TN, USA) as previously described in section 4.1.1. The protocol aimed to study subjects twice with VPM PET on the same day whenever possible with a two and a half hour break out of the PET camera between scans. In all subjects, a 60 minute VPM PET scan was performed to assess Pgp function. The pharmacoresistant mTLE patients and healthy controls underwent a second set of VPM-PET scans on the same day starting 60 minute after the end of a 30 minute intravenous infusion of 2 or 3 mg/kg TQD. Baseline and inhibitor scans were acquired in fixed order because of the long half-life of tariquidar (18-36

hours). Seizure-free patients did not receive TD because of the remote possibility that the interaction of TQD with AEDs could lead to seizure recurrence (Giacomini et al. 2010). The injection doses of VPM for the baseline scans in pharmacoresistant and healthy controls were 540 ± 37 MBq and 558 ± 21 MBq, respectively, and 533 ± 55 MBq, 551 ± 41 MBq for pharmacoresistant mTLE patients and healthy controls for the inhibitor scans after administration of TQD (Figure 4).

For 27 subjects, it was possible to perform both scans on the same day with a standardized protocol for lunch in-between. However, due to technical (scanner/hardware failure), we had to re-schedule the inhibitor scan on a different visit, but also at the same time of the day for two healthy controls. TQD plasma levels were measured at 95, 110 and 170 minutes after start of TQD infusion.

6.2.4 MRI data acquisition

For all subjects, a T1-weighted MRI brain scan was acquired on a 3-Tesla GE Excite II scanner (General Electric, Milwaukee, WI, USA) for co-registration with the PET images, as previously described in section 4.2.1.

6.2.5 PET data analysis

As shown recently in rodent models of Pgp-overactivity (Bankstahl et al. 2011), partial Pgp-inhibition increases VPM-K_1, but this increase is attenuated in areas of high Pgp-activity, since a fixed dose of Pgp-inhibitor (2 or 3mg/kg) inhibits a lower proportion of Pgp binding sites in areas of high Pgp-activity. It has

previously been reported in healthy controls (Bankstahl et al. 2011) that TQD did not alter VPM peripheral metabolism in pharmacoresistant mTLE patients. Subjects served as their own control, which eliminated the need for ratio images.

The asymmetry index (AI) was calculated as:

$$AI(\%) = \frac{ipsi - contra}{contra} \text{x}100$$

All image processing steps were performed in SPM8, Wellcome Trust Centre for Neuroimaging London, UK as previously described in section 4.3.2.

6.2.6 Statistical Analysis

The statistical analyses were performed using SPSS 19.0 as previously described in section 4.4.1 and the level of significance was set at $p<0.05$.

6.3 RESULTS

6.3.1 Pgp overactivity in pharmacoresistant mTLE compared to healthy controls

After 2mg/kg TQD, pharmacoresistant mTLE patients had significantly reduced increases in VPM-K_1 globally (26%, n=6) compared to healthy controls (52%, n=7, $p<0.001$). A recent study showed a sigmoidal relationship between TQD inhibition and VPM-K_1 in healthy controls with a half-maximum effect of about 3mg/kgTQD (Bauer, Zeitlinger et al. 2012). To further support our basic assumption that partial Pgp-inhibition increases the difference between areas of Pgp overactivity and normality, we scanned an additional seven pharmacoresistant mTLE patients and six healthy controls with the higher dose of 3 mg/kg TQD. Increases of VPM-K_1 were also significantly different after 3mg/kg TQD globally between both groups (48% for pharmacoresistant mTLE patients (n=7), compared to 70% in healthy controls (n=6), p=0.001, Figure 20 and 21) suggesting Pgp overactivity in pharmacoresistant mTLE.

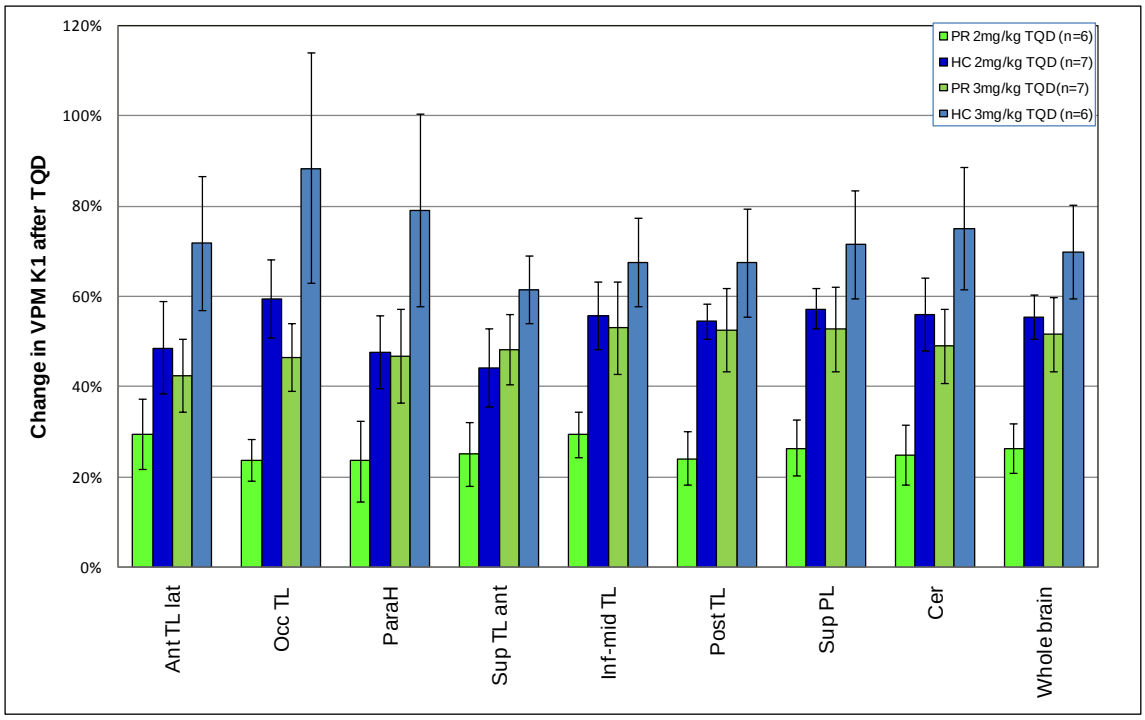

Figure 20: Change in VPM-K_1 after TQD

% change in VPM-K_1 is shown after 2 and 3mg/kg tariquidar for six different temporal lobe ROIs as well as cerebellum and whole brain for 13 healthy controls (HC), 14 pharmacoresistant (PR) mTLE patients. Ant TL lat, lateral anterior temporal lobe; OccTL, occipitotemporal gyrus; ParaH, parahippocampal and ambient gyrus; Sup TL ant, anterior superior temporal gyrus; Inf-mid TL, inferior temporal gyrus; Post TL, posterior temporal lobe; Sup PL, superior parietal gyrus; Cer, cerebellum. Error bars represent SEM.

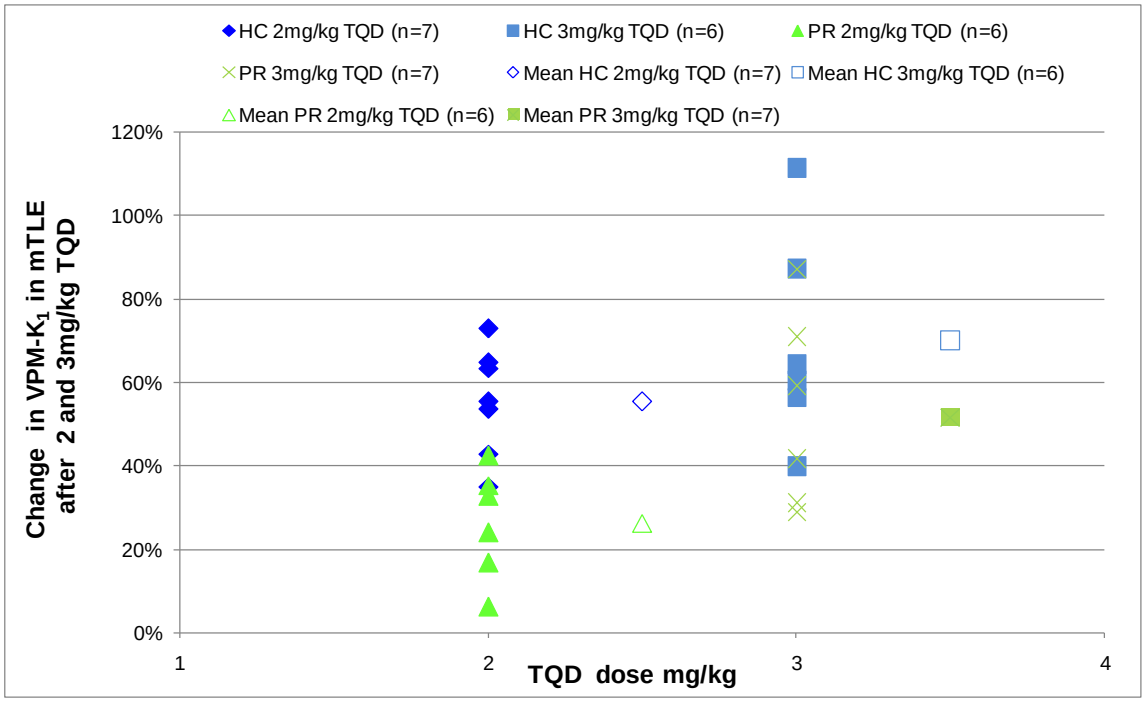

Figure 21: Change in VPM-K_1 for whole brain after TQD
% change in VPM-K_1 is shown after 2 and 3mg/kg tariquidar for the whole brain as well as the mean for 13 healthy controls (HC), 14 pharmacoresistant (PR) mTLE patients.

6.3.2 Tariquidar plasma levels not different between mTLE patients and healthy controls

Average TQD plasma levels were not significantly different between healthy controls and pharmacoresistant mTLE patients after 2mg/kg TQD (360 vs. 226 ng/ml, respectively, p=0.080) or 3mg/kg TQD (418 vs. 324 ng/ml, respectively, p=0.115). As in healthy controls, TQD did not alter the peripheral metabolism of VPM (Figure 22). Average TQD plasma levels for healthy controls and pharmacoresistant mTLE patients are shown in table 3.

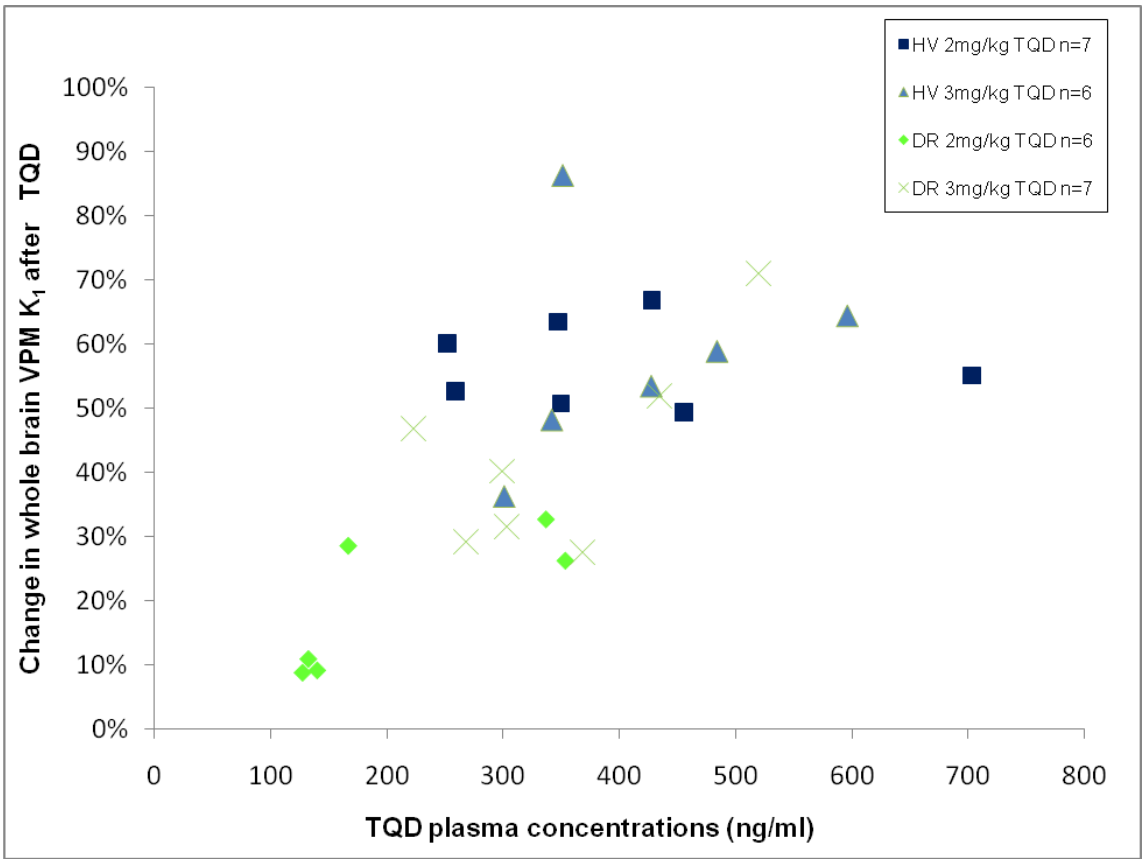

Figure 22: Correlation of TQD plasma level with change in VPM-K_1 for whole brain after TQD
% change in VPM-K_1 is shown after 2 and 3mg/kg tariquidar for the whole brain as well as the mean for 13 healthy controls (HC), 14 pharmacoresistant (PR) mTLE patients.

6.3.3 Differences in asymmetry index after Pgp inhibition with Tariquidar

After Pgp inhibition with 2mg/kg TQD pharmacoresistant mTLE patients had a significantly reduced asymmetry index (i.e. increases of VPM-K_1 contralateral>ipsilateral hence Pgp activity > ipsilateral) in the posterior temporal lobe ($p=0.019$). There was no significant difference in the AI index in any of the other brain regions either after 2 or 3 mg/TQD ($p>0.159$, Figure 23).

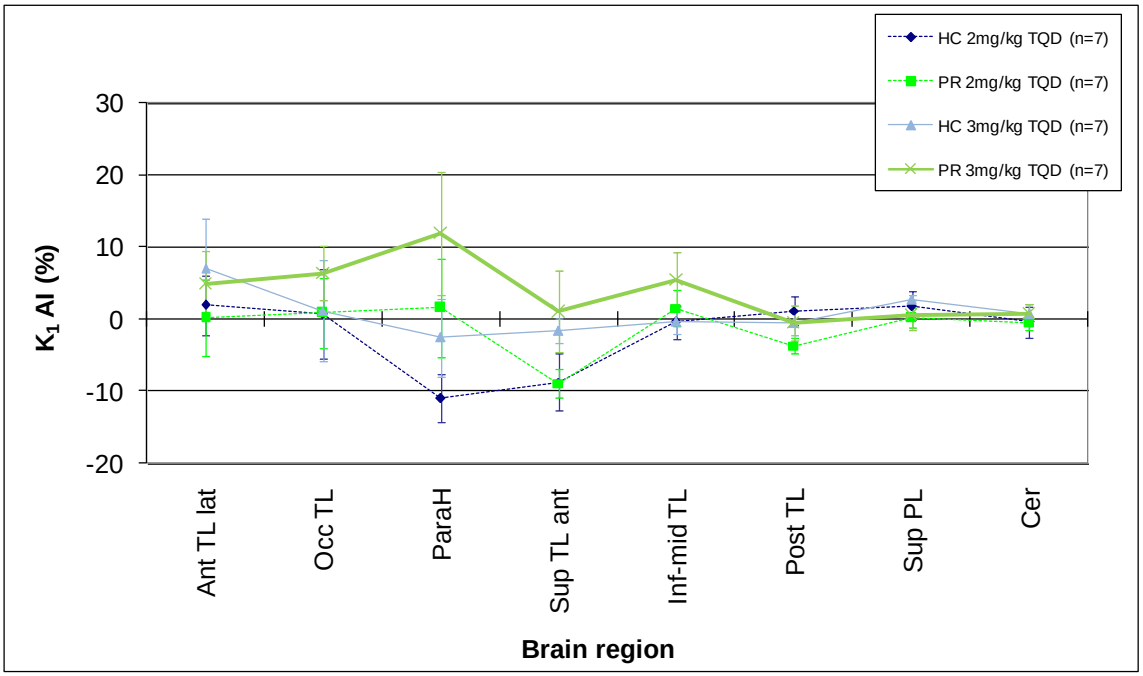

Figure 23: Differences in asymmetry index of VPM-K_1 after TQD
Asymmetry indedx is shown after 2 and 3mg/kg tariquidar for six different temporal lobe ROIs as well as cerebellum and whole brain for 13 healthy controls (HC), 14 pharmacoresistant (PR) mTLE patients. Ant TL lat, lateral anterior temporal lobe; OccTL, occipitotemporal gyrus; ParaH, parahippocampal and ambient gyrus; Sup TL ant, anterior superior temporal gyrus; Inf-mid TL, inferior temporal gyrus; Post TL, posterior temporal lobe; Sup PL, superior parietal gyrus; Cer, cerebellum. Error bars represent SEM.

6.3.4 Tariquidar induced AED side-effects

Five controls and six pharmacoresistant mTLE patients experienced mild adverse events possibly related to TQD such as phlebitis (two controls, two patients), hypotension (two controls, one patient) and nausea (one control, three patients); one control also reported a metallic taste. One pharmacoresistant mTLE patient (PR 2, table 2) developed AED-related side-effects starting 24 hours after the end of the TQD infusion: blurred vision, nausea and ataxia, with increasing severity over the following 24 hours during which the patient

continued taking regular AEDs before reporting the effects to the investigators. These symptoms were typical of concentration-dependent AED side-effects and subsided once AEDs were stopped for 24 hours, about 60 hours after TQD infusion. Following the TQD administration, the patient was seizure-free for four weeks, compared to seizure-frequency over the preceding six months of at least 12 seizures per month. This is a significant improvement as determined by the „rule of three-to-six" (Westover et al. 2012), which accounts for expected variation in seizure-frequency in individuals who a priori are known to probably respond or not respond to AED changes: if an individual goes without seizures for 6 times the average pre-intervention inter-seizure interval that is statistically unlikely to have happened by chance.

6.4 DISCUSSION

We provide the first direct, in-vivo evidence for Pgp overactivity in human pharmacoresistant mTLE, as pharmacoresistant mTLE patients have two-fold lower increases in VPM-K_1 after TQD compared to healthy controls. As shown in rodent models of Pgp overactivity (Bankstahl et al. 2011), partial Pgp inhibition increases VPM- K_1, but this increase is attenuated in areas of high Pgp activity, since a fixed dose of the Pgp-inhibitor TQD (2 or 3 mg/kg) inhibits a lower proportion of binding sites in areas of high Pgp activity than in areas of low activity. Hereby, it is important that Pgp activity is only partially inhibited. In the case of full Pgp inhibition, VPM-K_1 would be driven entirely by passive diffusion, and, thus, would not delineate regional differences in Pgp function (Löscher and Langer 2010). So far only studies in healthy volunteers with paired VPM-PET

scans, before and after TQD have been performed (Wagner et al. 2009; Bauer et al. 2010). So far two Pgp inhibitors have been used in human PET studies, CsA (Sasongko et al. 2005; Eyal et al. 2010) and TQD (Wagner et al. 2009). The third-generation Pgp inhibitor TQD is safer than the non-selective CsA (Fox and Bates 2007). More importantly TQD has no effect on VPM metabolism or plasma protein binding (Bankstahl et al. 2008b; Wagner et al. 2009). Accordingly, the average TQD plasma levels were not significantly different between healthy controls and pharmacoresistant mTLE patients after 2 or mg/kg TQD. One of 16 pharmacoresistant patients showed signs of AED-intoxication after Pgp-inhibitor TQD (PR 2, table 2). The timeline of side-effects in this patient was in keeping with the known half-life of TQD (18-36 hours). In-vitro experiments have shown that Pgp can undergo long-lasting conformational change with functional consequences after molecular modulation, which could be a molecular explanation for this observation (Kimchi-Sarfaty et al. 2007). We hypothesise that significant Pgp-inhibition following TQD led to higher intracellular AED brain concentrations resulting in an unusually long period of seizure freedom. However, only one of 16 patients suffered from AED-concentration-related side-effects, which reflects that Pgp and its inhibition might not be as relevant in humans, as in rodent models. TQD had 10 times greater effect sizes in rats than in humans, with similar doses resulting in half-maximum blockade (Kuntner et al. 2010)..

6.5 CONCLUSION

In conclusion, our findings provide direct in-vivo evidence for Pgp overactivity in pharmacoresistant mTLE with VPM-PET showing attenuated increases of VPM brain uptake after partial Pgp-inhibition by TQD globally in pharmacoresistant mTLE patients compared to healthy controls. However, differences in VPM brain uptake were reduced globally and voxel-based analysis may elicit regional differences.

CHAPTER VII (R)-[^{11}C]VERAPAMIL PET AT BASELINE IN PHARMACORESISTANT AND –SENSITIVE MTLE PATIENTS VERSUS HEALTHY CONTROLS – VOXEL-BASED ANALYSIS

7.1 BACKGROUND

At baseline by using the regional VPM analysis we failed to detect a difference of VPM-K_1 between healthy controls or between pharmacoresistant and seizure-free mTLE patients in brain ROIs. VPM is a high-affinity Pgp substrate and its brain uptake is very low, so that small differences in regional Pgp activity cannot easily be measured (Kuntner et al. 2010). On the other hand, we may not have detected differences between the three groups because the ROI analysis is less sensitive for this radiotracer with low brain uptake and small differences between groups. ROI analysis is used with either manually delineated, anatomically defined ROIs within the brain or by using a probability atlas of the brain (Hammers et al. 2003). ROI refers to selecting a cluster of voxels or brain region a priori when investigating a region for effects. The ROI method has many strengths, namely anatomical validity. However, it also has limitations, including the time-consuming nature of manual ROI drawings, both in delineating a priori-defined regions and in the rigorous training needed to ensure reliability, which does not easily allow for comparison of many brain regions or large subject groups (Kubicki et al. 2002). Additionally, it is generally the case that regions specified in this approach will be relatively large and that even if the region is significantly active, this activation may only occur in a small proportion of voxels

in the ROI. This suggests that simply averaging across the entire region could swamp the signal from this small number of voxels with noise from the remaining non-activated voxels. Another approach to analyse PET data is to employ voxel-based analysis by using SPM (Friston et al. 1995), Using voxel-based SPM analysis, has several benefits compared with traditional ROI analysis. The central idea of SPM analysis is that no a priori hypotheses are required, enabling the analysis of the entire brain volume. Thus, changes also outside of a priori specified regions can be detected. Furthermore, SPM explores every voxel, provides improved sensitivity of statistical analysis, and is more objective than manual ROI analysis (Kemppainen et al. 2006). In chapter 5 we based our VPM data analysis on the traditional ROI analysis of selected brain regions. Here we used voxel-based SPM analysis exploring the whole brain without any a priori hypothesis of involved brain regions. Group differences in VPM uptake were explored between pharmacoresistant and seizure-free mTLE patients and healthy controls. We hypothesise that VPM uptake is reduced in pharmacoresistant mTLE compared to seizure-free mTLE and healthy control. Additionally, we hypothesise that voxel-based SPM analysis further improves the diagnostic yield of our VPM-PET data and that voxel-based SPM analysis of this same data set would complement and extend the ROI findings.

7.2 METHODS

The common methods are described in Chapter 4, and the specific methods for this study are described here.

7.2.1 Subjects

Thirteen healthy controls (from the age range 35-55 years) and 14 pharmacoresistant and eight seizure-free mTLE patients (from the age range 18-60 years) with unilateral hippocampal sclerosis (HS) were included in this study as previously described in section 4.5. Clinical details of the pharmacoresistant and seizure-free patients are in table 2.

7.2.2 Radiochemistry

(R)-[^{11}C]verapamil was synthesised as previously described in section 4.1.4.

7.2.3 PET Image acquisition

The PET scans were performed at the Wolfson Molecular Imaging Centre, Manchester, UK, on the High Resolution Research Tomograph (CTI/Siemens, TN, USA) and the PET data was acquired as previously described in section 4.1.1.

7.2.4 MRI data acquisition

For all subjects, a T1-weighted MRI brain scan was acquired on a 3-Tesla GE Excite II scanner (General Electric, Milwaukee, WI, USA) for co-registration with the PET images as previously described in section 4.2.1.

7.2.5 PET data analysis

For the voxel-based SPM analysis, we generated parametric VPM-K_1 maps as previously described in section 4.3.3.

All image processing steps were performed in SPM 8, Wellcome Trust Centre for Neuroimaging London, UK. MRI and co-registered VPM-K_1 maps were spatially normalized using a symmetrical and centered gray matter DARTEL template. To determine changes ipsi- and contralateral to the sclerotic hippocampus, VPM-K_1 maps were also right-left reversed and normalised to the same DARTEL template as previously described in section 4.3.3.2.

To normalise for differences in peripheral metabolism of VPM, we created PET images corrected for differences in whole brain radiotracer uptake; we first calculated the mean whole brain gray matter VPM K_1 for patients and controls separately, and then normalised to the mean of the two. We used these globally normalised images when comparing patients with healthy controls. For differences between pharmacoresistant and seizure free mTLE patients we used the original VPM K_1 maps which were not normalised for whole brain differences as there was no difference in metabolism between the two patient groups as described in section 5.3.2.

Since the CP has the highest VPM uptake resulting in spill-over of radioactivity into the neighbouring hippocampus, the CP was individually masked out as described in section 4.3.3.4. The masked VPM-K_1 maps and globally normalised images were finally smoothed using an isotropic 8-mm Gaussian filter.

7.2.6 Statistical Analysis

The statistical analysis of voxel-based PET analysis was performed as previously described in section 4.4.2.

7.3 RESULTS

7.3.1 Pgp overactivity in pharmacoresistant compared to seizure-free mTLE patients

The voxel-based SPM analysis showed that at baseline, compared to seizure-free patients, pharmacoresistant mTLE patients had significantly lower regional VPM-K_1, which corresponds to increased Pgp activity, in the ipsilateral amygdala (15.5%, VPM-K_{1-PR} 0.031; VPM-K_{1-SF} 0.036, p=0.014), and bilateral parahippocampal (16.7%, VPM-K_{1-PR} 0.032; VPM-K_{1-SF} 0.037; <0.0001), fusiform (16.3%, VPM-K_{1-PR} 0.036; VPM-K_{1-SF} 0.041; p<0.0001), inferior (ITG) (15.4%, ITG; VPM-K_{1-PR} 0.035; VPM-K_{1-SF} 0.041; p<0.0001) and middle temporal gyri (MTG) (15.3%, MTG; VPM-K_{1-PR} 0.038; VPM-K_{1-SF} 0.044; p<0.0001; Figure 24a). When comparing pharmacoresistant to seizure-free patients, no area of significant increase in VPM-K_1 was detected.

7.3.2 Pgp overactivity correlates with seizure frequency

In pharmacoresistant mTLE patients, VPM-K_1 correlated inversely with average monthly seizure frequency, measured at the time of the baseline PET scan (correlation for whole brain: r =-0.651, p= 0.016; hippocampus: r =-0.604, p=0.029; Figure24b).

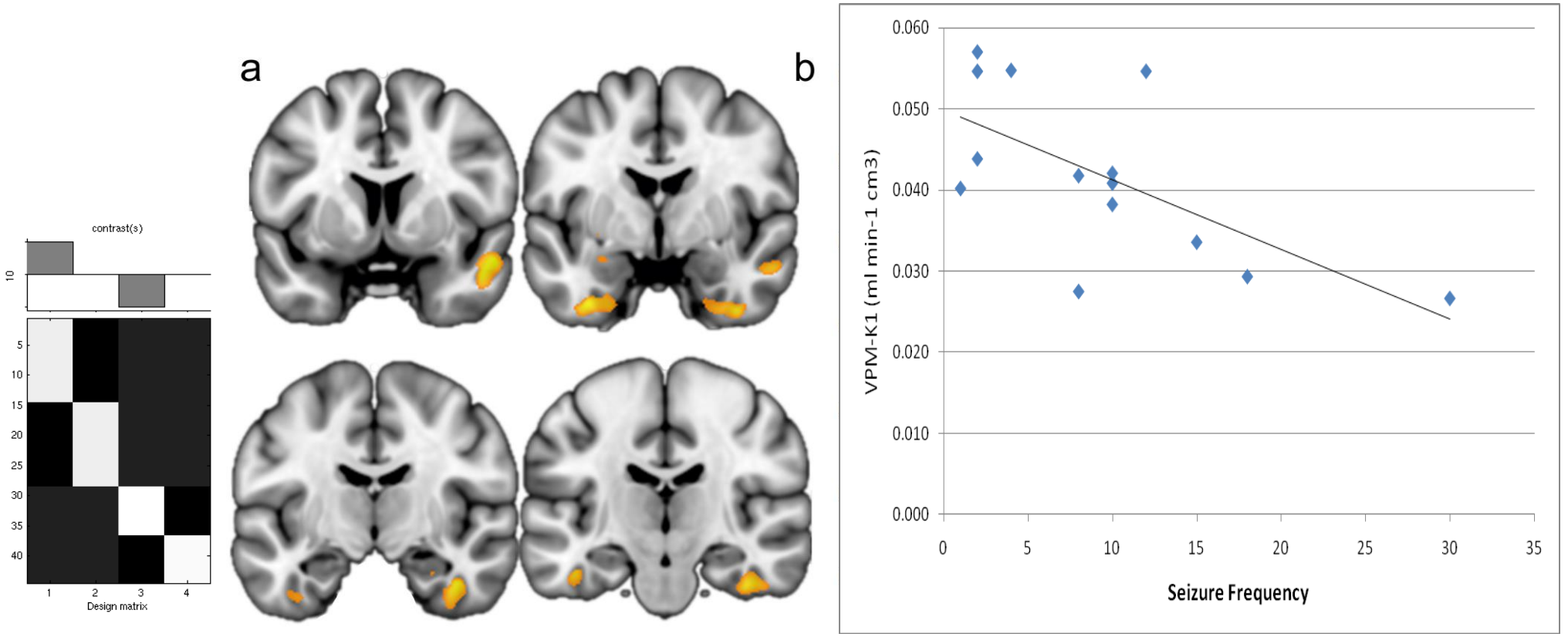

Figure 24: Differences in VPM-K_1 uptake between pharmacoresistant and seizure-free mTLE patients
VPM-K_1 brain uptake at baseline is lower bilaterally in the temporal lobe in the 14 pharmacoresistant compared to the eight seizure-free mTLE patients (a). Areas of significantly reduced K_1 in pharmacoresistant and seizure-free mTLE patients are superimposed in yellow on a coronal T1-weighted MRI template image. Seizure frequency per month inversely correlates with VPM-K_1 in the hippocampus of pharmacoresistant mTLE patients (b).

7.3.3 Pgp overactivity in pharmacoresistant mTLE patients compared to healthy controls

Because of differences in VPM metabolism between mTLE patients and healthy controls we created individual VPM-K_1 images, which were normalised for global whole brain differences in VPM-K_1 arisen from this measure being a composite of parent VPM and its metabolites. These globally normalized images were then used for further analysis to detect regional differences between healthy controls (HC) and the two mTLE patient groups.

Voxel-based comparison of globally normalised images revealed 12.6% lower VPM-K_1 in pharmacoresistant mTLE patients (VPM-$K_{1\text{-}PR}$ 0.038) compared to healthy controls in MTG (VPM-$_{K1\text{-}HC}$ 0.043; $p<0.0001$) and 14.2% lower VPM-K_1 in superior temporal gyrus (STG) (VPM-$K_{1\text{-}PR}$ 0·037; VPM-$K_{1\text{-}HC}$ 0.042, $p<0·.0001$) bilaterally. There was no area of significant difference between seizure-free patients and healthy controls.

7.4 DISCUSSION

Our voxel-based SPM analysis revealed that at baseline the VPM brain uptake is lower in the temporal lobes of patients with pharmacoresistant mTLE compared to seizure-free patients and healthy controls. We translated findings from animal rodent studies (Bankstahl et al. 2011) and our in-vivo PET measurements of Pgp activity are in keeping with the hypothesis that there is localized Pgp overactivity in pharmacoresistant mTLE. Additionally, in agreement with our ROI analysis we found an association between Pgp activity and seizure frequency. Since Pgp overexpression in the epileptic focus region is an important mechanism of pharmacoresistance in epilepsy patients (Löscher and Potschka 2005a), a validated method for in vivo detection of regionally increased Pgp activity would be a valuable tool for predicting the individual risk of an epilepsy patient not responding to pharmacological treatment with antiepileptic drugs that are Pgp substrates. In contrast to the traditional ROI analysis we were able to detect differences between pharmacoresistant and seizure-free mTLE patients and healthy controls by using voxel-based SPM analysis. Employing voxel-based SPM analysis to the VPM data compared to ROI analyses appears to have several potential advantages. For example, voxel-based SPM analysis enables regional comparisons throughout the whole brain without restriction to a few selected areas in the typical ROI methodology. Traditionally, statistical analyses of PET data are derived from ROI analysis or voxel-by-voxel approaches. ROI analyses are used to test hypotheses about specific regions. In this type of analysis, functional or anatomical regions are drawn for each individual subject based on his or her PET or structural image or

a probability brain atlas/template is applied. The alternative, a voxel-by-voxel approach, requires that all images be spatially transformed to a template space. This process, known as stereotaxic normalization, assumes that each voxel corresponds to the same anatomical region across subjects. Statistical analyses are therefore performed for every voxel across all subjects. This approach to analyzing PET data is more exploratory than the ROI approach because it requires no prior hypothesis about the expected location of the effect. Indeed by using voxel-based SPM analysis we found differences in regions not examined in our ROI study and the reduction in VPM brain uptake is not restricted to ipsilateral epileptogenic regions but also extends to contralateral temporal lobe regions, implying a wider area of Pgp overexpression than the epileptogenic focus. Furthermore it also raises the question whether epilepsy, uncontrolled seizures or chronic AED treatment stimulate a global rather than regional response of Pgp function.

7.5 Conclusion

By using voxel-based SPM analysis we provide direct in-vivo evidence for Pgp overactivity in pharmacoresistant mTLE, with VPM-PET showing lower focal VPM uptake in pharmacoresistant compared to seizure-free mTLE patients and healthy controls. Furthermore, Pgp overactivity in the ipsilateral hippocampus of pharmacoresistant mTLE patients correlates with seizure frequency.

CHAPTER VIII (R)-[^{11}C]VERAPAMIL PET AFTER PGP INHIBITION WITH TARIQUIDAR IN PHARMACORESISTANT MTLE PATIENTS COMPARED TO HEALTHY CONTROLS – VOXEL-BASED ANALYSIS

8.1 BACKGROUND

Our ROI analysis provided in-vivo evidence for Pgp overactivity in pharmacoresistant mTLE with VPM-PET showing attenuated increases of VPM-uptake after partial Pgp-inhibition by TQD in temporal lobe regions in pharmacoresistant mTLE patients compared to healthy controls (chapter 6). However, the differences in reduced VPM uptake were observed globally rather than regionally in all temporal regions and the whole brain. By applying voxel-based SPM analysis to the VPM-PET data at baseline compared to ROI analysis we were able to detect differences between pharmacoresistant and seizure-free mTLE patients and controls (chapter 7). Voxel-based analysis allows for comparisons throughout the whole brain without restriction to a few selected areas in the typical ROI methodology. Here, we performed PET scans with the Pgp substrate VPM in pharmacoresistant mTLE patients and healthy controls before and after partial Pgp inhibition with TQD and employed voxel-based SPM analysis to the VPM-PET data to assess specific regional changes. We hypothesize that voxel-based SPM analysis of the same data would complement the ROI findings and elicit regional differences in VPM-K_1 brain uptake before and after partial TQD inhibition in pharmacoresistant mTLE

patients and healthy controls and that the brain uptake of VPM is reduced in the epileptogenic relative to contralateral regions and compared to healthy controls.

8.2 METHODS

The common methods are described in Chapter 4, and the specific methods for this study are described here.

8.2.1 Subjects

Pharmacoresistant patients and healthy controls were recruited as previously described in section 4.5. Thirteen healthy controls (from the age range 35-55 years) and 14 pharmacoresistant mTLE patients (from the age range 18-60 years) with unilateral hippocampal sclerosis (HS) were included in this study. Clinical details of the pharmacoresistant are in table 2.

8.2.2 Radiochemistry

(R)-[^{11}C]verapamil was synthesised as previously described in section 4.1.4.

8.2.3 PET Image acquisition

The PET scans were performed at the Wolfson Molecular Imaging Centre, Manchester, UK, on the High Resolution Research Tomograph (CTI/Siemens, TN, USA) and the PET data was acquired as previously described in section 4.1.1. The pharmacoresistant mTLE patients and healthy controls underwent a second set of VPM-PET scans on the same day starting 60 minutes after the end of a 30 minute intravenous infusion of 2 or 3 mg/kg TQD (Figure 4).

8.2.4 MRI data acquisition

For all subjects, a T1-weighted MRI brain scan was acquired on a 3-Tesla GE Excite II scanner (General Electric, Milwaukee, WI, USA) for co-registration with the PET images, as previously described in section 4.2.1.

8.2.5 PET data analysis

For the voxel-based SPM analysis, we generated parametric VPM-K_1 maps as previously described in section 4.3.3. All image processing steps were performed in SPM 8, Wellcome Trust Centre for Neuroimaging London, UK. MRI and co-registered VPM-K_1 maps were spatially normalized using a symmetrical and centered gray matter DARTEL template. To determine changes ipsi- and contralateral to the sclerotic hippocampus, VPM-K_1 maps were also right-left reversed and normalised to the same DARTEL template as previously described in section 4.3.3.2. Since the CP has the highest VPM uptake resulting in spill-over of radioactivity into the neighbouring hippocampus, the CP was individually masked out as described in section 4.3.3.4. The masked VPM-K_1 maps and globally normalised images were finally smoothed using an isotropic 8-mm Gaussian filter. Subjects served as their own control, which eliminated the need for ratio images.

8.2.6 Statistical Analysis

The statistical analysis of voxel-based PET analysis was performed as previously described in section 4.4.2.

8.3 RESULTS

8.3.1 Maximum Pgp overactivity in hippocampus

Our voxel-based SPM analysis showed that in pharmacoresistant mTLE patients TQD-induced increase in VPM-K_1 was globally attenuated following 2mg/kg TQD, pointing to increased Pgp activity (21.9%; VPM-$K_{1\text{-PR-baseline}}$ 0.047; VPM-$K_{1\text{-PR-TQD}}$ 0.057) compared to controls (56.8%; VPM-$K_{1\text{-HC}}$-baseline 0.030; VPM-$K_{1\text{-HC-TQD}}$ 0.047; $p<0.0001$).

There were no differences at baseline between the two groups of pharmacoresistant mTLE patients scanned either after 2 or 3mg/kg TQD, but VPM-K_1 increases after 3 mg/kg TQD were globally higher (42.6%; VPM-$K_{1\text{-PR-baseline}}$ 0.051; VPM-$K_{1\text{-PR-TQD}}$ 0.074) than after 2 mg/kg TQD (21.9%; VPM-$K_{1\text{-PR-baseline}}$ 0.047; VPM-$K_{1\text{-PR-TQD}}$ 0.057; $p=0.016$). VPM-K_1 in healthy controls did not increase significantly more with 3mg/kg TQD (57.9%; VPM-$K_{1\text{-HC-baseline}}$ 0.036; VPM-$K_{1\text{-HC-TQD}}$ 0.056) compared to 2mg/kg TQD ($p=0.874$). Voxel-based SPM analysis before and after TQD showed significant differences in increases of VPM-K_1 between pharmacoresistant mTLE patients and healthy controls, suggestive of increased Pgp activity in TLE patients, only in the ipsilateral hippocampus (Figure 25) .

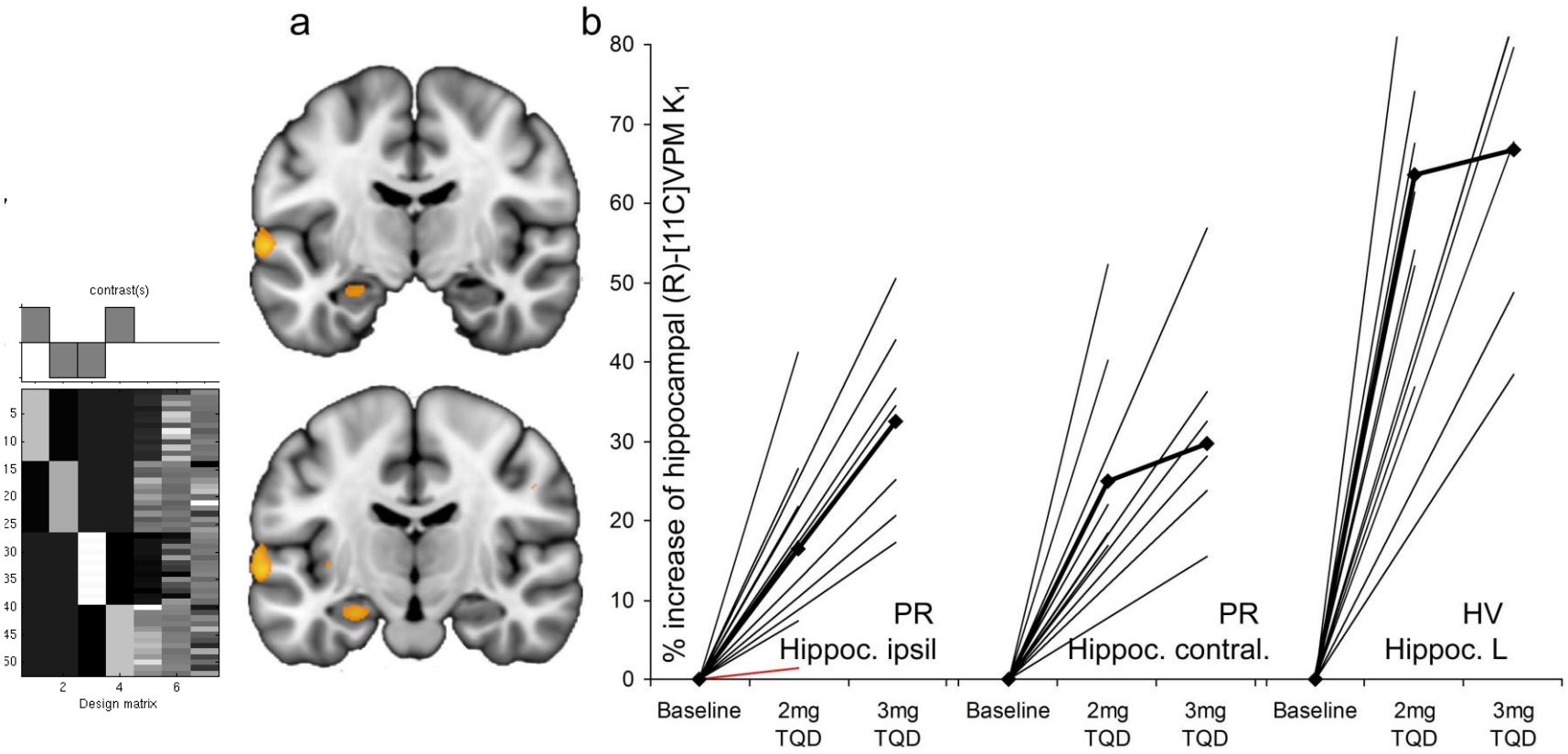

Figure 25: Differential effects of Pgp inhibition with TQD on VPM-K_1 in pharmacoresistant mTLE patients

VPM-K_1 brain uptake after 2 and 3 mg/kg tariquidar is reduced in the epileptogenic hippocampus in the 14 pharmacoresistant compared to 13 healthy controls (a). Area of significantly reduced VPM-K_1 brain in pharmacoresistant mTLE patients is superimposed in yellow on a coronal T1-weighted MRI template image. Increases in VPM-K_1 brain uptake after 2 and 3 mg/kg tariquidar in the hippocampus are shown for the ipsi and contralateral side for the pharmacoresistant mTLE patients and healthy controls (b). The bold line indicates the mean for each group. Pharmacoresistant patient 2, who became temporarily seizure-free and had side-effects associated with antiepileptic drug use after tariquidar, is indicated by a red line. TQD=tariquidar.

The difference between mTLE patients and healthy controls was more pronounced after 2 mg/kg TQD (+16.5%; VPM-$K_{1\text{-PR-baseline}}$ 0.038; VPM-$K_{1\text{-PR-TQD}}$ 0.042; versus +63.5%; VPM-$K_{1\text{-HC-baseline}}$ 0.023; VPM-$K_{1\text{-HC-TQD}}$ 0.038; $p<0.0001$) than after 3 mg/kg TQD, (+32.4% (VPM-$K_{1\text{-PR-baseline}}$ 0.041; VPM-$K_{1\text{-PR-TQD}}$ 0.056) versus +66.8% (VPM-$K_{1\text{-HC-baseline}}$ 0.025; VPM-$K_{1\text{-HC-TQD}}$ 0.041); $p=0.002$). Differences in TQD-induced increase in VPM-K_1 between patients and controls could not be explained by differences in TQD plasma levels between groups (Table 3, Figure 22).

The maximum difference between pharmacoresistant mTLE patients and healthy controls was in the hippocampus, suggesting that there is regionally specific Pgp overactivity for the epileptogenic hippocampus which is functionally relevant.

Table 3: VPM-K_1 and % change in VPM-K_1 in pharmacoresistant mTLE patients and healthy controls after TQD

Pat No	TQD level (ng/ml)	Ipsilateral hippocampus $K_{1\text{-baseline}}$/ $K_{1\text{-TQD}}$ (% change)	Ipsilateral middle temporal gyrus $K_{1\text{-baseline}}$/ $K_{1\text{-TQD}}$ (% change)	Ipsilateral inferior temporal gyrus $K_{1\text{-baseline}}$/ $K_{1\text{-TQD}}$ (% change)	Whole brain $K_{1\text{-baseline}}$/ $K_{1\text{-TQD}}$ (% change)
Pharmacoresistant (PR) patients 2mg/kg TQD					
1	384	0.020/0.024 (21.8)	0.026/0.034 (33.2)	0.025/0.030 (19.3)	0.025/0.033 (32.6)
2	140	0.054/0.055 (1.4)	0.061/0.063 (3.2)	0.052/0.053 (1.1)	0.058/0.063 (9.1)
3	348	0.029/0.034 (17.4)	0.041/0.047 (14.9)	0.032/0.041 (27.4)	0.035/0.044 (26.2)
4	160	0.034/0.036 (7.4)	0.040/0.053 (34.4)	0.035/0.044 (25.5)	0.041/0.053 (28.5)
5	130	0.044/0.044 (0.1)	0.052/0.056 (7.2)	0.045/0.050 (11.7)	0.051/0.056 (10.9)
6	113	0.042/0.059 (41.2)	0.067/0.071 (5.4)	0.057/0.063 (9.9)	0.066/0.072 (8.8)
7	312	0.041/0.052 (26.6)	0.051/0.074 (44.6)	0.049/0.073 (49.8)	0.057/0.078 (37.3)
Pharmacoresistant (PR) patients 3mg/kg TQD					
8	212	0.027/0.039 (42.7)	0.042/0.065 (54.5)	0037/0.058 (56.2)	0.040/0.059 (46.8)
9	491	0.042/0.051 (20.6)	0.040/0.071 (79.4)	0.035/0.065 (86.6)	0.040/0.069 (71.0)
10	269	0.057/0.067 (17.3)	0.064/0.078 (22.4)	0.058/0.079 (36.2)	0.059/0.076 (29.3)
11	326	0.038/0.058 (50.4)	0.057/0.073 (27.7)	0.047/0.065 (36.9)	0.058/0.075(27.6)
12	287	0.040/0.050 (25.1)	0.059/0.084 (41.8)	0.051/0.079 (53.8)	0.056/0.078 (40.2)
13	396	0.027/0.036 (34.4)	0.034/0.050 (46.0)	0.030/0.053 (76.4)	0.034/0.052 (51.8)
14	291	0.055/0.075 (36.6)	0.067/0.099 (48.3)	0.059/0.088 (47.9)	0.071/0.093 (31.6)
Healthy controls (HC) 2mg/kg TQD					
1	661	0.020/0.033 (67.4)	0.024/0.041 (70.8)	0.024/0.035 (46.7)	0.024/0.038 (55.1)
2	349	0.017/0.028 (61.4)	0.030/0.046 (53.1)	0.028/0.047 (64.4)	0.029/0.047 (63.4)
3	246	0.026/0.052 (98.7)	0.039/0.056 (42.5)	0.036/0.050 (38.6)	0.035/0.054 (52.6)
4	225	0.026/0.045 (74.1)	0.033/0.058 (76.3)	0.031/0.050 (61.9)	0.034/0.054 (60.1)
5	453	0.025/0.039 (54.1)	0.033/0.051 (51.9)	0.030/0.042 (39.4)	0.032/0.048 (49.3)
6	380	0.027/0.037 (36.8)	0.030/0.049 (62.6)	0.027/0.045 (68.4)	0.027/0.045 (66.8)
7	328	0.022/0.033 (52.2)	0.031/0.044 (41.9)	0.026/0.043 (62.3)	0.030/0.044 (50.6)
Healthy controls (HC) 3mg/kg TQD					
8	332	0.030/0.054 (79.6)	0.053/0.077 (45.6)	0.049/0.071 (42.8)	0.050/0.074 (48.3)
9	449	0.019/0.028 (48.7)	0.023/0.038 (65.7)	0.018/0.032 (80.2)	0.023/0.036 (58.9)
10	388	0.028/0.052 (83.2)	0.052/0.076 (46.5)	0.043/0.063 (45.1)	0.048/0.074 (53.5)
11	590	0.024/0.040 (67.7)	0.029/0.047 (61.3)	0.025/0.050(100.7)	0.030/0.049 (64.5)
12	323	0.015/0.027 (83.0)	0.021/0.042 (95.0)	0.017/0.034(100.1)	0.022/0.042 (86.3)
13	303	0.033/0.046 (38.5)	0.047/0.064 (36.4)	0.040/0.058 (44.6)	0.046/0.062 (36.3)

Data are baseline K_1/ K_1 (mL/min/cm³) after tariquidar (% change from baseline), unless otherwise stated. Mean tariquidar plasma concentrations (ng/mL) calculated from two samples taken 15 min and 60 min after injection of VPM.

8.3.2 Different response to Tariquidar in pharmacoresistant mTLE patients taking carbamazepine

The observed whole brain increases in VPM-K_1 in response to TQD administration showed a relatively large spread of values amongst pharmacoresistant mTLE patients when using the voxel-based analysis, ranging from +8.8 to 37.3% following 2 mg/kg (VPM-$K_{1\text{-PR-baseline}}$ range: 0.025; to 0.066; VPM-$K_{1\text{-PR-TQD}}$ range: 0.033; to 0·.78) and +27.6 to 71% after 3 mg/kg (VPM-$K_{1\text{-PR-baseline}}$ range; 0.034; to 0.071; VPM-$K_{1\text{-PR-TQD}}$ range: 0.052; to 0.093). Those pharmacoresistant mTLE patients who had lower increases in VPM-K_1 following TQD than any of the healthy controls, suggestive of highest Pgp activity, were all taking the AED carbamazepine (n=6), in different combinations with other AEDs. None of the other patients were taking carbamazepine. There was no difference in age of onset of epilepsy, duration of epilepsy, average monthly seizure frequency, time since last seizure before PET scan, or TQD plasma concentrations between patients taking carbamazepine and the other patients.

8.4 DISCUSSION

Our voxel-based analysis complements results from the ROI analysis and provides in-vivo evidence for Pgp overactivity in human pharmacoresistant mTLE, manifesting as attenuated TQD-induced increases in VPM brain uptake. Differences between pharmacoresistant mTLE patients and healthy controls became more pronounced after partial Pgp-inhibition: increased VPM-K_1 in pharmacoresistant mTLE patients were less than half of that seen in healthy controls, with the maximum difference between patients and controls found in

the ipsilateral hippocampus. The response to TQD was not uniform in our cohort, in keeping with the suggestion that Pgp-overactivity is only a relevant mechanism of pharmacoresistance in a subset of patients. Six of our 14 pharmacoresistant patients showed whole brain increases of VPM-K_1, which was below the lowest TQD-induced increase in healthy controls. All those six patients were taking carbamazepine, which was not being taken by any of the other patients. We cannot determine if this is a causal relationship. Studies with fewer AED combinations are required to address the effect of specific AEDs. A central question of the transporter hypothesis is whether AEDs are meaningful substrates for Pgp. There is general agreement that phenytoin, phenobarbital, lamotrigine, levetiracetam, topiramate, and carbamazepine-epoxide are substrates of human Pgp, but not valproic acid and carbamazepine (Baltes et al. 2007a; Zhang et al. 2011). One possible explanation for the observed association of high Pgp-activity and carbamazepine usage in our cohort is that carbamazepine might be better tolerated in those patients because the toxic metabolite, carbamazepine-epoxide, is transported out by Pgp (Zhang et al. 2011). Pgp induction by carbamazepine (Lombardo et al. 2008) does not explain the observed intra-subject regional variation, with the maximum difference between pharmacoresistant patients and healthy controls found in the epileptogenic hippocampus. The variation in response across the pharmacoresistant mTLE patient group is likely to be multifactorial.

8.5 CONCLUSION

In conclusion, our findings provide direct in-vivo evidence for Pgp overactivity in pharmacoresistant mTLE with VPM-PET showing attenuated increases of VPM uptake after partial Pgp-inhibition by TQD in pharmacoresistant mTLE patients compared to healthy controls. TQD being least effective in increasing VPM uptake in the epileptogenic hippocampus in pharmacoresistant mTLE patients compared to healthy controls suggests that Pgp overactivity is pronounced in the region of the focus and thus, potentially functionally relevant.

CHAPTER IX EX-VIVO ANALYSIS OF PGP AND COMPARISON WITH (R)-[^{11}C]VERAPAMIL PET

9.1 BACKGROUND

The direct evidence for increased expression of Pgp in humans at the blood-brain barrier (BBB) is limited to studies from post-mortem and from epileptic tissues removed during epilepsy surgery from patients with pharmacoresistant epilepsy (Tishler et al. 1995; Dombrowski et al. 2001; Sisodiya et al. 2002; Aronica et al. 2004; Liu et al. 2012), which have substantiated assumptions implicit in the transporter hypothesis that Pgp is likely to be the most important transporter in pharmacoresistant epilepsy at a structural level. However, the functional relevance of this increased expression in humans cannot be assessed ex vivo. Using in vivo PET with the Pgp substrate radiotracer (R)-[^{11}C]verapamil (VPM) before and after Pgp inhibition with Tariquidar (TQD), we studied pharmacoresistant patients with mesial temporal lobe epilepsy (mTLE) due to unilateral hippocampal sclerosis (HS) and compared the results of their VPM-PET scans with their epileptic tissues removed during epilepsy surgery, testing the hypotheses that Pgp overactivity demonstrated with VPM-PET correlates with Pgp expression established in surgically-resected brain tissue.

9.2 METHODS

This study was approved by the Joint Research Ethics Committee of the National Hospital for Neurology and Neurosurgery (NHNN)/University College London (UCL) Institute of Neurology; use of tissue was in accordance with UK Human Tissue Authority guidelines. Written informed consent was obtained from surgical patients. We studied surgically-resected brain tissue from patients with pharmacoresistant mTLE, who had pre-surgical VPM-PET scans, to measure Pgp function, before and after Pgp inhibition with TQD. Five of the 14 pharmacoresistant mTLE patients had anterior temporal lobe resection 5.7±4.7 months later at the NHNN. The recruitment of the pharmacoresistant mTLE patients was as previously described in section 4.5.1. In the interval between PET scanning and resection, no patient had any drug changes or episodes of status.

9.2.1 Tissue Sampling

Drs Joan Liu and Maria Thom from the Institute of Neurology, University College London, helped with this analysis. A 5mm-thick block of the surgically-resected hippocampus (mid-level) and temporal cortex (posterior-level) of each case was removed and stored in a -80ºC freezer. The remaining specimens were then fixed in 10% neutral-buffered formalin overnight. Fixed tissue was dissected anteroposteriorly into 5mm-thick blocks. Blocks were processed and embedded in paraffin wax within a week following sampling. 5µm sections were cut from each region and mounted on to adhesive microscopic slides (Superfrost, VWR International, UK).

9.2.2 Immunohistochemistry

The surgically-resected brain tissue was analysed by immunohistochemistry using antibodies against Pgp (JSB-1, C219 and C494) as previously described in Liu et al., 2012 (Liu et al. 2012).

9.2.3 Qualitative and quantitative assessments

All immunolabelled sections were qualitatively examined under a light microscope (Nikon Eclipse 80i) using 10x, 20x and 60x objective lenses. Quantitative studies were performed as previously described in Liu et al., 2012 (Liu et al. 2012) for anti-Pgp and anti-BCRP antibodies. In brief, the head of the hippocampus (inclusive of dentate gyrus and all cornu Ammonis subfields), and the grey matter of the temporal pole, middle temporal gyrus (MTG) and inferior temporal gyrus (ITG) were outlined using image analysis software (ImagePro Plus, Media cybernetics, UK) under 2.5x objective. Images were acquired in a random systematic sequence within the ROI under 20 x objectives using a CCD camera (JVC, USA). Positive immunolabelling was segmented (thresholded) using the ColorCube module of the ImagePro Plus software (Media Cybernetics, Inc. USA): positive labelling was manually selected by centering a 5x5 pixel selection grid on the darkest pixel in the image with the highest sensitivity option selected. The final results for each region of each case were expressed as the percentage area of the region of interest that was positively immunolabelled per case per marker.

9.2.4 Statistical Analysis

For the correlation of voxel-based analysis with immunohistochemistry Spearman rank tests were applied. The results are shown as mean ± SD and he level of significance was set at $p<0.05$.

9.3 RESULTS

The histological diagnosis for cases with pharmacoresistant mTLE is summarised in Table 4. In summary, all five cases with epilepsy from UCL showed a loss of NeuN-immunopositive cells in the CA1, 3, and 4 of the hippocampus, which is consistent with classical HS. 3/5 cases additionally showed neuronal cell loss, or increased numbers of ectopic white matter neurons in the temporal cortex. Regions of neuronal cell loss were accompanied by gliosis and an infiltration of CD68-immunopositive microglial cells.

Table 4: Histological diagnosis for cases with pharmacoresistant mTLE who underwent epilepsy surgery

Pat No	Resected regions	Histological diagnosis
PR 3	Hippocampus, Temporal cortex	FCD IIIA. Classical HS and temporal lobe sclerosis. Severe neuronal cell loss was observed in CA1,3, and 4 of the hippocampus and the superficial layers of the temporal cortex (particularly MTG and ITG).
PR 6	Hippocampus, Temporal cortex	Classical HS and mild malformation of cortical development (MCD type II). Neuronal cell loss was observed in the CA1, 3, and 4 of the hippocampus. An increase in the number of single neurons in the white matter, leading to mild dysplasia or mild MCD were observed.
PR 7	Hippocampus, Temporal cortex	FCD IIIA. Classical HS and temporal lobe sclerosis. Severe neuronal cell loss was observed in CA1,(3), and 4 of the hippocampus and the superficial layers of the temporal cortex.
PR 10	Hippocampus, Temporal cortex	Classical HS. Neuronal cell loss was observed in the CA1, 3, and 4 of the hippocampus.
PR 11	Hippocampus, Temporal cortex	Classical HS. Neuronal cell loss was observed in the CA1, 3, and 4 of the hippocampus.

9.3.1 Pgp expression in post-surgical pharmacoresistant mTLE specimens

Pgp immunoreactivity was observed in the blood vessels, glia and neurons in the hippocampus and temporal cortex of all pharmacoresistant mTLE cases. No evidence of 'double-cuff' or type 2 blood vessels was noted. Results from the quantification analysis are shown in Table 5.

Table 5: Percentage area of Pgp immunopositive labelling

		PR 3	PR 6	PR 7	PR 10	PR 11
Region	Level	Percentage area of Pgp immunopositive labelling				
Hippocampus	Pole	0.41	0.69	0.74	0.82	0.66
	Anterior	0.26	0.58	0.57	0.78	0.50
	Middle	0.53	0.48	0.71	0.65	0.54
	Posterior	0.93	0.52	0.86	0.88	0.71
	Average	0.57	0.57	0.72	0.78	0.60
Temporal lobe	Pole	0.35	0.81	0.87	0.68	0.59
Middle temporal lobe	Anterior	0.58	0.84	0.54	0.55	0.59
	Middle	0.54	0.86	0.62	0.83	0.73
	Posterior	0.39	0.81	0.6	1.03	0.71
	Average	0.50	0.84	0.59	0.80	0.68
Inferior temporal lobe	Anterior	0.55	0.6	n/a	0.49	0.56
	Middle	0.3	0.67	n/a	0.62	0.55
	Posterior	0.36	0.8	n/a	0.82	0.71
	Average	0.40	0.69	0.00	0.64	0.61

9.3.2 Pgp expression in post-surgical specimens correlate with in-vivo PET measurements of Pgp activity in pharmacoresistant mTLE

Pgp immunoreactivity was observed in the blood vessels, glia, and neurons in the hippocampus and temporal cortex of the five PET-scanned pharmacoresistant mTLE patients who underwent surgery. In three pharmacoresistant mTLE patients (PR 3,7 and 10, table 2), increases in VPM-K_1 after TQD were less pronounced, suggesting relatively higher Pgp activity, in the ipsilateral (sclerotic) hippocampus (20.4% ±5.3) than the ipsilateral temporal neocortex (combined inferior, middle, and superior temporal gyrus 31.7% ±11.6; figure 26). In accordance with this observation, the same three pharmacoresistant mTLE patients also showed a higher percentage area of Pgp immunopositive labelling in the sclerotic hippocampus (0.68% ±0.10) compared with the ipsilateral neocortex (0.59% ±0.13). The remaining two pharmacoresistant mTLE patients (PR 6 and 11, table 2), had less pronounced increases of VPM-K_1 in the ipsilateral neocortex (+20% ±6.5) than in the hippocampus (+45.8% ±14.8), and correspondingly higher Pgp immunopositive labelling in the neocortex (+0.70% ±0.08) compared with the hippocampus (+0.56% ±0.04; Spearman, $r=-0.900$, $p=0.034$; figure 26C).

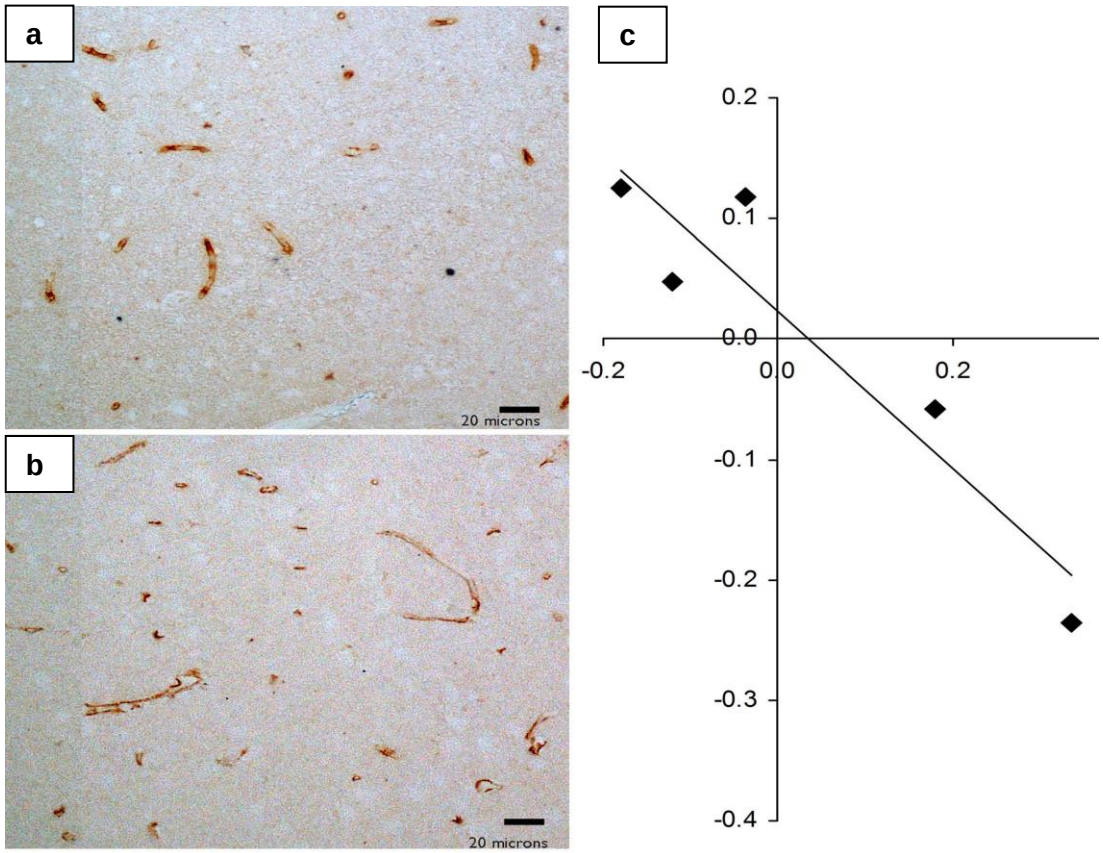

Figure 26: In-vivo and ex-vivo correlation of Pgp activity
Immunolabelling of ipsilateral hippocampus (a) and temporal neocortex (b; defined as combined inferior, middle, and superior temporal gyrus) from one of the five patients with pharmacoresistant mTLE who underwent surgery with anterior temporal lobe resection. Immunolabelling P-glycoprotein (brown) of ipsilateral hippocampus and temporal neocortex (defined for corresponding PET analysis as combined inferior, middle, and superior temporal gyrus). (c) Negative correlation in patients with pharmacoresistant mTLE who underwent epilepsy surgery (n=5), and differences in VPM-K_1 after tariquidar compared with areas of Pgp immunopositive labelling in the hippocampus as a percentage of that in the neocortex. This correlation shows less increase or greater Pgp activity for hippocampus than neocortex (i.e. negative values) and greater hippocampal than neocortical Pgp expression (i.e. positive values) in three of five patients (left upper quadrant).

9.4 DISCUSSION

Our in-vivo PET measurements of Pgp activity correlated with ex-vivo Pgp expression in the surgical temporal lobe specimens of those patients who had undergone surgery, in keeping with the hypothesis that there is localized Pgp overactivity in pharmacoresistant mTLE. This is the first study to date comparing in-vivo Pgp activity by using VPM-PET before and after Pgp inhibition with ex-vivo Pgp expression from pharmacoresistant mTLE patients who underwent temporal lobe resections. Recently Bauer et al. (Bauer et al. 2014) examined seven patients with mTLE in a longitudinal study using VPM-PET before and after temporal lobe resections to assess whether postoperative changes in seizure frequency and AED load are associated with changes in Pgp function and correlated their in-vivo VPM-PET measurements of Pgp function with ex - vivo immunohistochemistry from surgical temporal lobe specimens. However, they only performed VPM-PET scans at baseline and did not perform PET scans after Pgp inhibition. The seven patients were followed up for a median of six years (range 4–7) after epilepsy surgery. They found that pharmacoresistant mTLE patients who became seizure-free after surgery had lower VPM-K_1 values, hence increased temporal lobe Pgp activity before surgery, increased Pgp expression in their surgically resected hippocampal specimens, and reduced global Pgp activity postoperatively, i.e. higher VPM-K_1 values postoperatively, compared with patients who continued to have seizures postoperatively and had a poorer surgical outcome. Their results are consistent with our findings in seizure-free mTLE patients who have higher VPM-K_1 values, i.e. reduced Pgp

activity, compared to pharmacoresistant mTLE patients. In line with this a immunohistochemistry study in postmortem brain tissue also showing almost no Pgp overexpression in the sclerotic hippocampus of patients with epilepsy who had entered terminal remission before death (Liu et al. 2012). Several other previous studies have demonstrated Pgp expression in surgically resected specimens from patients with pharmacoresistant epilepsy with a variety of structural abnormalities, including hippocampal sclerosis (Tishler et al. 1995) (Tishler et al. 1995; Dombrowski et al. 2001; Sisodiya et al. 2002; Aronica et al. 2004; Liu et al. 2012). Investigating Pgp expression in the surgically resected tissue of our pharmacoresistant mTLE patients we could also observe Pgp immunoreactivity in the blood vessels, glia and neurons in the hippocampus. In particular, our study is the first study to assess whether this Pgp overexpression in pharmacoresistant mTLE is functionally relevant by combining in-vivo VPM-PET investigated Pgp activity with ex-vivo analysis of Pgp expression in surgically resected tissue.

9.5 Conclusion

The pre-operative results showed that the hippocampus of pharmacoresistant mTLE patients has a smaller percentage difference in Pgp function between the VPM-K_1 pre- and post-TQD, suggesting that the Pgp activity or expression might be higher in the hippocampus than temporal cortex of patients with pharmacoresistant mTLE patients. This was confirmed with the immunohistochemistry data where we observed a higher percentage area of Pgp in the hippocampus than temporal cortex in three of five cases

demonstrating that the Pgp overexpression in the epileptic focus of pharmacoresistant mTLE patients is functionally relevant.

CHAPTER X PERIPHERAL BIOMARKERS OF PGP EXPRESSION, BLOOD-BRAIN BARRIER DAMAGE AND ABCB1 GENETIC ANALYSIS

10.1 BACKGROUND

In human pharmacoresistant epileptic brain tissue (Tishler et al. 1995; Sisodiya et al. 2002; Aronica et al. 2004), as well as in the epileptic rat brain (Volk and Loescher 2005; van Vliet et al. 2007), Pgp is overexpressed in endothelial cells, neurons, and glial cells and this overexpression may lead to increased extrusion of AEDs from the brain to the blood, preventing the attainment of appropriate AED concentrations at therapeutic targets (Van Vliet et al. 2006). In addition to brain cells Pgp is also expressed by peripheral blood mononuclear cells (PBMCs). Ban et al. (Ban et al. 2012) and Kumar et al. (Kumar et al. 2014) have observed higher Pgp expression in PBMCs in pharmacoresistant epilepsy patients.

Pgp is the product of the ABCB1 (MDR-1) gene. As an indirect evidence of enhanced Pgp expression, several studies studied the ABCB1 gene polymorphism in human subjects with pharmacoresistant epilepsy. It has been speculated that the common SNP C3435T in the MDR 1 gene, specifically the 3435CC genotype, is associated with pharmacoresistance to AEDs. The first phamacogenetic study on this matter suggested a significant association between the C/C genotype than the T/T genotype in the ABCB1 C3435T polymorphism and pharmacoresistant epilepsy (Siddiqui et al. 2003). Although several association studies on the MDR 1 gene with drug disposition and

disease susceptibility have been completed to date, the data remain unclear and incongruous.

Dysfunction of the BBB is a hallmark of epileptogenic brain injuries, regardless of their aetiology (Loescher et al. 2013). S100B is a calcium binding protein and is a biomarker for BBB dysfunction (Kapural et al. 2002). Although it is found in a wide variety of vertebrates with very little structural variation, its biological function is not fully known. S100B protein is present in and secreted from both normal and transformed glial cells in the brain. Structural damage to the glial cells causes leakage of S100B protein into the extracellular compartment and then into CSF, eventually entering the blood stream (Heizmann et al. 2013). Studies suggest that the concentration of S100B protein in CSF and serum could be a useful marker for damage to the nervous system. High CSF and serum levels of S100B have been reported in Alzheimer's disease, stroke, traumatic brain injury and acute subarachnoid haemorrhage (Chaves et al. 2010; Wunderlich et al. 1999; Kleindienst et al. 2007). Central nervous system dysfunction and injury occur in patients sustaining generalized seizures. As a marker of epilepsy S100B protein has been studied in a few studies which have reported controversial results (Lu et al. 2010; Calik et al. 2013).

Here, we evaluate Pgp activity measuring PBMC ABCB1 mRNA levels as well as the ABCB1 polymorphism and S100B level in pharmacoresistant compared to seizure-free mTLE patients and healthy controls. We hypothesise that patients with pharmacoresistant mTLE have higher PBMC ABCB1 mRNA levels, present the haplotype CC and have higher Protein S100B levels.

10.2 METHODS

The common methods are described in Chapter 4, and the specific methods for this study are described here.

Professor Joan Abbott and colleagues at Kings College performed the S100 protein analysis. Drs Joan Liu and Maria Thom from the Institute of Neurology, University College London, did the genotypic analysis and Dr Dickens and Professor Pirmohamed from University of Liverpool helped with the PBMC analysis.

10.2.1 PBMC isolation and analysis of ABCB1 mRNA expression

Seventeen healthy controls, 16 patients with pharmacoresistant mTLE and eight seizure-free mTLE patients had PBMC isolation and analysis of ABCB1 mRNA expression. The recruitment of the mTLE patients and healthy controls was as previously described in section 4.5. The isolation of PBMCs using Ficoll-Paque was performed according to the manufacturer's instructions.

10.2.2 RNA extraction and quantitative RT-PCR

PBMCs were resuspended in Hank's Balanced Salt Solution (HBSS) and centrifuged at 250× g for 5 minutes. The resultant cell pellet was resuspended in Tri reagent (1 mL) for subsequent RNA extraction as described in the manufacturer's instructions. Following RNA extraction, reverse transcription utilising TaqMan® Reverse Transcription Reagents (Applied Biosystems, Paisley, UK) was performed. The samples were prepared for real-time polymerase chain reaction (qPCR); 80 ng cDNA was combined with universal master mix, sense and antisense primers (0.4 µM each) and oligonucleotide

probe (0.2 µM). Assays on demand primer and probe mixes for ABCB1 and glyceraldehyde 3-phophate dehydrogenase (GAPDH, 4310884) were purchased from Applied Biosystems. GAPDH was included as a housekeeping gene. Thermal cycling conditions for all assays consisted of 15 minutes at 95°C followed by 50 cycles of 15 s at 95°C and 60 s at 60°C. Quantification of PCR products occurred in real time and was analysed using a Bio-Rad Chromo4 real-time qPCR machine. Expression data were normalized to GAPDH expression using the Δ Ct method to determine expression of ABCB1 mRNA (Pfaffl 2001).

10.2.3 Genotyping Analysis

Blood samples were collected from 17 healthy controls, 16 patients with pharmacoresistant mTLE and eight seizure-free mTLE patients. DNA was extracted from blood samples of all cases. The recruitment of the mTLE patients and healthy controls was as previously described in section 4.5. DNA from patients with epilepsy were typed using the Illumina Infinium 550K/ Illumina Human 610-Quad genome-wide genotyping array chip, and DNA from healthy controls were typed at ABCB1. Written informed consent was obtained from all participants.

10.2.4 Protein S100B

Ten healthy controls, ten pharmacoresistant mTLE patients and one seizure-free mTLE patient had Protein S100 levels. The recruitment of the mTLE patients and healthy controls was as previously described in section 4.5. The S100B kit was distributed by Diasorin, Charles House, Toutley Road, Wokingham, Berkshire. This kit is run on the Liaison chemiluminescence analyser.

This assay is a two-site chemiluminescence immunoassay for the measurement of S100B in human serum. It utilises paramagnetic particles coated with two mouse monoclonal antibodies to human S100B and one mouse monoclonal antibody labelled with an isoluminol derivative. S100B is sandwiched between these antibodies. The formation of a soluble sandwich complex occurs only in the presence of S100B molecules, which bridge the two antibodies. Therefore, only peptides that bridge these two antibodies can be quantitated. See figure 27 below.

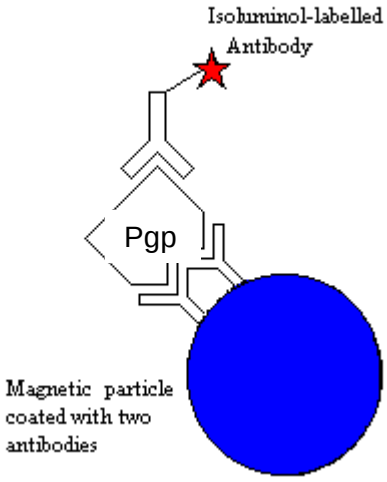

Figure 27: Principle of the S100 assay
The figure was kindly provided by Prof Roy Sherwood, Professor of Clinical, Biochemistry, King's College London.

10.2.4.1 Sensitivity

The minimal detectable dose is 0.02 µg/L.

10.2.4.2 Reference range

The normal range for S100B protein is 0.02 - 0.2 µg/L.

10.2.5 Radiochemistry

(R)-[^{11}C]verapamil was synthesised as previously described in section 4.1.4.

10.2.6 PET Image acquisition

The PET scans were performed at the Wolfson Molecular Imaging Centre, Manchester, UK, on the High Resolution Research Tomograph (CTI/Siemens, TN, USA) and the PET data was acquired as previously described in section 4.1.1.

10.2.7 MRI data acquisition

For all subjects, a T1-weighted MRI brain scan was acquired on a 3-Tesla GE Excite II scanner (General Electric, Milwaukee, WI, USA) for co-registration with the PET images as previously described in section 4.2.1.

10.2.8 PET data analysis

For the voxel-based SPM analysis, we generated parametric VPM-K_1 maps as previously described in section 4.3.3.

All image processing steps were performed in SPM 8, Wellcome Trust Centre for Neuroimaging London, UK. MRI and co-registered VPM-K_1 maps were spatially normalized using a symmetrical and centered gray matter DARTEL template. To determine changes ipsi- and contralateral to the sclerotic hippocampus, VPM-K_1 maps were also right-left reversed and normalised to the same DARTEL template as previously described in section 4.3.3.2. To normalize for differences in peripheral metabolism of VPM, we created PET images corrected for differences in global means; first we calculated the mean whole brain gray matter concentrations for patients and controls separately, and

then normalized to the average of the two. Since the CP has the highest VPM uptake resulting in spill-over of radioactivity into the neighbouring hippocampus, the CP was individually masked out as described in section 4.3.3.4. The masked VPM-K_1 maps and globally normalised images were finally smoothed using an isotropic 8-mm Gaussian filter.

10.2.9 Statistical Analysis

The analyses were performed using SPSS 19.0 (SPSS Inc., Chicago). We used independent t-tests to compare the means between two groups. To compare multiple groups, we used analysis of variance (ANOVA), calculated Pearson correlation coefficients for normally distributed data, or Spearman's rank-order correlations otherwise. For the genotyping data allele frequencies were compared between groups with use of chi-square tests and the level of significance was set at $p<0.05$.

10.3 RESULTS

10.3.1 No correlation with PBMC ABCB1 mRNA expression and Pgp activity

The level of PBMC ABCB1 mRNA expression was not different for healthy controls (mean±SD.: 4.6±5.9, n=17) from pharmacoresistant (9.2±12.8, p=0.222, n=16) and seizure-free (7.9±12.7, p=0.476, n=8) mTLE patients and the level of PBMC ABCB1 mRNA expression was not different between both patient groups (p=0.777, Figure 28).

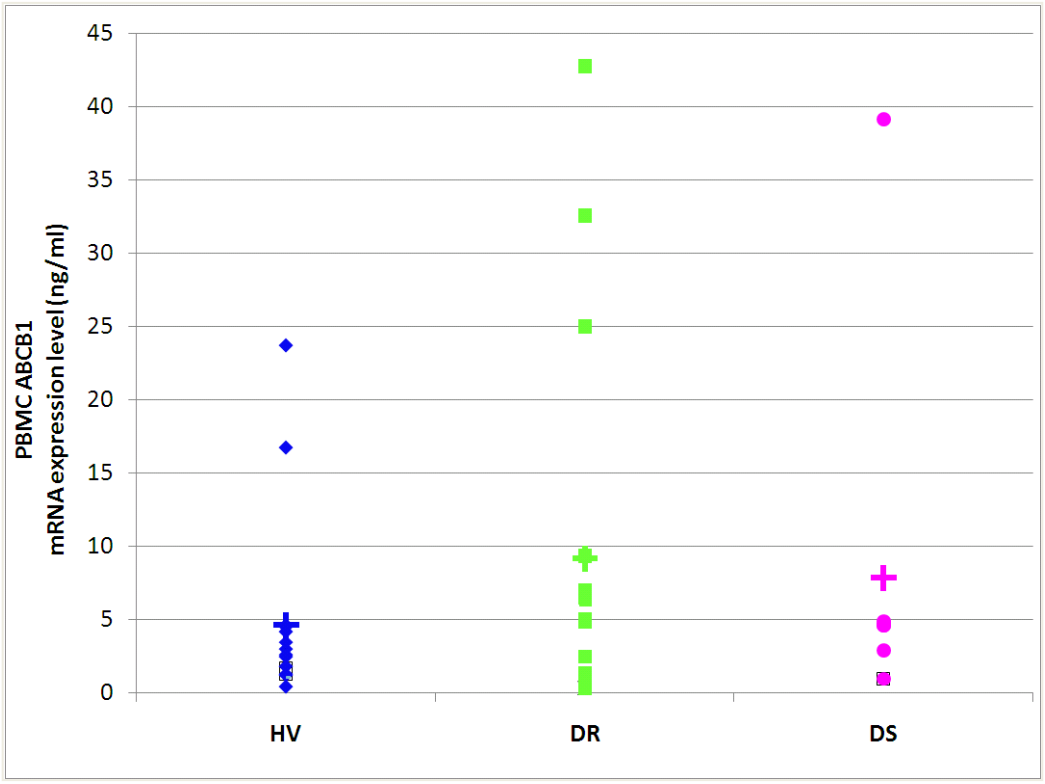

Figure 28: PBMC ABCB1 mRNA expression level for the three groups
PBMC ABCB1 mRNA expression data is shown for 17 healthy controls (HC), 16 pharmacoresistant (PR) and eight seizure-free (SF) mTLE patients. The cross represents the mean for each group.

The level of PBMC ABCB1 mRNA expression did not correlate with VPM-K_1 or its increase after TQD for either the regional analysis (whole brain VPM-K_1 at

baseline r=0.253, p=0.405; whole brain VPM-K_1 after blocking with TQD r=0.247, p=0.415; whole brain increase after TQD r=-0.112, p=0.729, n=14) or voxel based analysis in pharmacoresistant mTLE patients (whole brain VPM-K_1 at baseline r=0.350, p=0.241; whole brain VPM-K_1 after blocking with TQD r=0.377, p=0.204; whole brain increase after TQD r=-0.286, p=0.344, n=14).

The level of PBMC ABCB1 mRNA expression did not correlate with clinical parameters of pharmacoresistant mTLE such as duration of epilepsy (Spearman, r= 0.250, p= 0.409, n=16), time of last seizure before PET scan (r=0.456, p=0.118, n=16), seizure frequency (r=-0.211, p=0.490, n=16) or age at onset of mTLE (r=-0.365, p=0.222, n=16). There was no difference in the level of PBMC ABCB1 mRNA expression in pharmacoresistant mTLE patients who were taking Carbamazepine (4.2±5.1, n=5) and pharmacoresistant mTLE patients who were taking other AEDs (12.19±3.9, n=11, p=0.237).

10.3.2 No difference in genotyping data between the three groups

The frequency of the three different alleles did not differ significantly between pharmacoresistant, seizure free mTLE patients and healthy controls (χ^2= 1.56, p=0.816; Table 6, Figure 29).

Table 6: Frequency of genotyping data for the three different groups

Phenotype	Number of cases genotyped			
		CC No. %	CT No. %	TT No. %
Pharmacoresistant mTLE	14	3 (21)	6 (43)	5 (36)
Seizure-free mTLE	8	2 (25)	5(63)	1(13)
Healthy controls	13	3 (23)	7 (54)	3 (23)

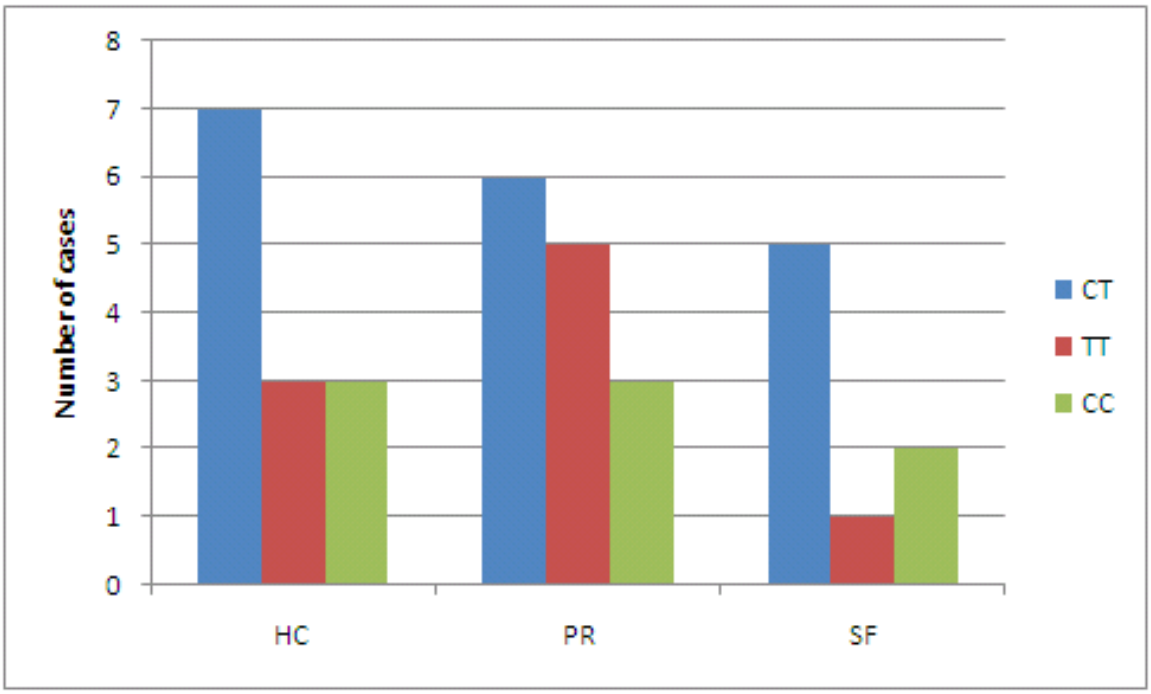

Figure 29: Differences in Pgp genotyping data between the three groups
The genotyping data is shown for 13 healthy controls (HC), 14 pharmacoresistant (PR) and eight seizure-free mTLE patients for the three Pgp genotypes CT, TT and CC.

The genotyping data did not correlate with VPM-K_1 or increase after TQD for either the regional analysis (Spearman, whole brain VPM-K_1 at baseline r=-0.254, p=0.380; whole brain VPM-K_1 after blocking with TQD r=-0.071, p=0.810; whole brain increase after TQD r=0.048, p=0.877, n=14) or voxel based analysis in pharmacoresistant mTLE patients (whole brain VPM-K_1 at baseline r=-0.210 p=0.471; whole brain VPM-K_1 after blocking with TQD r=-0.486, p=0.078; whole brain increase after TQD r=-0.191, p=0.513, n=14 increase in ipsilateral hippocampus after TQD r=-0.090, p=0.761, n=14).

The genotyping data did not correlate with clinical parameters of pharmacoresistant mTLE such as duration of epilepsy (Spearman, r= 0.491, p=

0.075, n=14), time of last seizure before PET scan (r=-0.174, p=0.553, n=14), seizure frequency (r=-0.069, p=0.815, n=14) or age at onset of mTLE (r=0.211, p=0.468, n=14).

10.3.3 Protein S100B does not correlate with blood-brain barrier damage in pharmacoresistant mTLE

All results for S100B were below the normality threshold of 0.2 µg/L for pharmacoresistant, seizure-free mTLE patients as well as healthy controls and therefore did not show an increase in Protein S100B in any of the three groups. For pharmacoresistant mTLE patients the blood samples for protein S100B samples were taken on average 11 days (range 1-60 days) after the last CPS.

10.4 DISCUSSION

We compared the PBMC ABCB1 mRNA expression between pharmacoresistant, seizure-free mTLE and healthy controls and analysed the data with clinical parameters as well as compared it to the Pgp function measured with (R)-[^{11}C]verapamil PET. We could not find a difference between the PBMC ABCB1 mRNA expression between the three groups and there was no correlation of the PBMC ABCB1 mRNA expression with clinical parameters or Pgp function measured with (R)-[^{11}C]verapamil PET. Very few studies have investigated the Pgp expression on peripheral blood mononuclear cells in patients with refractory epilepsy. Kumar et al. (Kumar et al. 2014) used peripheral blood mononuclear cells to evaluate the Pgp expression and function in 29 children with Lennox-Gastaut syndrome, a well-defined refractory childhood epilepsy syndrome, and compared the expression/function of Pgp on PBMCs to 23 children with other epilepsies, and 19 healthy children. The authors found a higher Pgp expression/function in Lennox-Gastaut syndrome, a higher percent positive cells as compared to children with other epilepsy ($p < 0.001$) and to healthy controls ($p = 0.012$), higher Pgp expression as compared to healthy controls ($p = 0.003$), a higher total Pgp expression as compared to children with other epilepsies ($p < 0.001$) and healthy controls ($p < 0.001$), and a higher Pgp function as compared to children with other epilepsies ($p = 0.001$) and healthy controls ($p = 0.002$). Similarly, Ban et al. (Ban et al.) collected MDR-1 data on PBMcs from 140 patients with epilepsy, 30 healthy volunteers, and 20 control patients taking antiepileptic drugs. MDR1 profiles were also analyzed according to various clinical parameters, including seizure frequency and

number of medications used in epilepsy patients. Epilepsy patients had a higher basal MDR1 level than non-epilepsy groups (p=0.01). Among epilepsy patients, there was a tendency for the higher seizure frequency group to have higher basal MDR1 levels (p = 0.059). Additionally, the MDR1 conformational change level was significantly higher in the high-medication-use group than the low-use group (p = 0.028). Basal MDR1 (OR = 1.16 [95% CI: 1.060–1.268]) and conformational change level (OR = 1.11 [95% CI: 1.02–1.20]) were independent predictors for seizure frequency and number of medications, respectively. They concluded that the MDR1 profile of PBMNCs is associated with high seizure frequency and medication conditions in patients with epilepsy. However, both studies did not correlate the Pgp expression/function on peripheral blood mononuclear cells with other tissues including brain cells.

Our genotype analyses for ABCB1 polymorphism did not show a difference in frequency of the CT, TT or CC alleles between pharmacoresistant, seizure-free mTLE patients and healthy controls. The single nucleotide polymorphism C3435T in exon 26 is one of more than 100 polymorphic variants of this gene that have been discovered to date. This polymorphism correlates with altered expression levels of Pgp, range of drug response and clinical conditions. However, the nature of this relationship is still unclear (Sterjev et al. 2012). Siddiqui et al. (Siddiqui et al. 2003) were the first to compare the frequencies of the ABCB1 C3435T variant in 315 patients with epilepsy and classified 200 patients as pharmacoresistant and 115 as drug-responsive patients and compared them to 200 controls without epilepsy. They found that

pharmacoresistant patients were more likely to have the CC genotype as ABCB1 3435 than the TT genotype (odds ratio, 2.66; 95% confidence interval, 1.32 to 5.38; p=0.006). However, 22 replication studies were conducted to evaluate this hypothesis but only nine found significant association in which three reported that the T/T genotype was more frequent in pharmacoresistant patients (Haerian et al. 2010). In addition, four meta-analyses, the first involving 1073 Caucasian patients (Leschziner et al. 2007), the second 3371 (Bournissen et al. 2009), the third 3996 (Nurmohamed et al. 2010), and the fourth 6755 Asian and Caucasian patients (Haerian et al. 2010) did not confirm this association in the total study population or in the ethnic subgroups (Haerian et al. 2011). It is unclear why these reports have found such contradictory results and how such conflicting results can be interpreted.

Furthermore the peripheral marker of BBB permeability Protein S100B was not elevated in pharmacoresistant, seizure-free mTLE patients or healthy controls. Astrocytosis may be an etiology for mTLE. Reactive astrocytosis could generate local synaptic dysfunction and lead to deficits in neuronal inhibition. An imbalance between excitatory and inhibitory synapses may lead to epileptiform firing in epilepsy. S100B is a cytokine produced and released predominantly by astrocytes in the CNS. S100B is involved in the regulation of astrocyte proliferation and the differentiation or apoptosis of neurons. Elevated S100B concentration has been detected in epilepsy animal models or post surgery specimens from epilepsy patients. Here the overexpression of S100B by reactive astrocytosis was detected in sections and homogenates of resected

hippocampus of pharmacoresistant mTLE compared with controls. Additionally, cerebral spinal fluid S100B levels were elevated in pharmacoresistant mTLE. But only a few studies have examined peripheral blood S100B level in–vivo in epilepsy patients. Lu et al. (Lu et al. 2010) investigated S100B levels in 28 patients with mTLE and compared them to 28 healthy controls. They found that patients showed significantly elevated S100B levels compared to healthy controls ($p=0.018$). Moreover, S100B levels were significantly higher in female patients than those in male patients ($p=0.027$). On the other hand Portela et al. (Portela et al. 2003) found normal Serum S100B level in 19 patients with focal epilepsy and in 20 patients with epilepsy secondary to neurocysticercosis ($p > 0.39$). Additionally, serum S100B levels were not affected by antiepileptic drugs, frequency and type of seizures. However, significantly higher levels of S100B were observed in patients with bilateral EEG findings than in patients with unilateral and normal EEG findings ($p < 0.05$). Furthermore, Atici et al. (Atici et al. 2012) investigated whether S100B level were elevated in children with febrile seizures (FS), the most common convulsive disorder during childhood. Although the prognosis associated with FS is generally considered good, the long-term effects of FS on brain development have not yet been clearly identified, particularly its effects associated with neuronal damage and neurocognitive functions. The relationship between FS and mesial temporal sclerosis (MTS) has been one of the most contentious issues in epileptology. For instance, some evidence suggests that prolonged FS directly damages the hippocampus and surrounding structures, while other authors contend that an independent underlying pathology may be responsible for FS and development of MTS (Atici

et al. 2012). In this study S100B level of 39 children with FS were compared to age-matched and sex-matched controls including 30 patients with fever and 30 healthy subjects. Two serum samples were obtained for S100B from the study group at 0–1 hours and 6–24 hours following seizures. No significant differences were detected in serum S100B levels of children with FS at 0–1 hours or 6–24 hours when compared to the control groups.

S100B has been used as a marker for the extent of glial cell damage in a variety of other neurological conditions: strokes, traumatic head injury, sub-arachnoid haemorrhage, encephalitis and hypoxic brain damage. The cut-off for serum S100B that gives the best negative and positive predictive values for poor outcome varies depending on the neurological condition being investigated, but falls in the range 0.2-0.6 mg/L. Serum S100B concentrations above 0.6 mg/L are almost invariably associated with residual cognitive dysfunction, persistent vegetative state or death. Peak S100B levels have been reported within the first 24 h in hypoxic brain damage after traumatic brain injury (Sandler et al. 2010). Additionally, de Oliveira et al. (De Oliveira et al. 2008) showed elevated CSF S100B levels 24 hours after pilocarpine induced status epilepticus in rats. In our study, analysis for protein S100B was limited as blood samples for pharmacoresistant epilepsy patients were taken on average 11 days (range 1-60 days) after the last CPS. An association of elevated Protein S100B levels in pharmacoresistant mTLE patients and Pgp overactivity/expression may be found when blood samples are taken 24 hours after the last seizure. However, in the present study, a sensitive method was employed, which detected S100B in

serum of controls and patients with epilepsy. We postulated that patients with pharmacoresistant mTLE would increase peripheral S100B levels. But our results do not support this hypothesis, as no differences in S100B levels between controls, pharmacoresistant or seizure-free mTLE patients were found.

Overall, a limitation of our study was small numbers and larger studies would be needed to investigate a correlation between Pgp activity/expression and peripheral markers of Pgp.

CHAPTER XI (R)-[^{11}C]VERAPAMIL PET BEFORE AND AFTER PGP INHIBITION WITH TARIQUIDAR IN PATIENTS WITH FOCAL CORTICAL DYSPLASIA COMPARED TO HEALTHY CONTROLS

11.1 BACKGROUND

Focal cortical dysplasia (FCD) is not only a congenital maldevelopment of the cortical tissue but also one of the most common causes of refractory epilepsy. Several studies demonstrating the overexpression of Pgp in brain tissues of patients with mTLE have been reported, however; studies to the neuronal expression and function of Pgp in patients with FCD are scarce (Ak et al. 2007). We assessed Pgp activity in vivo in patients with mTLE by using PET and the Pgp substrate VPM together with the Pgp inhibitor TQD (Feldmann et al. 2013). When using voxel-based analysis we detected that pharmacoresistant patients had lower baseline VPM-K_1, corresponding to higher baseline Pgp activity, than seizure-free patients and healthy controls ($p<0.0001$). Additionally, there were lower increases of VPM- K_1 after TQD in patients with pharmacoresistant mesial temporal lobe epilepsy compared to healthy controls and this difference in TQD response was most pronounced in the sclerotic hippocampus ($p<0.0001$).

One of the major drawbacks of performing PET studies using Pgp substrate radiotracers in patients with mTLE is that the region of most interest, the hippocampus, is difficult to quantify due to a spillover from the adjacent CP into the hippocampus. In our voxel-based analysis we individually masked out the CP using individual thresholds in order to assess the hippocampus. This is a

time consuming and complex task (see section 4.3.3.4). Therefore other epilepsy forms such as FCD, where the seizure focus is far away from the CP thereby avoiding partial volume effects into the region of interest, may possibly be better suited for direct analysis of epileptogenic brain regions to further elucidate the role of Pgp in pharmacoresistant epilepsy.

Here, we report the application of our methodology to three patients with FCD and pharmacoresistant epilepsy and performed PET scans with the Pgp substrate radiotracer VPM together with the Pgp inhibitor TQD.

11.2 METHODS

The common methods are described in Chapter 4, and the specific methods for this study are described here.

11.2.1 Subjects

Pharmacoresistant patients and healthy controls were recruited as previously described in section 4.5. Three pharmacoresistant patients (two male) with quantitative MRI findings of FCD were recruited. Pharmacoresistance was defined as on-going seizure activity despite trials with at least two AEDs given in sufficient doses. In one pharmacoresistant patient (case 2) the inhibitor scan could not be acquired due to radiochemistry failure.

Thirteen healthy controls (seven male, median age 45, range 35-55years), free of relevant, particularly neurological, condition and no regular or recent intake of medication known to be a substrate or inhibitor for Pgp or MPR1 were included in this study. Patients' and control characteristics summarized in Table 7.

Subjects	Gender	Age (yrs)	Weight (kg)	Epilepsy Syndrome	MRI	Onset of epilepsy (age in yrs)	Duration seizures (yrs)	Medication
Case 1	M	62	85	Left TLE	FCD left inferior temporal gyrus	17	45	ZON, LEV, CLB, OXC
Case 2	F	37	58	FLE	FCD posterior part of right calloso-marginal sulcus	19	18	CBZ, TPM
Case 3	M	24	96	Left posterior central seizures	FCD left posterior central gyrus	5	19	CBZ, LEV
Mean SD	2M/1F	41 19	80 20			11 7	35 15	
Control 1	M	47	110	n/a	n/a	n/a	n/a	n/a
Control 2	F	35	133	n/a	n/a	n/a	n/a	n/a
Control 3	F	42	74	n/a	n/a	n/a	n/a	n/a
Control 4	F	37	63	n/a	n/a	n/a	n/a	n/a
Control 5	M	36	93	n/a	n/a	n/a	n/a	n/a
Control 6	M	47	89	n/a	n/a	n/a	n/a	n/a
Control 7	M	51	89	n/a	n/a	n/a	n/a	n/a
Control 8	F	42	57	n/a	n/a	n/a	n/a	n/a
Control 9	M	44	80	n/a	n/a	n/a	n/a	n/a
Control 10	F	53	60	n/a	n/a	n/a	n/a	n/a
Control 11	M	45	90	n/a	n/a	n/a	n/a	n/a
Control 12	M	48	89	n/a	n/a	n/a	n/a	n/a
Control 13	F	35	71	n/a	n/a	n/a	n/a	n/a
Mean SD	7M/6F	43 6	84 21					

Table 7: Clinical data of FCD patients and healthy controls

M, male; F, female; LEV, levetiracetam; OXC, oxcarbazepine; CBZ, carbamazepine; CLOB, clobazam; ZON, zonisamide; TPM, topiramate; TLE, temporal lobe epilepsy, FLE, frontal lobe epilepsy; FCD, focal cortical dysplasia; PR, pharmacoresistant FCD patients; HC, healthy controls, yrs, years. Case 2 is highlighted in red as the inhibitor scan could not be performed due to radiochemistry failure and only the baseline scan is available for analysis.

11.2.2 Radiochemistry

(R)-[^{11}C]verapamil was synthesised as previously described in section 4.1.4.

11.2.3 PET Image acquisition

The PET scans were performed at the Wolfson Molecular Imaging Centre, Manchester, UK, on the High Resolution Research Tomograph (CTI/Siemens, TN, USA) and the PET data was acquired as previously described in section 4.1.1. The pharmacoresistant FCD patients and healthy controls underwent a second set of VPM-PET scans on the same day starting 60 minutes after the end of a 30 minute intravenous infusion of 2 or 3 mg/kg TQD (Figure 4). The transfer rate constant from plasma to brain, K_1, was estimated using a single-tissue compartment model with a VPM-in-plasma arterial input function. Analysis was performed as previously described in section 4.1.3 on the first ten minutes of dynamic data containing limited radiolabeled metabolites (Muzi et al. 2009). Since we administer the Pgp substrate PET tracer VPM intravenously, its entry into the brain is limited by Pgp activity, and the net effect is measured as K_1, the transport rate constant from plasma to brain; a low net influx from plasma to brain, indicated by a low VPM-K_1 value, therefore indicates high efflux from the brain and, thus, high Pgp activity. As shown in rodent models of Pgp overactivity, (Bankstahl et al. 2011) partial Pgp inhibition increases VPM-K_1, but this increase is attenuated in areas of high Pgp activity, since a fixed dose of Pgp inhibitor inhibits a lower proportion of binding sites in areas of high Pgp activity than in areas of low activity.

11.2.4 MRI data acquisition

For all subjects, a T1-weighted MRI brain scan was acquired on a 3-Tesla GE Excite II scanner (General Electric, Milwaukee, WI, USA) for co-registration with the PET images, as previously described in section 4.2.1.

11.2.5 PET data analysis

For the voxel-based analysis, we generated parametric VPM-K_1 maps as previously described in section 4.3.3. Parametric VPM-PET images of pharmacoresistant FCD patients were compared to healthy controls (n=13; “one-against-all-analysis”) using the factorial analysis of the SPM8 software package, Wellcome Trust Centre for Neuroimaging London, UK, with equal variance between groups and with overall grand mean scaling. The analysis was restricted to voxels belonging to gray matter by applying a gray matter mask (generation of gray mask explained above). Activations are shown in the figures as $p< 0.01$, uncorrected with clusters > 10 voxels.

11.2.6 Statistical Analysis

Statistical Analysis was performed using SPSS 19.0 and results are shown as mean ± sd. As numbers were small in the FCD group we used independent non-parametric-tests to compare the means between the two groups. The level of significance was set at $p <0.05$.

11.3 RESULTS

There was no statistically significant difference in age, weight or injected doses of (R)-[^{11}C]verapamil between the FCD patients and the healthy controls ($p>0.05$).

11.3.1 Case 1

At baseline there was a significantly reduced uptake of VPM corresponding to the area of FCD in the left inferior temporal gyrus (Figure 30) implying Pgp overexpression in this epileptic region. This was not only restricted to the area of FCD but also spread to other areas within the ipsilateral temporal lobe such as there was reduced VPM uptake in the ipsilateral middle temporal gyrus, superior temporal pole and rolandic operculum ($p<0.01$) implying the Pgp overactivity extended further than the area of FCD identified by MRI.

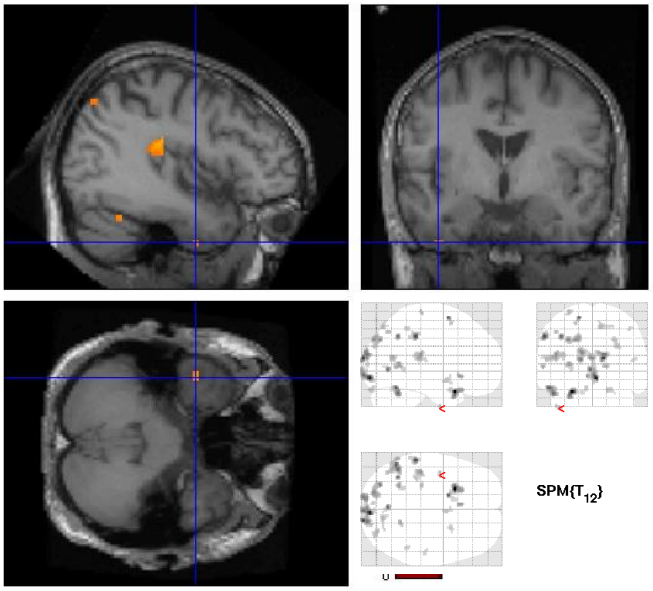

Figure 30: Parametric map of VPM-K_1 for FCD case 1 at baseline
Parametric map of VPM-K_1 for FCD case 1 at baseline is shown compared to 13 healthy controls. There is reduced VPM-K_1 uptake in the area of FCD inferior temporal gyrus, as well as in the ipsilateral medial temporal gyrus and rolandic operculum.

After Pgp inhibition with TQD the uptake of VPM was increased but this increase was significantly attenuated in the corresponding area of FCD the inferior temporal gyrus as well as the ipsi lateral hippocampus. There was also a reduced uptake of VPM in the contralateral amygdala ($p<0.01$; (Figure 31).

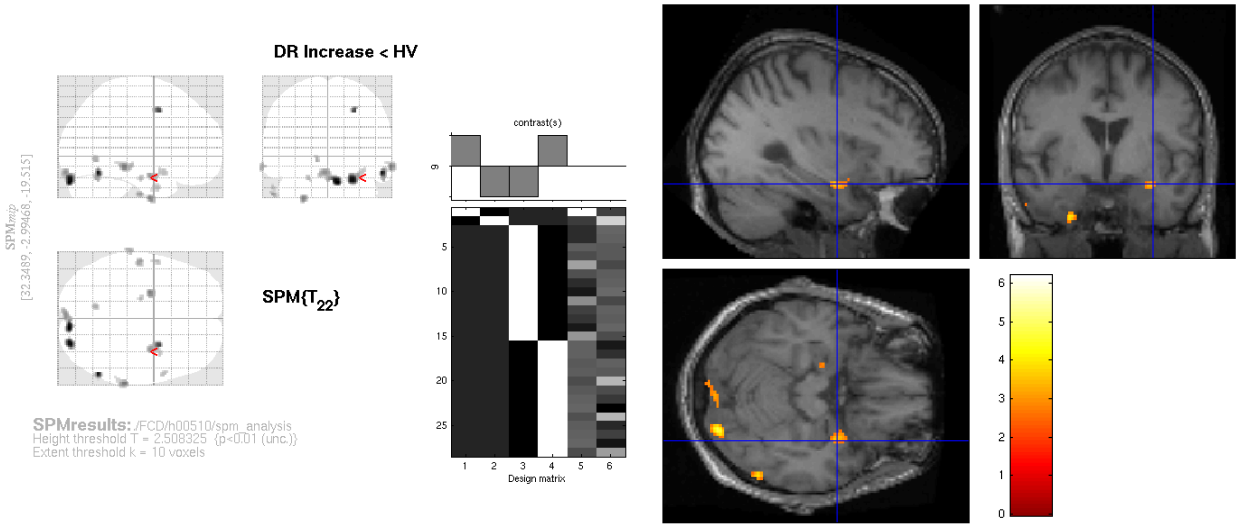

Figure 31: Parametric map of VPM-K_1 for FCD case 1 after TQD
Parametric map of VPM-K_1 for FCD case 1 after blocking with the Pgp inhibitor tariquidar compared to 13 healthy controls. There are reduced increases of VPM-K_1 uptake in the area of FCD in the inferior temporal gyrus, as well as ipsilateral hippocampus and contralateral amygdala.

There were no areas of significantly increased VPM uptake in case 1 compared to healthy controls.

11.3.2 Case 2

At baseline case 2 had significantly reduced uptake of VPM in areas adjacent to the area of FCD (posterior part of right callosomarginal sulcus) in the ipsilateral post central gyrus, precuneus, frontal superior gyrus as well as superior motor area ((p<0.01; Figure 32) implying Pgp overactivity in these epileptic regions.

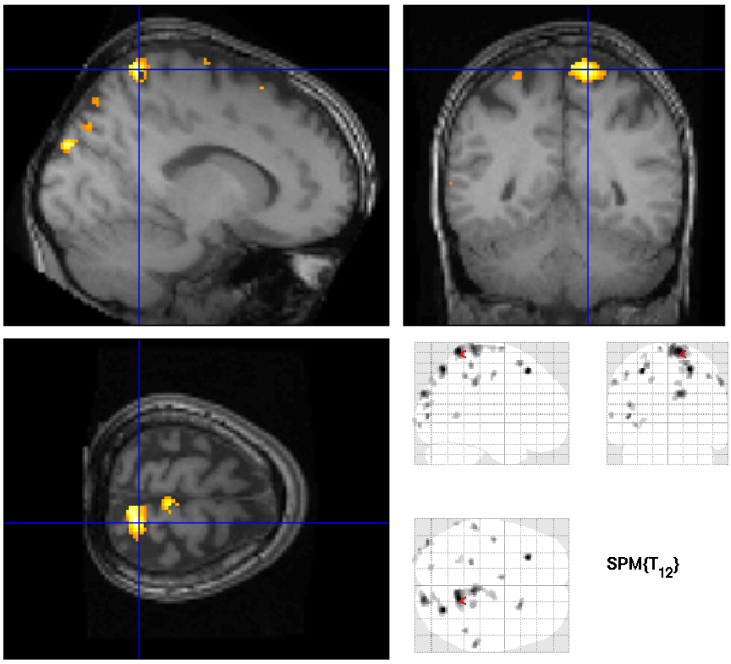

Figure 32: Parametric map of VPM-K_1 for FCD case 2 at baseline
Parametric map of VPM-K_1 for FCD case 2 at baseline compared to 13 healthy controls. There is reduced VPM-K_1 uptake in areas adjacent to the area of FCD in the ipsilateral postcentral gyrus, precuneus, frontal superior gyrus and superior motor area.

Unfortunately, the inhibitor scan could not be performed for this subject due to radiochemistry failure.

There were no areas of significantly increased VPM uptake in case 2 compared to healthy controls.

11.3.3 Case 3

At baseline there was significantly reduced uptake of VPM corresponding to the area of focal cortical dysplasia in the ipsilateral post central gyrus (Figure 33) implying Pgp overactivity in this epileptic region. There were additional areas of reduced VPM uptake on the ipsilateral occipital lobe as well as the contralateral occipital lobe and cuneus ($p<0.01$).

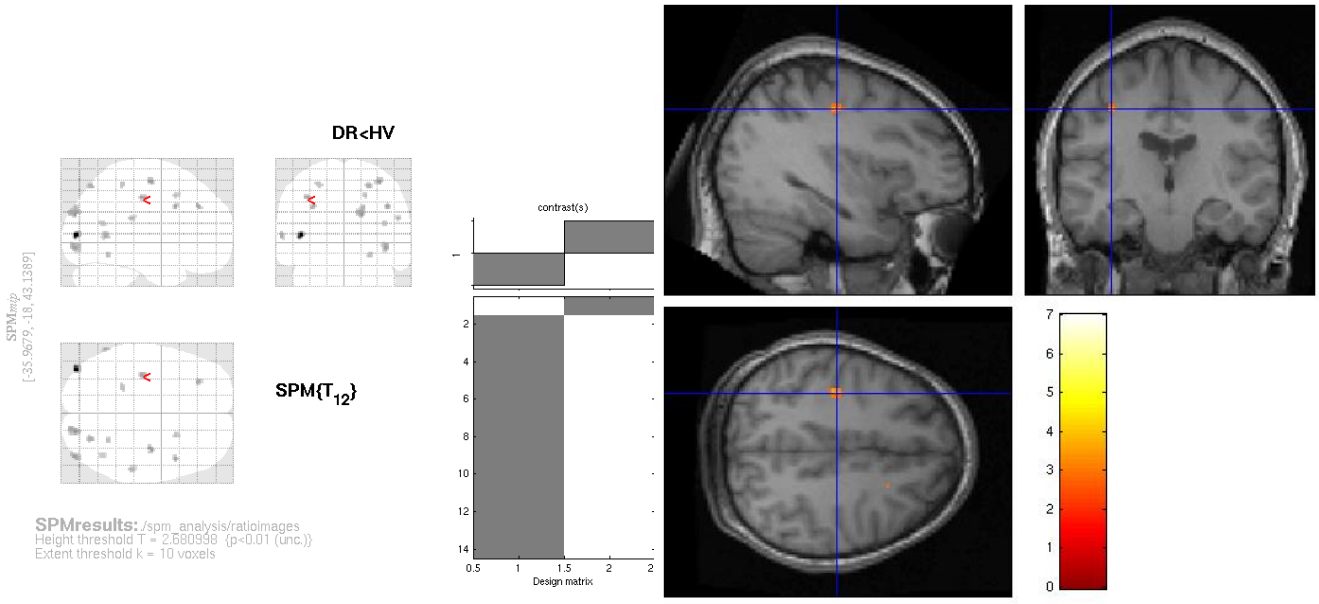

Figure 33: Parametric map of VPM-K_1 for FCD case 3 at baseline
Parametric map of VPM-K_1 for FCD case 3 at baseline compared to 13 healthy controls. Lower VPM-K_1 uptake in the area of FCD is observed in the ipsilateral postcentral gyrus, as well as bilateral occipital lobe and contralateral cuneus.

After inhibition with TQD the VPM uptake increased but this increase was significantly attenuated in the corresponding area of focal cortical dysplasia in the ipsilateral post central gyrus but also extended further to the inferior parietal gyrus, insula, superior temporal lobe and Heschl gyrus. There were also contralateral reduced uptake in the precuneus and inferior temporal lobe (Figure

34). There were no areas of significantly increased VPM uptake in case 3 compared to healthy controls.

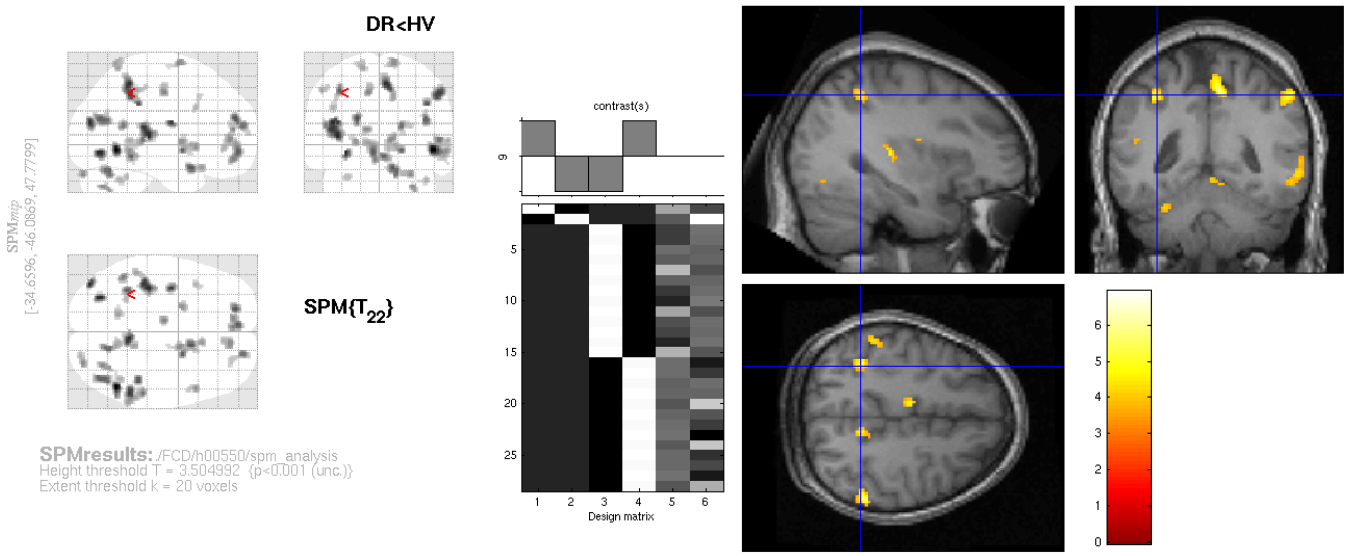

Figure 34: Parametric map of VPM-K_1 for FCD case 3 after TQD
Parametric map of VPM-K_1 for FCD case 3 after inhibition with the Pgp inhibitor tariquidar compared to 13 healthy controls. There are reduced increases of VPM-K_1 uptake in the area of FCD in the ipsilateral postcentral gyrus but it also extends further to the ipsilateral inferior parietal gyrus, superior temporal lobe, insula and to the contralateral precuneus and inferior gyrus.

11.4 DISCUSSION

This is the first in-vivo human PET study investigating Pgp function in patients with FCD compared to healthy controls. We showed that pharmacoresistant FCD patients have reduced uptake of VPM in close proximity to the area of FCD identified in the MRI implying that there is Pgp overexpression in the epileptogenic seizure onset-zone. Previous PET experiments were restricted to investigating Pgp function in TLE (Langer et al. 2007; Feldmann et al. 2013; Bauer et al. 2014). Evidence for Pg expression in FCD has mainly been

performed in epileptogenic human brain tissue resected during epilepsy surgery. Sisodiya et al. (Sisodiya et al. 2001) were the first to show an overexpression of Pgp in FCD. They studied four samples of surgically resected FCD and compared the findings with normal necropsy brain tissue. They showed an overexpression of Pgp in abnormal giant dysplastic neurons, glial cells, and in perivascular distribution in epileptogenic tissue. The authors extended their work by increasing the number of patients and included 14 patients with FCD in their study (Sisodiya et al. 2002). Their findings confirmed their previous work demonstrating an overexpression of Pgp also in astrocytes, dysmorphic neurons and balloon cells of patients with FCD. These findings have since been confirmed in several other studies (Aronica et al. 2003; Aronica et al. 2005; Ak et al. 2007; Oh et al. 2008). Ak et al. included a higher number of patients than the previously reported and studied the expression of Pgp in the epileptic tissues resected surgically in 28 patients with FCD and compared the results with 10 normal necropsy brain tissues (Ak et al. 2007). Normal brain showed no Pgp expression in neurons and astrocytes. In contrast to normal brain Pgp is intensely expressed in both neurons and reactive astrocytes in the vast majority of dysplastic tissues and endothelial cells of patients with FCD. These findings supported the ‘transporter hypothesis’ that overexpression of multidrug efflux transporters in epileptogenic brain regions may lower drug concentrations and thereby reducing their antiepileptic effects, which may explain the refractoriness to AEDs in FCD. However, although increased multidrug efflux transporter expression has been demonstrated in human tissue of patients with FCD that had been resected in surgery it may not be functionally relevant. Therefore non

invasive brain imaging of multidrug efflux transporter function in pharmacoresistant epilepsy patients are a strategy to evaluate whether the overexpression of multidrug efflux transporters at the BBB as postulated in the 'transporter hypothesis' have any functional consequences that underlie pharmacoresistance in epilepsy. Additionally, PET tracers for multidrug efflux transporters could be useful to identify epilepsy patients with increased multidrug efflux transporter activity who will benefit from treatment with drug transporter modulation drugs and therefore hold great promises for individualized medicine (Ak et al. 2007; Sisodiya 2003). We observed that the reduced uptake of VPM extends further to other ipsilateral regions implying that the distribution of Pgp overexpression is spread across to other cortical regions. One possible mechanism could be that seizures induce Pgp overexpression and hence the Pgp expression follows the seizure spread through neuronal network connections. In rodent models of mTLE, experimentally induced seizures have been shown to increase the expression of Pgp in brain capillary endothelial cells, astrocytes and neurons in the dentate gyrus, amygdala, hippocampus, piriform and parietal gyrus (Zhang et al. 1999; Seegers et al. 2002; Löscher and Potschka 2005b). Furthermore, FCD has a relative poor surgical outcome compared with TLE with hippocampal sclerosis. Whereas approximately 80% of patients became seizure free after surgical treatment for mesial TLE related to HS (Jeong et al. 2005) the efficacy of surgical treatment for FCD was consistently less favourable, with approximately 33–75% of individuals becoming seizure free (Tassi et al. 2002). The relative poor prognosis can be explained by that FCD is often invisible on MRI which leads to the difficulty to

define epileptogenic zone. The other factor affecting the relative poor surgical outcome is that even after the removal of all visible lesions on MRI, residual microscopic lesion can still be epileptogenic, which means that dysplastic tissues tend to be more extensive than is apparent on MRI and we therefore may elicit epileptogenic lesions with Pgp overactivity with our VPM PET study (Sisodiya et al. 1995; Aaron et al. 2004; Lee and Kim 2013).

Our study is limited by the small number of patients studied to date and a larger group is needed. Because of the small number of patients, no further subgroup analysis was possible to take into account genetic information (ie, polymorphisms) or correlations with seizure frequency or duration of epilepsy.

11.5 CONCLUSION

This is the first study demonstrating Pgp overactivity in pharmacoresistant epilepsy patients due to FCD in-vivo by using VPM PET showing that VPM uptake is reduced in the area of FCD and also extends further to other ipsilateral regions suggesting widespread abnormalities in FCD. We provide support for the ‘transporter hypothesis’ that there is overexpression of Pgp which may contribute to the pharmacoresistance of epilepsy caused by focal cortical dysplasia.

CHAPTER XII OVERALL CONCLUSION

12.1 INTRODUCTION

This thesis aimed to evaluate Pgp activity and expression in pharmacoresistant mTLE. We assessed Pgp activity in vivo by using the imaging technique PET and performed PET scans with the Pgp substrate VPM in pharmacoresistant and seizure-free mesial temporal lobe epilepsy patients and healthy controls before and after the Pgp inhibitor TQD. We compared the results of the in vivo VPM-PET scans with ex vivo epileptic tissues removed during epilepsy surgery correlating Pgp activity measured with VPM-PET with Pgp expression established in surgically-resected brain tissue. Furthermore, we evaluated Pgp activity by measuring additional peripheral markers of Pgp function: PBMC ABCB1 mRNA level as well as the ABCB1 polymorphism and S100B level in pharmacoresistant mTLE and compared them to seizure-free mTLE patients and healthy controls. Finally, we extended our study to other epilepsy syndromes by applying the methodology of measuring in-vivo Pgp activity with PET using the Pgp substrate VPM together with the Pgp inhibitor TQD to three patients with FCD and pharmacoresistant epilepsy.

12.2 SUMMARY OF THE MAIN FINDINGS

- Using ROI analysis we showed that there are differences in VPM metabolism between mTLE patients and healthy controls which is caused by AED-mediated hepatic cytochrome P450 enzyme induction in mTLE patients requiring images to be normalised for global brain differences.

- ROI analysis at baseline showed no difference of VPM K_1 ratios in pharmacoresistant compared to seizure-free mTLE patients or healthy controls.

- ROI analysis after partial Pgp-inhibition with TQD showed attenuated global increases of VPM brain uptake in pharmacoresistant mTLE patients compared to healthy controls but there where no regional differences.

- Voxel-based SPM analysis at baseline, showed that pharmacoresistant mTLE patients have significantly reduced VPM uptake compared to seizure free mTLE patients and healthy controls in the temporal lobes. However, the reduction is not restricted to ipsilateral epileptogenic regions but also extends to contralateral temporal lobe regions, implying a wider area of Pgp overexpression than the epileptogenic focus.

- Pharmacoresistant mTLE patients who have frequent seizures have the lowest VPM uptake, substantiating the contribution of seizures to the induction of Pgp overexpression in epilepsy.

- Voxel-based SPM analysis after partial blockade of Pgp with TQD, pharmacoresistant mTLE patients have attenuated increases of VPM uptake in the whole brain and more so in the ipsilateral epileptogenic area of the hippocampus compared to healthy controls, implicating functionally elevated Pgp function primarily in the epileptogenic hippocampus in pharmacoresistant epilepsy.

- A case-by-case comparison of epilepsy patients with focal cortical dysplasia against a group of healthy controls revealed that VPM uptake is reduced not only in close proximity to the area of FCD identified by MRI but also that the reduction extends further to other ipsilateral regions, supplementing the findings in mTLE patients that Pgp overexpression is not limited to the epileptogenic seizure-onset zone but also spreads across to other cortical regions.

- The difference in percentage change in VPM uptake after Pgp inhibition with tariquidar in the hippocampus compared to a reference temporal lobe region is inversely correlated with the corresponding difference in percentage area of Pgp immunopositive labelling in pharmacoresistant

mTLE patients who underwent anterior temporal lobe resection for surgical treatment, demonstrating that imaging with PET and a radiolabeled Pgp substrate is a suitable tool to assess Pgp function in vivo in humans.

- There was no difference in peripheral markers of Pgp activity measured by PBMC ABCB1 mRNA level expression and S100B level as well as with the ABCB1 genetic polymorphism in pharmacoresistant compared to seizure-free mTLE patients and healthy controls.

12.3 NEUROBIOLOGICAL AND CLINICAL IMPLICATIONS

We provide the first direct in-vivo evidence for Pgp overactivity in human pharmacoresistant temporal lobe epilepsy manifesting as attenuated tariquidar-induced increases in VPM brain uptake in six of our 14 patients. We directly translated findings of Pgp overexpression from rodent studies (Rizzi et al. 2002; Seegers et al. 2002; Van Vliet et al. 2006; Bankstahl et al. 2008b) and ex-vivo studies in epileptogenic tissues removed during surgery from patients with pharmacoresistant epilepsy and post-mortem tissue (Sisodiya et al. 2002; Aronica et al. 2004; Liu et al. 2012) in-vivo and showed that Pgp is a functionally relevant mechanism in pharmacoresistant temporal lobe epilepsy. Using this imaging technique we can identify individual patients where pharmacoresistance is caused by Pgp overactivity and potentially individualise treatment. Moreover, comparative studies between pharmacoresistant and seizure-free epilepsy patients can enable testing for a correlation between Pgp function and the pharmacoresponse. This imaging technique can also guide patient selection for future clinical studies. In particular, PET imaging of Pgp function may allow individualized application of approaches to overcome Pgp–associated pharmacoresistance. Our study provides useful information for future combined imaging and clinical trials of novel treatment strategies, such as Pgp inhibitors or modulators of overexpression in patients who have Pgp overactivity on VPM-PET. Targeting Pgp by modulators can enhance the efficacy of antiepileptic drugs. The compound verapamil is a substrate for Pgp at low concentrations (which is used in PET), but, like many substrates, verapamil is also an inhibitor for Pgp at high concentrations (Kannan et al. 2009). Verapamil

was among the first identified inhibitors of Pgp and it may function to block Pgp–modulated efflux of AEDs in the brain, thereby raising the intracellular concentration of AEDs (Summers et al. 2004). The third-generation modulator TQD increased the efficacy of phenytoin in a chronic rat epilepsy model and helped to overcome pharmacoresistance to phenobarbital in chronic rat epilepsy models (Van Vliet et al. 2006). On the other hand, first- and second-generation inhibitors are not specific for Pgp alone and can exert additional pharmacodynamic and pharmacokinetic effects. Third-generation inhibitors are considered fairly specific. But there is recent evidence for the third-generation inhibitor TQD that it can also affect the efflux transporter BCRP/ABCG2. Moreover, long-term inhibition of this transporter needs to take into account that Pgp serves as a protective mechanism and gatekeeper in several blood tissue barriers as well as hematopoietic cells (Huls et al. 2009). In addition to limiting access of harmful xenobiotics to sensitive tissues or cells, Pgp also accelerates extrusion of xenobiotics based on its efflux function in the liver and kidneys. Therefore, alternate approaches that leave basal transporter expression and function unaffected might offer advantages for tolerability and safety issues. Preventing seizure-associated transporter upregulation might offer an intriguing alternate approach to overcoming transporter associated pharmacoresistance (Potschka). In addition our study provides further support for an association between Pgp activity and seizure frequency. As already stated, experimental data indicate that seizure activity is the main factor upregulating Pgp in the epileptic brain. In rodent models of mTLE, Pgp expression increases significantly as early as 24 hours after experimentally induced SE (Rizzi et al.

2002; Seegers et al. 2002; Bankstahl et al. 2008a). The excitatory neurotransmitter glutamate, which is excessively released by seizures, upregulates Pgp expression in brain capillary endothelial cells, astrocytes and neurons in the dentate gyrus, amygdala, hippocampus, piriform and parietal gyrus (Zhang et al. 1999; Seegers et al. 2002; Zhu and Liu 2004; Bankstahl et al. 2008a; Bankstahl et al. 2011). In a recent study published by our department in post-mortem tissue, we showed Pgp overexpression in the sclerotic hippocampus in all eight individuals with pharmacoresistant epilepsy, but not in post-mortem tissue from a seizure-free individual, eight of eight post-mortem controls, or non-epileptogenic tissue from 14 of 14 patients with epilepsy with electrode-related injuries, indicating that the occurrence of seizures appear central to Pgp overexpression (Liu et al. 2012). These findings suggest that there is measurable, localised Pgp overactivity in pharmacoresistant temporal lobe epilepsy which is related to seizure activity; Pgp overexpression was not seen in the patient who was seizure free. Pgp overactivity might thus explain why pre-treatment seizure density is one factor predicting poor response to antiepileptic drugs.

12.4 LIMITATIONS OF THE STUDY

Although our study was relatively large for a PET study and sufficiently statistically powered, all studies in this thesis contain relatively small numbers of patients and our findings will have to be confirmed in other and larger populations of patients with epilepsy.

A further limitation of our study is that only five of our pharmacoresistant patients have undergone epilepsy surgery so far, and the correlation between in-vivo and ex-vivo measures of Pgp activity needs to be investigated in larger studies.

Our aim was to show a difference between groups of pharmacoresistant and seizure-free patients with temporal lobe epilepsy. Because of the small number of patients, no further subgroup analysis was possible to take into account genetic information (ie, polymorphisms), psychiatric co-morbidities, or potential differences in Pgp activity due to race or previous drug use. Association genetics requires large cohort sizes and to further refine the multidrug resistant phenotype a sufficient number of patients will have to be included.

Direct labelling of antiepileptic drugs is possible than could represent an alternative strategy for directly probing the clinical relevance in patients showing resistance to individual antiepileptic drugs. PET scans performed with the weak Pgp substrate [^{11}C]diphenylhydantoin long before the transporter hypothesis was formulated did not show any difference in binding between pharmacoresistant patients and non-epileptic patients. The greater affinity of (R)-[^{11}C]verapamil and [^{11}C]diphenylhydantoin for Pgp might explain why we were able to detect not

only whole brain but also regional differences in Pgp activity at baseline. Experiments with a Pgp inhibitor and ^{11}C]diphenylhydantoin have not been done, but will be important to increase the sensitivity to detect group differences between patients and controls.

The manual delineation of the CP is a time-consuming, potentially error-prone and subjective task. Since the CP has the highest VPM uptake resulting in spill-over of radioactivity into the neighbouring hippocampus, the CP has to be masked out when assessing mTLE patients. An erroneous CP mask effects the results of the hippocampus therefore developing automated segmentation methods for the partial volume correction of the CP would be useful so that the hippocampus can be accurately assessed in a timely-manner.

Finally, currently the clinical application of VPM PET is limited by the need for a cyclotron on-site, the significant expense, the injection of a radiolabeled tracer thus limiting the number of studies that can be performed in a particular subject and the invasive arterial line. In the future a fluorine-18 VPM PET tracer with a longer half-life without the need for an on-site cyclotron as well as the development of image derived input functions would improve the clinical application of VPM PET.

12.5 FUTURE WORK

Clinically it is what happens to individual patients that is important and the next step in the validation of these techniques will involve similar studies with larger numbers of patients. These should include also other epilepsy syndromes. Furthermore, the correlation between in-vivo and ex-vivo measures of Pgp activity by comparing VPM-PET scans with surgical tissue of pharmacoresistant patients undergone epilepsy surgery as well as the genotyping analysis will need to be extended to larger studies. In the future larger studies are needed to assess the effect of age and gender on Pgp activity and expression in pharmacoresistant epilepsy.

The next step in the future will be to combine imaging and clinical trials of novel treatment strategies, with Pgp inhibitors or modulators in patients who have Pgp overactivity on VPM-PET aimed at reversing drug resistance with selection of optimal patients and assessment of molecular targets. But further development of the approach needs to also consider tolerability issues specific to the different targets (Potschka 2010). In particular more evaluation is needed in view of the controversial findings which AEDs are Pgp substrates and, thus, determine the penetration of which particular AEDs are affected by Pgp. Of course, evidence that some antiepileptic drugs are affected by the human Pgp isoform and that others are not substrates, needs to be considered when drawing conclusions about the future promises of any approach to modulate Pgp expression or function. Modulating Pgp might, therefore, only help to overcome resistance to selected antiepileptic drugs, but might not help to overcome multidrug

resistance. More precise knowledge about substrate specificities is, therefore, crucial to guide the putative future application of respective diagnostics as well as therapeutic strategies to selected patients.

Finally, although here we provide the proof of concept for the transporter hypothesis and show that there is functionally relevant Pgp overactivity in pharmacoresistant mTLE, the critical question remains whether it sufficient to overcome Pgp overexpression as one putative mechanism of a multifactorial problem or that other mechanisms such as intrinsic disease severity, alterations in targets, different gene variants or network alterations need to be taken into account and in the future further investigated. Given the complexity of epilepsy, it is unlikely that pharmacoresistant epilepsy is caused by a single mechanism but instead is due to several mechanisms which may even occur in the same patient. Overcoming pharmacoresistance in epilepsy represents a challenge and will necessitate a multifactorial approach and the combined efforts of basic and clinical epilepsy researchers (Loescher et al. 2013).

REFERENCE LIST

Aaron, A. C.-G., Ã. z. Korey, A. B. Richard, H. K. Jung and D. S. Dennis (2004). "Long-term outcome after epilepsy surgery for focal cortical dysplasia." Journal of Neurosurgery **101**(1): 55-65.

Abrahim, A., G. Luurtsema, M. Bauer, R. Karch, M. Lubberink, E. Pataraia, C. Joukhadar, K. Kletter, A. Lammertsma, C. Baumgartner, M. Müller and O. Langer (2008). "Peripheral metabolism of (R)-[11C]verapamil in epilepsy patients." Eur J Nucl Med Mol Imaging. **35**: 116-23.

Ak, H., B. Ay, T. Tanriverdi, G. Sanus, Is, M, , Sar M, B. Oz, C. Ozkara, E. Ozyurt and M. Uzan (2007). "Expression and cellular distribution of multidrug resistancerelated proteins in patients with focal cortical dysplasia." Seizure (16): 493–503.

Al-Otaibi, F., S. S. Baeesa, A. G. Parrent, J. P. Girvin and D. Steven (2012). "Surgical Techniques for the Treatment of Temporal Lobe Epilepsy." Epilepsy Research and Treatment: 374848.

Ambroziak, K., K. Kuteykin-Teplyakov, C. Luna-Tortós, M. Al-Falah, M. Fedrowitz and W. Loescher (2010). "Exposure to antiepileptic drugs does not alter the functionality of P-glycoprotein in brain capillary endothelial and kidney cell lines." European Journal of Pharmacology **628**: 57-66.

Ambudkar, S., S. Dey, C. Hrycyna, M. Ramachandra, I. Pastan and M. Gottesman (1999). "Biochemical, cellular, and pharmacological aspects of the multidrug transporter." Annu Rev Pharmacol Toxicol.: 361-98.

Anton-Rodriguez, J. M., M. Sibomana, M. D. Walker, M. C. Huisman, J. C. Matthews, M. Feldmann, S. H. Keller and M. C. Asselin (2010). "Investigation of motion induced errors in scatter correction for the HRRT brain scanner " Nuclear Science Symposium Conference Record (NSS/MIC), 2010 IEEE: 2935 –2940.

Arida, R., F. Scorza, C. Scorza and E. Cavalheiro (2009). "Is physical activity beneficial for recovery in temporal lobe epilepsy? Evidences from animal studies." Neuroscience & Biobehavioral Reviews **33**(3): 422-431.

Aronica, E. and P. Crino (2011). "Inflammation in epilepsy: clinical observations." Epilepsia. **52**: 26-32.

Aronica, E., J. A. Gorter, G. H. Jansen, C. W. M. van Veelen, P. C. van Rijen, S. Leenstra, M. Ramkema, G. L. Scheffer, R. J. Scheper and D. Troost (2003). "Expression and cellular distribution of multidrug transporter proteins in two major causes of medically intractable epilepsy: focal cortical dysplasia and glioneuronal tumors." Neuroscience **118**(2): 417-429.

Aronica, E., J. A. Gorter, S. Redeker, E. A. Van Vliet, M. Ramkema, G. L. Scheffer, R. J. Scheper, P. Van Der Valk, S. Leenstra, J. C. Baayen, W. G. M. Spliet and D. Troost (2005). "Localization of Breast Cancer Resistance Protein (BCRP) in Microvessel Endothelium of Human Control and Epileptic Brain." Epilepsia **46**(6): 849-857.

Aronica, E., F. Özbas-Gerçeker, S. Redeker, M. Ramkema, W. G. M. Spliet, P. C. van Rijen, S. Leenstra, J. A. Gorter and D. Troost (2004). "Expression and cellular distribution of high- and low-affinity neurotrophin receptors in malformations of cortical development." Acta Neuropathologica **108**(5): 422-434.

Ashburner, J. (2007). "A fast diffeomorphic image registration algorithm." Neuroimage. **38**: 95-113.

Ashburner, J. and K. Friston (1997). "Multimodal Image Coregistration and Partitioning-A Unified Framework." NeuroImage **6**(3): 209-217.

Ashburner, J. and K. J. Friston (2005). "Unified segmentation." NeuroImage **26**(3): 839-851.

Atici, Y., F. Alehan, T. Sezer, N. Tuygun, A. Haberal, A. Yazici and C. Karacan (2012). "Serum S100B levels in children with simple febrile seizures." Seizure - European Journal of Epilepsy **21**(3): 175-177.

Babalola, K., B. Patenaude, P. Aljabar, J. Schnabel, D. Kennedy, W. Crum, S. Smith, T. Cootes, M. Jenkinson and D. Rueckert (2009). "An evaluation of four automatic methods of segmenting the subcortical structures in the brain." Neuroimage. **47**: 1435-47.

Bailey, D. (1998). "Transmission scanning in emission tomography." Eur J Nucl Med. **25**: 774-87.

Balosso, S., T. Ravizza, M. Pierucci, E. Calcagno, R. Invernizzi, G. Di Giovanni, E. Esposito and A. Vezzani (2009). "Molecular and functional interactions between tumor necrosis factor-alpha receptors and the glutamatergic system in the mouse hippocampus: implications for seizure susceptibility." Neuroscience. **161**: 293-300.

Baltes, S., M. Fedrowitz, C. L. Tortós, H. Potschka and W. Löscher (2007a). "Valproic Acid Is Not a Substrate for P-glycoprotein or Multidrug Resistance Proteins 1 and 2 in a Number of in Vitro and in Vivo Transport Assays." Journal of Pharmacology and Experimental Therapeutics **320**(1): 331-343.

Baltes, S., A. M. Gastens, M. Fedrowitz, H. Potschka, V. Kaever and W. Löscher (2007b). "Differences in the transport of the antiepileptic drugs phenytoin, levetiracetam and carbamazepine by human and mouse P-glycoprotein." Neuropharmacology **52**(2): 333-346.

Ban, J.-J., K.-H. Jung, K. Chu, S.-T. Lee, D. Jeon, K.-I. Park, H.-J. Moon, H. Kim, S. Kim, S. K. Lee and J.-K. Roh "Profiles of Multidrug Resistance Protein-1 in the Peripheral Blood Mononuclear Cells of Patients with Refractory Epilepsy." PLoS ONE **7**(5): e36985.

Banerjee, J., S. Chandra, N. Kurwale and M. Tripathi (2014). "Epileptogenic networks and drug-resistant epilepsy: Present and future perspectives of epilepsy research-Utility for the epileptologist and the epilepsy surgeon." Ann Indian Acad Neurol **17**: 134-40.

Bankstahl, J., M. Bankstahl, C. Kuntner, J. Stanek, T. Wanek, M. Meier, X. Ding, M. Müller, O. Langer and W. Löscher (2011). "A novel positron emission tomography imaging protocol identifies seizure-induced regional overactivity of P-glycoprotein at the blood-brain barrier." J Neurosci. **31**: 8803-11.

Bankstahl, J., K. Hoffmann, K. Bethmann and W. Löscher (2008a). "Glutamate is critically involved in seizure-induced overexpression of P-glycoprotein in the brain." Neuropharmacology **54**: 1006-16.

Bankstahl, J., C. Kuntner, A. Abrahim, R. Karch, J. Stanek, T. Wanek, W. Wadsak, K. Kletter, M. Mueller, W. Löscher and O. Langer (2008b). "Tariquidar-Induced P-Glycoprotein Inhibition at the Rat Blood Brain Barrier Studied with (R)-11C-Verapamil and PET." Journal of Nuclear Medicine **49**(8): 1328-1335.

Bankstahl, J. and W. Löscher (2008). "Resistance to antiepileptic drugs and expression of P-glycoprotein in two rat models of status epilepticus. ." Epilepsy research **82**: 70–85.

Baram, T., M. Eghbal-Ahmadi and R. Bender (2002). "Is neuronal death required for seizure-induced epileptogenesis in the immature brain?" Prog Brain Res. **135**: 365-75.

Baron, J., D. Roeda, C. Munari, C. Crouzel, J. Chodkiewicz and D. Comar (1983). "Brain regional pharmacokinetics of 11C-labeled diphenylhydantoin: positron emission tomography in humans." Neurology **33**: 580-5.

Bart, J., A. T. M. Willemsen, H. J. M. Groen, W. T. A. van der Graaf, T. D. Wegman, W. Vaalburg, E. G. E. de Vries and N. H. Hendrikse (2003). "Quantitative assessment of P-glycoprotein function in the rat blood-brain barrier by distribution volume of [11C]verapamil measured with PET." NeuroImage **20**(3): 1775-1782.

Bartels, A. L., R. Kortekaas, J. Bart, A. T. M. Willemsen, O. L. de Klerk, J. J. de Vries, J. C. H. van Oostrom and K. L. Leenders (2009). "Blood-brain barrier P-glycoprotein function decreases in specific brain regions with aging: A possible role in progressive neurodegeneration." Neurobiology of Aging **30**(11): 1818-1824.

Bartmann, H., C. Fuest, C. La Fougère, G. Xiong, T. Just, J. Schlichtiger, P. Winter, G. Böning, B. Wängler, A. Pekcec, J. Soerensen, P. Bartenstein, P. Cumming and H. Potschka (2010). "Imaging of P-glycoprotein-mediated pharmacoresistance in the hippocampus: proof-of-concept in a chronic rat model of temporal lobe epilepsy." Epilepsia. **51**: 1780-90.

Basic, S., S. Hajnsek, N. Bozina, I. Filipcic, D. Sporis, D. Mislov and A. Posavec (2008). "The influence of C3435T polymorphism of ABCB1 gene on penetration of phenobarbital across blood-brain barrier in patients with generalized epilepsy. ." Seizure Eur. J. Epilepsy. **17**: 524–530.

Bauer, B. (2008). "Seizure-induced up-regulation of P-glycoprotein at the blood-brain barrier through glutamate and cyclooxygenase-2 signalling." Mol. Pharmacol. **73**: 1444-1453.

Bauer, B. r., A. M. S. Hartz, A. Pekcec, K. Toellner, D. S. Miller and H. Potschka (2008). "Seizure-Induced Up-Regulation of P-Glycoprotein at the Blood-Brain Barrier through Glutamate and Cyclooxygenase-2 Signaling." Molecular Pharmacology **73**(5): 1444-1453.

Bauer, M., R. Karch, F. Neumann, C. Wagner, K. Kletter, M. Müller, W. Löscher, M. Zeitlinger and O. Langer (2010). "Assessment of regional differences in tariquidar-induced P-glycoprotein modulation at the human blood-brain barrier." J Cereb Blood Flow Metab. **30**: 510-5.

Bauer, M., R. Karch, M. Zeitlinger, J. Liu, M. Koepp, M. Asselin, S. Sisodiya, J. Hainfellner, W. Wadsak, M. Mitterhauser, M. Müller, E. Pataraia and O. Langer (2014). "In vivo P-glycoprotein function before and after epilepsy surgery." Neurology **83**: 1326-1331

Bauer, M., R. Karch, M. Zeitlinger, J. Stanek, C. Philippe, W. Wadsak, M. Mitterhauser, W. Jäger, H. Haslacher, M. Müller and O. Langer (2013). "Interaction of 11C-tariquidar and 11C-elacridar with P-glycoprotein and breast cancer resistance protein at the human blood-brain barrier." J Nucl Med. **54**: 1181-7.

Baxendale, S. and P. Thompson (2010). "Beyond localization: the role of traditional neuropsychological tests in an age of imaging." Epilepsia **51**: 2225-30.

Beaulieu, E., M. Demeule, L. Ghitescu and R. Béliveau (1997). "P-glycoprotein is strongly expressed in the luminal membranes of the endothelium of blood vessels in the brain." Biochem J. **326**: 539-44.

Bebawy, M. and M. Chetty (2009). "Gender differences in P-glycoprotein expression and function: effects on drug disposition and outcome. ." Curr Drug Metab. **10**: 322–328.

Beghi, E. (2011). "New classification proposals for epilepsy: A real advancement in the nosography of the disease?" Epilepsia **52**: 1197–1198.

Ben-Ari, Y., E. Tremblay and O. P. Ottersen (1980). "Injections of kainic acid into the amygdaloid complex of the rat: An electrographic, clinical and histological study in relation to the pathology of epilepsy." Neuroscience **5**(3): 515-528.

Berg, A., S. Berkovic, M. Brodie, J. Buchhalter, J. Cross, W. vanEmde Boas, J. Engel, J. French, T. Glauser, G. Mathern, S. Moshe, D. Nordli, P. Plouin and I. Scheffer (2010). "Revised terminology and concepts for organization of seizures and epilepsies: report of the ILAE Commission on Classification and Terminology, 2005–2009." Epilepsia **51**: 676–685.

Bilevicius, E., C. Yasuda, M. Silva, C. Guerreiro, I. Lopes-Cendes and F. Cendes (2010). "Antiepileptic drug response in temporal lobe epilepsy: A clinical and MRI morphometry study." Neurology **75**(19): 1695-1701.

Binder, J., J. Frost, T. Hammeke, R. Cox, S. Rao and T. Prieto (1997). "Human brain language areas identified by functional magnetic resonance imaging." J Neurosci. **17**: 353-62.

Blair, R. D. G. (2012). "Temporal Lobe Epilepsy Semiology." Epilepsy Research and Treatment **Article ID 751510**.

Bonilha, L., J. Halford, C. Rorden, D. Roberts, Z. Rumboldt and M. Eckert (2009). "Automated MRI analysis for identification of hippocampal atrophy in temporal lobe epilepsy." Epilepsia. **50**: 228-33.

Bonilha, L., C. Rorden, G. Castellano, F. Pereira, P. Rio, F. Cendes and L. Li (2004). "Voxel-based morphometry reveals gray matter network atrophy in refractory medial temporal lobe epilepsy." Archives of neurology **61**: 1379-1384.

Bournissen, F. G., M. E. Moretti, D. N. Juurlink, G. Koren, M. Walker and Y. Finkelstein (2009). "Polymorphism of the MDR1/ABCB1 C3435T drug-transporter and resistance to anticonvulsant drugs: A meta-analysis." Epilepsia **50**(4): 898-903.

Brandt, C., K. Bethmann, A. M. Gastens and W. Loescher (2006). "The multidrug transporter hypothesis of drug resistance in epilepsy: Proof-of-principle in a rat model of temporal lobe epilepsy." Neurobiology of Disease **24**(1): 202-211.

Brasse, D., P. E. Kinahan, C. Lartizien, C. Comtat, M. Casey and C. Michel (2005). "Correction methods for random coincidences in fully 3D whole-body PET: impact on data and image quality." Journal of nuclear medicine **46**(5): 859-867.

Brooks-Kayal, A., M. Shumate, H. Jin, T. Rikhter and D. Coulter (1998). "Selective changes in single cell GABA(A) receptor subunit expression and function in temporal lobe epilepsy." Nat Med. **4**: 1166-72.

Brunner, M., O. Langer, R. Sunder-Plassmann, G. Dobrozemsky, U. Muller, W. Wadsak, A. Krcal, R. Karch, C. Mannhalter, R. Dudczak, K. Kletter, I. Steiner, C. Baumgartner and M. Muller (2005). "Influence of functional haplotypes in the drug transporter gene ABCB1 on central nervous system drug distribution in humans." Clin Pharmacol Ther **78**(2): 182-190.

Calik, M., M. Abuhandan, A. Sonmezler, H. Kandemir, I. Oz, A. Taskin, S. Selek and A. Iscan (2013). "Elevated serum S-100B levels in children with temporal lobe epilepsy." Seizure : the journal of the British Epilepsy Association **22**(2): 99-102.

Cascino, G. (1990). "Intractable partial epilepsy: evaluation and treatment." Mayo Clin Proc. **65**: 1578-86.

Cascino, G. (2008). "When drugs and surgery don't work." Epilepsia. **49**: 79-84.

Cendes, F., Z. Caramanos, F. Andermann, F. Dubeau and D. Arnold (1997). "Proton magnetic resonance spectroscopic imaging and magnetic resonance imaging volumetry in the lateralization of temporal lobe epilepsy: a series of 100 patients." Ann Neurol. **42**(5): 737-46.

Chaves, M., A. Camozzato, E. Ferreira, I. Piazenski, R. Kochhann, O. Dall'Igna, G. Mazzini, D. Souza and L. Portela (2010). "Serum levels of S100B and NSE proteins in Alzheimer's disease patients." Journal of Neuroinflammation **7**(1): 6.

Cherry, S. (2001). "Fundamentals of positron emission tomography and applications in preclinical drug development." J Clin Pharmacol. **41**: 482-91.

Chung, M., T. Walczak, D. Lewis, D. Dawson and R. Radtke (1991). "Temporal Lobectomy and Independent Bitemporal Epileptiform Activity: What degree of lateralization is sufficient?" Epilepsia **32**: 195-201.

Chupin, M., A. Hammers, R. S. N. Liu, O. Colliot, J. Burdett, E. Bardinet, J. S. Duncan, L. Garnero and L. Lemieux (2009). "Automatic segmentation of the hippocampus and the amygdala driven by hybrid constraints: Method and validation." Neuroimage **46**(3): 749-761.

Cleary, R., S. Baxendale, P. Thompson and J. Foong (2013a). "Predicting and preventing psychopathology following temporal lobe epilepsy surgery." Epilepsy Behav. **26**: 322-34.

Cleary, R., Thompson, PJ, M. Thom and J. Foong (2013b). "Postictal psychosis in temporal lobe epilepsy: risk factors and postsurgical outcome?" Epilepsy Res. **106**: 264-72.

Clinckers, R., I. Smolders, A. Meurs, G. Ebinger and Y. Michotte (2005). "Quantitative in Vivo Microdialysis Study on the Influence of Multidrug Transporters on the Blood-Brain Barrier Passage of Oxcarbazepine: Concomitant Use of Hippocampal Monoamines as Pharmacodynamic Markers for the Anticonvulsant Activity." Journal of Pharmacology and Experimental Therapeutics **314**(2): 725-731.

Cole, S., G. Bhardwaj, J. Gerlach, J. Mackie, C. Grant, K. Almquist, A. Stewart, E. Kurz, A. Duncan and R. Deeley (1992). "Overexpression of a transporter gene in a multidrug-resistant human lung cancer cell line." Science. **258**: 1650-4.

Conseil, G., R. Deeley and S. Cole (2005). "Polymorphisms of MRP1 (ABCC1) and related ATP-dependent drug transporters." Pharmacogenet Genomics. **15**: 523-33.

Coulter, D., D. McIntyre and W. Löscher (2002). "Animal models of limbic epilepsies: what can they tell us?" Brain Pathol. **12**: 240-56.

Croop, J., M. Raymond, D. Haber, A. Devault, R. Arceci, P. Gros and D. Housman (1989). "The three mouse multidrug resistance (mdr) genes are expressed in a tissue-specific manner in normal mouse tissues." Mol Cell Biol. **9**: 1346-50.

Crowe, A. and Y.-K. Teoh (2006). "Limited P-glycoprotein mediated efflux for anti-epileptic drugs." Journal of Drug Targeting **14**(5): 291-300.

Dagenais, C., J. Zong, J. Ducharme and G. Pollack (2001). "ffect of mdr1a P-glycoprotein gene disruption, gender, and substrate concentration on brain uptake of selected compounds." E Pharm Res **18**: 957–963.

De Lange, E. (2004). "Potential role of ABC transporters as a detoxification system at the blood-CSF barrier." Adv Drug Deliv Rev. **56**: 1793-809.

De Oliveira, D. L., A. Fischer, R. S. Jorge, M. C. Da Silva, M. Leite, C. A. Gonçalves, J. A. Quillfeldt, D. O. Souza, T. M. E Souza and S. Wofchuk (2008). "Effects of early-life LiCl-Pilocarpine-induced status epilepticus on memory and anxiety in adult rats are associated with mossy fiber sprouting and elevated CSF S100B protein." Epilepsia **49**(5): 842-852.

Dean, M., A. Rzhetsky and R. Allikmets (2001). "The human ATP-binding cassette (ABC) transporter superfamily." Genome Res. **11**: 1156-66.

Defrise, M., D. Townsend, D. Bailey, A. Geissbuhler, C. Michel and T. Jones (1991). "A normalization technique for 3D PET data." Phys Med Biol. **36**: 939-52.

Deisz, R. (2002). "Cellular mechanisms of pharmacoresistance in slices from epilepsy surgery." Novartis Found Symp **243**: 186-99.

Demeule, M., A. Régina, J. Jodoin, A. Laplante, C. Dagenais, F. Berthelet, A. Moghrabi and R. Béliveau (2002). "Drug transport to the brain: key roles for the efflux pump P-glycoprotein in the blood-brain barrier." Vascul Pharmacol. **38**: 339-48.

Didelot, A., F. Mauguière, J. Redouté, S. Bouvard, A. Lothe, A. Reilhac, A. Hammers, N. Costes and P. Ryvlin (2010). "Voxel-based analysis of asymmetry index maps increases the specificity of 18F-MPPF PET abnormalities for localizing the epileptogenic zone in temporal lobe epilepsies." J Nucl Med **51**: 1732-9.

Dombrowski, S. M., S. Y. Desai, M. Marroni, L. Cucullo, K. Goodrich, W. Bingaman, M. R. Mayberg, L. Bengez and D. Janigro (2001). "Overexpression of Multiple Drug Resistance Genes in Endothelial Cells from Patients with Refractory Epilepsy." Epilepsia **42**(12): 1501-1506.

Doyle, L., W. Yang, L. Abruzzo, T. Krogmann, Y. Gao, A. Rishi and D. Ross (1998). "A multidrug resistance transporter from human MCF-7 breast cancer cells." Proc Natl Acad Sci U S A. **95**: 15665-70.

Duncan, J. (2010). "Imaging in the surgical treatment of epilepsy." Nature Reviews Neurology **6**: 537-550.

Duncan, J. (2011). "Epilepsy in 2010: Refinement of optimal medical and surgical treatments." Nat Rev Neurol. **7**: 72-4.

Dupont, W. D. and W. D. Plummer Jr (1990). "Power and sample size calculations: A review and computer program." Controlled Clinical Trials **11**(2): 116-128.

Echizen, H., T. Brecht, S. Niedergesäss, B. Vogelgesang and M. Eichelbaum (1985). "The effect of dextro-, levo-, and racemic verapamil on atrioventricular conduction in humans." Am Heart J. **109**: 210-7.

Eckford, P. and F. Sharom (2009). "ABC efflux pump-based resistance to chemotherapy drugs." Chem Rev. **109**: 2989-3011.

Eisenblätter, T., S. Hüwel and H. Galla (2003). "Characterisation of the brain multidrug resistance protein (BMDP/ABCG2/BCRP) expressed at the blood-brain barrier." Brain Res. **971**: 221-31.

Elsinga, P., E. Franssen, N. Hendrikse, L. Fluks, A. Weemaes, W. van der Graaf, E. de Vries, G. Visser and W. Vaalburg (1996). "Carbon-11-labeled daunorubicin and verapamil for probing P-glycoprotein in tumors with PET." J Nucl Med. **37**: 1571-5.

Engel, J. (1984). "The use of positron tomographic scanning in epilepsy. ." Ann Neurol. **15**: 180–191.

Engel, J., Jr. (1996). "Introduction to temporal lobe epilepsy." Epilepsy Research **26**(1): 141-150.

Engel, J. J. (1998). "Classifications of the International League Against Epilepsy: time for reappraisal." Epilepsia. **39**(9): 1014-7.

Evers, R., G. Zaman, L. van Deemter, H. Jansen, J. Calafat, L. Oomen, R. Oude Elferink, P. Borst and A. Schinkel (1996). "Basolateral localization and export activity of the human multidrug resistance-associated protein in polarized pig kidney cells." J Clin Invest. **97**: 1211-8.

Eyal, S., B. Ke, M. Muzi, J. Link, D. Mankoff, A. Collier and J. Unadkat (2010). "Regional P-glycoprotein activity and inhibition at the human blood-brain barrier as imaged by positron emission tomography." Clin Pharmacol Ther. **87**: 579-85.

Fang, M., Z. Xi, Y. Wu and X. Wang (2011). "A new hypothesis of drug refractory epilepsy: neural network hypothesis." Med Hypotheses **76**: 871-6.

Farwell, M., D. Chong, Y. Iida, S. Bae, B. Easwaramoorthy and M. Ichise (2013). "Imaging P-glycoprotein function in rats using [(11)C]-N-desmethyl-loperamide." Ann Nucl Med. **27**: 618-24.

Feldmann, M., M.-C. Asselin, J. Liu, S. Wang, A. McMahon, J. Anton-Rodriguez, M. Walker, M. Symms, G. Brown, R. Hinz, J. Matthews, M. Bauer, O. Langer, M. Thom, T. Jones, C. Vollmar, J. S. Duncan, S. M. Sisodiya and M. J. Koepp (2013). "P-glycoprotein expression and function in patients with temporal lobe epilepsy: a case-control study." The Lancet Neurology **12**(8): 777-785.

Ferrari-Marinho, T., L. Caboclo, M. Marinho, R. Centeno, R. Neves, M. Santana, F. Brito, H. Junior and E. Yacubian (2012). "Auras in temporal lobe epilepsy with hippocampal sclerosis: Relation to seizure focus laterality and post surgical outcome." Epilepsy & Behavior **24**(1): 120-125.

Fox, E. and S. Bates (2007). "Tariquidar (XR9576): a P-glycoprotein drug efflux pump inhibitor." Expert Rev Anticancer Ther. **7**: 447-59.

French, J., P. Williamson, V. Thadani, T. Darcey, R. Mattson, S. Spencer and D. Spencer (1993). "Characteristics of medial temporal lobe epilepsy: I. Results of history and physical examination." Ann Neurol. **34**: 774-80.

Friston, K., A. Holmes, K. Worsley, J. Poline, C. Frith and R. Franckowiak (1995). "Statistical parametric maps in functional imaging. A general approach." Hum Brain Map **2**: 189–210.

Friston, K. J. (1997). "Testing for anatomically specified regional effects. Hum Brain Mapp 5:133–136 " Hum Brain Mapp(5): 133–136

Froklage, F., S. Syvänen, N. Hendrikse, M. Huisman, C. Molthoff, Y. Tagawa, J. Reijneveld, J. Heimans, A. Lammertsma, J. Eriksson, E. de Lange and R. Voskuyl (2012). "[11C]Flumazenil brain uptake is influenced by the blood-brain barrier efflux transporter P-glycoprotein." EJNMMI Res. **2**: 12.

Fromm, M. (2004). "Importance of P-glycoprotein at blood-tissue barriers." Trends Pharmacol Sci. **25**: 423-9.

Gastaut, H. (1969). "Classification of the epilepsies. Proposal for an international classification." Epilepsia **10**: 14-21.

Gastaut, H. (1970). "Clinical and electroencephalographic classification of epileptic seizures." Epilepsia **11**: 102.

Georgiadis, I., E. Kapsalaki and K. Fountas (2013). "Temporal lobe resective surgery for medically intractable epilepsy: a review of complications and side effects." Epilepsy Res Treat. **2013**(Article ID 752195): 12 pages.

Germano, I., N. Poulin and A. Olivier (1994). "Reoperation for recurrent temporal lobe epilepsy." J Neurosurg. **8**: 31-6.

Ghersi-Egea, J. and N. Strazielle (2002). "Choroid plexus transporters for drugs and other xenobiotics." J Drug Target. **10**: 353-7.

Giacomini, K., S. Huang, D. Tweedie, L. Benet, K. Brouwer, X. Chu, A. Dahlin, R. Evers, V. Fischer, K. Hillgren, K. Hoffmaster, T. Ishikawa, D. Keppler, R. Kim, C. Lee, M. Niemi, J. Polli, Y. Sugiyama, P. Swaan, J. Ware, S. Wright, S. Yee, M. Zamek-Gliszczynski and L. Zhang (2010). "Membrane transporters in drug development." Rev Drug Discov **9**(3): 215-36. .

Gloor, P., A. Olivier, L. Quesney, F. Andermann and S. Horowitz (1982). "The role of the limbic system in experiential phenomena of temporal lobe epilepsy." Ann Neurol. **12**(2): 129-44.

Goddard, G. (1967). "Development of epileptic seizures through brain stimulation at low intensity." Nature. **214**: 1020-1.

Golden, P. and G. Pollack (2003). "Blood-brain barrier efflux transport." J Pharm Sci. **92**: 1739-53.

Gottesman, M. M., T. Fojo and S. E. Bates (2002). "Multidrug resistance in cancer: role of ATP-dependent transporters." Nat Rev Cancer **2**(1): 48-58.

Gunn, R., S. Gunn and V. Cunningham (2001). "Positron emission tomography compartmental models." J Cereb Blood Flow Metab **21**: 635-52.

Haerian, B. S., K. S. Lim, C. T. Tan, A. A. Raymond and Z. Mohamed (2011). "Association of ABCB1 gene polymorphisms and their haplotypes with response to antiepileptic drugs: a systematic review and meta-analysis." Pharmacogenomics **12**(5): 713-725.

Haerian, B. S., H. Roslan, A. A. Raymond, C. T. Tan, K. S. Lim, S. Z. Zulkifli, E. H. M. Mohamed, H. J. Tan and Z. Mohamed (2010). "ABCB1 C3435T polymorphism and the risk of resistance to antiepileptic drugs in epilepsy: A systematic review and meta-analysis." Seizure **19**(6): 339-346.

Hammers, A., R. Allom, M. J. Koepp, S. L. Free, R. Myers, L. Lemieux, T. N. Mitchell, D. J. Brooks and J. S. Duncan (2003). "Three-dimensional maximum probability atlas of the human brain, with particular reference to the temporal lobe." Human Brain Mapping **19**(4): 224-247.

Hammers, A., M.-C. Asselin, F. E. Turkheimer, R. Hinz, S. Osman, G. Hotton, D. J. Brooks, J. S. Duncan and M. J. Koepp (2007a). "Balancing bias, reliability, noise properties and the need for parametric maps in quantitative ligand PET: [11C]diprenorphine testâ€“retest data." NeuroImage **38**(1): 82-94.

Hammers, A., S. Bouvard, N. Costes, N. PereiradeSouza, S. Keihaninejad, D. Le Bars and e. al. (2010). "Impact of P-glycoprotein on the distribution of [18F]-MPPF in pharmacoresistant temporal lobe epilepsia." Epilepsia **51**: 48.

Hammers, A., R. Heckemann, M. J. Koepp, J. S. Duncan, J. V. Hajnal, D. Rueckert and P. Aljabar (2007b). "Automatic detection and quantification of hippocampal atrophy on MRI in temporal lobe epilepsy: A proof-of-principle study." NeuroImage **36**(1): 38-47.

Heinemann, U., D. Kaufer and A. Friedman (2012). "Blood-brain barrier dysfunction, TGFβ signaling, and astrocyte dysfunction in epilepsy." Glia **60**: 1251-7.

Heizmann, C. W., R. Astrand, J. Undén and B. Romner (2013). Clinical Use of the Calcium-Binding S100B Protein. Calcium-Binding Proteins and RAGE, Humana Press. **963:** 373-384.

Hendrikse, N. H., A. H. Schinkel, E. G. E. De Vries, E. Fluks, W. T. A. Van der Graaf, A. T. M. Willemsen, W. Vaalburg and E. J. F. Franssen (1998). "Complete in vivo reversal of P-glycoprotein pump function in the blood-brain barrier visualized with positron emission tomography." British Journal of Pharmacology **124**(7): 1413-1418.

Hogan, R., R. Carne, C. Kilpatrick, M. Cook, A. Patel, L. King and T. O'Brien (2008). "Hippocampal deformation mapping in MRI negative PET positive temporal lobe epilepsy." J Neurol Neurosurg Psychiatry. **79**: 636-40.

Holmes, M., C. Dodrill, A. Wilensky, L. Ojemann and G. Ojemann (1996). "Unilateral Focal Preponderance of Interictal Epileptiform Discharges as a Predictor of Seizure Origin." Arch Neurol. **53**: 228-232.

Huang, Y., J. Doherty and R. Dingledine (2002). "Altered histone acetylation at glutamate receptor 2 and brain-derived neurotrophic factor genes is an early event triggered by status epilepticus. ." J Neurosci **22**: 8422–8428. .

Hughes, J. R. (2008). "One of the hottest topics in epileptology: ABC proteins. Their inhibition may be the future for patients with intractable seizures." Neurol. Res. **30**: 920-925.

Huls, M., F. G. M. Russel and R. Masereeuw (2009). "The Role of ATP Binding Cassette Transporters in Tissue Defense and Organ Regeneration." Journal of Pharmacology and Experimental Therapeutics **328**(1): 3-9.

ILAE (1981). "Commission of Classification and Terminology of the International League Against Epilepsy: proposal for revised clinical and electroencephalographic classification of epileptic seizures. ." Epilepsia **22**: 489–501.

ILAE (1989). "Commission on Classification and Terminology of the International League Against Epilepsy: proposal for revised classification of epilepsies and epileptic syndromes." Epilepsia **30**: 389–399.

Innis, R., V. Cunningham, J. Delforge, M. Fujita, A. Gjedde, R. Gunn, J. Holden, S. Houle, S. Huang, M. Ichise, H. Iida, H. Ito, Y. Kimura, R. Koeppe, G. Knudsen, J. Knuuti, A. Lammertsma, M. Laruelle, J. Logan, R. Maguire, M. Mintun, E. Morris, R. Parsey, J. Price, M. Slifstein, V. Sossi, T. Suhara, J. Votaw, D. Wong and R. Carson (2007). "Consensus nomenclature for in vivo imaging of reversibly binding radioligands." J Cereb Blood Flow Metab. **27**: 1533-9.

Ishiwata, K., K. Kawamura, K. Yanai and N. Hendrikse (2007). "In vivo evaluation of P-glycoprotein modulation of 8 PET radioligands used clinically. ." J Nucl Med. **48**: 81–87.

Jack, C., F. Sharbrough, G. Cascino, K. Hirschorn, P. O'Brien and W. Marsh (1992). "Magnetic resonance image-based hippocampal volumetry: correlation with outcome after temporal lobectomy. ." Ann Neurol. **31**: 138–146.

Jackson, G., S. Berkovic, B. Tress, R. Kalnins, G. Fabinyi and P. Bladin (1990). "Hippocampal sclerosis can be reliably detected by magnetic resonance imaging. ." Neurology **40**: 1869–1875.

Jackson, G. D., A. Connelly, J. S. Duncan, R. A. Grunewald and D. G. Gadian (1993). "Detection of hippocampal pathology in intractable partial epilepsy: increased sensitivity with quantitative magnetic resonance T2 relaxometry." Neurology: 1793–1799.

Jandová, K., D. Päsler, L. Antonio, C. Raue, S. Ji, M. Njunting, O. Kann, R. Kovács, H. Meencke, E. Cavalheiro, U. Heinemann, S. Gabriel and T. Lehmann (2006). "Carbamazepine-resistance in the epileptic dentate gyrus of human hippocampal slices." Brain. **129**: 3290-306.

Jensen, S., A. DiPaolo, M. Lastella, P. Erba, M. Baldini, D. Perini, C. Pecori, R. Danesi, A. Iudice,

Mariani, G, , M. Del Tacca and L. Murri (2006). "Pharmacogenetics of ABCB1 and brain kinetics of 99m-Tc-MIBI in epilepsy patients. ." Epilepsia **47 (Suppl. 3)**: 88-89.

Jeong, S.-W., S. K. Lee, K.-S. Hong, K.-K. Kim, C.-K. Chung and H. Kim (2005). "Prognostic Factors for the Surgery for Mesial Temporal Lobe Epilepsy: Longitudinal Analysis." Epilepsia **46**(8): 1273-1279.

Jones, P. and A. George (2004). "The ABC transporter structure and mechanism: perspectives on recent research." Cell Mol Life Sci. **61**: 682-99.

Juliano, R. and V. Ling (1976). "A surface glycoprotein modulating drug permeability in Chinese hamster ovary cell mutants." Biochim Biophys Acta. **455**: 152-62.

Jutila, L., M. Aikiä, A. Immonen, E. Mervaala, I. Alafuzoff and R. Kälviäinen (2014). "Long-term memory performance after surgical treatment of unilateral temporal lobe epilepsy (TLE)." Epilepsy Res. **108**: 1228-37.

Kannan, P., C. John, S. S. Zoghbi, C. Halldin, M. M. Gottesman, R. B. Innis and M. D. Hall (2009). "Imaging the Function of P-Glycoprotein With Radiotracers: Pharmacokinetics and In Vivo Applications." Clin Pharmacol Ther **86**(4): 368-377.

Kapural, M., L. Krizanac-Bengez, G. Barnett, J. Perl, T. Masaryk, D. Apollo, P. Rasmussen, M. R. Mayberg and D. Janigro (2002). "Serum S-100β as a possible marker of blood-brain barrier disruption." Brain Research **940**(1â€“2): 102-104.

Kasperaviciute, D. and S. M. Sisodiya (2009). "Epilepsy pharmacogenetics." Pharmacogenomics **10**(5): 817-836.

Kellner, U., L. Hutchinson, A. Seidel, H. Lage, M. Danks, M. Dietel and S. Kaufmann (1997). "Decreased drug accumulation in a mitoxantrone-resistant gastric carcinoma cell line in the absence of P-glycoprotein." Int J Cancer. **71**: 817-24.

Kemppainen, N., S. Aalto, I. Wilson, K. Någren, S. Helin, A. Brück, V. Oikonen, M. Kailajärvi, M. Scheinin, M. Viitanen, R. Parkkola and J. Rinne (2006). "Voxel-based analysis of PET amyloid ligand [11C]PIB uptake in Alzheimer disease." Neurology. **67**: 1575-80.

Kimchi-Sarfaty, C., J. Oh, I. Kim, Z. Sauna, A. Calcagno, S. Ambudkar and M. Gottesman (2007). "A "silent" polymorphism in the MDR1 gene changes substrate specificity." Science **315**: 525-8.

Klein, O. and Y. Nishina (1929). "Über die Streuung von Strahlung durch freie Elektronen nach der neuen relativistischen Quantendynamik von Dirac." Z. Phys. **52**: 853 and 869.

Kleindienst, A., F. Hesse, M. R. Bullock, M. Buchfelder and T. W. a. A. I. R. M. John (2007). The neurotrophic protein S100B: value as a marker of brain damage and possible therapeutic implications. Progress in Brain Research, Elsevier. **Volume 161:** 317-325.

Knowlton, R., K. Laxer, M. Aminoff, T. Roberts, S. Wong and H. Rowley (1997). "Magnetoencephalography in partial epilepsy: clinical yield and localization accuracy." Ann Neurol. **42**: 622-31.

Kobow, K., A. El-Osta and I. Blümcke (2013). "The methylation hypothesis of pharmacoresistance in epilepsy." Epilepsia. **54**: 41-7.

Kobow, K., I. Jeske, M. Hildebrandt, J. Hauke, E. Hahnen, R. Buslei, M. Buchfelder, D. Weigel, H. Stefan, B. Kasper, E. Pauli and I. Blumcke (2009). "Increased reelin promoter methylation is associated with granule cell dispersion in human temporal lobe epilepsy." Neuropathol Exp Neurol **68**: 356–364. .

Koepp, M. (2014). "Neuroimaging of drug resistance in epilepsy." Curr Opin Neurol. **27**: 192-8.

Kotagal, P., H. Luders, H. Morris, D. Dinner, E. Wyllie, J. Godoy and A. Rothner (1989). "Dystonic posturing in complex partial seizures of temporal lobe onset: a new lateralizing sign." Neurology **39**: 196–201.

Kreisl, W., J. Liow, N. Kimura, N. Seneca, S. Zoghbi, C. Morse, P. Herscovitch, V. Pike and R. Innis (2010). "P-glycoprotein function at the blood-brain barrier in humans can be quantified with the substrate radiotracer 11C-N-desmethyl-loperamide." J Nucl Med **51**: 559-66.

Kubicki, M., M. Shenton, D. Salisbury, Y. Hirayasu, K. Kasai, R. Kikinis, F. Jolesz and R. McCarley (2002). "Voxel-based morphometric analysis of gray matter in first episode schizophrenia." Neuroimage. **17**: 1711-9.

Kuhl, D., J. J. Engel, M. Phelps and A. Kowell (1978). "Epileptic patterns of local cerebral metabolism and perfusion in man: investigation by emission computed tomography of 18F-fluorodeoxyglucose and 13N-ammonia." Trans Am Neurol Assoc **103**: 52–53.

Kuhl, D., J. Hale and W. Eaton (1966). "Transmission scanning: a useful adjunct to conventional emission scanning for accurately keying isotope deposition to radiographic anatomy." Radiology **87**: 278-84.

Kullmann, D., S. Schorge, M. Walker and R. Wykes (2014). "Gene therapy in epilepsy-is it time for clinical trials?" Nat Rev Neurol. **10**: 300-4.

Kumar, A., D. Tripathi, V. K. Paliwal, Z. Neyaz and V. Agarwal (2014). "Role of P-Glycoprotein in Refractoriness of Seizures to Antiepileptic Drugs in Lennox-Gastaut Syndrome." Journal of Child Neurology.

Kuntner, C., J. Bankstahl, M. Bankstahl, J. Stanek, T. Wanek, G. Stundner, R. Karch, R. Brauner, M. Meier, X. Ding, M. Müller, W. Löscher and O. Langer (2010). "Dose-response assessment of tariquidar and elacridar and regional quantification of P-glycoprotein inhibition at the rat blood-brain barrier using (R)-[(11)C]verapamil PET." European Journal of Nuclear Medicine and Molecular Imaging **37**(5): 942-953.

Kuzniecky, R. and O. Devinsky (2007). "Surgery Insight: surgical management of epilepsy." Nat Clin Pract Neurol. **3**: 673-81.

Kuzniecky, R., J. Hugg, H. Hetherington, R. Martin, E. Faught, R. Morawetz and F. Gilliam (1999). "Predictive value of 1H MRSI for outcome in temporal lobectomy." Neurology. **53**: 694-8.

Kwan, P., A. Arzimanoglou, A. Berg, M. Brodie, W. Allen Hauser, Mathern G, S. Moshe, E. Perucca, S. Wiebe and J. French (2010). "Definition of drug resistant epilepsy: Consensus proposal by the ad hoc Task Force of the ILAE Commission on Therapeutic Strategies. ." Epilepsia **51**: 1069-1077.

Kwan, P. and M. J. Brodie (2005). "Potential Role of Drug Transporters in the Pathogenesis of Medically Intractable Epilepsy." Epilepsia **46**(2): 224-235.

La Fougère, C., G. Böning, H. Bartmann, B. Wängler, S. Nowak, T. Just, E. Wagner, P. Winter, A. Rominger, S. Förster, F. Gildehaus, P. Rosa-Neto, L. Minuzzi, P. Bartenstein, H. Potschka and P. Cumming (2010). "Uptake and binding of the serotonin 5-HT1A antagonist [18F]-MPPF in brain of rats: Effects of the novel P-glycoprotein inhibitor tariquidar." NeuroImage **49**(2): 1406-1415.

La Fougère, C., A. Rominger, S. Foerster, J. Geisler and P. Bartenstein (2009). "PET and SPECT in epilepsy: A critical review." Epilepsy & Behavior **15**(1): 50-55.

Laćan, G., A. Plenevaux, D. Rubins, B. Way, C. Defraiteur, C. Lemaire, J. Aerts, A. Luxen, S. Cherry and W. Melega (2008). "Cyclosporine, a P-glycoprotein modulator, increases [18F]MPPF uptake in rat brain and peripheral tissues: microPET and ex vivo studies." Eur J Nucl Med Mol Imaging. **35**: 2256-66.

Langer, O., M. Bauer, A. Hammers, R. Karch, E. Pataraia, M. Koepp, A. Abrahim, G. Luurtsema, M. Brunner, R. Sunder-Plassmann, F. Zimprich, C. Joukhadar, S. Gentzsch, R. Dudczak, K. Kletter, M. Müller and C. Baumgartner (2007). "Pharmacoresistance in epilepsy: a pilot PET study with the P-glycoprotein substrate R-[(11)C]verapamil." Epilepsia. **48**(9): 1774-84.

Lee, D. H., F. Q. Gao, J. M. Rogers, I. Gulka, I. R. Mackenzie, A. G. Parrent, C. S. Kubu, D. G. Munoz, R. S. McLachlan, W. T. Blume and J. P. Girvin (1998). "MR in temporal lobe epilepsy: analysis with pathologic confirmation." American Journal of Neuroradiology **19**(1): 19-27.

Lee, E. M., K. C. Im, J. H. Kim, J. K. Lee, S. H. Hong, Y. J. No, S.-A. Lee, J. S. Kim and J. K. Kang (2009). "Relationship between hypometabolic patterns and ictal scalp EEG patterns in patients with unilateral hippocampal sclerosis: An FDG-PET study." Epilepsy research **84**(2): 187-193.

Lee, G., S. Dallas, M. Hong and R. Bendayan (2001). "Drug transporters in the central nervous system: brain barriers and brain parenchyma considerations." Pharmacol Rev. **53**: 569-96.

Lee, S. K. and D.-W. Kim (2013). "Focal Cortical Dysplasia and Epilepsy Surgery." Journal of Epilepsy Research **3**(2): 43-47.

Leschziner, G. D., T. Andrew, J. P. Leach, D. Chadwick, A. J. Coffey, D. J. Balding, D. R. Bentley, M. Pirmohamed and M. R. Johnson (2007). "Common ABCB1 polymorphisms are not associated with multidrug resistance in epilepsy using a gene-wide tagging approach." Pharmacogenetics and Genomics **17**(3): 217-220 10.1097/01.fpc.0000230408.23146.b1.

Lhatoo, S., J. Solomon, A. McEvoy, N. Kitchen, S. Shorvon and J. Sander (2003). "A prospective study of the requirement for and the provision of epilepsy surgery in the United Kingdom." Epilepsia. **44**: 673-6.

Li, L., F. Cendes, S. Antel, F. Andermann, W. Serles, F. Dubeau, A. Olivier and D. Arnold (2000). "Prognostic value of proton magnetic resonance spectroscopic imaging for surgical outcome in patients with intractable temporal lobe epilepsy and bilateral hippocampal atrophy." Ann Neurol. **47**: 195-200.

Librizzi, L., F. Noè, A. Vezzani, M. de Curtis and R. T. (2012). "Seizure-induced brain-borne inflammation sustains seizure recurrence and blood-brain barrier damage." Ann Neurol. **72**: 82-90.

Liow, J., W. Kreisl, S. Zoghbi, N. Lazarova, N. Seneca, R. Gladding, A. Taku, P. Herscovitch, V. Pike and R. Innis (2009). "P-glycoprotein function at the blood-brain barrier imaged using 11C-N-desmethyl-loperamide in monkeys." J Nucl Med. **50**: 108-15.

Litman, T., T. Druley, W. Stein and S. Bates (2001). "From MDR to MXR: new understanding of multidrug resistance systems, their properties and clinical significance." Cell Mol Life Sci. **58**: 931-59.

Liu, J., M. Thom, C. Catarino, L. Martinian, D. Figarella-Branger, F. Bartolomei, M. Koepp and S. Sisodiya (2012). "Neuropathology of the blood-brain barrier and pharmaco-resistance in human epilepsy." Brain **135**

Loescher, W., H. Klitgaard, R. Twyman and D. Schmidt (2013). "New avenues for anti-epileptic drug discovery and development." Nature Reviews Drug Discovery(12): 757-776.

Loescher, W. and H. Potschka (2005). "Role of drug efflux transporters in the brain for drug disposition and treatment of brain diseases." Progress in Neurobiology **76**(1): 22-76.

Lombardo, L., R. Pellitteri, M. Balazy and V. Cardile (2008). "Induction of Nuclear Receptors and Drug Resistance in the Brain Microvascular Endothelial Cells Treated with Antiepileptic Drugs." Current Neurovascular Research **5**(2): 82-92.

Löscher, W. (2011). "Critical review of current animal models of seizures and epilepsy used in the discovery and development of new antiepileptic drugs." Seizure **20**(5): 359-368.

Löscher, W. and C. Brandt (2010). "High seizure frequency prior to antiepileptic treatment is a predictor of pharmacoresistant epilepsy in a rat model of temporal lobe epilepsy." Epilepsia. **51**: 89-97.

Löscher, W., H. Klitgaard, R. Twyman and D. Schmidt (2013). "New avenues for anti-epileptic drug discovery and development." Nature Reviews Drug Discovery(12): 757-776.

Löscher, W., U. Klotz, F. Zimprich and D. Schmidt (2009). "The clinical impact of pharmacogenetics on the treatment of epilepsy." Epilepsia **50**(1): 1-23.

Löscher, W. and O. Langer (2010). "Imaging of P-glycoprotein function and expression to elucidate mechanisms of pharmacoresistance in epilepsy." Curr Top Med Chem. **10**: 1785-91.

Löscher, W. and H. Potschka (2005a). "Blood-Brain Barrier Active Efflux Transporters: ATP-Binding Cassette Gene Family." NeuroRx. **2**: 86–98.

Löscher, W. and H. Potschka (2005b). "Drug resistance in brain diseases and the role of drug efflux transporters." Nature Rev. Neurosci. **6**: 591-602.

Loup, F., F. Picard, Y. Yonekawa, H. Wieser and J. Fritschy (2009). "Selective changes in GABAA receptor subtypes in white matter neurons of patients with focal epilepsy." Brain **132**: 2449-63.

Lu, C., J. Li, W. Sun, L. Feng, L. Li, A. Liu, J. Li, W. Mao, H. Wei, L. Gao, X. Zhang, Z. Huang, X. Meng and Y. Wang (2010). "Elevated plasma S100B concentration is associated with mesial temporal lobe epilepsy in Han Chinese: A case-control study." Neuroscience Letters **484**(2): 139-142.

Lubberink, M., G. Luurtsema, B. N. M. van Berckel, R. Boellaard, R. Toornvliet, A. D. Windhorst, E. J. F. Franssen and A. A. Lammertsma (2006). "Evaluation of tracer kinetic models for quantification of P-glycoprotein function using (R)-[11C]verapamil and PET." J Cereb Blood Flow Metab **27**(2): 424-433.

Luna-Tortos, C., M. Fedrowitz and W. Loescher (2008). "Several major antiepileptic drugs are substrates for human P-glycoprotein." Neuropharmacology **55**(8): 1364-1375.

Luna-Tortós, C., B. Rambeck, U. Jürgens and W. Löscher (2009). "The Antiepileptic Drug Topiramate is a Substrate for Human P-glycoprotein but Not Multidrug Resistance Proteins." Pharmaceutical Research **26**(11): 2464-2470.

Luurtsema, G., C. F. M. Molthoff, R. C. Schuit, A. D. Windhorst, A. A. Lammertsma and E. J. F. Franssen (2005). "Evaluation of (R)-[11C]verapamil as PET tracer of P-glycoprotein function in the blood-brain barrier: kinetics and metabolism in the rat." Nuclear medicine and biology **32**(1): 87-93.

Luurtsema, G., A. D. Windhorst, M. P. J. Mooijer, J. D. M. Herscheid, A. A. Lammertsma and E. J. F. Franssen (2002). "Fully automated high yield synthesis of (R)- and (S)-[11C]verapamil for measuring P-glycoprotein function with positron emission tomography." Journal of Labelled Compounds and Radiopharmaceuticals **45**(14): 1199-1207.

Mairinger, S., T. Erker, M. Muller and O. Langer (2011). "PET and SPECT radiotracers to assess function and expression of ABC transporters in vivo." Curr Drug Metab. **12**: 774-92.

Mairinger, S., T. Wanek, C. Kuntner, Y. Doenmez, S. Strommer, J. Stanek, E. Capparelli, P. Chiba, M. Müller, N. Colabufo and O. Langer (2012). "Synthesis and preclinical evaluation of the radiolabeled P-glycoprotein inhibitor [(11)C]MC113." Nucl Med Biol. **39**: 1219-25.

Marchi, N., L. Angelov, T. Masaryk, V. Fazio, T. Granata, N. Hernandez, K. Hallene, T. Diglaw, L. Franic, I. Najm and D. Janigro (2007). "Seizure-promoting effect of blood-brain barrier disruption." Epilepsia. **48**: 732-42.

Marchi, N., T. Granata and D. Janigro (2014). "Inflammatory pathways of seizure disorders." Trends Neurosci. **37**: 55-65.

Mark, L., D. Daniels, T. Naidich and A. Williams (1993). "Hippocampal anatomy and pathologic alterations on conventional MR images." AJNR Am J Neuroradiol. **14**(5): 1237-40.

Markiewicz, P., M. Tamal, P. Julyan, D. Hastings and A. Reader (2007). "High accuracy multiple scatter modelling for 3D whole body PET." Phys Med Biol. **52**: 829-47.

McAndrews, M. and M. Cohn (2012). "Neuropsychology in temporal lobe epilepsy: influences from cognitive neuroscience and functional neuroimaging." Epilepsy Res Treat. **2012**(Article ID 925238): 13 pages.

McClelland, S., C. Flynn, C. Dubé, C. Richichi, Q. Zha, A. Ghestem, M. Esclapez, C. Bernard and T. Baram (2011). "Neuron-restrictive silencer factor-mediated hyperpolarization-activated cyclic nucleotide gated channelopathy in experimental temporal lobe epilepsy." Ann Neurol. **70**: 454-64.

McNamara, J. O. (1999). "Emerging insights into the genesis of epilepsy." Nature **399**(Supplementary): A15-A22.

Muzi, M., D. A. Mankoff, J. M. Link, S. Shoner, A. C. Collier, L. Sasongko and J. D. Unadkat (2009). "Imaging of Cyclosporine Inhibition of P-Glycoprotein Activity Using 11C-Verapamil in the Brain: Studies of Healthy Humans." Journal of Nuclear Medicine **50**(8): 1267-1275.

Nakagawa, M., E. Schneider, K. Dixon, J. Horton, K. Kelley, C. Morrow and K. Cowan (1992). "Reduced intracellular drug accumulation in the absence of P-glycoprotein (mdr1) overexpression in mitoxantrone-resistant human MCF-7 breast cancer cells." Cancer Res. **52**: 6175-81.

Neligan, A., G. S. Bell, J. W. Sander and S. D. Shorvon (2011). "How refractory is refractory epilepsy? Patterns of relapse and remission in people with refractory epilepsy." Epilepsy Research **96**(3): 225-230.

Neville, B. and Gindner (2010). "Febrile seizures are a syndrome of secondarily generalized hippocampal epilepsy." DMCN **52**: 1151–1153.

Nurmohamed, L., F. Garcia-Bournissen, R. J. Buono, M. W. Shannon and Y. Finkelstein (2010). "Predisposition to epilepsy—Does the ABCB1 gene play a role?" Epilepsia **51**(9): 1882-1885.

O'Brien, T. J., E. L. So, B. P. Mullan, M. F. Hauser, B. H. Brinkmann, C. R. Jack, G. D. Cascino, F. B. Meyer and F. W. Sharbrough (1999). "Subtraction SPECT co-registered to MRI improves postictal SPECT localization of seizure foci." Neurology **52**(1): 137.

Oakes, T. R., V. Sossi and T. J. Ruth (1997). Normalization in 3D PET: comparison of detector efficiencies obtained from uniform planar and cylindrical sources. Nuclear Science Symposium, 1997. IEEE, IEEE.

Oh, H.-S., M.-C. Lee, H.-S. Kim, J.-S. Lee, J.-H. Lee, M.-K. Kim, Y.-J. Woo, J.-H. Kim, H.-I. Kim and S.-U. Kim (2008). "Pathophysiologic characteristics of balloon cells in cortical dysplasia." Child's Nervous System **24**(2): 175-183.

Owen, A., M. Pirmohamed, J. N. Tettey, P. Morgan, D. Chadwick and B. K. Park (2001). "Carbamazepine is not a substrate for P-glycoprotein." British Journal of Clinical Pharmacology **51**(4): 345-349.

Panayiotopoulos, C. (2005). "The Epilepsies: Seizures, Syndromes and Management. ." Oxfordshire (UK): Bladon Medical Publishing.

Pardridge, W. (1999). "Blood-brain barrier biology and methodology." J Neurovirol. **5**: 556-69.

Pekcec, A. (2009). "Targeting prostaglandin E2 EP1 receptors prevents seizure-associated P-glycoprotein up-regulation." J. Pharmacol. Exp. Ther. **330**: 939-947.

Pfaffl, M. W. (2001). "A new mathematical model for relative quantification in real-time RT-PCR." Nucleic Acids Research **29**(9): e45.

Portela, L. V. C., A. B. L. Tort, R. Walz, M. Bianchin, P. C. Trevisol-Bittencourt, P. R. Wille, R. C. Cardoso, M. M. I. Ishida, A. VonWangenheim, E. C. Grisard, M. Steindel, C. A. Gonçalves and D. O. Souza (2003). "Interictal serum S100B levels in chronic neurocysticercosis and idiopathic epilepsy." Acta Neurologica Scandinavica **108**(6): 424-427.

Potschka, H. (2010). "Modulating P-glycoprotein regulation: Future perspectives for pharmacoresistant epilepsies?" Epilepsia **51**(8): 1333-1347.

Potschka, H. (2013). "Animal and human data: where are our concepts for drug-resistant epilepsy going?" Epilepsia. **54** 29-32.

Potschka, H. and W. Löscher (2002). "A comparison of extracellular levels of phenytoin in amygdala and hippocampus of kindled and non-kindled rats." NeuroReport **13**(1): 167-171.

Potschka, H., H. Volk and W. Löscher (2004). "Pharmacoresistance and expression of multidrug transporter P-glycoprotein in kindled rats." NeuroReport **15**(10): 1657-1661.

Provenzale, J., D. Barboriak, K. VanLandingham, J. MacFall, D. Delong and D. Lewis (2008). "Hippocampal MRI signal hyperintensity after febrile status epilepticus is predictive of subsequent mesial temporal sclerosis." AJR Am J Roentgenol. **190**: 976-83.

Pugliatti M, Beghi E, Forsgren L, Ekman M and S. P. (2007). "Estimating the cost of epilepsy in Europe: a review with economic modeling." Epilepsia **48**(12): 2224-33.

Racine, R. (1972). "Modification of seizure activity by electrical stimulation. I. After-discharge threshold." Electroencephalogr Clin Neurophysiol. **32**: 269-79.

Ranicar, A., C. Williams, L. Schnorr, J. Clark, C. Rhodes, P. Bloomfield and T. Jones (1991). "The on-line monitoring of continuously withdrawn arterial blood during PET studies using a single BGO/photomultiplier assembly and non-stick tubing. ." Med Prog Technol **17**: 259–64.

Rao, V., J. Dahlheimer, M. Bardgett, A. Snyder, R. Finch, A. Sartorelli and D. Piwnica-Worms (1999). "Choroid plexus epithelial expression of MDR1 P glycoprotein and multidrug resistance-associated protein contribute to the blood-cerebrospinal-fluid drug-permeability barrier." Proc Natl Acad Sci U S A **96**: 3900-5.

Rathore, C., J. Dickson, R. Teotónio, P. Ell and J. Duncan (2014). "The utility of 18F-fluorodeoxyglucose PET (FDG PET) in epilepsy surgery." Epilepsy Res. **108**: 1306-14.

Regesta, G. and P. Tanganelli (1999). "Clinical aspects and biological bases of drug-resistant epilepsies." Epilepsy Res. **34**: 109-22.

Remy, S., S. Gabriel, B. Urban, D. Dietrich, T. Lehmann, C. Elger, U. Heinemann and H. Beck (2003). "A novel mechanism underlying drug resistance in chronic epilepsy." Ann Neurol. **53**: 469-79.

Rivers, F., T. J. O'Brien and R. Callaghan (2008). "Exploring the possible interaction between anti-epilepsy drugs and multidrug efflux pumps; in vitro observations." European Journal of Pharmacology **598**(1â€“3): 1-8.

Rivest, S. (2010). "Interactions between the immune and neuroendocrine systems." Prog Brain Res. **181**: 43-53.

Rizzi, M., S. Caccia, G. Guiso, C. Richichi, J. Gorter, E. Aronica, M. Aliprandi, R. Bagnati, R. Fanelli, M. D'Incalci, R. Samanin and A. Vezzani (2002). "Limbic seizures induce P-glycoprotein in rodent brain: functional implications for pharmacoresistance." J Neurosci. **22**: 5833-9.

Rosenow, F. and H. Lüders (2001). "Presurgical evaluation of epilepsy." Brain. **124**: 1683-700.

Ryvlin, P., S. Bouvard, D. Le Bars, G. De Lamérie, M. Grégoire, P. Kahane, J. Froment and F. Mauguière (1998). "Clinical utility of flumazenil-PET versus [18F]fluorodeoxyglucose-PET and MRI in refractory partial epilepsy. A prospective study in 100 patients." Brain **121** 2067-81.

Sanchez, M. B., J. L. Herranz, C. Leno, R. Arteaga, A. Oterino, E. M. Valdizan, J. M. Nicolas, J. Adin and J. A. Armijo (2010). "Genetic factors associated with drug-resistance of epilepsy: Relevance of stratification by patient age and aetiology of epilepsy." Seizure **19**(2): 93-101.

Sandler, S. I., A. Figaji and P. D. Adelson (2010). "Clinical applications of biomarkers in pediatric traumatic brain injury." Child's Nervous System **26**(2): 205-213.

Sarkisian, M. (2001). "Overview of the Current Animal Models for Human Seizure and Epileptic Disorders." Epilepsy Behaviour **2**: 201-216.

Sasongko, L., J. Link, M. Muzi, D. Mankoff, X. Yang, A. Collier, S. Shoner and J. Unadkat (2005). "Imaging P-glycoprotein transport activity at the human blood-brain barrier with positron emission tomography." Clin Pharmacol Ther. **77**: 503-14.

Schinkel, A. and J. Jonker (2003). "Mammablian drug efflux transporters of the ATP binding cassette (ABC) family: an overview." Adv Drug Deliv Rev. **55**: 3-29.

Schinkel, A. H. (1999). "P-Glycoprotein, a gatekeeper in the blood-brain barrier." Adv. Drug Deliv. Rev. **36**: 179-194.

Schmidt, D. and W. Löscher (2009). "New developments in antiepileptic drug resistance: an integrative view." Epilepsy Curr **9**: 47-52.

Schuetz, E. G., K. N. Furuya and J. D. Schuetz (1995). "Interindividual variation in expression of P-glycoprotein in normal human liver and secondary hepatic neoplasms." Journal of Pharmacology and Experimental Therapeutics **275**(2): 1011-1018.

Scott, R., D. Gadian, M. King, W. Chong, T. Cox, B. Neville and A. Connelly (2002). "Magnetic resonance imaging findings within 5 days of status epilepticus in childhood." Brain. **125**: 1951-9.

Seegers, U., H. Potschka and W. Loescher (2002). "Transient increase of P-glycoprotein expression in endothelium and parenchyma of limbic brain regions in the kainate model of temporal lobe epilepsy." Epilepsy Research **51**(3): 257-268.

Seneca, N., S. S. Zoghbi, J.-S. Liow, W. Kreisl, P. Herscovitch, K. Jenko, R. L. Gladding, A. Taku, V. W. Pike and R. B. Innis (2009). "Human Brain Imaging and Radiation Dosimetry of 11C-N-Desmethyl-Loperamide, a PET Radiotracer to Measure the Function of P-Glycoprotein." Journal of Nuclear Medicine **50**(5): 807-813.

Sharma, A. K., R. Y. Reams, W. H. Jordan, M. A. Miller, H. L. Thacker and P. W. Snyder (2007). "Mesial Temporal Lobe Epilepsy: Pathogenesis, Induced Rodent Models and Lesions." Toxicologic Pathology **35**(7): 984-999.

Sharom, F. (2008). "ABC multidrug transporters: structure, function and role in chemoresistance." Pharmacogenomics **9**: 105-27.

Shorvon, S. (2009). "A history of neuroimaging in epilepsy 1909–2009." Epilepsia **50**: 39–49.

Shorvon, S. (2010). "Handbook of Epilepsy Treatment." Blackwell

Siddiqui, A., R. Kerb, M. E. Weale, U. Brinkmann, A. Smith, D. B. Goldstein, N. W. Wood and S. M. Sisodiya (2003). "Association of Multidrug Resistance in Epilepsy with a Polymorphism in the Drug-Transporter Gene ABCB1." New England Journal of Medicine **348**(15): 1442-1448.

Siegel, A., H. Wieser, W. Wichmann and G. Yasargil (1990). "Relationships between MR-imaged total amount of tissue removed, resection scores of specific mediobasal limbic subcompartments and clinical outcome following selective amygdalohippocampectomy." Epilepsy Res. **6**: 56-65.

Silfvenius, H. (1999). "Cost-benefit of epilepsy surgery." Acta Neurol Belg. **99**: 266-74.

Sills, G. J. (2008). "Antiepileptic Drug Transport-Of Mice and Men." Epilepsy Currents **8**(2): 48-50.

Sisodiya, S. (2003). "Mechanisms of antiepileptic drug resistance." Curr Opin Neurol. **16**: 197-201.

Sisodiya, S. M. and S. E. Bates (2006). "Treatment of drug resistance in epilepsy: one step at a time." The Lancet Neurology **5**(5): 380-381.

Sisodiya, S. M., S. L. Free, J. M. Stevens, D. R. Fish and S. D. Shorvon (1995). Widespread cerebral structural changes in patients with cortical dysgenesis and epilepsy.

Sisodiya, S. M., W. R. Lin, B. N. Harding, M. V. Squier and M. Thom (2002). "Drug resistance in epilepsy: expression of drug resistance proteins in common causes of refractory epilepsy." Brain **125**(1): 22-31.

Sisodiya, S. M., W. R. Lin, M. V. Squier and M. Thom (2001). "Multidrug-resistance protein 1 in focal cortical dysplasia." The Lancet **357**(9249): 42-43.

Smith, S. J. M. (2005). "EEG in the diagnosis, classification, and management of patients with epilepsy." J Neurol Neurosurg Psychiatry **76**: Suppl 2:ii2-7.

Smith, S. M. (2002). "Fast robust automated brain extraction." Human Brain Mapping **17**(3): 143-155.

Sommer, W. (1880). "Erkrankung des Ammonshorns als aetiologisches Moment der Epilepsie." Archiv für Psychiatrie und Nervenkrankheiten **10**(3): 631-675.

Sorokin, A. (2004). "Cyclooxygenase-2: potential role in regulation of drug efflux and multidrug resistance phenotype." Curr Pharm Des. **10**: 647-57.

Spencer, S. and L. Huh (2008). "Outcomes of epilepsy surgery in adults and children." Lancet Neurol. **7**: 525-37.

Stavchansky, S. A., R. S. Tilbury, J. M. McDonald, C. T. Ting and H. B. Kostenbauder (1978). "In Vivo Distribution of Carbon-11 Phenytoin and its Major Metabolite, and Their Use in Scintigraphic Imaging." Journal of Nuclear Medicine **19**(8): 936-941.

Sterjev, Z., G. K. Trencevska, E. Cvetkovska, I. Petrov, I. Kuzmanovski, J. T. Ribarska, A. K. Nestorovska, N. Matevska, Z. Naumovska, S. Jolevska-Trajkovic, A. Dimovski and L. Suturkova (2012). "The association of C3435T single-nucleotide polymorphism, Pgp-glycoprotein gene expression levels and carbamazepine maintenance dose in patients with epilepsy." Neuropsychiatric Disease and Treatment **8**: 191-196.

Summers, M. A., J. L. Moore and J. W. McAuley (2004). "Use of Verapamil as a Potential P-Glycoprotein Inhibitor in a Patient with Refractory Epilepsy." Annals of Pharmacotherapy **38**(10): 1631-1634.

Sureau, F. C., A. J. Reader, C. Comtat, C. Leroy, M.-J. Ribeiro, I. n. Buvat and R. g. Trebossen (2008). "Impact of Image-Space Resolution Modeling for Studies with the High-Resolution Research Tomograph." Journal of Nuclear Medicine **49**(6): 1000-1008.

Sweatt, D. (2009). "Mechanisms of Memory." Elsevier, Burlington, MA.

Syvaenen, S., G. Blomquist, M. Sprycha, A. Urban Hoeglund, M. Roman, O. Eriksson, M. Hammarlund-Udenaes, B. Langstroem and M. Bergstroem (2006). "Duration and degree of cyclosporin induced P-glycoprotein inhibition in the rat blood-brain barrier can be studied with PET." NeuroImage **32**(3): 1134-1141.

Syvänen, S., M. Labots, Y. Tagawa, J. Eriksson, A. Windhorst, A. Lammertsma, E. de Lange and R. Voskuyl (2012). "Altered GABAA receptor density and unaltered blood-brain barrier transport in a kainate model of epilepsy: an in vivo study using 11C-flumazenil and PET." J Nucl Med **53**: 1974-83.

Syvänen, S., V. Russmann, J. Verbeek, J. Eriksson, M. Labots, C. Zellinger, N. Seeger, R. Schuit, M. Rongen, R. van Kooij, A. Windhorst, A. Lammertsma, E. de Lange, R. Voskuyl, M. Koepp and H. Potschka (2013). "[11C]quinidine and [11C]laniquidar PET imaging in a chronic rodent epilepsy model: impact of epilepsy and drug-responsiveness." Nucl Med Biol. **40**: 764-75.

Szakacs, G., J. K. Paterson, J. A. Ludwig, C. Booth-Genthe and M. M. Gottesman (2006). "Targeting multidrug resistance in cancer." Nat Rev Drug Discov **5**(3): 219-234.

Takano, A., H. Kusuhara, T. Suhara, I. Ieiri, T. Morimoto, Y.-J. Lee, J. Maeda, Y. Ikoma, H. Ito, K. Suzuki and Y. Sugiyama (2006). "Evaluation of In Vivo P-Glycoprotein Function at the Blood-Brain Barrier Among MDR1 Gene Polymorphisms by Using 11C-Verapamil." Journal of Nuclear Medicine **47**(9): 1427-1433.

Tassi, L., N. Colombo, R. Garbelli, S. Francione, G. Lo Russo, R. Mai, F. Cardinale, M. Cossu, A. Ferrario, C. Galli, M. Bramerio, A. Citterio and R. Spreafico (2002). Focal cortical dysplasia: neuropathological subtypes, EEG, neuroimaging and surgical outcome.

Téllez-Zenteno, J., L. Ronquillo and S. Wiebe (2005). "Sudden unexpected death in epilepsy: evidence-based analysis of incidence and risk factors." Epilepsy Res. **65**: 101-15.

Thiebaut, F., T. Tsuruo, H. Hamada, M. Gottesman, I. Pastan and M. Willingham (1987). "Cellular localization of the multidrug-resistance gene product P-glycoprotein in normal human tissues." Proc Natl Acad Sci U S A. **84**: 7735-8.

Thom, M. (2009). "Hippocampal sclerosis: progress since Sommer." Brain Pathol. **19**: 565-72.

Thom, M. (2014). "Review: Hippocampal sclerosis in epilepsy: a neuropathology review." Neuropathol Appl Neurobiol. **40**: 520-43.

Thom, M., G. Mathern, J. Cross and E. Bertram (2010). "Mesial temporal lobe epilepsy: How do we improve surgical outcome?" Ann Neurol. **68**: 424-34. .

Tishler, D., K. Weinberg, D. Hinton, N. Barbaro, G. Annett and R. C. (1995). "MDR1 gene expression in brain of patients with medically intractable epilepsy " Epilepsia **36**: 1-6.

Tournier, N., S. Cisternino, M. Peyronneau, S. Goutal, F. Dolle, J. Scherrmann, M. Bottlaender, W. Saba and H. Valette (2012). "Discrepancies in the P-glycoprotein-mediated transport of (18)F-MPPF: a pharmacokinetic study in mice and non-human primates." Pharm Res. **29**: 2468-76.

Traynelis, S. and R. Dingledine (1988). "Potassium-induced spontaneous electrographic seizures in the rat hippocampal slice." J Neurophysiol. **59**: 259-76.

Turkheimer, F., N. Boussion, A. Anderson, N. Pavese, P. Piccini and D. Visvikis (2008). "PET image denoising using a synergistic multiresolution analysis of structural (MRI/CT) and functional datasets." J Nucl Med **49**: 657-66.

van Assema, D. l. M. E., M. Lubberink, R. Boellaard, R. C. Schuit, A. D. Windhorst, P. Scheltens, A. A. Lammertsma and B. N. M. van Berckel (2012). "P-Glycoprotein Function at the Blood-Brain Barrier: Effects of Age and Gender." Molecular Imaging and Biology **14**(6): 771-776.

Van Paesschen, W. (2004). "Ictal SPECT." Epilepsia **45**: 35-40.

Van Vliet, E., E. Aronica, S. Redeker, N. Marchi, M. Rizzi, A. Vezzani and J. Gorter (2004). "Selective and persistent upregulation of mdr1b mRNA and P-glycoprotein in the parahippocampal cortex of chronic epileptic rats." Epilepsy Res **60**: 203–213.

Van Vliet, E., R. van Schaik, P. Edelbroek, R. Voskuyl, S. Redeker, E. Aronica, W. Wadman and J. Gorter (2007). "Region-specific overexpression of P-glycoprotein at the blood-brain barrier affects brain uptake of phenytoin in epileptic rats." J Pharmacol Exp Ther **322**: 141-7.

Van Vliet, E., G. Zibell, A. Pekcec, J. Schlichtiger, P. Edelbroek, L. Holtman, E. Aronica, J. Gorter and H. Potschka (2010). "COX-2 inhibition controls P-glycoprotein expression and promotes brain delivery of phenytoin in chronic epileptic rats." Neuropharmacology **58**: 404–412.

Van Vliet, E. A., R. Van Schaik, P. M. Edelbroek, S. Redeker, E. Aronica, W. J. Wadman, N. Marchi, A. Vezzani and J. A. Gorter (2006). "Inhibition of the Multidrug Transporter P-Glycoprotein Improves Seizure Control in Phenytoin-treated Chronic Epileptic Rats." Epilepsia **47**(4): 672-680.

Verma, A. and R. Radtke (2006). "EEG of partial seizures." J Clin Neurophysiol. **23**: 333-9.

Vezzani, A., E. Aronica, A. Mazarati and Q. Pittman (2013). "Epilepsy and brain inflammation." Exp Neurol. **244**: 11-21.

Vezzani, A., J. French, T. Bartfai and T. Baram (2011). "The role of inflammation in epilepsy." Nat Rev Neurol. **7**: 31-40.

Vezzani, A. and T. Granata (2005). "Brain inflammation in epilepsy: experimental and clinical evidence." Epilepsia. **46**: 1724-43.

Vinton, A. B., R. Carne, R. J. Hicks, P. M. Desmond, C. Kilpatrick, A. H. Kaye and T. J. O'Brien (2007). "The extent of resection of FDG-PET hypometabolism relates to outcome of temporal lobectomy." Brain **130**(2): 548-560.

Vogelgesang, B., H. Echizen, E. Schmidt and M. Eichelbaum (1984). "Stereoselective first-pass metabolism of highly cleared drugs: studies of the bioavailability of L- and D-verapamil examined with a stable isotope technique." Br J Clin Pharmacol. **18**: 733-40.

Volk, H. A. and W. Loescher (2005). "Multidrug resistance in epilepsy: rats with drug-resistant seizures exhibit enhanced brain expression of P-glycoprotein compared with rats with drug-responsive seizures." Brain **128**(6): 1358-1368.

Wagner, C., T. Feurstein, R. Karch, M. Bauer, S. Kopp, P. Chiba, k. Kletter, M. Mueller, M. Zeitlinger and O. Langer (2009). "A pilot study to assess the efficacy of tariquidar to inhibit P-glycoprotein at the human blood-brain barrier with (R)[11C]verapamil and PET." J Nucl Med **50**: 1192.

Walker, M., M. Feldmann, J. Matthews, J. Anton-Rodriquez, S. Wang, M. Koepp and M. Asselin (2012). "Optimization of methods for quantification of rCBF using high-resolution [15 O]H 2 O PET images." Physics in Medicine and Biology **57**(8): 2251.

Watabe, H., Y. Ikoma, Y. Kimura, M. Naganawa and M. Shidahara (2006). "PET kinetic analysis--compartmental model." Ann Nucl Med. **20**: 583-8.

Watson, C. C. (1997). "A technique for measuring the energy response of a PET tomograph using a compact scattering source." IEEE Trans. Nucl. Sci. **44**: 2500-8.

Watson, C. C. (2000). "New, faster, image-based scatter correction for 3D PET." IEEE Trans. Nucl. Sci. **47**: 1587-94.

Wehner, T., E. Lapresto, J. Tkach, P. Liu, W. Bingaman, R. Prayson, P. Ruggieri and B. Diehl (2007). "The value of interictal diffusion-weighted imaging in lateralizing temporal lobe epilepsy." Neurology. **68**: 122-7.

Wehner, T. and H. Lüders (2008). "Role of neuroimaging in the presurgical evaluation of epilepsy." J Clin Neurol. **4**: 1-16.

Wendling, A., E. Hirsch, I. Wisniewski, C. Davanture, I. Ofer, J. Zentner, S. Bilic, J. Scholly, A. Staack, M. Valenti, A. Schulze-Bonhage, P. Kehrli and B. Steinhoff (2013). "Selective amygdalohippocampectomy versus standard temporal lobectomy in patients with mesial temporal lobe epilepsy and unilateral hippocampal sclerosis." Epilepsy Res. **104**: 94-104.

Westover, M., J. Cormier, M. Bianchi, M. Shafi, R. Kilbride, A. Cole and S. Cash (2012). "Revising the "Rule of Three" for inferring seizure freedom." Epilepsia. **53**: 368-76.

Wiebe, S., W. Blume, J. Girvin and M. Eliasziw (2001). "A randomized, controlled trial of surgery for temporal lobe epilepsy." N Engl J Med **345**: 311–318.

Wieshmann, U. (2003). "Clinical application of neuroimaging in epilepsy." J Neurol Neurosurg Psychiatry **74**: 466–470.

Wijnholds, J., E. deLange, G. Scheffer, D. van den Berg, C. Mol, M. van der Valk, A. Schinkel, R. Scheper, D. Breimer and P. Borst (2000). "Multidrug resistance protein 1 protects the choroid plexus epithelium and contributes to the blood-cerebrospinal fluid barrier." J Clin Invest. **105**: 279-85.

Williamson, P., V. Thadani, J. French, T. Darcey, R. Mattson, S. Spencer and D. Spencer (1998). "Medial temporal lobe epilepsy: videotape analysis of objective clinical seizure characteristics." Epilepsia **39**: 1182–1188.

Willmann, O., R. Wennberg, T. May, F. G. Woermann and B. Pohlmann-Eden (2007). "The contribution of 18F-FDG PET in preoperative epilepsy surgery evaluation for patients with temporal lobe epilepsy: A meta-analysis." Seizure : the journal of the British Epilepsy Association **16**(6): 509-520.

Winston, G. P., M. J. Cardoso, E. J. Williams, J. L. Burdett, P. A. Bartlett, M. Espak, C. Behr, J. S. Duncan and S. Ourselin (2013). "Automated hippocampal segmentation in patients with epilepsy: Available free online." Epilepsia **54**(12): 2166-2173.

Wolf, A., B. Bauer and A. Hartz (2012). "ABC Transporters and the Alzheimer's Disease Enigma." Frontiers in Psychiatry **3**.

Won, H. J., K.-H. Chang, J.-E. Cheon, H. D. Kim, D. S. Lee, M. H. Han, I.-O. Kim, S. K. Lee and C.-K. Chung (1999). "Comparison of MR Imaging with PET and IctalSPECT in 118 Patients with Intractable Epilepsy." American Journal of Neuroradiology **20**(4): 593-599.

Wunderlich, M. T., A. D. Ebert, T. Kratz, M. Goertler, S. Jost and M. Herrmann (1999). "Early Neurobehavioral Outcome After Stroke Is Related to Release of Neurobiochemical Markers of Brain Damage." Stroke **30**(6): 1190-1195.

Wyler, A. R., B. P. Hermann and G. Somes (1995). "Extent of Medial Temporal Resection on Outcome from Anterior Temporal Lobectomy: A Randomized Prospective Study." Neurosurgery **37**(5): 982-991.

Yamamoto, S., M. Amano, S. Miura, H. Iida and I. Kanno (1986). "Deadtime correction method using random coincidence for PET." Journal of nuclear medicine: official publication, Society of Nuclear Medicine **27**(12): 1925-1928.

Zentner, J., A. Hufnagel, H. Wolf, B. Ostertun, E. Behrens, M. Campos, L. Solymosi, C. Elger, O. Wiestler and J. Schramm (1995). "Surgical treatment of temporal lobe epilepsy: clinical, radiological, and histopathological findings in 178 patients. ." J Neurol Neurosurg Psychiatry **58**: 666–73.

Zhang, C., P. Kwan, Z. Zuo and L. Baum (2010). "In vitro concentration dependent transport of phenytoin and phenobarbital, but not ethosuximide, by human P-glycoprotein." Life Sciences **86**: 899-905.

Zhang, C., Z. Zuo, P. Kwan and L. Baum (2011). "In vitro transport profile of carbamazepine, oxcarbazepine, eslicarbazepine acetate, and their active metabolites by human P-glycoprotein." Epilepsia **52**(10): 1894-1904.

Zhang, L., W. Ong and T. Lee (1999). " Induction of P-glycoprotein expression in astrocytes following intracerebroventricular kainate injections. ." Experimental Brain Research **126**: 509-516.

Zhu, H. and G. Liu (2004). "Glutamate up-regulates P-glycoprotein expression in rat brain microvessel endothelial cells by an NMDA receptor-mediated mechanism. ." Life Sciences **75**: 1313-1322.

Zumsteg, D. and H. Wieser (2000). "Presurgical evaluation: current role of invasive EEG." Epilepsia. **41**: 55-60.